Enantioselective Synthesis using Azides: Mechanism and Methods

A Dissertation

SUBMITTED TO THE FACULTY OF THE

UNIVERSITY OF MINNESOTA

BY

Amy A. Ott

IN PARTIAL FULFILLMENT OF THE REQUIREMENTS FOR THE DEGREE OF

DOCTOR OF PHILOSOPHY

Professor Joseph Topczewski, Advisor

May 2020

May 2020

ACKNOWLEDGEMENTS

I would like to give thanks to my supervisor, Prof. Joe Topczewski. Joe's passion and enthusiasm for science is contagious. I have learned so much from him over the past five years. He has always pushed me to be the best researcher possible. I am proud to have helped him start his academic career.

I am grateful for the community in the chemistry department at the University of Minnesota. In particular, thank you to Patrick, Hannah, Mary, Curtis, Grant, Ryan, Subhasree and Johannes for your friendship and scientific discussion. I am thankful for the helpful scientific discussions, guidance, and support from the chemistry faculty members including Chris Douglas, Steve Kass, and Nick Race.

Thank you to Prof. Emeritus Wayland Noland and the University of Minnesota chemistry department for the Excellence in Graduate Studies Fellowship (2017) and the University of Minnesota graduate school for the Doctoral Dissertation Fellowship (2019).

I am very grateful for my family and friends because this would not have been possible without their love and support.

I dedicate this thesis to my parents, Tammy and Barry.

Abstract

With the increasing demand of complex sp^3-hybridized molecules and the importance of sustainability and environmental impact, it is imperative for chemists to develop creative and efficient synthetic methods to synthesize these molecules. As a molecular subclass, chiral-α,α-disubstituted amines are particularly challenging to access via traditional methods. Our approach has focused on developing dynamic kinetic resolutions (DKR) to access chiral amines from azides. DKR is a fundamentally interesting strategy because racemic starting materials can be converted into enantioenriched products in high yield and stereoselectivity. This work describes the initial discovery of a dynamic kinetic resolution of allylic azides (Chapter 2), followed by subsequent fundamental mechanistic investigations (Chapter 3). Insights from these fundamental studies led in exploration of catalysts to promote racemization of activated azides (Chapter 4). This racemization was used to recycle the excess scalemic starting material in a kinetic resolution of cyclic secondary azides (Chapter 5). Finally, efforts to utilize the catalyst-promoted racemization in a dynamic kinetic resolution are discussed (Chapter 6).

Table of Contents

Abstract ... iii

List of Tables ... vi

List of Figures ... vii

List of Schemes ... viii

List of Abbreviations ... x

Chapter 1. Introduction ... 1

1.1. Methods for Resolution ... 2

1.1.2 Classic Resolution. ... 2

1.1.2 Kinetic Resolution ... 4

1.1.3. Dynamic Kinetic Resolution (DKR) ... 8

1.2. Chiral Amines ... 11

1.2.1. Synthesis of Chiral Amines via Nucleophilic Addition to Imine ... 11

1.2.2. [3,3]-Sigmatropic Rearrangements to Access Chiral Amines ... 14

1.2.3. Allylic Azide Rearrangement ... 18

1.3 References ... 22

2. Dynamic Kinetic Resolution of Allylic Azides via Asymmetric Dihydroxylation. 29

2.1 Introduction ... 29

2.2 Substrate Synthesis ... 31

2.3 Results and Discussion ... 32

2.4 Conclusion ... 37

2.5 References ... 38

Chapter 3. Evidence for a Sigmatropic and an Ionic Pathway in the Winstein Rearrangement ... 41

3.1 Introduction ... 41

3.2 Results and Discussion ... 43

3.2.1 Effect of Conjugation on K_{eq} ... 43

3.2.2 ^{15}N-Labelling Experiment ... 44

3.2.3 *E* to *Z* Isomerization ... 45

3.2.4 Chiral Acyclic Allylic Azide ... 47

3.2.5 Synthesis of Allylic Azides ... 50

3.2.5 Identifying a Racemization Pathway ... 51

3.3 Conclusion ... 53

3.4 References ... 54

Chapter 4. Catalytic Racemization of Activated Organic Azides ... 57

4.1 Introduction ... 57

4.2 Results and Discussion ... 59

4.3 Conclusion 66
4.4 Experimental 66
4.5 References 68
5. Kinetic Resolution of Cyclic Secondary Azides using an Enantioselective Copper(I) Catalyzed Azide-Alkyne Cycloaddition 70
5.1 Introduction 70
5.2 Results and Discussion 72
5.3 Conclusion 78
5.4 References 79
Chapter 6. Efforts Towards a DKR with Activated Azides 81
6.1 Introduction 81
6.2 E-CuAAC Reaction via DKR of Azides 82
6.3 Azide Reduction using Chiral Catalysts 86
6.4 Azide Reduction using Chiral Rhodium Catalyst and Acceptor/Acceptor Diazo 93
6.5 Conclusions 99
6.6 Experimental 100
6.7 References 117
Bibliography 119
Appendix. HPLC and NMR Images 137

List of Tables

Table 1.1 Conversions Necessary to Recover Starting Material with Desired ee at 23 °C ……6

Table 2.1 Optimization for Sharpless Asymmetric Dihydroxylation ……33

Table 2.2 Substrate Scope of SAD-Based DKR…….....35

Table 4.1 Initial Screen for Racemization Catalyst……..…….60

Table 4.2 Scope of Racemization…….…….63

Table 4.3 Alternate Racemization Catalysts…….…....64

Table 5.1 E-CuAAC Optimization by Kinetic Resolution…….....73

Table 6.1 Effect of Racemization Catalyst on er of Triazole **6.5**…….....84

Table 6.2 Catalytic Racemization of Azide **6.1**…….....85

Table 6.3 Reduction of Azide **6.8** Using Ruthenium Catalysts….……...88

Table 6.4 Reduction of Azide **6.8** using H_2 with Ruthenium Catalysts……89

Table 6.5 Reduction of azide **6.8** using $Pd_2(dba)_3$ and H_2[a] ……..……90

Table 6.6 Reduction of Azide **6.12** using [Ru] catalyst ……...……91

Table 6.7 Reduction of azide **6.12** using H_2 with [Ir] or [Rh] catalysts……92

Table 6.8 Racemization of azide **6.1** with $B(C_6F_5)_3$……..……....97

Table 6.9 Effect of Ag(I) Salt and Chiral Catalysts……..…98

Table 6.10 Chiral Rhodium Catalysts with Azide **6.12**…….99

Table 6.11 Racemization of Azide **6.1** with $B(C_6F_5)_3$…….……106

Table 6.12 Racemization of Azide **6.27**…….……..107

Table 6.13 Racemization of Azide **6.1** with Dowex 50Wx4……107

List of Figures

Figure 1.1 Examples of Chiral Amines and Amine Derivatives ……..…..11

Figure 3.1 a) Plot of log(k/k_0) vs σ^+ for substituent effects on the racemization of azides **3.36-3.41** in MeOH. Rates were measured in duplicate, replicates shown. b) Plot of log(k/k0) vs σ+ for substituent effects on the solvolysis of azides **3.36-3.41** in MeOH. Rates were measured in duplicate, replicates shown……53

Figure 4.1 Plot of log(k/k_0) vs. σ+ for substituent effects on the racemization of azides **1a** – **1e** using catalyst 4. Rates were measured in duplicate, replicates shown……..62

Figure 5.1 Representative Bioactive α-Chiral Triazoles……...70

Figure 6.1 Classes of Diazo Compounds…….……..95

List of Schemes

Scheme 1.1 Types of Resolution……..2

Scheme 1.2 Synthesis of Jacobsen's Catalyst……...3

Scheme 1.3 Classic Resolution in Synthesis of Crixivan®……..4

Scheme 1.4 General Equations in Kinetic Resolution…….6

Scheme 1.5 Jacobsen's Hydrolytic Kinetic Resolution……...7

Scheme 1.6 Dynamic Kinetic Resolution of Cyclopentenones……9

Scheme 1.7 Transition Metal and Enzyme Catalyzed DKR……...10

Scheme 1.8 Addition to Imine for Chiral Amine Synthesis……12

Scheme 1.9 Ellman's Auxiliary used to Access Chiral α,α-Disubstituted Amine……..14

Scheme 1.10 Rearrangement of Thiocyanate to Thioisocyanate……..…15

Scheme 1.11. a) Ichikawa's Method for Rearrangement of Allyl Cyanates b) Synthesis of (*S*)-Ketamine via Sigmatropic Rearrangement……...……16

Scheme 1.12. Overman Rearrangement to Access Unnatural α-Amino Acids…….....17

Scheme 1.13 a) Allylic Azide Rearrangement of Simple Allylic Azides. b) Rate Constants for Allylic Azide Rearrangement……...19

Scheme 1.14 Selective Dihydroxylation of Equilibrating Allylic Azide……19

Scheme 1.15 General Approach to Chiral Amines from Allylic Azide Rearrangement….20

Scheme 2.1 Winstein Rearrangement and Dynamic Kinetic Resolutions……..29

Scheme 2.2 Synthesis of Symmetric Azides Substrates……....32

Scheme 2.3 Elaboration of Product Diol……36

Scheme 3.1 Winstein Rearrangement……42

Scheme 3.2 Effects of Conjugation on K_{eq}…….....44

Scheme 3.3 Rearrangement of ^{15}N-Labeled Allylic Azide……..……...45

Scheme 3.4 Equilibration of Azides **3.27** and **3.28**…….46

Scheme 3.5 Equilibration of Chiral Allylic Azide……..48

Scheme 3.6 Relative Ionization Energies of Azide **3.30**…….50

Scheme 3.7 Synthesis of Enantioenriched Allylic Azides……..……..…51

Scheme 3.8 Racemization and Solvolysis of Cyclic Azides……...52

Scheme 4.1 Mechanisms of Azide Rearrangement and Racemization……...58

Scheme 4.2 Proposed Mechanism for Azide Racemization……..62

Scheme 4.3 Crossover Experiment……...…….66

Scheme 5.1 Azide Kinetic Resolution by E-CuAAC……71

Scheme 5.2 Substrate Scope of Alkyne Coupling Partner……....75

Scheme 5.3 Substrate Scope of Azide Coupling Partner……76

Scheme 5.4 Matched/Mismatched Experiment…….....77

Scheme 5.5 Gram Scale Reaction and Racemization of Recovered Azide……..…….78

Scheme 6.1 General DKR Strategy with Activated Azides…….…...81

Scheme 6.2 a) Kinetic Resolution of Azide **6.1**. b) Attempted DKR with Azide **6.1**.....82

Scheme 6.3 a) General Approach for DKR of Activated Azides using an E-CuAAC Reaction. b) Flow Chart of Requirements for Successful E-CuAAC Reaction…...….....83

Scheme 6.4 Synthesis of Azide **6.8** and Amine **6.9** …….…….……87

Scheme 6.5 Synthesis of Azide **6.12** and Amine **6.13**……91

Scheme 6.6 a) Rhodium-Catalyzed Reaction of Allylic Azide **6.14** with Aryldiazoacetate **6.15** b) Rhodium-Catalyzed Reaction of Tertiary Azide **6.8**……..……94

Scheme 6.7 Reactivity Screen of Diazo Compounds with Azide **6.8**……...……96

List of Abbreviations

Ac	acetate
AQN	anthraquinone
Ar	aryl
BACE1	Beta-secretase 1
BINAP	2,2′-Bis(diphenylphosphino)-1,1′-binaphthalene
CALB	*Candida antarctica* lipase B
calcd	calculated
$CDCl_3$	deuterated chloroform
CH_2Cl_2	dichloromethane
CHO	aldehyde
CLB	chlorobenzoate
CuAAC	Copper-catalyzed azide-alkyne cycloaddition
$Cu(hfac)_2$	Copper(II) hexafluoroacetylacetonate hydrate
DEAD	diethyl azodicarboxylate
DHQ	hydroquinine
DHQD	hydroquinidine
DIPEA	diisopropylethylamine
DKR	dynamic kinetic resolution
DME	dimethoxymethane
DMF	dimethylformamide
DPEN	1,2-Diphenyl-1,2-ethylenediamine
DPPTA	di-*p*-toluoyl tartaric acid
dr	diastereomeric ratio
EDCI	*N*-(3-Dimethylaminopropyl)-*N*′-ethylcarbodiimide hydrochloride
ee	enantiomeric excess
equiv	equivalents
er	enantiomeric ratio
ESI	electrospray ionization
Et_2O	ethyl ether
EtOAc	ethyl acetate

EtOH	ethanol
HCl	hydrochloric acid
Hex	hexanes
HFIP	1,1,1,3,3,3-hexafluoro-2-propanol
HOAc	acetic acid
HPLC	high performance liquid chromatography
HRMS	high resolution mass spectrometry
Hz	hertz
IPA	isopropyl alcohol
J	coupling constant (NMR)
KR	kinetic resolution
LA	Lewis acid
LDA	lithium diisopropylamide
m	multiplet (NMR)
m-CPBA	metachloroperoxy benzoic acid
MeOH	methanol
MEQ	4-methyl-2-quinolyl ether
min	minute
mL	milliliter
mmol	millimoles
MsCl	methane sulfonyl chloride
N	normal
$NaBH_4$	sodium borohydride
NaH	sodium hydride
NaOH	sodium hydroxide
^{n}BuLi	normal butyl lithium
NMO	*N*-methylmorpholine-*N*-oxide
NMR	nuclear magnetic resonance
Ph	phenyl
PHAL	phthalazine
PhCCH	phenyl acetylene

PhMe	toluene
PMHS	polymethylhydrosiloxane
PHN	phenanthryl ether
PPh_3	triphenyl phospine
p-TsOH	*para*-toluenesulfonic acid
PYR	diphenylpyrimidine
s	singlet (NMR)
SAD	Sharpless asymmetric dihydroxylation
t	triplet (NMR)
TBAF	tetrabutylammonium fluoride
TEA	triethylamine
THF	tetrahydrofuran
$Ti(i PrO)_4$	titanium isopropoxide
TLC	thin-layer chromatography
TMS	trimethylsilyl
δ	chemical shift in NMR
μM	micromolar

Chapter 1. Introduction

The ability to synthesize stereochemically-defined complex molecules is a central goal in the field of synthetic chemistry. This is especially critical as the number of stereochemically complex sp^3 hybridized molecules in pharmaceuticals, agrochemicals, polymers, and materials continues to rise.[1,2] There are three main strategies to achieve this desired outcome: i) using stereodefined starting materials, ii) inducing enantioselectivity via asymmetric catalysis, and iii) resolution of racemates. The chiral pool approach starts with commodity chemicals that contain pre-defined stereocenters.[3–5] Further transformations utilize the pre-existing stereocenters to install additional stereocenters in a diastereoselective manner. While this strategy has several advantages, this can be a problem if the desired diastereomer is disfavored due to the configuration of the starting material or if the desired molecule is difficult to access from the chiral pool. An alternate approach is asymmetric catalysis.[6–8] In this strategy, a chiral catalyst is used to impose asymmetry on a prochiral substrate. Work in this field has been highly regarded, as Sharpless, Noyori, and Knowles were awarded the Nobel Prize in chemistry in 2001 for their work on asymmetric transformations.[9] While certain motifs can be easily accessed using asymmetric methodologies (e.g. 1,2-diols), often it is easier and less expensive to access the racemate. Therefore, the ability to resolve a pair of enantiomers is necessary.[10–13] The concept of resolving racemic mixtures is paramount to this work and will be discussed in detail below. Further development of each of these strategies will advance efforts towards the efficient synthesis of enantioenriched molecules. This work will describe our efforts to expand the area of dynamic kinetic resolution to access chiral amines.

1.1. Methods for Resolution

Resolving enantiomers is a common approach to access enantioenriched compounds. Most mixtures of organic molecules are separated based on differences in their physical properties (e.g. polarity, solubility, or boiling point). However, enantiomers have the same physical properties in an achiral environment, thus, separation is less straightforward. Often the resolution of a racemic mixture requires modifying one or both enantiomers with another chiral agent. Common approaches include classic resolution, kinetic resolution, and dynamic kinetic resolution (Scheme 1.1). Excluding the chiral pool approach, resolution is the most commonly utilized strategy for obtaining chiral compounds in industry.[14]

Scheme 1.1 Types of Resolution

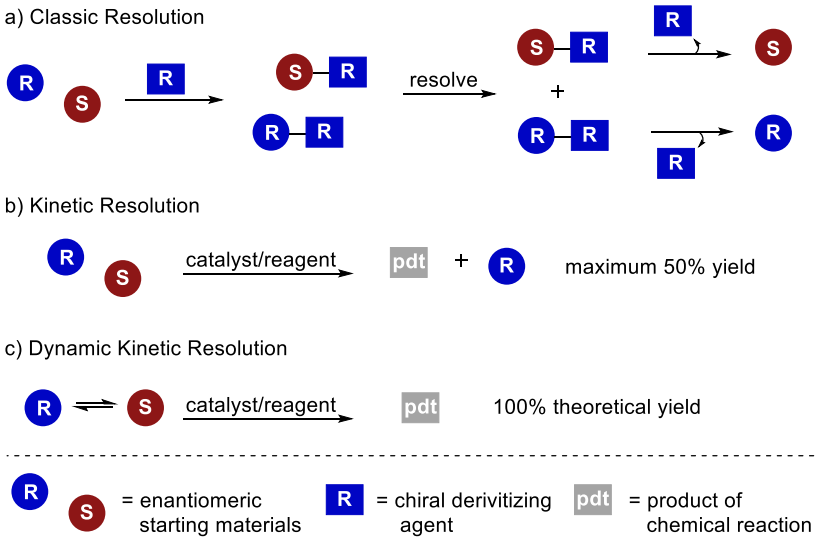

1.1.2 Classic Resolution

A classic resolution relies on a stoichiometric derivatization using a chiral molecule (Scheme 1.1a). Diastereomers are formed upon treatment of a racemic mixture with a chiral

resolving agent. Because diastereomers have different chemical properties, they can be separated. Separation can be accomplished using conventional purification techniques (e.g. chromatography or recrystallization) followed by removal of the resolving agent. Recrystallization is a common method for the separation of diastereomers that have appreciable differences in solubility. This includes salts that are not covalently bound (Scheme 1.2). This technique is prevalent in the pharmaceutical industry, which often requires the production of complex molecules with high levels of enantiopurity.

A classic resolution is the first step in the synthesis of Jacobsen's catalyst.[15] Diastereomeric salts are formed upon addition of enantiopure tartaric acid to trans-1,2-diamine (Scheme 1.2). Separation by selective crystallography is followed by a condensation reaction to afford the ligand backbone and is subsequently metallated to give Jacobsen's catalyst (**1.3**).

Scheme 1.2 Synthesis of Jacobsen's Catalyst

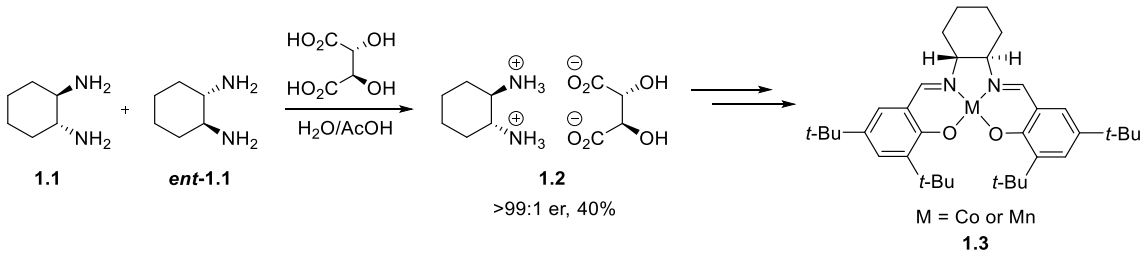

The synthesis of Crixivan®, an HIV-protease inhibitor drug developed by Merck, utilized a classic resolution to access the chiral piperazine fragment (Scheme 1.3).[16] Using (*S*)-PGA with the racemic piperazine **1.4** afforded a diastereomeric mixture of salts **1.5** and **1.6**. Selective crystallization of piperazine **1.5** left the desired salt **1.6** in the mother liquor. Exposure of salt **1.6** to Boc_2O and KOH resulted in piperazine **1.7** which was further

elaborated into Crixivan® (**1.8**). While this fragment had been accessed via asymmetric catalytic reduction and by bio-catalysis, Merck ultimately employed the classical resolution to access piperidine **1.6**.[16]

Scheme 1.3 Classic Resolution in Synthesis of Crixivan®

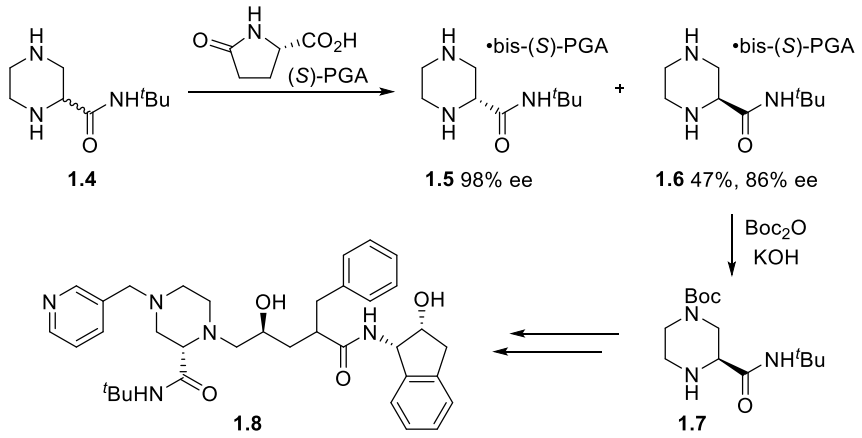

Unfortunately, not all pairs of diastereomers can be selectively crystallized. For these substrates, chromatography can be used as the method of separation.[17] It should be noted that enantiomers can be directly separated using preparative HPLC with a chiral column. This strategy is often used in industry to advance a chiral intermediate.[18–22] However, chiral chromatography can be expensive, often requiring long separation times and large amounts of solvent consumption.

1.1.2 Kinetic Resolution

Kinetic resolution differentiates a pair of enantiomers based on their rate of reactivity with a chiral catalyst or reagent (Scheme 1.4). Because the starting material is chiral and the catalyst/reagent is chiral, when they interact, they form diastereomeric

transition states. The selectivity arises from the difference in energy between the two diastereomeric transition states ($\Delta\Delta G^{\ddagger}$).[12] The larger $\Delta\Delta G^{\ddagger}$, the greater the selectivity between the two products. Similar to classic resolution, there is a maximum 50% yield in a kinetic resolution.

Obtaining good enantioselectivity and attaining a yield close to 50% requires a high selectivity factor. The selectivity factor (*s*) is equal to k_{rel} which is the ratio of k_{fast}/k_{slow} (Scheme 1.4, eq. 1). Unlike many enantioselective reactions, the ee of the product changes throughout the course of a kinetic resolution. In a kinetic resolution the relative concentration of the enantiomers changes as the reaction proceeds. A reaction rate is dependent on both the rate constant and the concentration. As the more reactive enantiomer is consumed, its concentration decreases. Therefore, the ability of the catalyst to differentiate between enantiomers decreases as conversion increases due to the concentration discrepancy between the two enantiomeric starting materials. Using this strategy, either the newly functionalized product or enantioenriched starting material may be the desired material. Depending on which is valuable, the reaction is either stopped early or extended past 50% conversion to achieve high enantiopurity. Table 1.1 shows the necessary conversions required to recover unreacted starting material in various levels of enantiopurity.[12] With an *s* value of ~10, the recovered starting material can be obtained in 98% ee and nearly 30% yield. The ability to utilize conversion as a tunable parameter for ee can be viewed as a benefit compared to asymmetric synthesis which solely depends on the $\Delta\Delta G^{\ddagger}$ of the diastereomeric transition state.[23] However, with a moderate k_{rel}, this results in a decreased yield.

Scheme 1.4 General Equations in Kinetic Resolution.

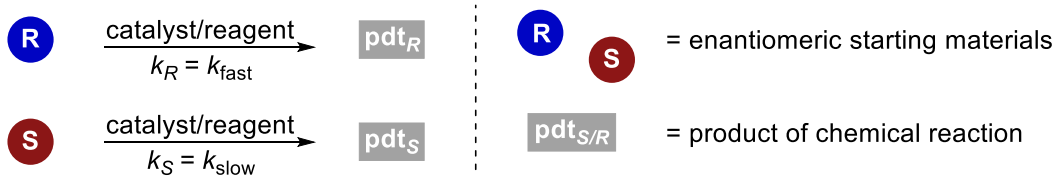

$$k_{rel} = s = k_{fast}/k_{slow} = e^{\Delta\Delta G^{\ddagger}/RT} \qquad \text{(eq. 1)}$$

Table 1.1 Conversions Necessary to Recover Starting Material with Desired ee at 23 °C.

k_{rel}	$\Delta\Delta G^{\ddagger}$ kcal/mol	Conversion (%) required to attain: 90% ee	98% ee	>99% ee
1.5	0.24	99.9	99.99	>99.999
2	0.41	97.2	99.5	>99.7
5	0.95	74.8	84.0	>86.6
10	1.35	62.1	69.7	>72.1
20	1.77	54.9	60.3	>62.2
50	2.31	50.4	54.0	>54.9
100	2.72	48.9	51.8	>52.4
500	3.66	47.7	50.0	>50.3

Several conditions must be met to make kinetic resolution a practical method: i) the racemate must be inexpensive, ii) the starting material and the product must be easily separable, and iii) the catalyst must be highly selective in preferably low loadings.[12] Initial development of kinetic resolutions focused on secondary alcohols using an enzymatic transformation, most commonly acetylation.[24–27] Because enzymes tend to have a limited substrate scope, efforts have been made to develop small molecule catalysts to accelerate similar transformations on a broader array of compounds.[28–31]

A classic example of this methodology is Jacobsen's hydrolytic kinetic resolution (HKR) of terminal epoxides (Scheme 1.5).[32] These reaction conditions provide high selectivity factors (s > 100) so both the product and the recovered starting material can be accessed with high levels of enantiopurity. For example, using racemic propylene oxide (**1.9** and ***ent*-1.9**) under HKR conditions affords highly enantioenriched diol **1.10** and unreacted epoxide ***ent*-1.9** with yields near 50%. Both enantiomers of the catalyst are readily accessible and only low catalyst loadings are required.[33] As well, the catalyst can be recovered and reused without diminished selectivity.[34] The reaction is scalable without loss of yield or enantiomeric excess. There are applications of HKR in total synthesis.[35–37] Also, Sigma Aldrich distributes chiral epoxides and 1,2-diols that are accessed via this method.[38]

Unfortunately, any kinetic resolution has a maximum of 50% yield. Jacobsen's HKR has very high selectivity factors and can attain yields close to 50%. However, most kinetic resolutions are not as selective and result in lower yields depending on the desired ee. This limitation can be overcome if there is a pathway for racemization, resulting in a more complex dynamic kinetic resolution.

Scheme 1.5 Jacobsen's Hydrolytic Kinetic Resolution (HKR)

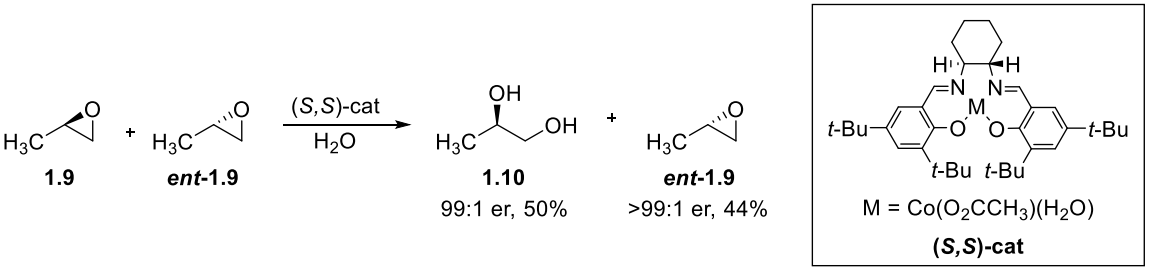

1.1.3. Dynamic Kinetic Resolution (DKR)

Similar to kinetic resolution, dynamic kinetic resolution (DKR) is predicated on differential rates of reactivity between a pair of enantiomers and a chiral catalyst/reagent. The key difference between the two modes of resolution is a DKR has a mechanism of racemization between the enantiomeric starting materials. As one enantiomer reacts to form the product, more of the reactive enantiomer is generated via the racemization pathway (Scheme 1.1c). While the ee of the product changes over time in a kinetic resolution, ideally the ee in a DKR remains constant over the course of the reaction. From the catalyst's perspective, there is always a racemic mixture of starting material as long as the rate of racemization is significantly faster than the rate of resolution. Ideally, a racemic mixture can be funneled to a single product in high yield with high levels of stereoselectivity. For this method to be viable, the rate of the racemization must be faster than the rate of reaction between the mismatched enantiomer and the catalyst. In an ideal situation, the rate of racemization is significantly faster than the rate of reaction of both starting enantiomers with the catalyst.[39] Because this form of resolution has the potential for 100% enantioselective yield from the racemate, research in this area has garnered significant attention over the past few decades.[11]

Buchwald developed a kinetic resolution using an asymmetric conjugate reduction of 2-alkyl cyclopentenones. It was discovered that upon the addition of base, a DKR was observed (Scheme 1.6).[40] The base allowed racemization of the α-stereocenter. Under the classic resolution conditions, yields below 50% were obtained with enantiomeric excesses (ee's) between 72-96%, while the DKR conditions provided yields >89% with ee's between 91-94%. One potential challenge with DKR is racemization of products under the

same conditions. To avoid this racemization, polymethylhydrosiloxane (PMHS) was used to trap the enolate intermediate as the silyl enol ether. Additionally, the PMHS allowed for catalyst turnover. In a subsequent step, tetrabutylammonium fluoride (TBAF) was used to remove the silyl group and reveal the enantioenriched cyclopentanones. In this example, developing a dynamic kinetic resolution from the kinetic resolution was straightforward. This is often not the case. This example also highlights the advantages of a DKR relative to a KR.

Scheme 1.6 Dynamic Kinetic Resolution of Cyclopentenones

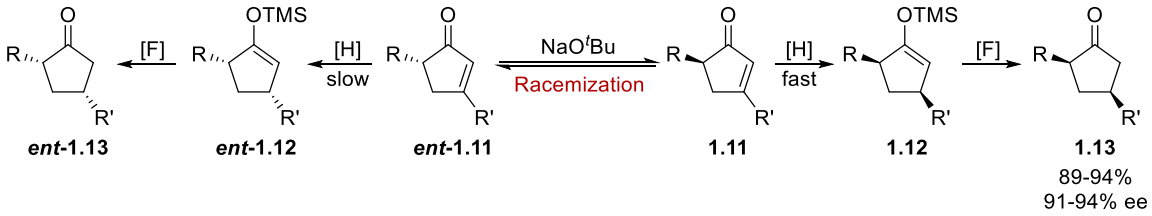

Because enzymes are often very selective, there are several examples of DKRs using enzymes as the chiral catalyst in combination with a secondary reagent for racemization. In some cases, a transition metal catalyst can be used to promote racemization. In 1992, Bäckvall et al. used a ruthenium catalyst with acetone to oxidize secondary alcohols.[41] Mechanistically, the Ru(II) catalyst dehydrogenates the alcohol and transfers the hydrogen to a hydrogen acceptor, in this case acetone.[42] During their studies of this reaction, it was observed that racemization of the alcohol stereocenter occurs due to hydrogen transfer back to the substrate. A few years later, Bäckvall et al. took advantage of this Ru(II) catalyzed racemization for DKR applications. After screening several enzymes for this DKR, their system included a ruthenium catalyst and *Candida antarctica* lipase B (CALB). Using this combination, racemic mixtures of secondary alcohols were

smoothly converted to enantioenriched acetates (Scheme 1.7).[43,44] Several other groups have reported using transition metals with enzymes to achieve a DKR.[45] In these examples, the transition metals promoted racemization while the enzymes selectively functionalized one enantiomer of the staring material.

Scheme 1.7 Transition Metal and Enzyme Catalyzed DKR

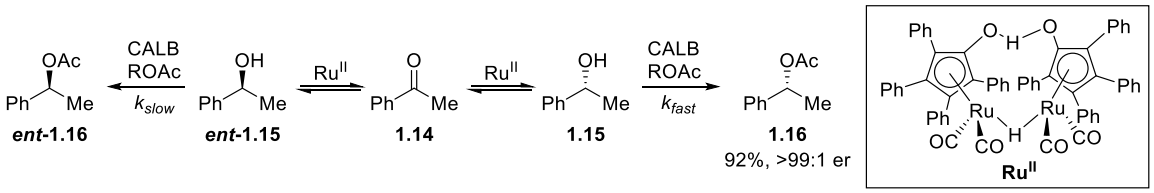

Like in the above example, often an external reagent or catalyst is required to provide a mechanism for racemization. One challenge associated with using a dual catalytic system is catalyst compatibility. While independently each catalyst may achieve the desired reaction, when combined the catalyst/catalyst interactions may inhibit or slow the reaction. As well, the catalyst used for racemization must be compatible with the product. For these reasons finding suitable conditions to conduct a DKR can be challenging.

Because there is an inherent requirement for a pathway of racemization in DKR, common substrates include alcohols (oxidation/reduction) and α-stereocenters (deprotonation/reprotonation).[11] While there are examples that fall outside of these categories, they are limited.[46,47] New substrate classes that have the potential for DKR would increase the utility of this approach for the efficient formation of enantioenriched molecules. This work explores the utility of azides as substrates for dynamic kinetic resolutions to access chiral amines.

1.2. Chiral Amines

The development of a DKR of azides would provide a synthetically useful approach toward chiral amines and amine derivatives. Chiral amines are common in natural products, ligands, polymers, and bioactive molecules (Figure 1.1). Because of their ubiquity, methods for their preparation have been widely studied and developed. In the words of Buchwald, "the synthesis of optically pure amines has long been recognized as a preeminent goal for organic synthesis."[48]

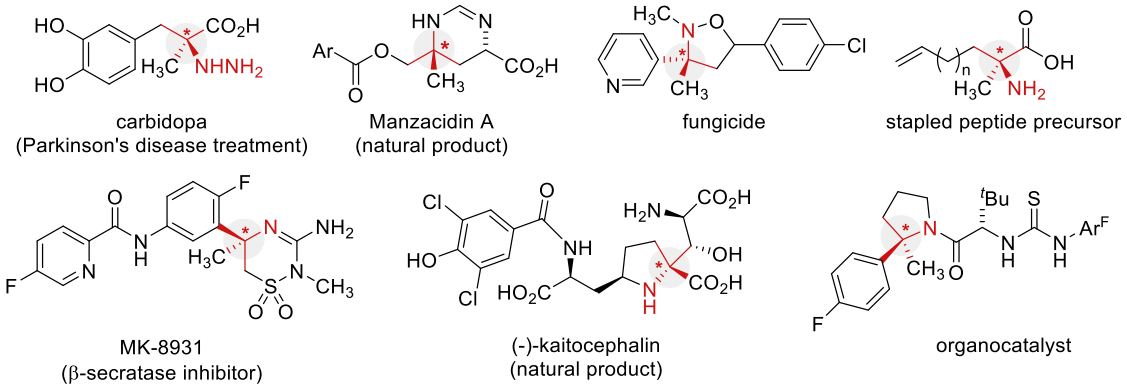

Figure 1.1 Examples of Chiral Amines and Amine Derivatives

1.2.1. Synthesis of Chiral Amines via Nucleophilic Addition to Imine

There are several successful methods for the synthesis of α-chiral amines, which include: imine addition, asymmetric reductive amination, asymmetric hydrogenation, transamination, hydroamination and C-H amination.[49–52] However, several of these methods, are fundamentally incapable of generating α,α-disubstituted amines because they require the formation or presence of a C-H bond**.**

There are few strategies capable of accessing the more congested of α,α-disubstituted amines. Even more challenging is the ability to do so enantioselectively. Both subclasses of chiral amines can be synthesized from the addition of a nucleophile into an imine (Scheme 1.8). The imine (**1.18**) is formed from condensation with either a ketone or aldehyde (**1.17**). After nucleophilic addition, the electron-withdrawing group can be cleaved to reveal the free amine (**1.20**). While imines are inherently less electrophilic than their carbonyl counterparts, methods have been developed to activate imines such that a wide variety of nucleophiles are viable.[53] Often, the imines will bear electron withdrawing substituents (e.g. sulfonyl group) to increase their electrophilicity and/or require a Lewis acid activator. Depending on the activating group, this method can be applicable for different nucleophiles including copper-[54,55] and rhodium-catalyzed[56–58] nucleophilic addition chemistry.

Scheme 1.8 Addition to Imine for Chiral Amine Synthesis

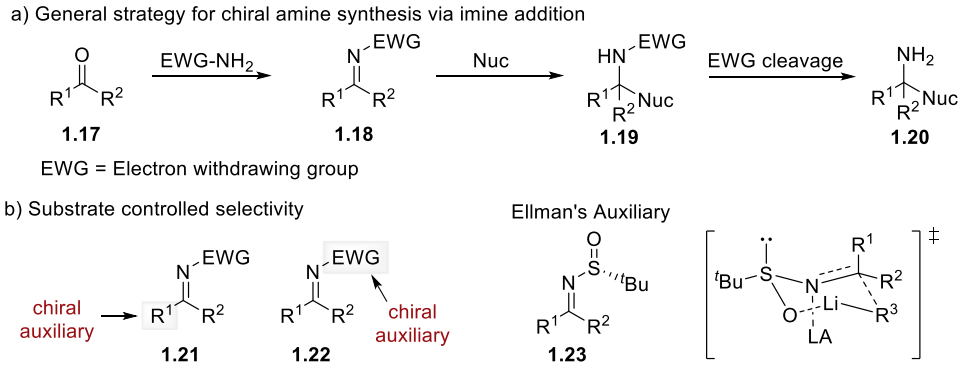

Either substrate or catalyst control can be used to attain selectivity during the nucleophilic addition (Scheme 1.8b). For substrate-controlled addition, the chiral component can be on either end of the C-N double bond. The condensation of chiral

aldehydes/ketones with amines affords a stereocenter on the imine backbone, while condensation with a chiral amine affords a stereocenter bound to the imine nitrogen. Depending on the substrate, there can be mixtures of E/Z ketimines, which can negatively affect the selectivity of the nucleophilic addition.

Ellman's auxiliary, *tert*-butylsulfinamide, is the most common auxiliary used for imine addition (Scheme 1.8b). The auxiliary can be prepared in two steps. Typically, nucleophiles add via a closed Zimmerman-Traxler transition state (Scheme 1.8b). However, certain conditions can promote addition via an open transition state.[59–61] Subsequent removal of the chiral auxiliary with strong acid affords the enantioenriched free amine. Ellman's auxiliary is state-of-the-art for the synthesis of chiral α,α-disubstituted amines, however it requires three steps with several stoichiometric reagents, the ketimines can be unstable, and there can be selectivity issues if the ketimine exists as a mixture of *E/Z* isomers.[62]

Bristol Myers Squibb reported BACE1 inhibitors containing an α,α-disubstituted amine, where Ellman's auxiliary was used to set the stereocenter (Scheme 1.9).[63] Condensation of the Ellman's auxiliary with ketone **1.24** provided imine **1.25** in modest yield. Enolate addition formed the chiral amine stereocenter in compound **1.26**. After reduction of the ketone, the chiral auxiliary was efficiently removed under acidic conditions to reveal the free amine (**1.28**). Further transformations afforded BACE1 inhibitor **1.29**. Several analogues were synthesized using this sequence.

Scheme 1.9 Ellman's Auxiliary Used to Access Chiral α,α-Disubstituted Amine

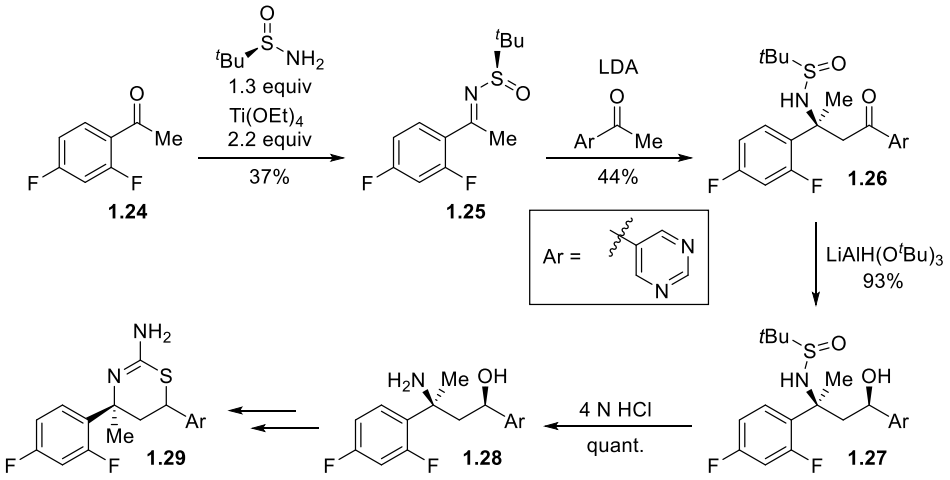

While other methods for the synthesis of these types of motifs exist, they are very substrate dependent and the scope is limited.[64–68] Ellman's auxiliary is the most common way to prepare these amines enantioselectively. Alternatively, as mentioned above, the amine can be prepared as the racemate and then separated using chiral chromatography, usually either chiral HPLC or SFC.[69–71]

Currently, a general and catalytic method to access α,α-disubstituted amines is lacking. This research project aims to develop a method that would allow for complete conversion of a racemic mixture of allylic azides to a single product with high enantioselectivity.

1.2.2. [3,3]-Sigmatropic Rearrangements to Access Chiral Amines

Due to the challenges of synthesizing chiral α,α-disubstituted amines, alternate approaches to access these chiral motifs have been investigated. One alternative strategy is utilizing rearrangements to form the highly congested stereocenter.[72–74] Many

rearrangements proceed through a cyclic transition state, thereby resulting in a high level of stereospecificity. As well, the components of the starting materials are also in the product, making this an atom economical approach.

The rearrangement of allyl thiocyanates to allyl isothiocyanates was contemporaneously discovered by Billeter and Gerlich in 1875.[75,76] Several experimental studies concluded this was likely a sigmatropic process.[77–79] Gonda and coworkers took advantage of this rearrangement utilized to construct a chiral α,α-disubstituted amine derivative (Scheme 1.10).[80] Microwave heating of thiocyanate **1.30** for two hours resulted in formation of isothiocyanate **1.31** as a single diastereomer. It was proposed that the diastereoselectivity was due to steric interactions from the 1,2-*O*-isopropylidine group. This intermediate is a precursor to (+)-myriocin and potentially other spingofungins.

Scheme 1.10 Rearrangement of Thiocyanate to Thioisocyanate.

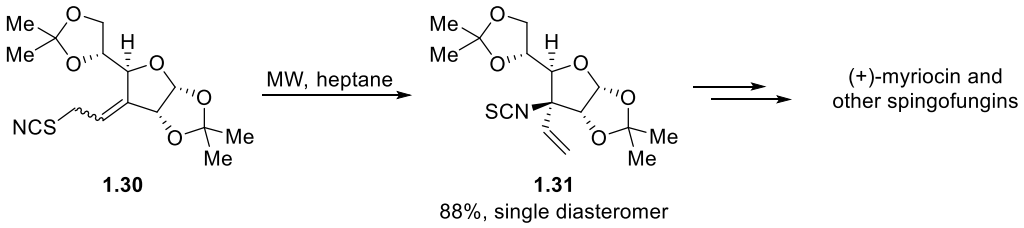

1.30 **1.31**
88%, single diasteromer

Holm and coworkers reported the first rearrangement of allyl cyanates to allyl isocyanates, however this rearrangement was not widely used due to the difficulty of accessing the starting allyl cyanates.[81,82] Several decades later, Ichikawa and coworker's developed mild conditions for the formation of allyl cyanates, allowing this rearrangement to be a more attractive synthetic approach (Scheme 1.11a).[83–85] The allyl cyanate (**1.33**) can be generated from dehydration of an easily accessible carbamate (**1.32**). Subsequent

rearrangement and trapping with methanol, or another nucleophile, affords the rearranged methyl carbamate (**1.34**).

Scheme 1.11. a) Ichikawa's Method for Rearrangement of Allyl Cyanates b) Synthesis of (*S*)-Ketamine via Sigmatropic Rearrangement

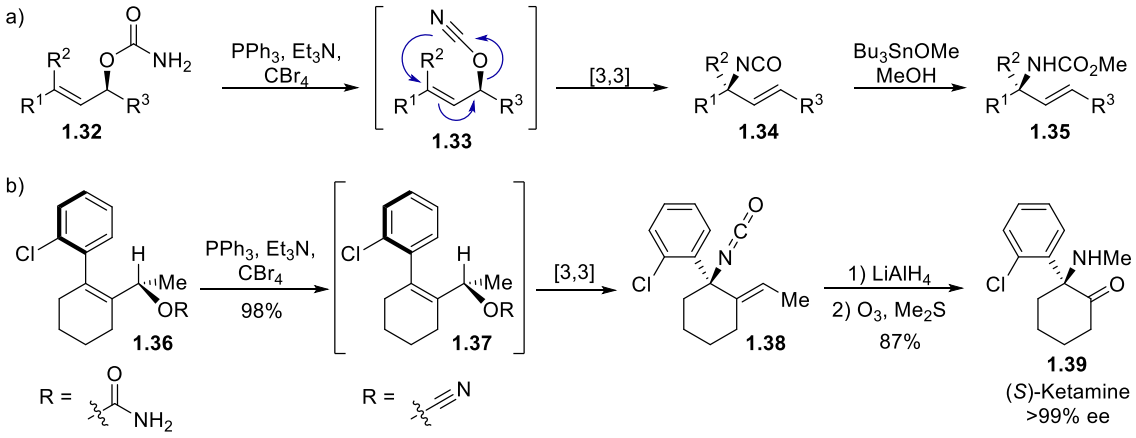

An asymmetric synthesis of (*S*)-ketamine used this rearrangement to set the α,α-disubstituted amine stereocenter (Scheme 1.11b).[86] Because the rearrangement is stereospecific, the key to high enantioselectivity of the desired product hinges on the enantiopurity of the starting carbamate which is derived from the corresponding alcohol. Enantioselective reduction of prochiral ketones to secondary alcohols has been well studied.[87–90] Therefore, this approach allows for a difficult α,α-disubstituted amine stereocenter to be generated from a relatively easy to access chiral alcohol. In this example, the prochiral ketone was reduced using Noyori conditions and subsequently converted to the rearrangement precursor **1.36**.[91,92] Dehydration of carbamate **1.36** resulted in allylic cyanate **1.37** which concomitantly rearranged to isocyanate **1.38** in 98% yield. Isocyanate **1.38** was reduced to the corresponding amine using $LiAlH_4$ and the exocyclic alkene was

subjected to ozonolysis to form (*S*)-ketamine (**1.39**) in >99% ee. This example highlights the utility of this stereospecific rearrangement to generate congested stereocenters. Other total syntheses have also taken advantage of this rearrangement as a key step in their synthetic route.[93,94]

Overman reported a thermal and a metal catalyzed rearrangement of trichloroacetimidates to trichloroacetamides, which is now referred to as the Overman rearrangement.[95,96] Like other sigmatropic rearrangements, this reaction proceeds via a chair-like transition state, therefore the chirality of the initial trichloracetimidate is conserved in the product.[96] Ramachandran and coworkers used the Overman rearrangement to synthesize allylic amines and α-amino acids (Scheme 1.12). Asymmetric allylboration of α,β-unsaturated aldehydes resulted in chiral secondary allylic alcohol **1.40**. Trichloroacetimidate **1.41** was formed by treatment of alcohol **1.40** with base and trichloroacetonitrile. The thermal Overman rearrangement proceeded smoothly with retention of configuration to afford amide **1.42**. Further transformations allowed access to α-amino acids (**1.43**). Others have utilized the thermal rearrangement in total syntheses.[97–100] The metal catalyzed rearrangement has been used to generate chiral α-amines staring from the primary acetimidates.[101] However, it has been challenging to access chiral α,α-disubstituted amines via this approach.[102–104]

Scheme 1.12. Overman Rearrangement to Access Unnatural α-Amino Acids

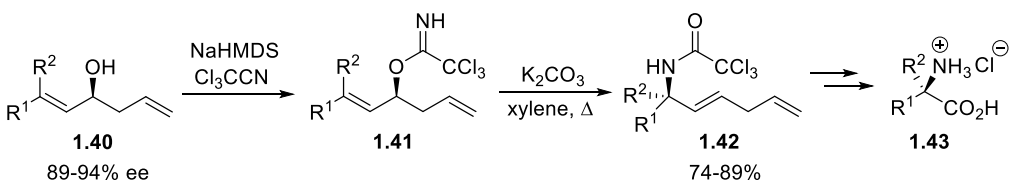

1.40 89-94% ee **1.41** **1.42** 74-89% **1.43**

1.2.3. Allylic Azide Rearrangement

While sigmatropic rearrangements are, in principle, reversible, the most synthetically useful rearrangements tend to have a thermodynamic driving force.[105] Often these rearrangements are promoted by elevated temperatures or a catalyst. Unlike these rearrangements, the allylic azide rearrangement occurs near room temperature and results in an equilibrium mixture of isomers.

Winstein and coworkers reported the allylic azide rearrangement (i.e. the Winstein rearrangement) in 1960.[106] Upon exposing prenyl chloride to sodium azide, a mixture of substitution products were observed. The two isomers could be isolated, but it was noted that at room temperature the isomers interconverted (Scheme 1.13a, azides **1.44** and **1.45**). This same phenomenon was observed with azide isomers **1.46** and **1.47** accessed from substitution with crotyl chloride. The ratio of isomers as well as the rate of isomerization was measured in a range of solvents ranging from pentane to 70% aqueous acetone (Scheme 1.13b). At equilibrium, the primary azide isomer was favored for both allylic azide substrates (75:25 eq. 2, 64:46 eq. 3). The rate of equilibration was not significantly affected by the dielectric constant of the solvent, as only a 10-20 fold increase was observed. This contrasts with the rate of isomerization or acid formation from prenyl chloride in which a rate enhancement of several orders of magnitude was observed between pentane and 70% aqueous acetone.[106] This lack of sensitivity to solvent is indicative of a cyclic, non-polarized, transition state.

Scheme 1.13 a) Allylic Azide Rearrangement of Simple Allylic Azides. b) Rate Constants for Allylic Azide Rearrangements.

a)

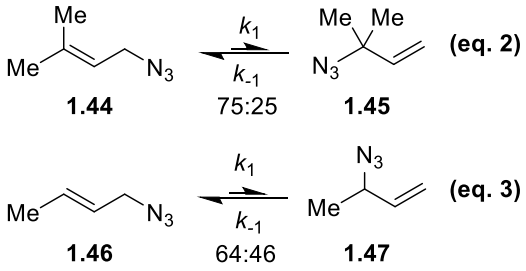

b)

solvent	eq. 2 $(k_1 + k_{-1})$ s^{-1}	eq. 3 $(k_1 + k_{-1})$ s^{-1}
n-C_5H_{12}	4.93×10^{-5}	1.88×10^{-5}
Et_2O	11.1×10^{-5}	4.28×10^{-5}
EtOH	24.1×10^{-5}	7.18×10^{-5}
70% aq. Me_2CO	90.6×10^{-5}	24.9×10^{-5}

Since Winstein's original report, there have been a few examples of selective functionalization of a single allylic azide isomer in the equilibrating mixture. Danishefsky and coworkers successfully functionalized a single azide isomer in an equilibrating mixture in their synthesis of *N*-acetylactinobolamine (Scheme 1.14).[107] The isomers were differentiated based on the electronics of the alkene. The azide isomer containing the more electron rich vinyl ether (**1.49**) reacted preferentially to afford diol **1.50** in good yield.

Scheme 1.14 Selective Dihydroxylation of Equilibrating Allylic Azide

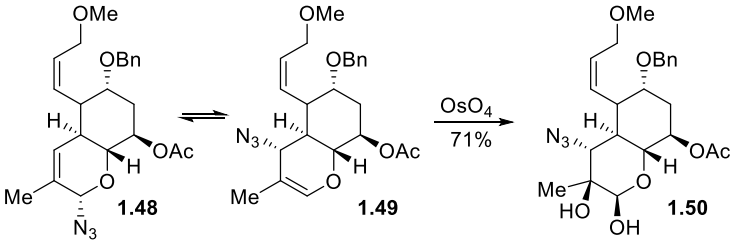

Our lab was inspired by the creative use of rearrangements to avoid the common pitfalls associated with synthesizing chiral α,α-disubstituted amines. Compared to other rearrangements, the Winstein rearrangement is likely underutilized because there is no thermodynamic driving force, resulting in a mixture of isomers. However, we plan to take advantage of this rearrangement as a mechanism of racemization to carry out a DKR for the synthesis of chiral amines (Scheme 1.15). As the more reactive enantiomer is pulled out of the equilibrium by selective functionalization, more is generated from the rearrangement. In principle, all the starting material can be converted to a single enantioenriched product (***ent*-1.53**). Reduction of the azide (***ent*-1.53**) by known methods would result in the free amine (***ent*-1.54**). This strategy requires several types of selectivity including: i) enantioselectivity, ii) isomer selectivity, iii) diastereoselelctivity, and iv) kinetic matching. This thesis describes my efforts to develop this methodology.

Scheme 1.15 General Approach to Chiral Amines from the Winstein Rearragement

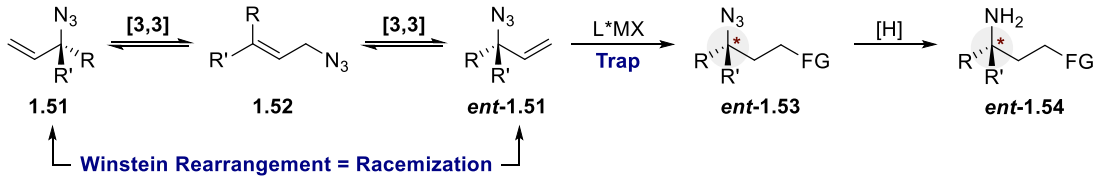

Initial efforts focused on a DKR of allylic azides via Sharpless asymmetric dihydroxylation (Chapter 2). Efforts to broaden the scope beyond symmetric allylic azides resulted in fundamental mechanistic investigations into the Winstein rearragement (Chapter 3). From these fundamental studies, we began to investigate catalysts that could

promote the racemization of allylic azides, as well as benzylic azides (Chapter 4). A KR of secondary benzylic azides was developed and the catalyst-promoted racemization was used to recycle the excess scalemic starting material (Chapter 5). Lastly, efforts to utilize the catalyzed racemization in a DKR are discussed (Chapter 6).

1.3 References

(1) Lovering, F.; Bikker, J.; Humblet, C. Escape from Flatland: Increasing Saturation as an Approach to Improving Clinical Success. *J. Med. Chem.* **2009**, *52*, 6752–6756.

(2) Lovering, F. Escape Form Flatland 2: Complexity and Promiscuity. *Medchemcomm* **2013**, *4*, 515–519.

(3) Brill, Z. G.; Condakes, M. L.; Ting, C. P.; Maimone, T. J. Navigating the Chiral Pool in the Total Synthesis of Complex Terpene Natural Products. *Chem. Rev.* **2017**, *117*, 11753–11795.

(4) Crosby, J. Synthesis of Optically Active Compounds: A Large Scale Perspective. *Tetrahedron* **1991**, *47*, 4789–4846.

(5) Paek, S. M.; Jeong, M.; Jo, J.; Heo, Y. M.; Han, Y. T.; Yun, H. Recent Advances in Substrate-Controlled Asymmetric Induction Derived from Chiral Pool α-Amino Acids for Natural Product Synthesis. *Molecules* **2016**, *21*, 951–963.

(6) Nugent, W. A.; RajanBabu, T. V.; Burk, M. J. Beyond Nature's Chiral Pool: Enantioselective Catalysis in Industry. *Science* **1993**, *259*, 479–483.

(7) Noyori, R. *Asymmetric Catalysis in Organic Synthesis*; John Wiley & Sons, Ltd: New York, 1994.

(8) Noyori, R. Asymmetric Catalysis: Science and Opportunities. *Adv. Synth. Catal.* **2003**, *345*, 15–30.

(9) Ault, A. The Nobel Prize in Chemistry for 2001. *J. Chem. Educ.* **2002**, *79*, 572–577.

(10) Jacques, J.; Collet, A.; Willen, S. H. *Enantiomers, Racemates, and Resolutions*; John Wiley & Sons, Ltd, 1981.

(11) Pellissier, H. H. Recent Developments in Dynamic Kinetic Resolution. *Tetrahedron* **2011**, *67*, 3769–3802.

(12) Keith, J. M.; Larrow, J. F.; Jacobsen, E. N. Practical Considerations in Kinetic Resolution Reactions. *Adv. Synth. Catal.* **2001**, *343*, 5–26.

(13) Porter, W. H. Resolution of Chiral Drugs. *Pure Appl. Chem.* **1991**, *63*, 1119–1122.

(14) Carey, J. S.; Laffan, D.; Thomson, C.; Williams, M. T. Analysis of the Reactions Used for the Preparation of Drug Candidate Molecules. *Org. Biomol. Chem.* **2006**, *4*, 2337–2347.

(15) Larrow, J. F.; Jacobsen, E. N. (R,R)-*N*,*N*'-Bis(3,5-Di-*Tert*-Butylsalicylidene)-1,2-Cyclohexanediamino Manganese(III) Chloride, A Highly Enantioselective Epoxidation Catalyst. *Org. Synth.* **1998**, *75*, 1–6.

(16) Reider, P. J. Advances in AIDS Chemotherapy: The Asymmetric Synthesis of Crixivan®. *Chimia* **1997**, *51*, 306–308.

(17) Ahuja, S. *Chiral Separations by Chromatography*; Oxford University Press: New York, 2000.

(18) Ahuja, S.; Zeid, R. L.; Amoss, C. A.; Maier, N. M.; Ning, J. G.; Ye, Y. K.; Webster, G. K.; DePianta, R.; Douville, K.; Nickerson, B.; et al. *Chiral Separation Methods for Pharmaceutical and Biotechnological Products*; John Wiley & Sons, Ltd: Hoboken, 2011.

(19) Zhang, Y.; Wu, D.-R.; Wang-Iverson, D. B.; Tymiak, A. A. Enantioselective Chromatography in Drug Discovery. *Drug Discov. Today* **2005**, *10*, 571–577.

(20) Rossi, D.; Marra, A.; Rui, M.; Brambilla, S.; Juza, M.; Collina, S. "Fit-for-Purpose" Development of Analytical and (Semi)Preparative Enantioselective High Performance Liquid and Supercritical Fluid Chromatography for the Access to a Novel Sigma-1 Recepotr Agonist. *J. Pharm. Biomed. Anal.* **2016**, *118*, 363–369.
(21) Nelson, T. D.; Welch, C. J.; Rosen, J. D.; Smitrovich, J. H.; Huffman, M. A.; Namara, J. M. M. C.; Mathre, D. J. Effective Use of Preparative Chiral HPLC in a Preclinical Drug Synthesis. *Chirality* **2004**, *16*, 609–613.
(22) Leek, H.; Andersson, S. Preparative Scale Resolution of Enantiomers Enables. *Molecules* **2017**, *22*, 158–166.
(23) Martin, V. S.; Woodard, S. S.; Katsuki, T.; Yamada, Y.; Ikeda, M. M.; Sharpless, K. B. Kinetic Resolution of Racemic Allylic Alcohols by Enantioselective Epoxidation. A Route to Substances of Absolute Enantiomeric Purity? *J. Am. Chem. Soc.* **1981**, *103*, 6237–6240.
(24) Adam, W.; Lazarus, M.; Boss, B.; Saha-mo, C. R. Enzymatic Resolution of Chiral 2-Hydroxy Carboxylic Acids by Enantioselective Oxidation with Molecular Oxygen Catalyzed by the Glycolate Oxidase from Spinach (Spinacia Oleracea). *J. Org. Chem.* **1997**, *3263*, 7841–7843.
(25) Dieth, S.; Tritsch, D.; Biellman, J.-F. Resolution of Allylic Alcohols by Cholesterol Oxidase Iosolated from Rhodococcus Erythropolis. *Tetrahedron Lett.* **1995**, *36*, 2243–2246.
(26) Patel, R. N.; Banerjee, A.; Nanduri, V.; Goswami, A.; Comezoglu, F. T. Enzymatic Resolution of Racemic Secondary Alcohols by Lipase B from *Candida Antarctica*. *J. Am. Oil Chem. Soc.* **2000**, *77*, 1015–1019.
(27) Sonnet, P. E.; Baillargeon, M. W. Kinetic Resolution of Secondary Alcohols with Commerical Lipases: Application to Rootworm Sex Pheromone Synthesis. *J. Chemcial Ecol.* **1987**, *13*, 1279–1292.
(28) Ruble, J. C.; Latham, H. A.; Fu, G. C. Effective Kinetic Resolution of Secondary Alcohols with a Planar-Chiral Analogue of 4-(Dimethylamino) Pyridine. Use of the Fe(C_5Ph_5) Group in Asymmetric Catalysis. *J. Am. Chem. Soc.* **1997**, *119*, 1492–1493.
(29) Spivey, A. C.; Fekner, T.; Spey, S. E. Axially Chiral Analogues of 4-(Dimethylamino) Pyridine: Novel Catalysts for Nonenzymatic Enantioselective Acylations. *J. Org. Chem.* **2000**, *65*, 3154–3159.
(30) Kawabata, T.; Nagato, M.; Takasu, K.; Fuji, K. Nonenzymatic Kinetic Resolution of Racemic Alcohols through an "Induced Fit" Process. *J. Am. Chem. Soc.* **1997**, *119*, 3169–3170.
(31) Vedejs, E.; Daugulis, O. 2-Aryl-4,4,8-Trimethyl-2-Phophabicyclo[3.3.0]Octanes:Reactive Chiral Phosphine Catalysts for Enantioselective Acylation. *J. Am. Chem. Soc.* **1999**, *121*, 5813–5814.
(32) Tokunaga, M.; Larrow, J. F.; Kakiuchi, F.; Jacobsen, E. N. Asymmetric Catalysis with Water: Efficient Kinetic Resolution of Terminal Epoxides by Means of Catalytic Hydrolysis. *Science* **1997**, *277*, 936–938.
(33) Jacobsen, E. N. Asymmetric Catalysis of Epoxide Ring-Opening Reactions. *Acc. Chem. Res.* **2000**, *33*, 421–431.
(34) Kim, G.-J.; Lee, H.; Kim, S.-J. Catalytic Activity and Recyclability of New Enantioselective Chiral Co-Salen Complexes in the Hydrolytic Kinetic Resolution

of Epichlorohydrine. *Tetrahdron Lett.* **2003**, *44*, 5005–5008.
(35) Dorling, E. K.; Elisabeth, Ö.; Mantoulidis, A.; Mulzer, J. Concise Synthesis of the C3-C14-Fragment of the Antitumor Agent Laulimalide. Application of Jacobsen's HKR Reaction. *Synlett* **2001**, 1105–1108.
(36) Chavez, D. E.; Jacobsen, E. N. Total Synthesis of Fostriecin (CI-920). *Angew. Chem. Int. Ed.* **2001**, *40*, 3667–3670.
(37) Jiang, S.; Liu, Z.; Sheng, G.; Zeng, B.; Cheng, X.; Wu, Y.-L.; Yao, Z.-J. Mimicry of Annonaceous Acetogenins: Enantioselective Synthesis of a (4*R*)-Hydroxy Analogue Having Potent Antitumor Activity. *J. Org. Chem.* **2002**, *67*, 3404–3408.
(38) HKR Epoxides. *Aldrich ChemFiles* **2005**, *5.4*, 17.
(39) Seeman, J. I.; Farone, W. A. Analytical Solution to the Curtin-Hammett/Winstein-Holness Kinetic System. *J. Org. Chem.* **1978**, *43*, 1854–1864.
(40) Jurkauskas, V.; Buchwald, S. L. Dynamic Kinetic Resolution via Asymmetric Conjugate Reduction: Enantio- and Diastereoselective Synthesis of 2,4-Dialkyl Cyclopentanones. *J. Am. Chem. Soc.* **2002**, *124*, 2892–2893.
(41) Wang, G.-Z.; Backvall, J.-E. Ruthenium-Catalysed Oxidation of Alcohols by Acetone. *J. Chem. Soc. Chem. Commun.* **1992**, 337–339.
(42) Almeida, M. L. S.; Beller, M.; Wang, G.; Backvall, J. Ruthenium(II)-Catalyszed Oppenauer-Type Oxidation of Secondary Alcohols. *Chem. Eur. J.* **1996**, *2*, 1533–1536.
(43) Larsson, A. L. E.; Persson, B. A.; Backvall, J.-E. Enzymatic Resolution of Alcohols Coupled with Ruthenium-Catalyzed Racemization of the Substrate Alcohol. *Angew. Chem. Int. Ed.* **1997**, *36*, 1211–1212.
(44) Leijondahl, K.; Borén, L.; Braun, R.; Bäckvall, J. E. Enzyme- and Ruthenium-Catalyzed Dynamic Kinetic Asymmetric Transformation of 1,5-Diols. Application to the Synthesis of (+)-Solenopsin A. *J. Org. Chem.* **2009**, *74*, 1988–1993.
(45) Steinreiber, J.; Griengl, H. De-Racemization of Enantiomers versus De-Epimerization of Diastereomers — Classification of Dynamic Kinetic Asymmetric. *Chem. - Eur. J.* **2008**, *14*, 8060–8072.
(46) Dornan, P. K.; Kou, K. G. M.; Houk, K. N.; Dong, V. M. Dynamic Kinetic Resolution of Allylic Sulfoxides by Rh-Catalyzed Hydrogenation: A Combined Theoretical and Experimental Mechanistic Study. *J. Am. Chem. Soc.* **2014**, *136*, 291–298.
(47) Arnold, S.; Nguyen, H. M. Rhodium-Catalyzed Dynamic Kinetic Asymmetric Transformations of Racemic Tertiary Allylic Trichloroacetimidates with Anilines. *J. Am. Chem. Soc.* **2012**, *134*, 8380–8383.
(48) Yang, Y.; Shi, S.-L.; Niu, D.; Liu, P.; Buchwald, S. L. Catalytic Asymmetric Hydroamination of Unactivated Internal Olefins to Aliphatic Amines. *Science* **2015**, *349*, 62–66.
(49) Nugent, T. C. *Chiral Amine Synthesis: Methods, Developments and Applications*; Wiley, 2010.
(50) Fleury-Brégeot, N.; de la Fuente, V.; Castillón, S.; Claver, C. Highlights of Transition Metal-Catalyzed Asymmetric Hydrogenation of Imines. *ChemCatChem* **2010**, *2*, 1346–1371.
(51) Hannedouche, J.; Schulz, E. Asymmetric Hydroamination: A Survey of the Most Recent Developments. *Chem. - Eur. J.* **2013**, *19*, 4972–4985.

(52) Trowbridge, A.; Walton, S. M.; Gaunt, M. J. New Strategies for the Transition-Metal Catalyzed Synthesis of Aliphatic Amines. *Chem. Rev* **2020**, *120*, 2613–2692.
(53) Kobayashi, S.; Ishitani, H. Catalytic Enantioselective Addition to Imines. *Chem. Rev.* **1999**, *99*, 1069–1094.
(54) Ukaji, Y.; Watai, T.; Sumi, T.; Fujisawa, T. Reversal of Diastereofacial Selectivity in the Addition Reaction of Organometallics to Chiral Imines. *Chem. Lett.* **1991**, 1555–1558.
(55) Fujihara, H.; Nagai, K.; Tomioka, K. Copper - Amidophosphine Catalyst in Asymmetric Addition of Organozinc to Imines. *J. Am. Chem. Soc.* **2000**, *122*, 12055–12056.
(56) Nishimura, T.; Yasuhara, Y.; Hayashi, T. Asymmetric Addition of Dimethylzinc to N-Tosylarylimines Catalyzed by a Rhodium− Diene Complex toward the Synthesis of Chiral 1-Arylethylamines. *Org. Lett.* **2006**, *8*, 979–981.
(57) Shintani, R.; Takeda, M.; Tsuji, T.; Hayashi, T. Rhodium-Catalyzed Asymmetric Arylation of N -Tosyl Ketimines Ketimines Provides Straightforward Access to Enantioenriched Chiral. **2010**, 13168–13169.
(58) Weix, D. J.; Shi, Y.; Ellman, J. A. Diastereoselective and Enantioselective Rh (I)-Catalyzed Additions of Arylboronic Acids to *N*-*Tert*-Butanesulfinyl and *N*-Diphenylphosphinoyl Aldimines. *J. Am.* **2005**, *127*, 1092–1093.
(59) Kuduk, S. D.; DiPardo, R. M.; Chang, R. K.; Ng, C.; Bock, M. G. Reversal of Diastereoselection in the Addition of Grignard Reagents to Chiral 2-Pyridyl *Tert*-Butyl (Ellman) Sulfinimines. *Tetrahedron Lett.* **2004**, *45*, 6641–6643.
(60) Han, Z.; Krishnamurthy, D.; Pflum, D.; Grover, P.; Wald, S. A.; Senanayake, C. H. First Application of Tunable Alkyl or Aryl Sulfinamides to the Stereoselective Synthesis of a Chiral Amine: Asymmetric Synthesis of (*R*)-Didesmethylsibutramine ((*R*)-DDMS) Using (*R*)-Triethylmethylsulfinamide ((*R*)-TESA). *Org. Lett.* **2002**, 4025–4028.
(61) Brinner, K. M.; Ellman, J. A. A Rapid and General Method for the Asymmetric Synthesis of 2-Substituted Pyrrolidines Using *Tert*-Butanesulfinamide. *Org. Biomol. Chem.* **2005**, *3*, 2109–2113.
(62) Robak, M. T.; Herbage, M. A.; Ellman, J. A. Synthesis and Applications of Tert-Butanesulfinamide. *Chem. Rev.* **2010**, *110*, 3600–3740.
(63) Wu, Y.; Guernon, J.; Shi, J.; Marcin, L.; Higgins, M.; Rajamani, R.; Muckelbauer, J.; Lewis, H.; Chang, C.; Camac, D.; et al. Discovery of S3-Truncated, C-6 Heteroaryl Substituted Aminothiazine B-Site APP Cleaving Enzyme-1 (BACE1) Inhibitors. *J. Med. Chem.* **2016**, *59*, 8593–8600.
(64) Shibasaki, M.; Kanai, M. Asymmetric Synthesis of Tertiary Alcohols and α-Tertiary Amines via Cu-Catalyzed C-C Bond Formation to Ketones and Ketimines. *Chem. Rev.* **2008**, *108*, 2853–2873.
(65) Jiang, C.; Lu, Y.; Hayashi, T. High Performance of a Palladium Phosphinooxazoline Catalyst in the Asymmetric Arylation of Cyclic N-Sulfonyl Ketimines. *Angew. Chem. Int. Ed.* **2014**, *53*, 9936–9939.
(66) Jiang, T.; Wang, Z.; Xu, M. H. Rhodium-Catalyzed Asymmetric Arylation of Cyclic N-Sulfonyl Aryl Alkyl Ketimines: Efficient Access to Highly Enantioenriched α-Tertiary Amines. *Org. Lett.* **2015**, *17*, 528–531.

(67) Wieland, L. C.; Vieira, E. M.; Snapper, M. L.; Hoveyda, A. H.; Hill, C. Mannich Reactions of Alpha-Ketoimine Esters . Development of a Method and Investigation of Its Mechanism. *J. Am. Chem. Soc.* **2009**, *131*, 570–576.
(68) Kalek, M.; Fu, G. C. Phosphine-Catalyzed Doubly Stereoconvergent Γ-Additions of Racemic Heterocycles to Racemic Allenoates: The Catalytic Enantioselective Synthesis of Protected α,α-Disubstituted A-Amino Acid Derivatives. *J. Am. Chem. Soc.* **2015**, *137*, 9438–9442.
(69) Mandal, M.; Wu, Y.; Misiaszek, J.; Li, G.; Buevich, A.; Caldwell, J. P.; Liu, X.; Mazzola, R. D.; Orth, P.; Strickland, C.; et al. Structure-Based Design of an Iminoheterocyclic β-Site Amyloid Precursor Protein Cleaving Enzyme (BACE) Inhibitor That Lowers Central Aβ in Nonhuman Primates. *J. Med. Chem.* **2016**, *59*, 3231–3248.
(70) Yan, T. Q.; Orihuela, C.; Swanson, D. The Application of Preparative Batch HPLC, Supercritical Fluid Chromatography, Steady-State Recycling, and Simulated Moving Bed for the Resolution of a Racemic Pharmaceutical Intermediate. *Chirality* **2008**, *20*, 139–146.
(71) Jr, W. R. L.; Henderson, D. W.; Miller, R. A.; Spencer, G. A.; Sudah, O. S.; Biba, M.; Welch, C. J. Strategic Use of Preparative Chiral Chromatography for the Synthesis of a Preclinical Pharmaceutical Candidate. *Chirality* **2007**, *19*, 693–700.
(72) Overman, L. E. Molecular Rearrangements in the Construction of Complex Molecules. *Tetrahedron*. 2009, 6432–6446.
(73) Clayden, J.; Donnard, M.; Lefranc, J.; Tetlow, D. J. Quaternary Centres Bearing Nitrogen (Alpha-Tertiary Amines) as Products of Molecular Rearrangements. *Chem. Commun.* **2011**, *47*, 4624–4639.
(74) Nocquet, P. A.; Henrion, S.; Macé, A.; Carboni, B.; Villalgordo, J. M.; Carreaux, F. The Allyl Cyanate/Isocyanate Rearrangement: An Efficient Tool for the Stereocontrolled Formation of Allylic C–N Bonds. *Eur. J. Org. Chem.* **2017**, 1295–1307.
(75) Billeter, O. Ueber Organische Sulfocyanverbindungen. *Ber. Dtsch. Chem. Ges* **1875**, *8*, 462–466.
(76) Gerlich, G. Ueber Psendoyropyl- Und Allylrhodaniir. *Justus Liebigs Ann. Chem* **1875**, *198*, 80–91.
(77) Billeter, O. Notice Sur La Transposisition Des Thiocyanates En Senevols. *Helv. Chim. Acta* **1925**, *11*, 337–338.
(78) Mumm, O.; Richter, H. Versuche Zur Theorie Der Allyl-Umlagerung. *Berichte der Dtsch. Chem. Gesellschaft* **1940**, *73*, 843–860.
(79) Smith, A. S.; Emerson, D. W. The Isomerization of Alkyl Thiocyanates to Isothiocyanates. *J. Am. Chem. Soc.* **1992**, *82*, 3076–3082.
(80) Gonda, J.; Martinkova, M.; Raschmanova, J.; Balentova, E. Creation of Quarternary Stereocentres via [3,3]- Sigmatropic Rearrangement of Allylic Thiocyanates. A Synthetic Appraoch to (+)-Myriocin. *Tetrahedron Asymmetry* **2006**, *17*, 1875–1882.
(81) Christophersen, C.; Holm, A. Formation of 1-Methylallyl and 2-Butenyl Isocyanate from Crotyl Bromide and Silver Cyanate. *Acta Chem. Scand.* **1970**, *24*, 1852–1854.
(82) Christophersen, C.; Holm, A. Alkyl Cyanates. XIV. Isomerization of Allylic

Cyanates and Allylic Thionoderivatives. *Acta Chemica Scandinavica*. 1970, pp 1512–1526.
(83) Ichikawa, Y. New Synthetic Method for Allylic Isocyanates Through [3,3] Sigmatropic Rearrangement of Allylic Cyanates. *Synlett* **1991**, 238–240.
(84) Ichikawa, Y. Evolution, Development and Personal Experience in Studies of the Allyl Cyanate-to-Isocyanate Rearrangement. *Synlett* **2007**, 2927–2936.
(85) Ichikawa, Y.; Okumura, K.; Matsuda, Y.; Hasegawa, T.; Nakamura, M.; Fujimoto, A.; Masuda, T.; Nakano, K.; Kotsuki, H. Synthesis of Manzacidin A and C: Efficient Construction of Quaternary Carbon Stereocenters Bearing Nitrogen Substituents. *Org. Biomol. Chem.* **2012**, *10*, 614–622.
(86) Yokoyama, R.; Matsumoto, S.; Nomura, S.; Higaki, T.; Yokoyama, T.; Kiyooka, S. Enantioselective Construction of Nitrogen-Substituted Quaternary Carbon Centers Adjacent to the Carbonyl Group in the Cyclohexane Ring: First Asymmetric Synthesis of Anesthetic (*S*) -Ketamine with High Selectivity. *Tetrahedron* **2009**, *65*, 5181–5191.
(87) Noyori, R.; Ohkuma, T. Asymmetric Catalysis by Architectural and Functional Molecular Engineering: Practical Chemo- and Stereoselective Hydrogenation of Ketones. *Angew. Chem. Int. Ed.* **2001**, *40*, 40–73.
(88) Yoshimura, M.; Tanaka, S.; Kitamura, M. Recent Topics in Catalytic Asymmetric Hydrogenation of Ketones. *Tetrahedron Lett.* **2014**, *55*, 3635–3640.
(89) Echeverria, P. G.; Ayad, T.; Phansavath, P.; Ratovelomanana-Vidal, V. Recent Developments in Asymmetric Hydrogenation and Transfer Hydrogenation of Ketones and Imines through Dynamic Kinetic Resolution. *Synth.* **2016**, *48*, 2523–2539.
(90) Shende, V. S.; Singh, P.; Bhanage, B. M. Recent Trends in Organocatalyzed Asymmetric Reduction of Prochiral Ketones. *Catal. Sci. Technol.* **2018**, *8*, 955–969.
(91) Noyori, R.; Tomino, I.; Yamada, M.; Nishizawa, M. Synthetic Applications of the Enantioselective Reduction by Binaphthol-Modified Lithium Aluminum Hydride Reagents. *J. Am. Chem. Soc.* **1984**, *106*, 6717–6725.
(92) Noyori, R.; Tomino, I.; Tanimoto, Y.; Nishizawa, M. Rational Designing of Efficient Chiral Reducing Agents. Highly Enantioselective Reduction of Aromatic Ketones by Binaphthol-Modified Lithium Aluminum Hydride Reagents. *J. Am. Chem. Soc.* **1984**, *106*, 6709–6716.
(93) Arbour, M.; Roy, S.; Godbout, C.; Spino, C. Stereoselective Synthesis of (+)-Euphococcinine and (-)-Adaline. *J. Org. Chem.* **2009**, *74*, 3806–3814.
(94) Roulland, E.; Monneret, C.; Florent, J.; Bennejean, C.; Renard, P. Enantioselective Synthesis of 12-Amino Alkylidenecyclopentenone Prostaglandins Biological Activities of Cyclopentenone Prostaglandins. *J. Org. Chem.* **2002**, No. 67, 4399–4406.
(95) Overman, L. E. Thermal and Mercuric Ion Catalyzed [3,3]-Sigmatropic Rearrangement of Allylic Trichloroacetimidates. The 1,3 Transposition of Alcohol and Amine Functions. *J. Am. Chem. Soc.* **1974**, *96*, 597–599.
(96) Overman, L. E. A General Method for the Synthesis of Amines by the Rearrangement of Allylic Trichloroacetimidates. 1,3 Transposition of Alcohol and Amine Functions. *J. Am. Chem. Soc.* **1976**, *1*, 2901–2910.

(97) Chida, N.; Takeoka, J.; Tsutsumi, N.; Ogawa, S. Total Syntheis of (+)-Lactacystin from D-Glucose. *J. Chem. Soc. Chem. Commun.* **1995**, *20*, 793–794.
(98) Kang, S. H.; Kang, S. Y.; Lee, H. S.; Buglass, A. J. Total Synthesis of Natural Tert-Alkylamino Hydroxy Carboxylic Acids. *Chem. Rev.* **2005**, *105*, 4537–4558.
(99) Nishikawa, T.; Asai, M.; Ohyabu, N.; Yamamoto, N.; Fukuda, Y.; Isobe, M. Synthesis of a Common Key Intermediate for (-)-Tetrodotoxin and Its Analogs. *Tetrahedron* **2001**, *57*, 3875–3883.
(100) Nishikawa, T.; Urabe, D.; Isobe, M. An Efficient Total Synthesis of Optically Active Tetrodotoxin. *Angew. Chem. Int. Ed.* **2004**, *43*, 4782–4785.
(101) Overman, L. E.; Owen, C. E.; Pavan, M. M.; Richards, C. J. Catalytic Asymmetric Rearrangement of Allylic N-Aryl Trifluoroacetimidates. A Useful Method for Transforming Prochiral Allylic Alcohols to Chiral Allylic Amines. *Org. Lett.* **2003**, *5*, 1809–1812.
(102) Xin, Z. Q.; Fischer, D. F.; Peters, R. Catalytic Asymmetric Formation of Secondary Allylic Amines by Aza-Claisen Rearrangement of Trifluoroacetimidates. *Synlett* **2008**, 1495–1499.
(103) Fischer, D. F.; Barakat, A.; Xin, Z. Q.; Weiss, M. E.; Peters, R. The Asymmetric Aza-Claisen Rearrangement: Development of Widely Applicable Pentaphenylferrocenyl Palladacycle Catalysts. *Chem. - Eur. J.* **2009**, *15*, 8722–8741.
(104) Fischer, D. F.; Xin, Z.; Peters, R. Asymmetric Formation of Allylic Amines with N-Substituted Quaternary Stereocenters by PdII-Catalyzed Aza-Claisen Rearrangements. *Angew. Chem. Int. Ed.* **2007**, *46*, 7704–7707.
(105) *Molecular Rearrangements in Organic Synthesis*; Rojas, C. M., Ed.; John Wiley and Sons, 2015.
(106) Gagneux, A.; Winstein, S.; Young, W. G. Rearrangement of Allyl Azides. *J. Am. Chem. Soc.* **1960**, *82*, 5956–5957.
(107) Askin, D.; Angst, C.; Danishefsky, S. A Total Syntheis of *N*-Acetylactinobolamine. *J. Org. Chem.* **1985**, *50*, 5005–5007.

2. Dynamic Kinetic Resolution of Allylic Azides via Asymmetric Dihydroxylation*

2.1 Introduction

The seminal report describing the rearrangement of allylic azides was authored by Winstein in 1960.[1] The rearrangement, which is thought to occur via a sigmatropic process, typically occurs at or near room temperature (Scheme 2.1a). While the Winstein rearrangement has been observed in many contexts,[2–8] selectivity challenges inherent in the azide mixture have limited its synthetic applications. In 2005, Sharpless and co-workers reported that site-selectivity could be achieved in some instances by exploiting different alkene substitution patterns (Scheme 2.1b).[9]

Scheme 2.1 Winstein Rearrangement and Dynamic Kinetic Resolutions

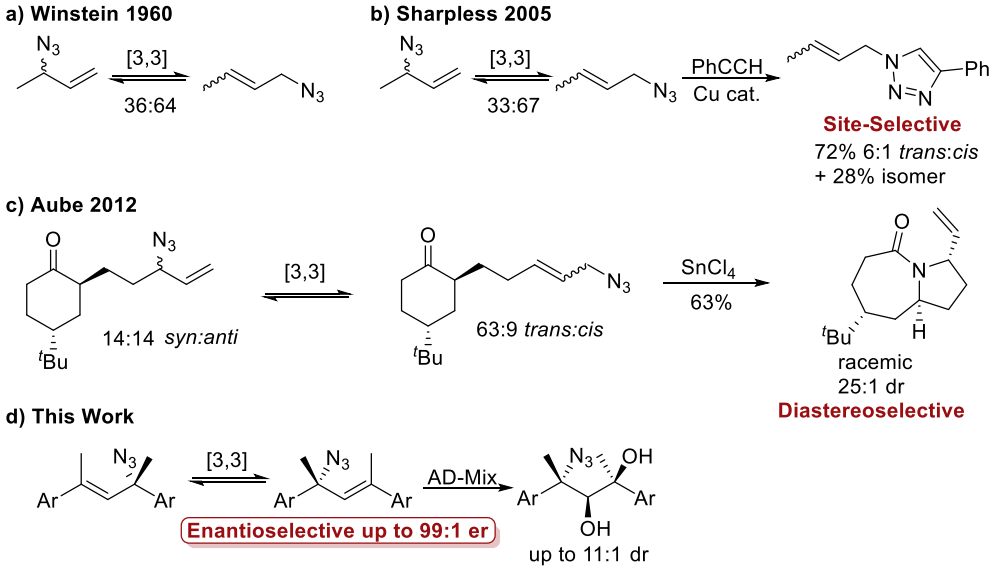

* Reprinted (adapted) with permission from Ott, A. A.; Goshey, C. S.; Topczewski, J. J. *J. Am. Chem. Soc.* **2017**, *139*, 7737 – 7740. Copyright (2017) American Chemical Society.

Subsequently, it was shown by Aubé and co-workers that the equilibrating mixture of azides could be differentially functionalized in an intramolecular Schmidt reaction that differentiated the azides based on the relative rates of ring closure (Scheme 2.1c).[10] Based on this precedent, we hypothesized that the Winstein rearrangement could be used as the racemization pathway in a dynamic kinetic resolution. Herein, we report the successful achievement of this goal.

Dynamic kinetic resolution (DKR) is a premier approach for asymmetric synthesis.[11–17,18–26] The principle attribute of DKR is the obtention of enantioenriched material from a racemic mixture. A wide array of catalysts can participate in a DKR including enzymes,[27] transition metal complexes,[28–31] Brønsted acids/bases,[32–34] and organocatalysts.[35–37] While DKR is a powerful approach to establish absolute configuration, it commonly suffers from several limitations including the (i) requirement for a mechanistic pathway for racemization, (ii) common need for two separate catalysts, which must be mutually compatible, and (iii) delicate balance of relative rates in the synchronized catalytic cycles. In practice, this has largely limited DKR to easily epimerizable α-carbonyl stereocenters, redox active sites (i.e. secondary alcohols), or hydrolysis reactions. [11–17] Employing sigmatropic reactions as the racemization pathway in a DKR is appealing because these reactions do not require an exogenous catalyst. However, this has only rarely been described, presumably due to the relatively high activation energies of these processes.[38] Thus, it appeared that the relatively low activation barrier of the Winstein rearrangement would make it a particularly powerful racemization pathway in DKR if a suitable alkene functionalization reaction was identified. A Winstein rearrangement-facilitated DKR would have the further attribute of directly affording

sterically congested amine equivalents present as stereodefined tertiary azides. Sterically congested chiral amines of this nature comprise a motif of considerable significance in the preparation of biologically relevant compounds including recent families of BACE-1 inhibitors.[39,40] Herein, we disclose our initial efforts in this regard by coupling the Winstein rearrangement with one of the most venerable alkene functionalization reactions, namely the Sharpless asymmetric dihydroxylation (SAD, Scheme 2.1d).[41]

2.2 Substrate Synthesis

The synthesis of azide **2.4** began from the self-dimerization of acetophenone.[42] Treatment of the resulting α,β-unsaturated ketone (**2.2**) with methyl lithium resulted in the tertiary alcohol. Exposure of the tertiary alcohol to a Lewis acid catalyst and TMS-N_3 gave azide **2.4**. In efforts with Prof. Joseph Topczewski and Charles Goshey, a series of azide substrates were synthesized using the same sequence with various substituted acetophenones. Most substrates used $Cu(hfac)_2$ as the Lewis acid catalyst for the conversion of the tertiary alcohol into the corresponding azide. However when $Cu(hfac)_2$ was ineffective, a Lewis acid screen was conducted to find a suitable catalyst. Generally screening was required for substrates bearing electron-withdrawing substituents on the arene as a stronger Lewis acid was required. There was a limit to the electron-density of the alcohols that could be transformed into the azides. More electron-donating substrates resulted in significant elimination rather than displacement with azide. With the symmetric allylic azide substrates in hand, we turned to optimization of the Sharpless asymmetric dihydroxylation (SAD).

Scheme 2.2 Synthesis of Symmetric Azides Substrates

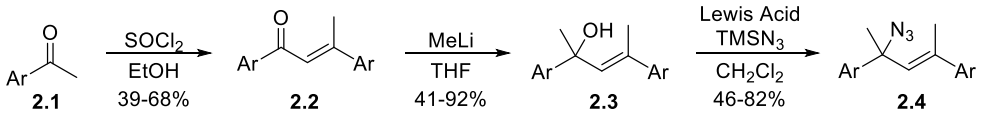

2.3 Results and Discussion

Our investigation began with azide **2.5**.[42] Exposure of azide **2.5** to standard SAD conditions provided poor conversion and modest enantioselectivity. Gratifyingly, a brief optimization afforded satisfactory results for the formation of diol **2.6** (82% yield 91:9 er, Table 2.1, entry 1) and a minor diastereomer. A screen of known SAD ligands (entries 2-6) led to the identification of DHQ-MEQ as the ligand of choice due to its excellent performance (entry 6, 82%, 99:1 er, 11:1 dr) and relatively low cost. The pseudoenantiomer DHQD-MEQ provided nearly identical results but provided the opposite enantiomer (entry 7). Given that the rate of racemization via the background rearrangement is temperature dependent, we examined the effect that temperature had on the reaction outcome (entries 8-11). Acceptable yields and enantioselectivity were maintained across the temperature range investigated, although 40 °C appeared to be optimal. The absolute configuration of the product was assigned based on the model of Sharpless.[41*]

[*] To see the Sharpless model applied to this system, please see "Discussion of Stereochemical Outcome and Diastereoselectivity" in the supporting information of this manuscript: *J. Am. Chem. Soc.* **2017**, *139*, 7737-7740.

Table 2.1 Optimization for Sharpless Asymmetric Dihydroxylation

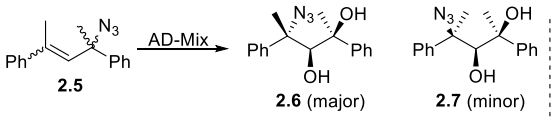

entry	ligand	temp (°C)	yield (%)	er	dr
1	$(DHQ)_2PHAL$	40	82	91:9	4:1
2	$(DHQ)_2AQN$	40	79	83:17	5.5:1
3	$(DHQ)_2PYR$	40	91	89:11	4.5:1
4	DHQ-CLB	40	86	86:14	8.5:1
5	DHQ-PHN	40	81	97:3	19:1
6	DHQD-MEQ	40	83	98:2	8:1
7	DHQ-MEQ	40	82	99:1	11:1
8	DHQ-MEQ	rt	85	99:1	8:1
9	DHQ-MEQ	30	87	98:2	7:1
10	DHQ-MEQ	50	86	97:3	8:1
11	DHQ-MEQ	60	78	95:5	7:1

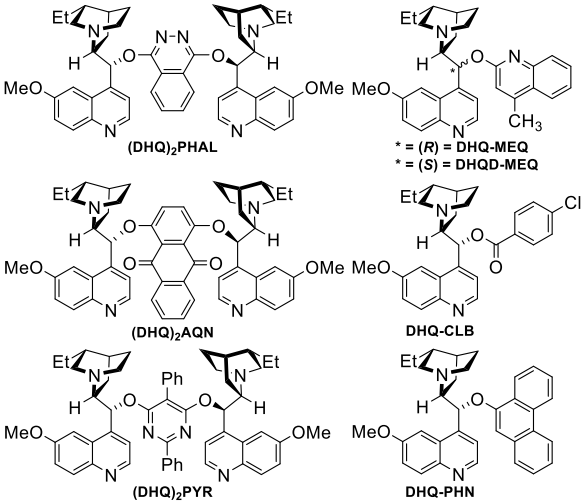

Reaction Conditions: substrate (0.08 - 0.2 mmol), ^{t}BuOH (10 mL/mmol), water (10 mL/mmol), K_2CO_3 (3 equiv), $MeSO_2NH_2$ (3 equiv), $K_3Fe(CN)_6$ (3 equiv), OsO_4 (5 mol %), L (10 mol %), under air, 48 h. Yields and dr where determined by ^{1}H NMR spectroscopic analysis using triphenylmethane as an internal standard. The represented dr is the integration ratio of the respective hydroxylated methine. The enantiomeric ratio was determined by chiral HPLC analysis. All values reported are the average of duplicate trials.

When at equilibrium, the starting azide **2.5** contains about 5% of the *Z* isomer by ^{1}H NMR analysis. It was not initially clear if the minor diastereomer **2.7** arose from dihydroxylation of the *Z* isomer or from the opposite enantiomer of the *E* isomer. The relative configuration of the major and minor diastereomer were assigned based on X-ray crystallographic analysis. The X-ray crystal structure of the major diastereomer **2.6** is shown in Table 2.2. The minor diastereomer differs in the relative arrangement of the azide and arises from dihydroxylation of the same face of the enantiomeric *E* azide isomer. No products were observed that arise from the *Z* isomer. Diastereocontrol in this system likely

arises from negative hyperconjugation.[43,44*] The high level of control in this system is due to a combination of enantioselectivity and diastereoselectivity. It is noteworthy that this catalytic process simultaneously establishes three consecutive stereocenters, two of which are to fully substituted carbons, in a single operation. Of the 8 possible stereoisomers that could arise from this reaction, ~90% of the product is a single stereoisomer.

We investigated the scope of this Winstein rearrangement tandem SAD based DKR (Table 2.2). The model system was isolated in acceptable yield (**2.6**). An array of other aromatic substituents were tolerated in this process including electron rich (**2.8**-**2.9**), halogenated (**2.10**-**2.12**), electron deficient (**2.13**), and 3-substituted arenes (**2.14**-**2.16**). Across this range of substituents, the selectivity was maintained and high levels of enantioselectivity were observed.

We examined substrates other than symmetric acetophenone derivatives. Highly substituted cyclohexane derivatives lacking any aryl rings provided excellent er in the diol product (**2.18**), as did less substituted cyclohexyl-rings (**2.19**). This process was capable of affording secondary azides with excellent enantioselectivity (**2.20**) and was viable on non-symmetric allylic azides (**2.21**). A derivative of *trans*-sobrerol was also dihydroxylated in satisfactory yield and selectivity.

[*] For more disucssion on the stereochemical models, please see "Discussion of Stereochemical Outcome and Diastereoselectivity" in the supporting information of this manuscript: *J. Am. Chem. Soc.***2017**, *139*, 7737-7740.

Table 2.2 Substrate Scope of SAD-Based DKR.

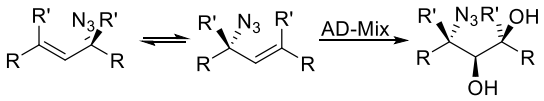

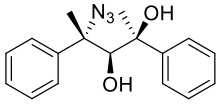

2.6, 79%, 99:1 er, 11:1 dr

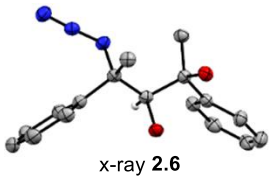

x-ray **2.6**

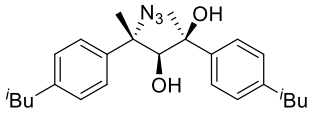

2.8, 81%, 95:5 er, 10:1 dr[a]

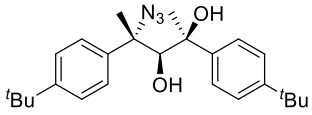

2.9, 77%, 99:1 er, 10:1 dr[a]

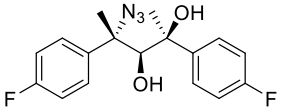

2.10, 75%, 98:2 er, 9.5:1 dr

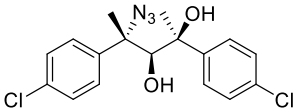

2.11, 80%, 98:2 er, 10:1 dr

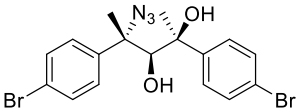

2.12, 72%, 98:2 er, 9:1 dr

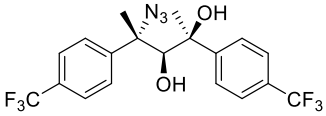

2.13, 73%, 97:3 er, 9:1 dr

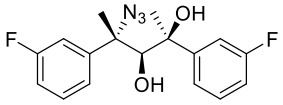

2.14, 76%, 98:2 er, 9:1 dr[a]

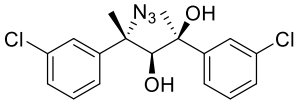

2.15, 81%, 97:3 er, 10:1 dr

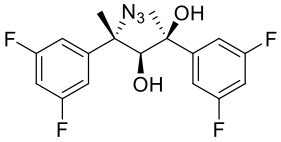

2.16, 65%, 96:4 er, 6:1 dr[a]

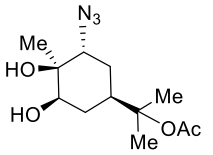

2.17, 91%, 72:28 er[b,c]

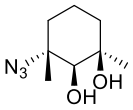

2.18, 82%, 95:5 er[b]

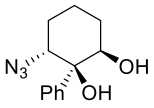

2.19, 81%, 84:16 er[b]

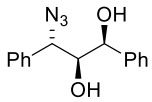

2.20, 83%, 98:2 er[b]

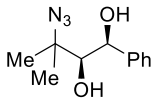

2.21, 82%, 98:2 er[b]

Reaction Conditions: substrate (0.3 - 0.4 mmol), ^{t}BuOH (10 mL/mmol), water (10 mL/mmol), K_2CO_3 (3 equiv), $MeSO_2NH_2$ (3 equiv), $K_3Fe(CN)_6$ (3 equiv), OsO_4 (5 mol %), ligand (10 mol %), 40 °C, under air, 48 h. Yields reported are for isolated material. The dr was determined by ^{1}H NMR spectroscopic analysis. The represented dr is the integration ratio of the respective hydroxylated methine. The enantiomeric ratio was determined by chiral HPLC analysis after purification. All values reported are the average of duplicate trials. [a]Reaction was conducted at 35 °C. [b]Reaction was conducted at room temperature. [c]Reaction conducted with commercial AD-mix-α.

This DKR is readily scalable and both the enantioselectivity and yield remained constant for a reaction performed using more than one gram of substrate (Scheme 2.3). Furthermore, the products formed from this dynamic kinetic resolution are of potential

synthetic value (Scheme 2.3). For instance, the diol was selectively protected and the azide reduced to the amine (compound **2.26**).

Scheme 2.3 Elaboration of Product Diol

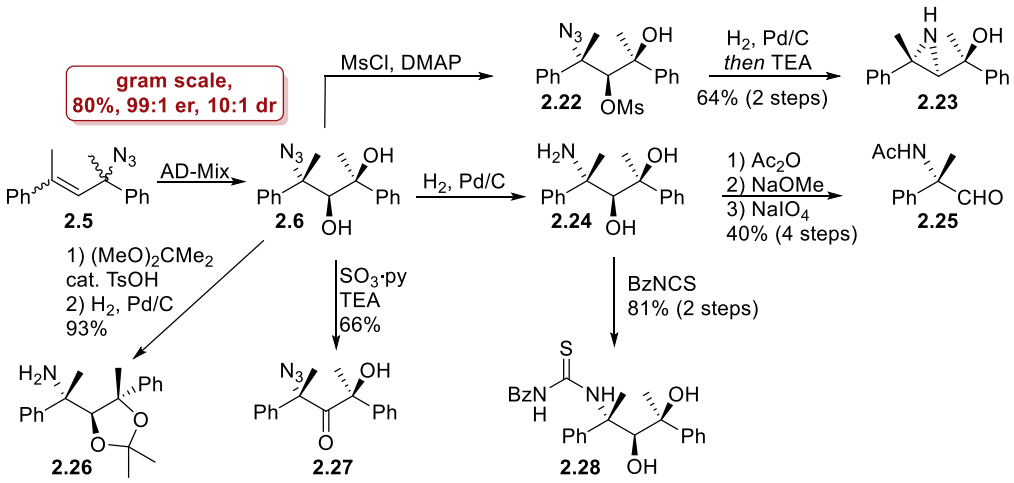

The secondary alcohol can be selectively oxidized to form ketone **2.27**. Alpha-azido ketones pose unique reactivity and are valuable intermediates.[45] Activation on the secondary alcohol and azide reduction affords aziridine **2.23**. The diol can be subjected to glycolytic cleavage to afford the corresponding α-amino aldehyde **2.25**. Finally, the azido diol can be converted to thiourea **2.28**, a direct aminothiazine precursor. Numerous aminothiazine based BACE-1 inhibitors have been reported and are currently under clinical investigation for the treatment of Alzheimer's disease.[39,40] The chiral amine motif in these BACE-1 inhibitors has been established almost exclusively by the use of Ellman's auxiliary.[46] Our DKR approach is a potential catalytic alternative for some of these inhibitors where the requisite hydroxyl group is also established during the DKR.

2.4 Conclusion

In conclusion, we have successfully accomplished the first DKR that takes advantage of the Winstein rearrangement as the racemization pathway. When this background rearrangement is coupled to a Sharpless asymmetric dihydroxylation, high levels of stereocontrol are observed in the resulting tertiary azide. This azide can be converted to products of interest or to other reactive intermediates. The Winstein rearrangement, acting as a racemization process, has the potential to be coupled with numerous other alkene functionalization reactions. Our continued efforts in this regard will be reported in due course.

2.5 References

(1) Gagneux, A.; Winstein, S.; Young, W. G. Rearrangement of Allyl Azides. *J. Am. Chem. Soc.* **1960**, *82*, 5956–5957.

(2) Vekariya, R. H.; Liu, R.; Aubé, J. A Concomitant Allylic Azide Rearrangement/Intramolecular Azide-Alkyne Cycloaddition Sequence. *Org. Lett.* **2014**, *16*, 1844–1847.

(3) Craig, D.; Harvey, J. W.; O'Brien, A. G.; White, A. J. P. Claisen Rearrangements of Equilibrating Allylic Azides. *Org. Biomol. Chem.* **2011**, *9*, 7057–7061.

(4) Lauzon, S.; Tremblay, F.; Gagnon, D.; Godbout, C.; Chabot, C.; Mercier-Shanks, C.; Perreault, S.; DeSeve, H.; Spino, C. Sterically Biased 3,3-Sigmatropic Rearrangement of Chiral Allylic Azides: Application to the Total Syntheses of Alkaloids. *J. Org. Chem.* **2008**, *73*, 6239–6250.

(5) Cardillo, G.; Fabbroni, S.; Gentilucci, L.; Perciaccante, R.; Piccinelli, F.; Tolomelli, A. Highly Diastereoselective Allylic Azide Formation and Isomerization . Synthesis of 3(2′-Amino)-β-Lactams. *Org. Lett.* **2005**, *3*, 5087–5090.

(6) Padwa, A.; Sa, M. M. Intramolecular O-H Insertion Reaction of Azido Substituted Diazoesters and Its Relevance to the Mechanism of the Allylic Azide Rearrangement. *Tetrahedron Lett.* **1997**, *38*, 5087–5090.

(7) Panek, J.; Yang, M.; Muler, I. Sequential Diastereoselective Addition and Allylic Azide Isomerization of Syn- and Anti-α-Azido-β-(Dimethylphenylsilyl)-(*E*)-Hex-4-Enoates with Acetals: Asymmetric Synthesis of γ- Hydroxy-α-Amino Acid Synthons. *J. Org. Chem.* **1992**, *54*, 4063–4064.

(8) VanderWerf, C. A.; Heasley, L. Studies on the Preparation and Rearrangements of Allylic Azides. *J. Org. Chem.* **1966**, *31*, 3534–3537.

(9) Feldman, A. K.; Colasson, B.; Sharpless, K. B.; Fokin, V. V. The Allylic Azide Rearrangement: Achieving Selectivity. *J. Am. Chem. Soc.* **2005**, *127*, 13444–13445.

(10) Liu, R.; Gutierrez, O.; Tantillo, D. J.; Aubé, J. Stereocontrol in a Combined Allylic Azide Rearrangement and Intramolecular Schmidt Reaction. *J. Am. Chem. Soc.* **2012**, *134*, 6528–6531.

(11) Pellissier, H. H. Recent Developments in Dynamic Kinetic Resolution. *Tetrahedron* **2011**, *67*, 3769–3802.

(12) Steinreiber, J.; Griengl, H. De-Racemization of Enantiomers versus De-Epimerization of Diastereomers — Classification of Dynamic Kinetic Asymmetric. *Chem. - Eur. J.* **2008**, *14*, 8060–8072.

(13) Pellissier, H. Recent Developments in Dynamic Kinetic Resolution. *Tetrahedron* **2008**, *64*, 1563–1601.

(14) Pellissier, H. H. Dynamic Kinetic Resolution. *Tetrahedron* **2003**, *59*, 8291–8327.

(15) Faber, K. Non-Sequential Processes for the Transformation of a Racemate into a Single Stereoisomeric Product : Proposal for Stereochemical Classification. *Chem. - Eur. J.* **2001**, *7*, 5004–5010.

(16) Pamies, O.; Backvall, J.-E. Combination of Enzymes and Metal Catalysts. A Powerful Approach In. *Chem. Rev.* **2003**, *103*, 3247–3261.

(17) Bhat, V.; Welin, E. R.; Guo, X.; Stoltz, B. M. Advances in Stereoconvergent

Catalysis from 2005 to 2015: Transition-Metal-Mediated Stereoablative Reactions, Dynamic Kinetic Resolutions, and Dynamic Kinetic Asymmetric Transformations. *Chem. Rev.* **2017**, *117*, 4528–4561.

(18) Chen, X.; Fong, J. Z. M.; Xu, J.; Mou, C.; Lu, Y.; Yang, S.; Song, B. A.; Chi, Y. R. Carbene-Catalyzed Dynamic Kinetic Resolution of Carboxylic Esters. *J. Am. Chem. Soc.* **2016**, *138*, 7212–7215.

(19) Koszelewski, D.; Brodzka, A.; Żądło, A.; Paprocki, D.; Trzepizur, D.; Zysk, M.; Ostaszewski, R. Dynamic Kinetic Resolution of 3-Aryl-4-Pentenoic Acids. *ACS Catal.* **2016**, 3287–3292.

(20) Piotrowski, D. W.; Kamlet, A. S.; Dechert-Schmitt, A. M. R.; Yan, J.; Brandt, T. A.; Xiao, J.; Wei, L.; Barrila, M. T. Regio- and Enantioselective Synthesis of Azole Hemiaminal Esters by Lewis Base Catalyzed Dynamic Kinetic Resolution. *J. Am. Chem. Soc.* **2016**, *138*, 4818–4823.

(21) Zhang, G.; Yang, S.; Zhang, X.; Lin, Q.; Das, D. K.; Liu, J.; Fang, X. Dynamic Kinetic Resolution Enabled by Intramolecular Benzoin Reaction: Synthetic Applications and Mechanistic Insights. *J. Am. Chem. Soc.* **2016**, *138*, 7932–7938.

(22) Zhang, Q.; Stockdale, D. P.; Mixdorf, J. C.; Topczewski, J. J.; Nguyen, H. M. Iridium-Catalyzed Enantioselective Fluorination of Racemic, Secondary Allylic Trichloroacetimidates. *J. Am. Chem. Soc.* **2015**, *137*, 11912–11915.

(23) Bhadra, S.; Yamamoto, H. Catalytic Asymmetric Synthesis of *N*-Chiral Amine Oxides. *Angew. Chem. Int. Ed.* **2016**, *55*, 13043–13046.

(24) Woods, B. P.; Orlandi, M.; Huang, C. Y.; Sigman, M. S.; Doyle, A. G. Nickel-Catalyzed Enantioselective Reductive Cross-Coupling of Styrenyl Aziridines. *J. Am. Chem. Soc.* **2017**, *139*, 5688–5691.

(25) Bartlett, S. L.; Keiter, K. M.; Johnson, J. S. Synthesis of Complex Tertiary Glycolates by Enantioconvergent Arylation of Stereochemically Labile α-Keto Esters. *J. Am. Chem. Soc.* **2017**, *139*, 3911–3916.

(26) Rasu, L.; John, J. M.; Stephenson, E.; Endean, R.; Kalapugama, S.; Clément, R.; Bergens, S. H. Highly Enantioselective Hydrogenation of Amides via Dynamic Kinetic Resolution Under Low Pressure and Room Temperature. *J. Am. Chem. Soc.* **2017**, *139*, 3065–3071.

(27) Applegate, G. A.; Berkowitz, D. B. Exploiting Enzymatic Dynamic Reductive Kinetic Resolution (DYRKR) in Stereocontrolled Synthesis. *Adv. Synth. Catal.* **2015**, *357*, 1619–1632.

(28) Noyori, R.; Ikeda, T.; Ohkuma, T.; Widhalm, M.; Kitamura, M.; Takaya, H.; Akutagawa, S.; Sayo, N.; Saito, T.; Taketomi, T.; et al. Stereoselective Hydrogenation via Dynamic Kinetic Resolution. *J. Am. Chem. Soc.* **1999**, *111*, 9134–9135.

(29) Trost, B. M.; Toste, F. D. Palladium-Catalyzed Kinetic and Dynamic Kinetic Asymmetric Transformation of Synthesis of (-) -Aflatoxin B Lactone. *J. Am. Chem. Soc.* **1999**, *121*, 3543–3544.

(30) Rainka, M. P.; Milne, J. E.; Buchwald, S. L. Dynamic Kinetic Resolution of α,β -Unsaturated Lactones through Asymmetric Copper-Catalyzed Conjugate Reduction: Application to the Total Synthesis of Eupomatilone-3. *Angew. Chem. Int. Ed.* **2005**, *44*, 6177–6180.

(31) Jurkauskas, V.; Buchwald, S. L. Dynamic Kinetic Resolution via Asymmetric

Conjugate Reduction: Enantio- and Diastereoselective Synthesis of 2,4-Dialkyl Cyclopentanones. *J. Am. Chem. Soc.* **2002**, *124*, 2892–2893.
(32) Petersen, K. S. Chiral Brønsted Acid Catalyzed Kinetic Resolutions. *Asian J. Org. Chem* **2016**, *5*, 308–320.
(33) Lu, G.; Birman, V. B. Dynamic Kinetic Resolution of Azlactones Catalyzed by Chiral Brønsted Acids. *Org. Lett.* **2011**, *13*, 356–358.
(34) Weisenburger, G. A.; Faibish, N. C.; Pippel, D. J.; Beak, P. Temperature- and Electrophile-Dependent Stereocontrol: A Structural and Mechanistic Investigation of (-)-Sparteine-Mediated Asymmetric Lithiation-Substitution Sequences of *N*-Boc-*N*-*p*-Methoxyphenyl) Cinnamylamine. *J. Am. Chem. Soc.* **1999**, *121*, 9522–9530.
(35) Pellissier, H. Organocatalyzed Dynamic Kinetic Resolution. *Adv. Synth. Catal.* **2011**, *353*, 659–676.
(36) Berkessel, A.; Cleemann, F.; Mukherjee, S.; Müller, T. N.; Lex, J. Highly Efficient Dynamic Kinetic Resolution of Azlactones by Urea-Based Bifunctional Organocatalysts. *Angew. Chem. Int. Ed.* **2005**, *44*, 807–811.
(37) Tang, L.; Deng, L. Dynamic Kinetic Resolution via Dual-Function Catalysis of Modified Cinchona Alkaloids : Asymmetric Synthesis of α-Hydroxy Carboxylic Acids. *J. Am. Chem. Soc.* **2002**, *124*, 2870–2871.
(38) Dornan, P. K.; Kou, K. G. M.; Houk, K. N.; Dong, V. M. Dynamic Kinetic Resolution of Allylic Sulfoxides by Rh-Catalyzed Hydrogenation: A Combined Theoretical and Experimental Mechanistic Study. *J. Am. Chem. Soc.* **2014**, *136*, 291–298.
(39) Wu, Y.; Guernon, J.; Shi, J.; Marcin, L.; Higgins, M.; Rajamani, R.; Muckelbauer, J.; Lewis, H.; Chang, C.; Camac, D.; et al. Discovery of S3-Truncated, C-6 Heteroaryl Substituted Aminothiazine B-Site APP Cleaving Enzyme-1 (BACE1) Inhibitors. *J. Med. Chem.* **2016**, *59*, 8593–8600.
(40) Ghosh, A. K.; Osswald, H. L. BACE1 (β-Secretase) Inhibitors for the Treatment of Alzheimer's Disease. *Chem. Soc. Rev.* **2014**, *43*, 6765–6813.
(41) Kolb, H. C.; VanNieuwenhze, M. S.; Sharpless, K. B. Catalytic Asymmetric Dihydroxylation. *Chem. Rev.* **1994**, *94*, 2483–2547.
(42) Hu, Z.; Liu, J.; Li, G.; Dong, Z.; Li, W. Synthesis of Asymmetric Triarylbenzenes by Using $SOCl_2$ -C_2H_5OH Reagent. *J. Chinese Chem. Soc.* **2004**, *51*, 581–583.
(43) Hoffmann, R.; Radom, L.; Pople, J. A.; Schleyer, P. von R.; Hehre, W. J.; Salem, L. Strong Conformational Consequences of Hyperconjugation. *J. Am. Chem. Soc.* **1972**, *94*, 6221–6223.
(44) Radom, L.; Hehre, W. J.; Pople, J. A. Molecular Orbital Theory of the Electronic Structure of Organic Compounds XIII. Fourier Component Analysis of Internal Rotation Potential Functions in Saturated Molecules. *J. Am. Chem. Soc.* **1972**, *94*, 2371–2381.
(45) Patonay, T.; Kónya, K.; Juhász-Tóth, É. Syntheses and Transformations of α-Azido Ketones and Related Derivatives. *Chem. Soc. Rev.* **2011**, *40*, 2797–2847.
(46) Robak, M. T.; Herbage, M. A.; Ellman, J. A. Synthesis and Applications of *Tert*-Butanesulfinamide. *Chem. Rev.* **2010**, *110*, 3600–3740.

Chapter 3. Evidence for a Sigmatropic and an Ionic Pathway in the Winstein Rearrangement*

3.1 Introduction

Sigmatropic rearrangements are central to organic chemistry and their synthetic applications are numerous. Famous examples include the Cope,[1] Claisen,[1] Wittig,[2] Carroll,[3] Sommelet-Hauser,[4] Mislow-Evans,[5] Meisenheimer,[6] and Overman[7] rearrangements or modifications thereof.[8–10] In principle, all of these reactions are reversible. However, the most heavily utilized sigmatropic rearrangements have a clear thermodynamic driving force. Most also require heating to achieve efficient reactivity. When viewed in this light, the Winstein rearrangement of allylic azides is an oddity because i) it occurs at or near room-temperature and ii) it results in an equilibrium mixture of allylic azides (Scheme 3.1a).[11] This is because the azide functional group is dipolar and symmetric. A C-N, N=N, and C=C bond is present in both the starting material and product of the azide rearrangement, making it near thermo-neutral. This parallels the Cope rearrangement, where, in most cases, the starting material and product are similar in energy, resulting in an equilibrium distribution.[12] This also parallels the rearrangement of allylic acetates.[13–15] These unusual properties make the allylic azide rearrangement an interesting candidate for further study.

The rearrangement of allylic azides was first described by Winstein and co-workers (Scheme 3.1a).[11] In hindsight, this rearrangement was likely observed but not recognized until later by VanderWerf and Heasley.[16,17] Winstein's initial report describes the rate constant and equilibrium constant for the rearrangement of prenyl azide and crotyl azide.

* Reprinted (adapted) with permission from Ott, A. A.; Packard, M. H.; Ortuno, M. A.; Johnson, A.; Suding, V. P.; Cramer, C. C.; Topczewski, J. J. *J. Org. Chem.* **2018**, *83*, 8214-8224. Copyright (2018) American Chemical Society.

These parameters were minimally sensitive to solvent polarity, indicating a relatively neutral transition state and implying a sigmatropic process. Le Noble found that at high pressure the reaction's activation volume was consistent with a neutral pathway.[18] Padwa provided the first evidence for stereoselectivity.[19] A single diastereomer was isolated from a tandem insertion rearrangement sequence (Scheme 3.1b). Spino observed stereoselectivity during a tandem Mitsunobu reaction rearrangement sequence (Scheme 3.1c).[20] A few reports describe an analysis of crotyl and prenyl systems computationally and concluded that the process is cyclic.[21–23] These observations are all consistent with a concerted [3,3] sigmatropic mechanism for the allylic azide rearrangement and the [3,3] mechanism has been generally accepted.

Scheme 3.1 Winstein Rearrangement

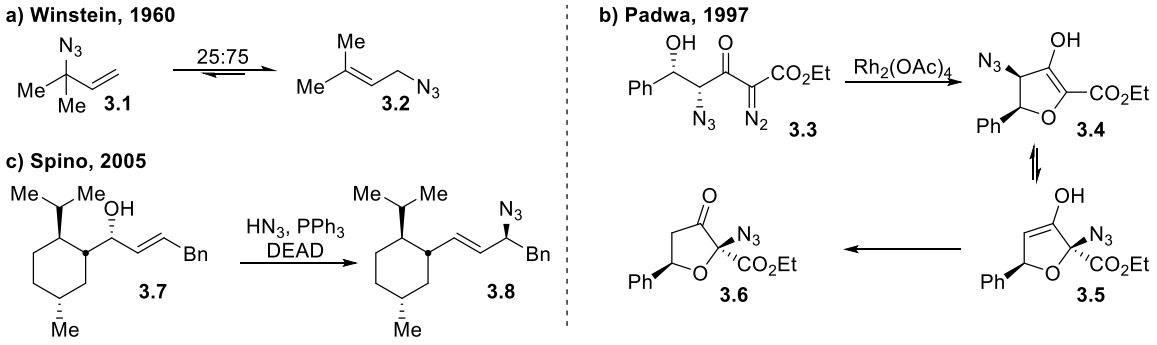

A unique aspect of the allylic azide rearrangement is the abnormally low activation barrier, which allows this process to occur at ambient temperature. The Winstein rearrangement has limited synthetic applications due to difficulties controlling the rearrangement.[24–30] We have an ongoing interest in using the Winstein rearrangement and

became interested in more precisely defining the parameters of the rearrangement on a broader set of allylic azides.[31–33] Presented herein is a summary of several experiments that more fully define the energetics and mechanism of this rearrangement. We investigated the effect of competitive conjugation on the equilibrium constant. A rearrangement with ^{15}N isotopically labeled allylic azide unambiguously confirms the [3,3] pathway. We describe a pathway for the *E* to *Z* isomerization of trisubstituted alkenes. These results led to us to probe whether racemization of chiral allylic azides could occur. Under certain conditions, these allylic azides racemize. A kinetic analysis supports an ionic pathway. Each of these pathways is supported by DFT calculations. These combined experiments indicate that more than one pathway is operable for allylic azide isomerization.

3.2 Results and Discussion

3.2.1 Effect of Conjugation on K_{eq}

Scattered reports provide insight into biasing the azide rearrangement. Hassner originally synthesized cinnamyl azide and reported only a single isomer (Scheme 3.2a).[34] In this example, conjugation to the phenyl ring strongly influences the equilibrium and results in a single observable isomer.[35] Panek observed a similar effect with γ-azido-α,β-unsaturated esters (Scheme 3.2b) and Evans made an analogous observation with 3-azido-vinyl sulfones (Scheme 3.2c).[36,37] In all cases, the conjugated compound is favored. This is reminiscent of strategies to render the Cope rearrangement effectively irreversible by forming a conjugated product.[38] We were interested in re-establishing a detectible equilibrium with conjugated azides. To this end, compounds **3.15** through **3.22** were synthesized (Scheme 3.2d). Each allylic terminus is substituted with a different group for conjugation. After isolation, samples were incubated at 40 °C for 48 h to allow

equilibration and then analyzed. The observed equilibrium ratio ranges from 2.3:1 to 1.2:1 for azides **3.15** through **3.20**, indicating that a detectible equilibrium can be re-established if both termini stabilize the system through conjugation. The effect seemed insensitive to the nature of the aryl (**3.17** vs **3.19**). For nitriles **3.21** and **3.22**, the other isomer was not detected. The remainder of this report describes allylic azides that are conjugated to an aryl ring. These systems were intentionally designed to minimize the number of isomers present in the mixture as a means of simplifying analysis.

Scheme 3.2 Effects of Conjugation on K_{eq}

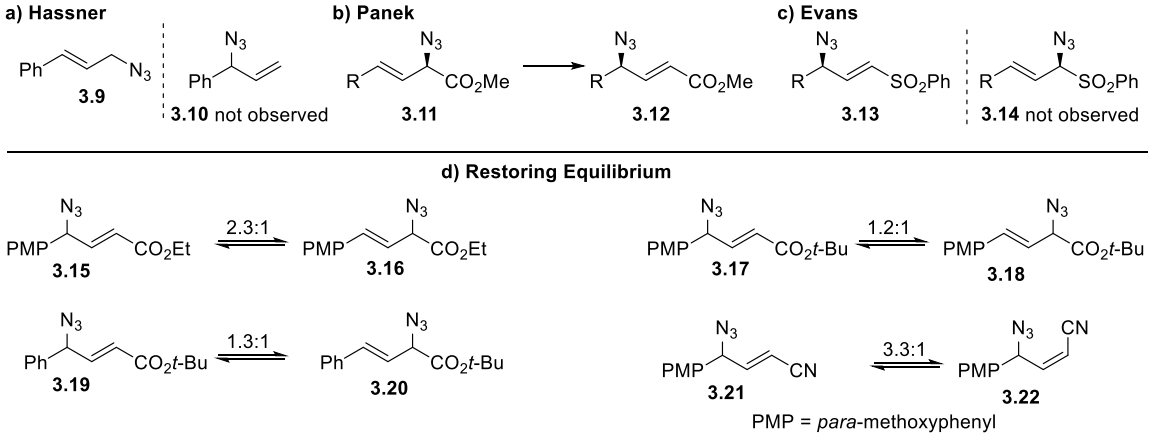

3.2.2 ^{15}N-Labelling Experiment

One means to unambiguously discern between a [1,3], [3,3], and ionic mechanism is to isotopically label one end of the azide group. Sodium azide containing a ^{15}N-label is commercially available; however, either end of the azide anion could attack an electrophilic carbon center. This would likely generate a 1:1 mixture of proximal and distal ^{15}N-azides, which would be difficult to analyze. Instead, we turned our attention to an alternate approach (Scheme 3.3). We synthesized ^{15}N-amine **3.23** in two steps from potassium ^{15}N-

phthalimide. The ^{15}N-label was evident by ^{15}N NMR and by HRMS.* The amine was subjected to diazo-transfer conditions, which formed azide **3.24**. This azide spontaneously rearranged to afford ^{15}N-cinnamyl azide (**3.25**), which was isolated as a single isomer due to conjugation. The label was again clearly evident by NMR, IR, and HRMS. Reduction of the azide liberated N_2 and afforded phosphoramidate **3.26**. Analysis of this product by NMR and HRMS indicated the complete loss of the ^{15}N label. An authentic sample of ^{15}N-**22** was synthesized by a separate route. This experiment provides direct evidence for the [3,3] mechanism of the Winstein rearrangement.

Scheme 3.3 Rearrangement of ^{15}N-Labeled Allylic Azide

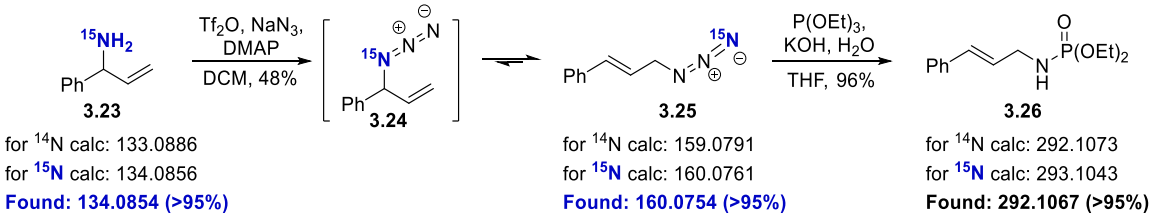

for ^{14}N calc: 133.0886
for ^{15}N calc: 134.0856
Found: 134.0854 (>95%)

for ^{14}N calc: 159.0791
for ^{15}N calc: 160.0761
Found: 160.0754 (>95%)

for ^{14}N calc: 292.1073
for ^{15}N calc: 293.1043
Found: 292.1067 (>95%)

3.2.3 *E* to *Z* Isomerization

Many allylic azides are isolated as a mixture of alkene isomers.[11,24,27,39,40] Typically, the observed distribution of isomers is related to the relative thermodynamic stability of the alkenes. Little is known regarding the mechanism of alkene isomerization via the Winstein rearrangement.[22] Labadie et. al, investigated several isoprenyl azides.[23] That report concluded that allylic azides conjugated to an aryl ring do not rearrange. This is

*Images of all mass spectra can be found in the supporting information of this manuscript: *J. Org. Chem.* **2018**, *83*, 8214-8224.

contrary to a prior report that *cis*-cinnamyl azide isomerizes to *trans*-cinnamyl azide.[41] We observed that azide **3.27** forms a mixture of *E* and *Z* isomers upon standing (Scheme 3.4a).

Scheme 3.4 Equilibration of Azides **3.27** and **3.28**

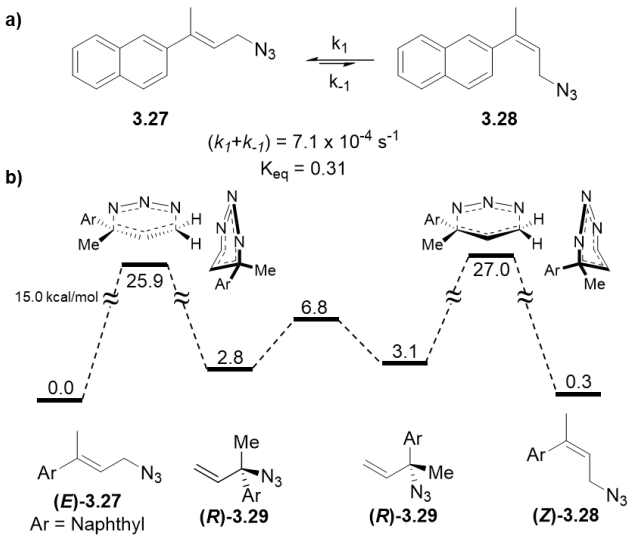

(a) Values determined by ^{1}H NMR. (b) Free energies (kcal/mol, 1 M standard state, 75 °C) computed at the SMD($CHCl_3$)/M06-2X/6- 311+G(2df,p)//SMD($CHCl_3$)/M06-2X/6-31G(d) level of theory. The vertical scale has been compressed by 15.0 kcal/mol between the ground states and transition states.

The naphthyl containing compound was studied because the isomers were separable by column chromatography.[42] We conducted a kinetic analysis of the *E* to *Z* isomerization by ^{1}H NMR at 75 °C in C_6D_6. The observed rate constant (k_1+k_{-1}) was 7.2 x 10^{-4} s^{-1} and the observed ratio of **3.27**:**3.28** was 3.2:1 at equilibrium (equilibrium reached after 90 min). The same approximate values were measured by monitoring the reverse *Z* to *E* rearrangement (k_1+k_{-1} = 6.9 x 10^{-4} s^{-1}, average reported in Scheme 3.4). The observed rate is slower than that reported by Winstein for crotyl azide.

We turned to density functional theory (DFT) calculations to describe the pathway for the observed alkene isomerization (Scheme 3.4b). These calculations were conducted

at the M06-2X level of theory, both in the gas phase and accounting for solvation effects implicitly with the SMD solvation model (e.g., chloroform, as shown in Scheme 3.4, see Computational Details).[43,44] The analysis indicates a three step process: (1) endothermic rearrangement to benzylic azide **3.29**, (2) sigma bond rotation, and (3) a second Winstein rearrangement to the conjugated isomer **3.28**. The calculated barriers and relative stationary point energetics are in good agreement with the experimental data. In both rearrangements, the transition-state structure is a fairly flat half chair (C-N-N-N-C in plane and C-C-C pucker). The rearrangement is relatively synchronous (CN bond lengths of 2.036 and 2.069 Å). This study did not address if the transition state is pericyclic or pseudopericyclic.[15,45,46] These results indicate that the Winstein rearrangement is kinetically viable on conjugated systems, even though the isomeric benzylic azide is present at too small a concentration to be readily detected by ^{1}H NMR.

3.2.4 Chiral Acyclic Allylic Azide

These results led us to consider whether azide **3.30** could racemize through the Winstein rearrangement (Scheme 3.5). Stereoselectivity is a key feature to effectively utilizing allylic azides in synthetic contexts.[20] Racemization can occur readily if one isomer is achiral[*] or if the product is the enantiomer of the starting material.[32,47] It was unclear whether a system such as azide **3.30** would racemize via a sigmatropic process.

[*] For the calculated profile for crotyl azide, see the supporting information of this manuscript: *J. Org. Chem.* **2018**, *83*, 8214-8224.

Scheme 3.5 Equilibration of Chiral Allylic Azide

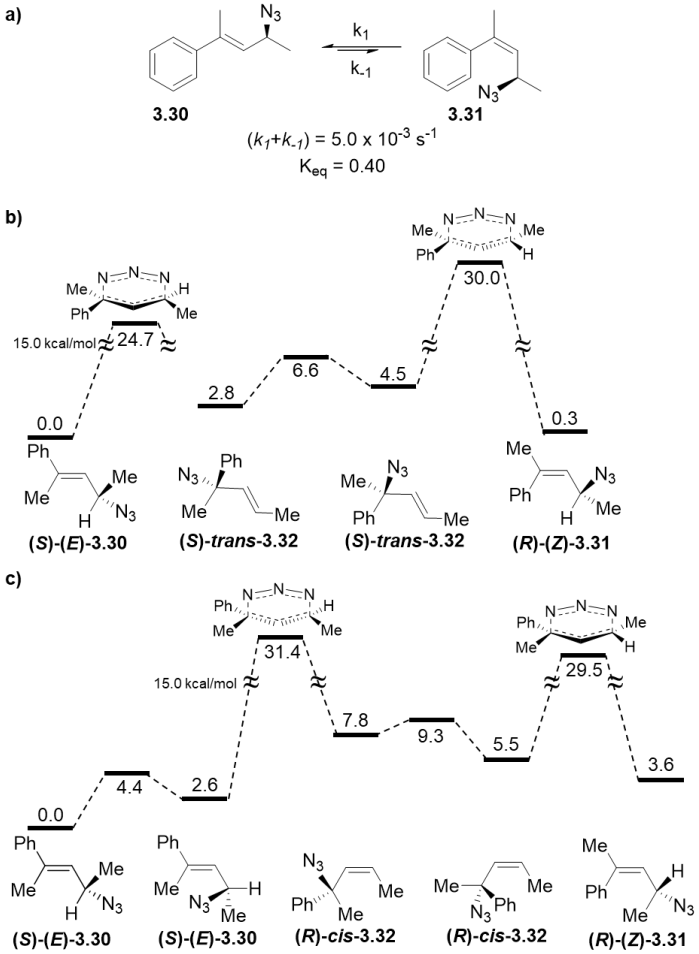

Values determined by ^{1}H NMR. (b,c) Free energies (kcal/mol, 1 M standard state, 75 °C) computed at the SMD($CHCl_3$)/M06-2X/6-311+G(2df,p)//SMD($CHCl_3$)/M06-2X/6-31G(d) level of theory. The vertical scale has been compressed by 15.0 kcal/mol between the ground states and transition states.

The examples from Padwa and Spino (Scheme 3.1b-c) document that racemization was not observed in those instances. However, the example from Padwa is cyclic, cannot form *E*/*Z* mixtures, and it is effectively irreversible (kinetically mediated). The example from Spino contains a *trans* alkene, which may not be able to adopt multiple reactive conformations. Azide **3.30** rapidly forms a mixture of *E*/*Z* isomers, with a rate constant (k_1+k_{-1}) of 5.0 x 10^{-3} s^{-1} in C_6D_6 at 75 °C and a 2.5:1 equilibrium ratio of **3.30**:**3.31**. Equilibrium is reached

considerably faster for compounds **3.30** and **3.31** (after 20 min) relative to **3.27** and **3.28** (90 min). The observation that an additional methyl group speeds the rearrangement is consistent with Winstein's work where k_{rel} for prenyl/crotyl azides ranged from 2.6-3.6 in a variety of solvents.[11] To determine if racemization occurs, we used semi-preparative chiral HPLC to isolate enantioenriched azide **3.30** (>99:1 er). The equilibration of compound **3.30** was monitored by ^{1}H NMR at 75 °C. Once equilibrium was reached, the enantiopurity of the sample was measured by chiral HPLC. Only a single enantiomer was observed for both the *E* isomer (>99:1 er) and *Z* isomer (>99:1 er). This indicates that racemization via a sigmatropic process is unlikely.

We investigated the [3,3] mechanism computationally (Scheme 3.5b-c). The lowest energy pathway is similar to that shown for compounds **3.27** and **3.28,** where a three step process is responsible for the alkene isomerization (Scheme 3.5b). The azide rearranges to *trans*-azide **3.32**, undergoes a bond rotation, and then rearranges for a second time to afford (*Z*)-azide **3.31**. For compounds **3.30** and **3.31**, a second sigmatropic pathway was identified, which is similar to the first except in the order of events. In the second pathway (Scheme 3.5c), (*E*)-azide **3.30** undergoes a sigma bond rotation and then a rearrangement to afford *cis*-azide **3.32**. This azide undergoes a second bond rotation and subsequent rearrangement to afford (*Z*)-azide **3.31**. In both pathways, the initial azide was intentionally assigned as (*S*)-(*E*)-azide **3.30** and the product of both pathways was (*R*)-(*Z*)-azide **3.31**. The stereoselectivity in both pathways is consistent with the experimental findings.

A third ionic pathway was identified which was significantly higher in energy. The azide ionizes to form free azide anion and a stabilized allylic cation (Scheme 3.6). In the gas phase and in chloroform, this pathway was significantly higher in energy relative to

the sigmatropic pathway (134.3 and 48.7 kcal/mol, respectively). However, in methanol, the ionic pathway was calculated to be much closer in energy to the sigmatropic pathway, at only 30.0 kcal/mol. This prompted further exploration.

Scheme 3.6 Relative Ionization Energies of Azide **3.30**

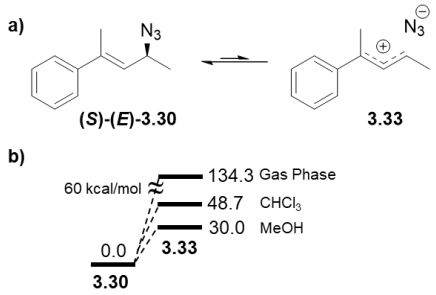

Free energies (kcal/mol, 1 M standard state, 75 °C) computed at the M06-2X/6-311+G(2df,p)//M06-2X/6-31G(d) level of theory for gas-phase and SMD-solvated reaction coordinates. The vertical scale has been compressed by 60.0 kcal/mol between chloroform and gas phase.

3.2.5 Synthesis of Allylic Azides

To examine the proposed ionic pathway, a new series of allylic azides was investigated. An example sequence is shown for the synthesis of chiral azide **3.36** (Scheme 3.7) The cyclohexyl ring prevents *E* to *Z* isomerization and simplifies analysis. Cyclohexenone was treated with a preformed organolithium reagent to access tertiary alcohol **3.35**. For some substrates a commercial Grignard reagent was used instead of forming the organolithium species. Using TMS-N_3 and catalytic $Zn(OTf)_2$, the secondary alcohol was converted to tertiary azide **3.36**. Presumably, the tertiary azide is formed which then undergoes rapid rearrangement to the more stable conjugated secondary azide **3.36**. The procedure allowed ready access to racemic azides **3.36-3.41**. However, to investigate

racemization of these substrates enantioenriched material was necessary. Each enantiomer was isolated using semi-preparative HPLC with a chiral column. After collection of each enantiomer, a sample was reinjected on the HPLC to determine the er. With a series of azides in hand, the proposed racemization was investigated (Scheme 3.8).

Scheme 3.7 Synthesis of Enantioenriched Allylic Azides

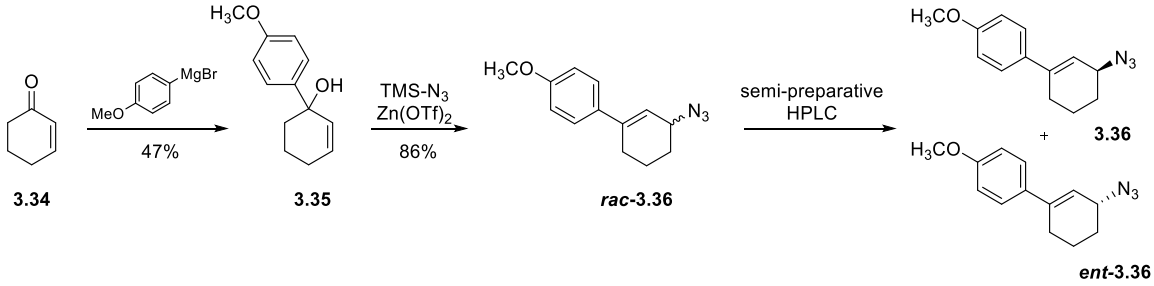

3.2.5 Identifying a Racemization Pathway

Azide **3.40** was subjected to prolonged heating in a variety of solvents. After one week at 100 °C no or negligible racemization was observed in hexanes, toluene, chloroform, and tetrahydrofuran. In these solvents, even after prolonged heating, these allylic azides can be thought of as static structures that are configurationally and isomerically stable. However, rapid racemization was observed in methanol at 100 °C. As an example, for azide **3.37** (4-Me), the er decreased considerably after only 1 h from >99:1 er to 74:26 er and full racemization occurred within 8 h. Solvent-dependent racemization is consistent with the pathway identified by DFT.

Scheme 3.8 Racemization and Solvolysis of Cyclic Azides

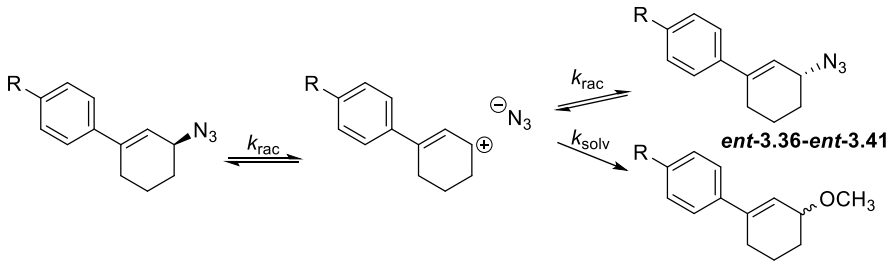

R = OCH_3, **3.36**
R = CH_3, **3.37**
R = $C(CH_3)_3$, **3.38**
R = F, **3.39**
R = H, **3.40**
R = CF_3, **3.41**

R = OCH_3, **3.42**
R = CH_3, **3.43**
R = $C(CH_3)_3$, **3.44**
R = F, **3.45**
R = H, **3.46**
R = CF_3, **3.47**

R = OCH_3, **3.48**
R = CH_3, **3.49**
R = $C(CH_3)_3$, **3.50**
R = F, **3.51**
R = H, **3.52**
R = CF_3, **3.53**

Intrigued by the observed racemization, we conducted a more detailed kinetic analysis. The rate of racemization was determined by chiral HPLC. Using the method of initial rates,[48] the rate was found to be first order in azide. Several analogous substrates were synthesized and subjected to the same analysis. A Hammett plot was generated for racemization (Figure 3.1a). The rate of racemization is highly correlated with the Hammett parameter σ^+ (R^2 = 0.99, ρ = - 3.9). The relative energies of the ions (**3.42-3.47**) were calculated at the SMD/M06-2X level. The ion stabilities ranged from 21.4 – 30.0 kcal/mol (SMD(MeOH)) and the stabilities were also correlated to σ^+.[*] This analysis is consistent with rate determining formation of an ion pair.

A more detailed analysis revealed a byproduct of the racemization process, identified as the corresponding methyl ether. At all-time points, the methyl ether is racemic. The appearance of this product is consistent with an ionic solvolysis reaction. Adding exogenous tetrabutylammonium azide did not noticeably inhibit the formation of the

[*] For correlation of computed ion stabilities to σ^+ see the supporting information for this manuscript. *J. Org. Chem.* **2018**, *83*, 8214-8224.

methyl ether. The rate of methyl ether formation is also correlated with the Hammett parameter σ^+ (Figure 3.1b, $R^2 = 0.92$, $\rho = -3.1$). When heated in methanol, acyclic azide **3.30** also racemizes, indicating that other azides can participate in this process.

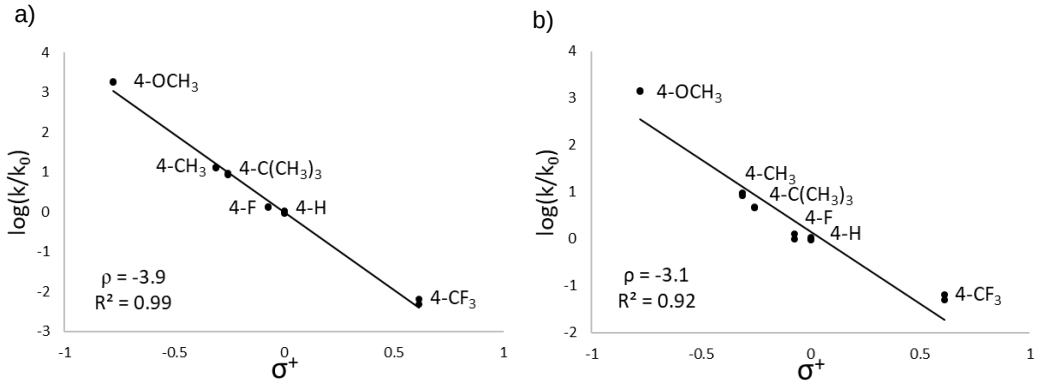

Figure 3.1 a) Plot of $\log(k/k_0)$ vs σ^+ for substituent effects on the racemization of azides **3.36-3.41** in MeOH. Rates were measured in duplicate, replicates shown. b) Plot of $\log(k/k_0)$ vs σ^+ for substituent effects on the solvolysis of azides **3.36-3.41** in MeOH. Rates were measured in duplicate, replicates shown.

3.3 Conclusion

Presented herein is a description of two competing pathways for the rearrangement of allylic azides. A ^{15}N-labeling experiment, supported by DFT calculations, indicates that under most circumstances, the rearrangement is sigmatropic. A pathway for the isomerization of a chiral allylic azide, with a trisubstituted alkene, is reported to occur without racemization. A second ionic pathway is available in highly polar media and we observed it in methanol. This reaction is Hammett constant (σ^+) correlated and is kinetically consistent with a solvolysis mechanism.

3.4 References

(1) Lutz, R. P. Catalysis of the Cope and Claisen Rearrangements. *Chem. Rev.* **1984**, *84*, 206–243.

(2) Nakai, T.; Mikami, K. [2,3]-Wittig Sigmatropic Rearrangements in Organic Synthesis. *Chem. Rev.* **1986**, *86*, 885–902.

(3) Wilson, S. R.; Price, M. F. The Ester Enolate Carroll Rearrangment. *J. Org. Chem.* **1984**, *49*, 722–725.

(4) Kantor, S. W.; Hauser, C. R. Rearrangements of Benzyltrimethylammonium Ion and Related Quaternary Ammonium Ions by Sodium Amide Involving Migration into the Ring. *J. Am. Chem. Soc.* **1951**, *73*, 4122–4131.

(5) Evans, D. A.; Andrews, G. C. Allylic Sulfoxides: Useful Intermediates in Organic Synthesis. *Acc. Chem. Res.* **1974**, *7*, 147–155.

(6) Albini, A. Synthetic Utility of Amine *N*-Oxides. *Synthesis* **1992**, 263–277.

(7) Overman, L. E. Allylic and Propargylic Imidic Esters in Organic Synthesis. *Acc. Chem. Res.* **1980**, *13*, 218–224.

(8) Nubbemeyer, U. Recent Advances in Asymmetric [3 ,3]-Sigmatropic Rearrangements. *Synthesis* **2003**, *7*, 961–1008.

(9) Jones, A. C.; May, J. A.; Sarpong, R.; Stoltz, B. M. Toward a Symphony of Reactivity : Cascades Involving Catalysis and Sigmatropic Rearrangements. *Angew. Chem. Int. Ed.* **2014**, *53*, 2556–2591.

(10) Ilardi, E. A.; Stivala, C. E.; Zakarian, A. [3,3]-Sigmatropic Rearrangements: Recent Applications in the Total Synthesis of Natural Products. *Chem. Soc. Rev.* **2009**, *38*, 3133–3148.

(11) Gagneux, A.; Winstein, S.; Young, W. G. Rearrangement of Allyl Azides. *J. Am. Chem. Soc.* **1960**, *82*, 5956–5957.

(12) Doering, W. V. E.; Roth, W. R. Thermal Rearrangements. *Angew. Chem. Int. Ed.* **1963**, *2*, 115–122.

(13) Overman, L. E.; Fredrick, K. M. Palladium (II)-Catalyzed Rearrangement of Allylic Acetates. *Tetrahedron Lett.* **1979**, *20*, 321–234.

(14) Marion, N.; Gealageas, R.; Nolan, S. P. [(NHC)Au(I)]-Catalyzed Rearrangement of Allyic Acetates. *Org. Lett.* **2007**, *9*, 2653–2656.

(15) Kreiman, H. W.; Batali, M. E.; Jamieson, C. S.; Lyon, M. A.; Duncan, J. A. CASSCF Calculations Reveal Competitive Chair (Pericyclic) and Boat (Pseudopericyclic) Transition States for the [3,3] Sigmatropic Rearrangement of Allyl Esters. *J. Org. Chem.* **2018**, *83*, 1717–1726.

(16) VanderWerf, C. A.; Heisler, R. V; McEwen, W. E. The Reaction of Sodium Azide with Some Representative Epoxides. *J. Am. Chem. Soc.* **1954**, *76*, 1231–1235.

(17) VanderWerf, C. A.; Heasley, L. Studies on the Preparation and Rearrangements of Allylic Azides. *J. Org. Chem.* **1966**, *31*, 3534–3537.

(18) Le Noble, W. J. The Effect of Pressure on the Equilibration of α- and γ-Methylallyl Azide. *J. Phys. Chem.* **1963**, *67*, 2451–2453.

(19) Padwa, A.; Sa, M. M. Intramolecular O-H Insertion Reaction of Azido Substituted Diazoesters and Its Relevance to the Mechanism of the Allylic Azide Rearrangement. *Tetrahedron Lett.* **1997**, *38*, 5087–5090.

(20) Gagnon, D.; Lauzon, S.; Godbout, C.; Spino, C. Sterically Biased 3,3-Sigmatropic

Rearrangement of Azides: Efficient Preparation of Nonracemic α-Amino Acids and Heterocycles. *Org. Lett.* **2005**, *7*, 4769–4771.
(21) Jabbari, A. Transition States and Activation Barriers for [3,3]-Sigmatropic Shift of Allyl Azides. *Org. Chem. J.* **2010**, *1*, 6–14.
(22) Kang, H.; Kang, Y. K. Allylic Azide Rearrangements Investigated by Density Functional Theory Calculations. *Bull. Korean Chem. Soc.* **2017**, *38*, 1419–1426.
(23) Porta, E. O. J.; Vallejos, M. M.; Bracca, A. B. J.; Labadie, G. R. Experimental and Theoretical Studies of the [3,3]- Sigmatropic Rearrangement of Prenyl Azides. *RSC Adv.* **2017**, *7*, 47527–47538.
(24) Askin, D.; Angst, C.; Danishefsky, S. A Total Syntheis of *N*-Acetylactinobolamine. *J. Org. Chem.* **1985**, *50*, 5005–5007.
(25) Liu, R.; Gutierrez, O.; Tantillo, D. J.; Aubé, J. Stereocontrol in a Combined Allylic Azide Rearrangement and Intramolecular Schmidt Reaction. *J. Am. Chem. Soc.* **2012**, *134*, 6528–6531.
(26) Vekariya, R. H.; Liu, R.; Aubé, J. A Concomitant Allylic Azide Rearrangement/Intramolecular Azide-Alkyne Cycloaddition Sequence. *Org. Lett.* **2014**, *16*, 1844–1847.
(27) Feldman, A. K.; Colasson, B.; Sharpless, K. B.; Fokin, V. V. The Allylic Azide Rearrangement: Achieving Selectivity. *J. Am. Chem. Soc.* **2005**, *127*, 13444–13445.
(28) Craig, D.; Harvey, J. W.; O'Brien, A. G.; White, A. J. P. Claisen Rearrangements of Equilibrating Allylic Azides. *Org. Biomol. Chem.* **2011**, *9*, 7057–7061.
(29) Moynihan, L.; Chadda, R.; Mcardle, P.; Murphy, P. V. Allylic Azide Rearrangement in Tandem with Huisgen Cycloaddition for Stereoselective Annulation: Synthesis of *C*-Glycosyl Iminosugars. *Org. Lett.* **2015**, *17*, 6226–6229.
(30) Chadda, R.; Mcardle, P.; Murphy, P. V. Allylic Azide Rearrangement in Tandem with Intramolecular Huisgen Cycloaddition for Iminosugar and Glycomimetic Synthesis: Functionalized Piperidine, Pyrrolidine, and Pyrrolotriazoles from D-Mannose. *Synthesis* **2017**, *49*, 2138–2152.
(31) Packard, M. H.; Cox, J. H.; Suding, V. P.; Topczewski, J. J. The Effect of Proximal Functionality on the Allylic Azide Equilibrium. *Eur. J. Org. Chem.* **2017**, 6365–6368.
(32) Ott, A. A.; Goshey, C. S.; Topczewski, J. J. Dynamic Kinetic Resolution of Allylic Azides via Asymmetric Dihydroxylation. *J. Am. Chem. Soc.* **2017**, *139*, 7737–7740.
(33) Porter, M. R.; Shaker, R. M.; Calcanas, C.; Topczewski, J. J. Stereoselective Dynamic Cyclization of Allylic Azides : Synthesis of Tetralins, Chromanes, and Tetrahydroquinolines. *J. Am. Chem. Soc.* **2018**, *140*, 1211–1214.
(34) Hassner, A.; Fibiger, R.; Andisik, D. Lewis Acid Catalyzed Conversion of Alkenes and Alcohols to Azides. *J. Org. Chem.* **1984**, *49*, 4237–4244.
(35) Carlson, A. S.; Calcanas, C.; Brunner, R. M.; Topczewski, J. J. Regiocontrolled Wacker Oxidation of Cinnamyl Azides. *Org. Lett.* **2018**, *20*, 1604–1607.
(36) Panek, J.; Yang, M.; Muler, I. Sequential Diastereoselective Addition and Allylic Azide Isomerization of Syn- and Anti-α-Azido-β-(Dimethylphenylsilyl)-(*E*)-Hex-4-Enoates with Acetals: Asymmetric Synthesis of γ- Hydroxy-α-Amino Acid

Synthons. *J. Org. Chem.* **1992**, *54*, 4063–4064.
(37) Doherty, W.; Evans, P. Aminooxylation Horner-Wadsworth-Emmons Sequence for the Synthesis of Enantioenriched γ-Functionalized Vinyl Sulfones. *J. Org. Chem.* **2016**, *81*, 1416–1424.
(38) Cope, A. C.; Hardy, E. M. The Introduction of Substituted Vinyl Groups. V. A Rearrangement Involving the Migration of an Allyl Group in a Three-Carbon System. *J. Am. Chem. Soc.* **1940**, *62*, 441–444.
(39) Safi, M.; Fahrang, R.; Sinou, D. Palladium(0)-Catalyzed Azidation of Allyl Esters with Trimethylsilyl Azide. *Tetrahedron Lett.* **1990**, *31*, 527–530.
(40) Maag, H.; J, R. M. R. An Allylic Azide Route to 4'-Azido Carbocyclic Nucleosides. Synthesis of (±)-(1'α,2'α,3'β)- and (±)-(1'α,2'β,3'β)-1-[1-Azido-2-Hydroxy-1-(Hydroxymethyl)-3-Cyclopentyl]Thymine. *J. Org. Chem.* **1992**, *57*, 5823–5831.
(41) Banert, K.; Hagedorn, M.; Liedtke, C.; Melzer, A.; Schöffler, C. Reactions of Unsaturated Azides, 12 Azido-1,2,3-Triphenylpropenes of Varying Stabilities: A Corrigendum of Structure Assignment. *Eur. J. Org. Chem.* **2000**, 257–267.
(42) Goswami, P. P.; Suding, V. P.; Carlson, A. S.; Topczewski, J. J. Direct Conversion of Aldehydes and Ketones into Azides by Sequential Nucleophilic Addition and Substitution. *Eur. J. Org. Chem.* **2016**, 4805–4809.
(43) Marenich, A. V; Cramer, C. J.; Truhlar, D. G. Universal Solvation Model Based on Solute Electron Density and on a Continuum Model of the Solvent Defined by the Bulk Dielectric Constant and Atomic Surface Tensions. *J. Phys. Chem. B.* **2009**, *113*, 6378–6396.
(44) Zhao, Y.; Truhlar, D. G. The M06 Suite of Density Functionals for Main Group Thermochemistry, Thermochemical Kinetics, Noncovalent Interactions, Excited States, and Transition Elements: Two New Functionals and Systematic Testing of Four M06-Class Functionals and 12 Other Function. *Theor. Chem. Acc.* **2008**, *120*, 215–241.
(45) Sharma, S.; Rajale, T.; Unruh, D. K.; Birney, D. M. Competitive Pseudopericyclic [3,3]- and [3,5]-Sigmatropic Rearrangements of Trichloroacetimidates. *J. Org. Chem.* **2015**, *80*, 11734–11743.
(46) Sharma, S.; Rajale, T.; Cordes, D. B.; Hung-Low, F.; Birney, D. M. Experimental and Computational Studies on the [3,3]- and [3,5]- Sigmatropic Rearrangements of Acetoxycyclohexadienones: A Non- Ionic Mechanism for Acyl Migration. *J. Am. Chem. Soc.* **2013**, *135*, 14438.
(47) Klepper, F.; Jahn, E. M.; Hickmann, V.; Carell, T. Synthesis of the Transfer-RNA Nucleoside Queuosine by Using a Chiral Allyl Azide Intermediate. *Angew. Chem. Int. Ed.* **2007**, *46*, 2325–2327.
(48) Espenson, J. H. *Chemical Kinetics and Reaction Mechanisms*; McGraw-Hill, Inc: New York, 1995.

Chapter 4. Catalytic Racemization of Activated Organic Azides*

4.1 Introduction

Synthetic methods that provide direct access to enantioenriched products are highly desired. A powerful platform for enantioselective synthesis is dynamic kinetic resolution (DKR).[1–6] DKR is especially powerful because racemic starting materials can be converted to enantioenriched products in both high yield and high selectivity. This surmounts the 50% maximum theoretical yield barrier inherent to kinetic resolution.[7] A mechanism for rapid racemization is crucial for DKR, which has limited this process to substrates containing easily racemizeable stereocenters. Common DKR substrates include carbonyl containing molecules with an α-stereocenter.[8–10] Alternatively, chiral secondary alcohols can be racemized via an oxidation/reduction sequence.[3] While other mechanisms of racemization are known,[2,11] the applications of DKR remain limited. Identifying new mechanisms of facile racemization for new substrate classes could potentially open unexplored avenues for the development of methods predicated on DKR. Azides are particularly interesting substrates because they are chiral amine equivalents, and chiral amines are an essential motif in many drugs and drug candidates.

Recently, our group has become interested in using organic azides as amine surrogates for DKR.[12–14] We hypothesized that the Winstein rearrangement[15–17] could serve as a suitable racemization pathway. An initial example afforded tertiary azides in high er.[12] These promising results led us to ask fundamental questions regarding the mechanism of the allylic azide rearrangement. Under most conditions, the rearrangement occurred via a [3,3] sigmatropic pathway and no racemization was observed (Scheme 4.1a).[18] A second

* Reprinted (adapted) with permission from Ott, A. A.; Topczewski, J. J. *Org. Lett.* **2018**, *20*, 7253-7256. Copyright (2018) American Chemical Society

solvolysis pathway led to azide racemization, which proceeded slowly in methanol at 100 °C (Scheme 4.1b).[18] While this was exciting, racemization was slow, required elevated temperatures, and resulted in significant decomposition of the azide through methanolysis. Therefore, these conditions could not be readily adapted to DKR. Nevertheless, the observed racemization prompted a search for a suitable racemization catalyst.

Scheme 4.1 Mechanisms of Azide Rearrangement and Racemization

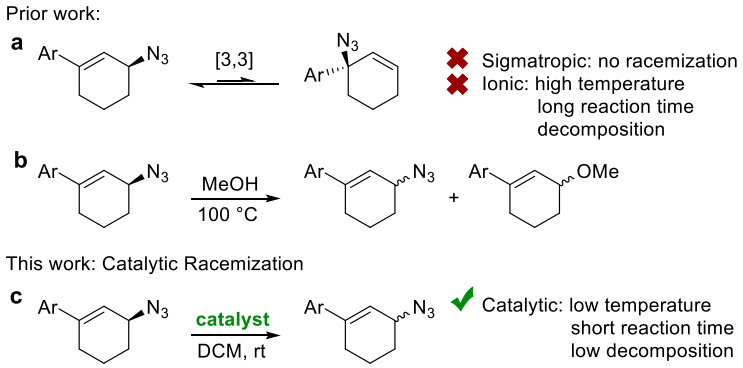

We sought to identify a catalyst for azide racemization that would i) significantly increase the rate of racemization, ii) proceed without significant decomposition of the azide, and iii) broaden the scope of azides that could be efficiently racemized. This report provides the first detailed account documenting the catalytic racemization of organic azides (Scheme 4.1c). Several catalysts for racemization are described that proceed with an exceptional rate enhancement relative to the solvolysis pathway (Scheme 4.1b vs 4.1c). This process is broad in scope and is tunable based on catalyst selection.

4.2 Results and Discussion

We began this study with allylic azide **4.1** (Table 4.1). Prior work indicated that this azide is configurationally stable in non-polar solvents at 100 °C for >1 week.[18] Catalysts were examined in dichloromethane at 50 °C so that any observed racemization could be attributed to the catalyst. Azide **4.1** (>99:1 er) was exposed to 10 mol % of various possible catalysts for 24 h and the reaction was monitored by chiral HPLC. Initially, transition metal catalysts were investigated (entries 1-4). As part of a report on an allylic substitution reactions, Trost and co-workers suggested that the presence of palladium may accelerate the allylic azide rearrangment.[19] Exposure of azide **4.1** to Pd(0) sources led to minimal racemization (entries 1-2). Exposure to a more electrophilic Pd(II) salt led to considerable racemization along with significant azide decomposition (entry 3). Based on Liu's observation,[20] Lewis acidic salts were investigated (entries 5 and 6). Several of these catalysts resulted in racemization along with appreciable decomposition of azide **4.1** (entries 4-6).[*] Gratifyingly, $Zn(OTf)_2$ led to full racemization with minimal azide decomposition (entry 6). Triflamide, as a Brønsted acid catalyst, was found to be minimally effective (entry 7). A report by Toste and co-workers suggested that cationic gold salts may cause partial racemization of some azides.[21] Catalyst 1 was chosen as a representative gold(I) complex. Exposure of azide **4.1** to 10 mol % of this catalyst led to complete racemization with minimal decomposition of the azide. Based on these results, $Zn(OTf)_2$ and gold catalyst 1 were selected for further study.

[*] For more screening of racemization catalysts see the supporting information for this manuscript: *Org. Lett*. **2018**, *20*, 7253-7256.

Table 4.1 Initial Screen for Racemization Catalyst

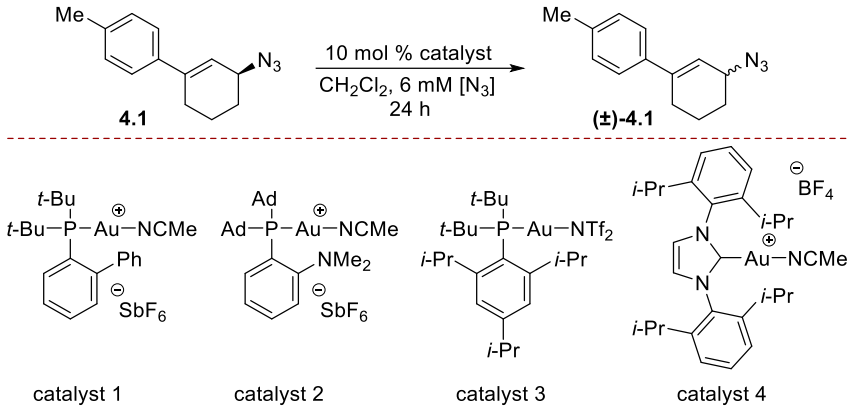

entry	catalyst	temp	er[a]	% azide remaining[b]
1	$Pd(PPh_3)_4$	50 °C	81:19	68
2	$Pd_2(dba)_3$	50 °C	98:2	89
3	$PdCl_2(NCPh)_2$	50 °C	64:36	76
4	$(cod)_2RhOTf$	50 °C	59:41	23
5	$Cu(OTf)_2$	50 °C	60:40	61
6	$Zn(OTf)_2$	50 °C	50:50	86
7	Tf_2NH	50 °C	82:18	65
8	catalyst 1	50 °C	50:50	88
9	$Zn(OTf)_2$	rt	82:18	94
10	catalyst 1	rt	50:50	88
11[c]	$Ph_3PAu(MeCN)SbF_6$	rt	50:50	84
12[c]	catalyst 2	rt	52:48	75
13[c]	catalyst 3	rt	78:22	85
14[c]	catalyst 4	rt	57:43	97
15[c,d]	catalyst 4	rt	98:2	99
16[e]	catalyst 4	50 °C	60:40	99
17	$AgSbF_6$	rt	50:50	72

[a]Measured using chiral HPLC analysis. [b]Determined by calibrated HPLC analysis using 4,4'-di-*tert*-butylbiphenyl as a standard. Reactions were run in duplicate, and the average yield and er values are reported. Room temperature = rt. [c]Reaction time of 10 min. [d]Reaction with 1 mol% catalyst. [e]Reaction with 1 mol% catalyst at 0.1 M [N_3] and at 3 h.

Other cationic gold(I) complexes were investigated (Table 4.1, entries 11-14). These results indicate that other gold(I) complexes with non-coordinating counter ions are suitable for racemization. Significantly, minimal azide decomposition was observed even with rapid racemization. Decreasing the catalyst loading slowed racemization (entry 15, and SI);[*] however, activity could be restored by increasing the temperature and concentration (entry 16). As a control experiment, $AgSbF_6$ was used as the catalyst (entry 17), which led to both racemization and significant azide decomposition. We proceeded to study catalyst 4 because it is readily available, fully soluble, provided rapid racemization at room temperature, and caused minimal azide decomposition.

With a catalyst identified, we were interested in illuminating the mechanism of racemization. Using the method of initial rates,[22] the reaction was found to be first order in both azide and gold catalyst. To gain more insight, a series of substituted azides was synthesized (Figure 4.1, **4.1** – **4.5**). For each azide, the initial rate of racemization was measured using chiral HPLC analysis. The rate of racemization correlated to the Hammett parameter σ^+ (Figure 4.1, $R^2 = 0.97$, $\rho = -5.9$), indicating build-up of positive charge in the transition state. The large negative ρ value is consistent with formation of a carbocation intermediate.[23] Based on the known binding mode of a similar gold complex to adamantyl azide[24] and the kinetic analysis, a mechanism is proposed (Scheme 4.2). The gold catalyst likely binds the azide (step i), ionizes the azide (step ii), recombines with the carbocation (step iii), and dissociates (step iv).

[*] See supporting information for this manuscript: *Org. Lett*. **2018**, *20*, 7253-7256.

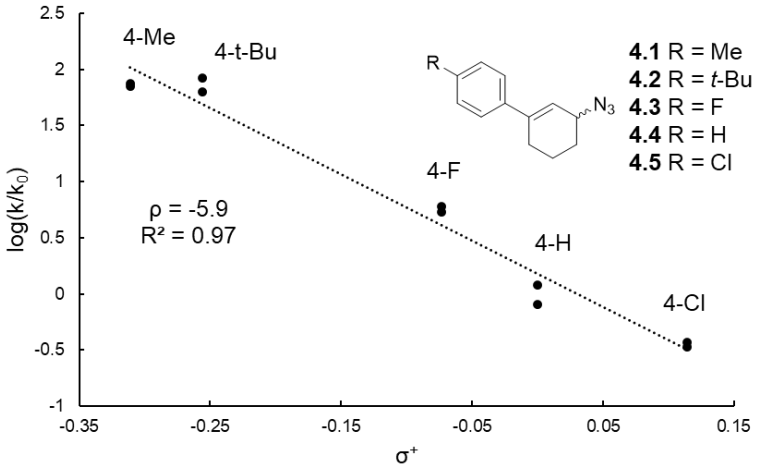

Figure 4.1 Plot of $\log(k/k_0)$ vs. σ+ for substituent effects on the racemization of azides 1a – 1e using catalyst 4. Rates were measured in duplicate, replicates shown.

Scheme 4.2 Proposed Mechanism for Azide Racemization

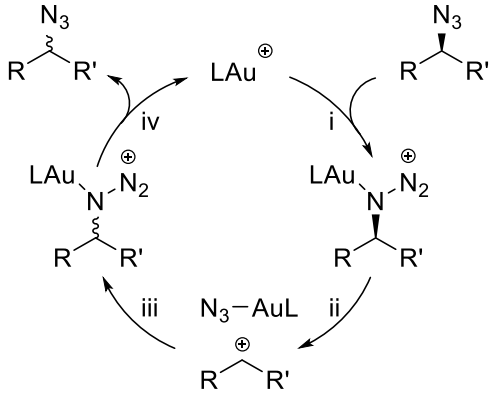

Other organic azides could be racemized under these gold catalyzed conditions (Table 4.2). In order to tease apart subtle differences in the rate of racemization, the following experiments were conducted under dilute conditions (5 mM). As expected based on the Hammett correlation, a tertiary allylic azide underwent rapid racemization (entry 1).

Table 4.2 Scope of Racemization

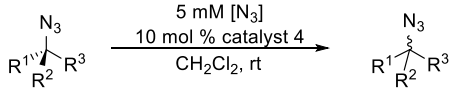

entry	azide	azide remaining[a], er[b] 1 h	6 h	24 h
1[c]	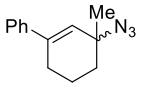 **4.6**	90% 50:50	81% 51:49	77% 51:49
2[d]	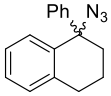 **4.7**	86% 74:26	71% 56:44	--
3[e]	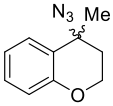 **4.8**	84% 83:17	86% 55:45	79% 50:50
4[f]	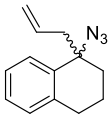 **4.9**	97% 98:2	93% 92:8	90% 88:12
5	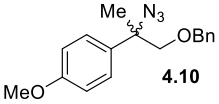 **4.10**	98% 97:3	95% 91:9	93% 81:19
6	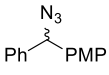 **4.11**	97% 57:43	95% 50:50	94% 50:50
7	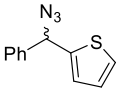 **4.12**	99% 50:50	96% 50:50	96% 50:50
8	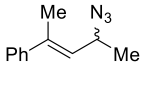 **4.13**	93% 84:16	92% 80:20	92% 70:30
9	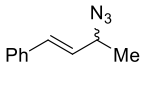 **4.14**	99% >99:1	99% 97:3	97% 93:7
10[e]	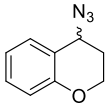 **4.15**	96% >99:1	96% >99:1	96% >99:1
11[e]	 **4.16**	99% >99:1	99% >99:1	99% >99:1
12	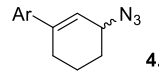 **4.17** Ar = 4-CF_3-C_6H_4	--	--	98% 98:2

[a]Determined by HPLC analysis using 4,4'-di-*tert*-butylbiphenyl as a standard. Reactions were run in duplicate, and the average yield and er values are reported. [b]Measured using chiral HPLC analysis. [c]Time points are 1 min, 5 min, and 10 min. [d]Time points are 1 h and 3.5 h. [e]Azide remaining determined by GC-FID analysis. [f]Time points are 1 h, 3.5 h, and 6 h. Room temperature = rt, PMP = *para*-methoxyphenyl.

A doubly benzylic and tertiary azide racemized and gradually decomposed to the corresponding styrene, which was independently verified (entry 2). Other tertiary benzylic azides demonstrated a range of activity based on the substituents (entries 3-5). Diaryl secondary azides reached a 50:50 er within 6 h (entries 6 and 7). These results are particularly exciting because they demonstrate that this process is not restricted to allylic azides and is operable on a much broader class of compounds. Less activated azides also

reacted, albeit at a decreased rate under these dilute conditions (entries 8 and 9). Secondary benzylic azides were stable under these conditions (entries 10 and 11).

Table 4.3 Alternate Racemization Catalysts

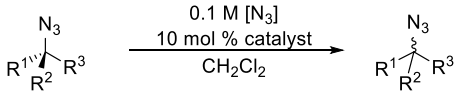

entry	azide	catalyst	temp.	azide remaining[a], er[b] 1 h	azide remaining[a], er[b] 5 h
1[c,d]	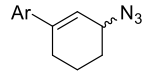 **4.1** Ar = 4-CH_3-C_6H_4	$AgPF_6$	rt	94% 63:37	93% 57:47
2[c]		$AgPF_6$/PPh_3	rt	92% 64:36	89% 59:41
3[e]	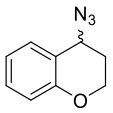 **4.15**	$AgPF_6$	rt	94% 67:23	95% 52:48
4[e]		$AgPF_6$	50 °C	92% 51:49	92% 50:50
5[f]	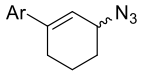 **4.17** Ar = 4-CF_3-C_6H_4	$AgPF_6$	rt	91% 52:48	88% 51:49
6	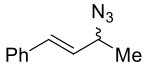 **4.14**	cat. 4	50 °C	90% 78:22	88% 68:32
7[f]	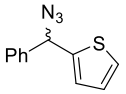 **4.12**	$Zn(OTf)_2$	50 °C	>99% 85:15	>99% 51:49
8[f]	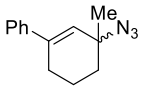 **4.6**	$Zn(OTf)_2$	rt	97% 71:29	95% 51:49

[a]Determined by HPLC analysis using 4,4'-di-*tert*-butylbiphenyl as a standard. Reactions were run in duplicate, and the average yield and er values are reported. [b]Measured using chiral HPLC analysis. [c]Time points are 10 min and 1 h at 6 mM [N_3]. [d]Reaction with 3 mol % catalyst loading. [e]Azide remaining determined by GC-FID analysis. [f]Time points are 1 h and 3 h. Room temperature = rt

With several suitable catalysts identified in the initial screen, we hypothesized that the catalyst and substrate combination could be fine-tuned to i) to increase the reactivity of less activated azides or ii) prevent decomposition for the most activated azides. For model

substrate **1a**, the use of a decreased $AgPF_6$ loading resulted in racemization with less decomposition (Table 4.3, entry 1). Furthermore, the reactivity of the silver salt could be tuned by the addition of ligand (entry 2). Secondary azides **4.15** and **4.17** were stable to catalyst 4, but treatment with $AgPF_6$ resulted in near complete racemization in under 5 h at room temperature (entries 3 and 5). Racemization could be further accelerated by mildly heating the reaction (entry 4). Racemization of azide **4.14** was sluggish under the initially optimized conditions but increasing the temperature and concentration resulted in moderate racemization in 5 h (entry 6). Highly active substrates can be efficiently racemized under more mild conditions with $Zn(OTf)_2$ (entries 7-8). While azide **4.6** began to decompose using catalyst 4, the use of $Zn(OTf)_2$ resulted in minimal decomposition (entry 8).

To further probe the mechanism, we conducted a crossover experiment using a substrate bearing an ^{15}N label (Scheme 4.3). This experiment would help determine whether the azide ion is held in a tight ion pair or whether it becomes solvent separated. ^{15}N-labelled azide **4.11'** was synthesized in one step from alcohol **4.18**. The alcohol was activated using MsCl, which was followed by displacement using $Na^{15}N_3$. Azide **4.12** and labelled azide **4.11'** were chosen for the crossover experiment because they have similar rates of racemization. The mixture of azides was treated with $IPrAuBF_4$ to promote racemization. After 1 h, an aliquot of the reaction mixture was analyzed by mass spectrometry. Labelled azide **4.12'** was not detected which indicates the azide ion is formed as a tight ion pair with the corresponding carbocation. Therefore, once the ion pair is formed, the azide anion re-traps the carbocation.

Scheme 4.3 Crossover Experiment

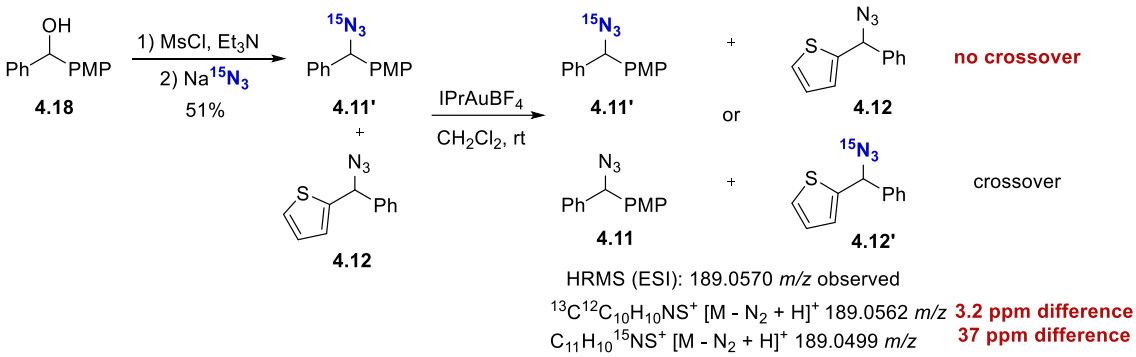

4.3 Conclusion

Herein we disclose the catalytic racemization of activated organic azides. The rate of the reaction is correlated to the Hammett constant σ^+, implicating the involvement of a carbocation intermediate. The reactivity can be modulated by the choice of catalyst. Investigations into utilizing this racemization for a downstream functionalization are currently underway.

4.4 Experimental

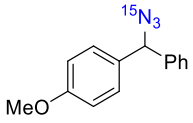

Azide 4.11'. To a solution of alcohol **4.18** (56 mg, 0.26 mmol) and MsCl (18 µL, 0.23 mmol) in Et_2O (0.25 mL) cooled in an ice bath was added Et_3N (70 µL, 0.52 mmol). After 10 min, $Na^{15}N_3$ (22 mg, 0.34 mmol) in DMF (0.25 mL) was added and the reaction mixture was heated to 50 °C. After 24 h, the reaction was diluted with Et_2O, washed with water (10 mL x 3). The aqueous layer was extracted with Et_2O (10 mL × 3). The combined organic phase was washed with brine, dried ($MgSO_4$), filtered, and concentrated under reduced

pressure. Final purification by flash chromatography (4 g cartridge, gradient elution 5%-30% EtOAc in hexanes) yielded azide **4.11'**(27 mg, 51%) as a colorless oil.

^{1}H NMR (500 MHz, $CDCl_3$) δ 7.40 – 7.35 (m, 2H), 7.35 – 7.30 (m, 3H), 7.25 (d, *J* = 8.7 Hz, 2H), 6.91 (d, *J* = 8.7 Hz, 2H), 5.70 (s, 1H), 3.83 (s, 3H). **^{13}C NMR (125 MHz, $CDCl_3$)** δ 159.4, 139.9, 131.8, 128.8, 128.6, 127.9, 127.2, 114.1, 68.1 (d, ^{15}N-C coupling, 4.1 Hz), 55.3. **IR (NaCl, thin film, cm^{-1})** 2076, 1511, 1247, 1174, 1033. **HRMS (ESI):** *m/z* calcd for $C_{14}H_{14}NO^+$ $[M - N_2 + H]^+$ 212.1270, found 212.1072, *m/z* calcd for $C_{14}H_{14}{}^{15}NO^+$ $[M - N_2 + H]^+$ 213.1040, observed 213.1056.

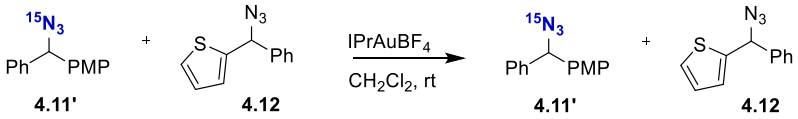

Crossover Experiment: To a solution of ^{15}N-labelled azide **4.11'** (4.0 mg, 17 µmol) and azide **4.12** (4.1 mg, 19 µmol) in CH_2Cl_2 (0.25 mL) was added $IPrAuBF_4$ (2.4 mg, 3.4 µmol) at room temperature. After 1 h, an aliquot of the reaction mixture was diluted in MeOH and analyzed by mass spectroscopy. The molecular ion for each azide was not observed by eithe EI and ESI. However, fragments containing one nitrogen $(M - N_2 - H)^+$ using EI and $(M - N_2 + H)^+$ using ESI were observed. Using HRMS, the exact mass of the observed ion from azide **4.12** was compared to ^{13}C $(M - N_2 + H)^+$ and ^{15}N $(M - N_2 + H)^+$.

HRMS (ESI): *m/z* calcd for $^{13}C_{11}H_{10}NS^+$ $[M - N_2 + H]^+$ 189.0562, *m/z* calcd for $C_{11}H_{10}{}^{15}NS^+$ $[M - N_2 + H]^+$ 189.0499, found 189.0570. The observed mass is 4.2 ppm off from $^{13}C_{11}H_{10}NS^+$ and 37 ppm off $C_{11}H_{10}{}^{15}NS^+$. In this experiment, the ^{15}N label does not scramble, indicating the azide ion does not dissipate from the substrate upon ionization.

4.5 References

(1) Pellissier, H. H. Recent Developments in Dynamic Kinetic Resolution. *Tetrahedron* **2011**, *67*, 3769–3802.

(2) Pellissier, H. H. Dynamic Kinetic Resolution. *Tetrahedron* **2003**, *59*, 8291–8327.

(3) Verho, O.; Bäckvall, J. E. Chemoenzymatic Dynamic Kinetic Resolution: A Powerful Tool for the Preparation of Enantiomerically Pure Alcohols and Amines. *J. Am. Chem. Soc.* **2015**, *137*, 3996–4009.

(4) Bhat, V.; Welin, E. R.; Guo, X.; Stoltz, B. M. Advances in Stereoconvergent Catalysis from 2005 to 2015: Transition-Metal-Mediated Stereoablative Reactions, Dynamic Kinetic Resolutions, and Dynamic Kinetic Asymmetric Transformations. *Chem. Rev.* **2017**, *117*, 4528–4561.

(5) El Gihani, M. T.; Williams, J. M. J. Dynamic Kinetic Resolution. *Curr. Opin. Chem. Biol.* **1999**, *3*, 11–15.

(6) Huerta, F.; Minidis, A. Racemisation in Asymmetric Synthesis. Dynamic Kinetic Resolution and Related Processes in Enzyme and Metal Catalysis. *Chem. Soc. Rev.* **2001**, *30*, 321–331.

(7) Keith, J. M.; Larrow, J. F.; Jacobsen, E. N. Practical Considerations in Kinetic Resolution Reactions. *Adv. Synth. Catal.* **2001**, *343*, 5–26.

(8) Tai, A.; Wantanabe, H.; Harada, T. Stereochemical Studies of the Hydrogenation with Asymmetrically Modified Nickel Catalysts; The Hydrogenation of Methyl 2-Alkyl-3-Oxobutyrate. *Bull. Chem. Soc. Jpn.* **1979**, *52*, 1468–1472.

(9) Noyori, R.; Ikeda, T.; Ohkuma, T.; Widhalm, M.; Kitamura, M.; Takaya, H.; Akutagawa, S.; Sayo, N.; Saito, T.; Taketomi, T.; et al. Stereoselective Hydrogenation via Dynamic Kinetic Resolution. *J. Am. Chem. Soc.* **1999**, *111*, 9134–9135.

(10) Jurkauskas, V.; Buchwald, S. L. Dynamic Kinetic Resolution via Asymmetric Conjugate Reduction: Enantio- and Diastereoselective Synthesis of 2,4-Dialkyl Cyclopentanones. *J. Am. Chem. Soc.* **2002**, *124*, 2892–2893.

(11) Carmona, J. A.; Hornillos, V.; Ramírez-López, P.; Ros, A.; Iglesias-Sigüenza, J.; Gómez-Bengoa, E.; Fernández, R.; Lassaletta, J. M. Dynamic Kinetic Asymmetric Heck Reaction for the Simultaneous Generation of Central and Axial Chirality. *J. Am. Chem. Soc.* **2018**, *140*, 11067–11075.

(12) Ott, A. A.; Goshey, C. S.; Topczewski, J. J. Dynamic Kinetic Resolution of Allylic Azides via Asymmetric Dihydroxylation. *J. Am. Chem. Soc.* **2017**, *139*, 7737–7740.

(13) Porter, M. R.; Shaker, R. M.; Calcanas, C.; Topczewski, J. J. Stereoselective Dynamic Cyclization of Allylic Azides : Synthesis of Tetralins, Chromanes, and Tetrahydroquinolines. *J. Am. Chem. Soc.* **2018**, *140*, 1211–1214.

(14) Ding, P. G.; Hu, X. S.; Zhou, F.; Zhou, J. Catalytic Enantioselective Synthesis of α-Chiral Azides. *Org. Chem. Front.* **2018**, *5*, 1542–1559.

(15) Gagneux, A.; Winstein, S.; Young, W. G. Rearrangement of Allyl Azides. *J. Am. Chem. Soc.* **1960**, *82*, 5956–5957.

(16) Feldman, A. K.; Colasson, B.; Sharpless, K. B.; Fokin, V. V. The Allylic Azide Rearrangement: Achieving Selectivity. *J. Am. Chem. Soc.* **2005**, *127*, 13444–13445.

(17) Liu, R.; Gutierrez, O.; Tantillo, D. J.; Aubé, J. Stereocontrol in a Combined Allylic Azide Rearrangement and Intramolecular Schmidt Reaction. *J. Am. Chem. Soc.* **2012**, *134*, 6528–6531.
(18) Ott, A. A.; Packard, M. H.; Ortuño, M. A.; Johnson, A.; Suding, V. P.; Cramer, C. J.; Topczewski, J. J. Evidence for a Sigmatropic and an Ionic Pathway in the Winstein Rearrangement. *J. Org. Chem.* **2018**, *83*, 8214–8224.
(19) Trost, B. M.; Pulley, S. R. On the Flexibility of Allylic Azides as Synthetic Intermediates. *Tetrahedron Lett.* **1995**, *36*, 8737–8740.
(20) Liu, R. A Combined Allylic Azide Rearrangement and Intramolecular Schmidt Reaction - Discovery, Development, And Application. *Ph.D Diss. Univ. Kansas* **2003**.
(21) Lalonde, R. L.; Sherry, B. D.; Kang, E. J.; Toste, F. D. Gold (I)-Catalyzed Enantioselective Intramolecular Hydroamination of Allenes. *J. Am. Chem. Soc.* **2007**, *129*, 2452–2453.
(22) Espenson, J. H. *Chemical Kinetics and Reaction Mechanisms*; McGraw-Hill, Inc: New York, 1995.
(23) Jaffe, H. H. A Reexamination of the Hammett Equation. *Chem. Rev.* **1973**, *53*, 191–261.
(24) Dash, C.; Yousufuddin, M.; Cundari, T. R.; Dias, H. V. R. Gold-Mediated Expulsion of Dinitrogen from Organic Azides. *J. Am. Chem. Soc.* **2013**, *135*, 15479–15488.

Chapter 5. Kinetic Resolution of Cyclic Secondary Azides using an Enantioselective Copper(I) Catalyzed Azide-Alkyne Cycloaddition*

5.1 Introduction

The copper(I) catalyzed azide-alkyne cycloaddition reaction (CuAAC)[1,2] is an important transformation. Applications for CuAAC penetrate numerous sub-disciplines, including chemical biology, medicinal chemistry, and polymer chemistry.[3–5] This click reaction[6] is operationally simple, functional group tolerant, high yielding, and broad in scope. Furthermore, the triazole ring is gaining recognition as a protease resistant peptidomimetic.[4] Biologically active α-chiral triazoles have been reported (Figure 5.1).[7–12]

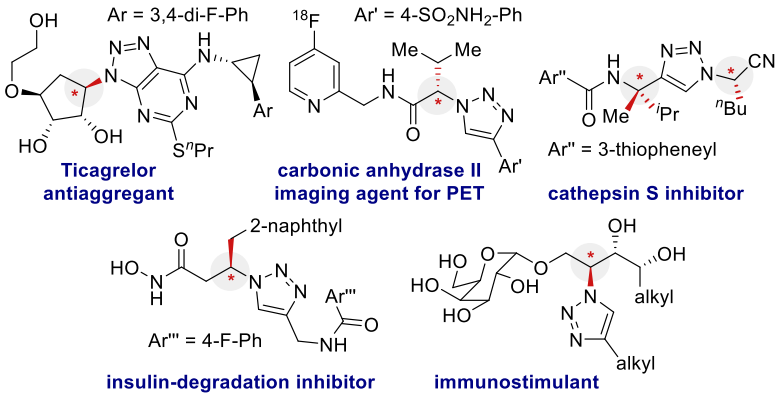

Figure 5.1 Representative Bioactive α-Chiral Triazoles

Due to the prevalence of α-amino acid derived amides, an enantioselective CuAAC (E-CuAAC) reaction would be useful for accessing α-*N*-chiral triazoles. However, E-CuAAC has proven challenging in part because i) both cycloaddition components have linear

*Reprinted (adapted) with permission from Alexander, J. R.; Ott, A. A.; Liu, E-C.; Topczewski, J. J. *Org. Lett.* **2019**, *21*, 4355-4358. Copyright (2019) American Chemical Society

geometries, ii) CuAAC does not require a ligand, and iii) the product triazole is a competent CuAAC ligand.[13] Therefore, E-CuAAC must kinetically outcompete the background CuAAC reaction.

A few reports describe kinetic resolution,[14–16] dynamic kinetic resolution,[17] or desymmetrization[18–21] for E-CuAAC.[22] The majority of successful E-CuAAC reactions generate α-*C*-chiral triazoles, where the new stereocenter is *alkyne* derived.[15,16,18,20,21] The original E-CuAAC reported by Fokin and Finn is the state-of-the-art E-CuAAC kinetic resolution for α-*N*-chiral triazole formation, where the new stereocenter is derived from the *azide* component (Scheme 5.1a).[14] The authors provided only two examples of kinetic resolution with a selectivity factor (*s*) of 3.2 and 8 respectively (ca. 70:30 er and 84:16 er, assuming 40% conversion of the azide). Using the same conditions, the desymmetrization of two *bis*-azides were reported to result predominantly in *bis*-triazole formation (not shown).

Scheme 5.1 Azide Kinetic Resolution by E-CuAAC

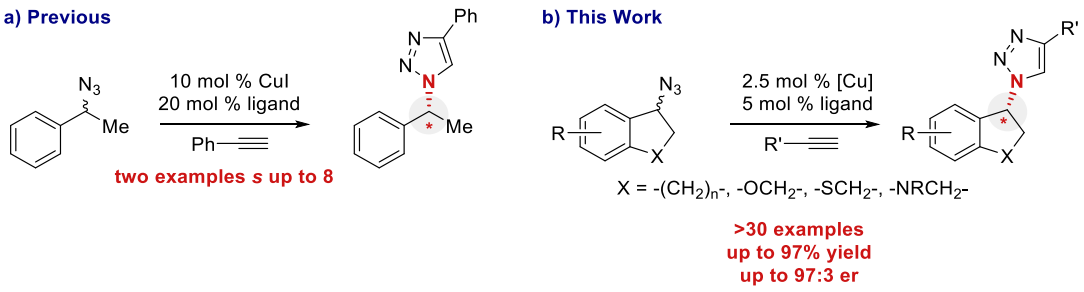

5.2 Results and Discussion

Our lab became interested in using the unique properties of allylic azides to establish α-*N*-chiral centers though dynamic kinetic resolution.[23–25] Recently, we reported the first E-CuAAC reaction by dynamic kinetic resolution.[17] This work prompted an exploration of E-CuAAC by azide kinetic resolution for α-*N*-chiral triazole synthesis (Scheme 5.1b). Reported herein is a successful expansion of the kinetic resolution by E-CuAAC.

Our investigation began with azide **5.1**, alkyne **5.2**, and commercially available PYBOX ligands (Table 5.1, entries 1-3). Minimal enantioselectivity was observed with these ligands, confirming the report from Fokin and Finn. A wide variety of chiral ligands were screened consisting of numerous ligand classes (entries 4-5 and Supporting Information).* Only the aryl-PYBOX ligands provided reasonable enantioselectivity, with ligand **L5** providing the best selectivity among the ligands screened. The data obtained are reported here with er instead of the selectivity parameter *s* because i) er is more synthetically meaningful, ii) er is directly obtained by chiral HPLC, and iii) several kinetic assumptions are made when deriving *s* which are likely faulty for E-CuAAC based on reported CuAAC kinetics.[26,27] One could convert the reported er to a presumed *s* by assuming 40% conversion for reactions approaching completion. Lowering the reaction temperature resulted in an increase in enantioselectivity, albeit at the cost of conversion (entries 6-8). The reaction was faster in DME or $PhCF_3$ as the solvent, relative to CH_2Cl_2, and the enantioselectivity was maintained. When using $PhCF_3$ as the solvent, the reaction

* See supporting information of this manuscript: *Org. Lett.* **2019**, *21*, 4355-4358.

was complete within 48 h (entry 11, see the Supporting Information for additional optimization).*

Table 5.1 E-CuAAC Optimization by Kinetic Resolution

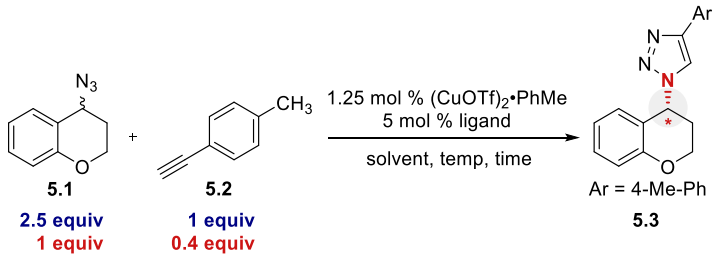

entry	ligand	solvent	temperature	yield (%)[a]	er[b]
1	(*R*)-L1	CH_2Cl_2	rt	**88** (**35**)	55:45
2	(*R*)-L2	CH_2Cl_2	rt	**55** (**22**)	50:50
3	(*R*)-L3	CH_2Cl_2	rt	**92** (**37**)	22:78
4	(*R*)-L4	CH_2Cl_2	rt	**95** (**38**)	21:79
5	(*S*)-L5	CH_2Cl_2	rt	**96** (**38**)	80:20
6[c]	(*S*)-L5	CH_2Cl_2	0 °C	**84** (**34**)	84:16
7[c,d]	(*S*)-L5	CH_2Cl_2	-15 °C	**64** (**26**)	86:14
8[c,e]	(*S*)-L5	CH_2Cl_2	-20 °C	**34** (**14**)	89:11
9[c,d]	(*S*)-L5	DME	-15 °C	**87** (**35**)	86:14
10[c,d]	(*S*)-L5	$PhCF_3$	-15 °C	**92** (**37**)	88:12
11[c,f]	(*S*)-L5	$PhCF_3$	-15 °C	**92** (**37**)	88:12

Reactions conducted with azide **5.1** (0.125 mmol) and alkyne **5.2** (0.05 mmol) at 0.1 M in varying solvent with $(CuOTf)_2$·PhMe (0.62 µmol) and varying ligand (2.5 µmol) for 24 h. All yield and er values reflect the average of duplicate trials. [a]Yield determined using calibrated GC with triphenylmethane as an internal standard. The yield is calculated based on either the **alkyne** (limiting reagent) or **azide** (kinetic resolution component, in parenthesis). [b]Chiral HPLC was used to determine er. [c]Concentration was 0.125 M. [d]Time was 72 h. [e]Time was 96 h. [f]Time was 48 h. rt = room temperature.

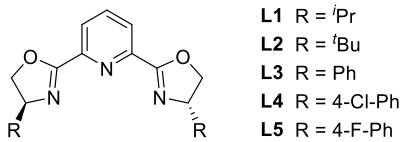

* See supporting information of this manuscript: *Org. Lett.* **2019**, *21*, 4355-4358.

With the optimized conditions in hand, the scope of the alkyne coupling partner was investigated (Scheme 5.2). The model substrate was isolated in comparable yield and er as expected (**5.3**). Other aryl alkynes were tolerated with electron rich (**5.4-5.5**), electron neutral (**5.6-5.7**), and electron deficient substituents (**5.8-5.10**) on the arene. Substituents *meta*- and *ortho*- on the aryl alkyne provided good enantioselectivity (**5.11-5.14**). Ethyl propiolate (**5.15**), cycloalkyl alkynes (**5.16-5.17**), and a heterocyclic alkyne (**5.18**) were tolerated, although several substrates required higher catalyst loadings or longer reaction times to reach higher conversion. It should be noted that long reaction times are not uncommon for other E-CuAAC reactions.[15,18,19]

The scope of the azide component that could be kinetically resolved was explored (Scheme 5.3). Substituents on the chromane arene core were tolerated including methyl (**5.19**) and halogens (**5.20-5.22**). Groups could also be added α to the oxygen atom (**5.23**). Azido-tetrahydroquinolines with various *N*-protecting groups (**5.24-5.26**) and the free NH (**5.27**) provided triazoles in high yield and acceptable enantioselectivity. Azido-thiochromanes (**5.28-5.29**), azido-benzofuran (**5.30**), and azido-indane (**5.31-5.32**) could also be resolved. Substrates **5.31-5.32** are noteworthy because the original E-CuAAC reported by Fokin and Finn described this as a problematic substrate ($s < 1.3$).[14] Acyclic substrate **5.33** provided slower conversion and slightly reduced selectivity.

Scheme 5.2 Substrate Scope of Alkyne Coupling Partner

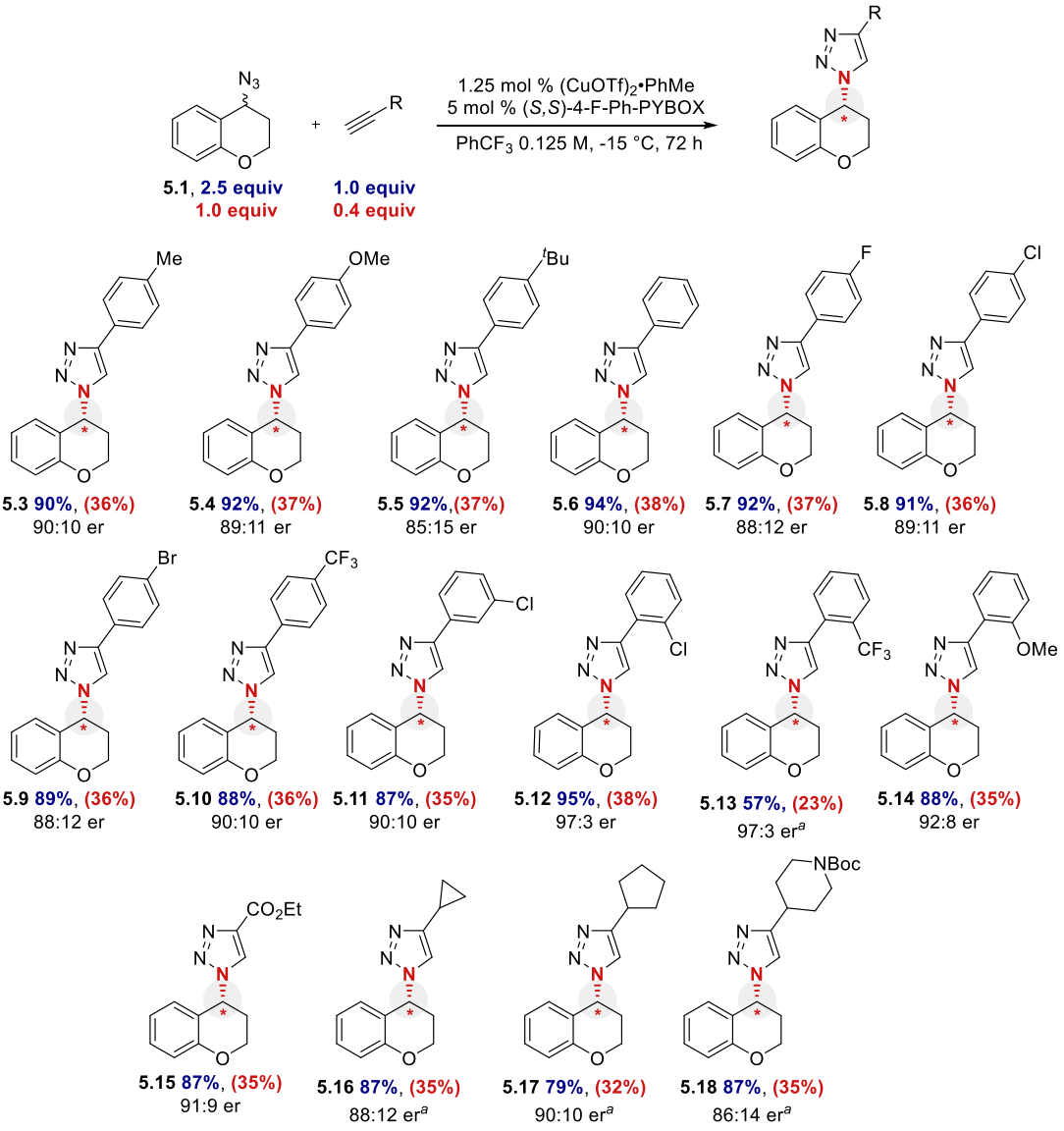

Isolated yields are reported. The yield is calculated based on either the **alkyne** (limiting reagent) or **azide** (kinetic resolution component, in parentheses). Enantiomeric ratio was determined by chiral HPLC. Yield and er values are the average of duplicate trials. [a]2.5 mol % $(CuOTf)_2 \cdot PhMe$, 10 mol% (*S,S*)-4-F-Ph-PYBOX and 0.1 M in $PhCF_3$.

Scheme 5.3 Substrate Scope of Azide Coupling Partner

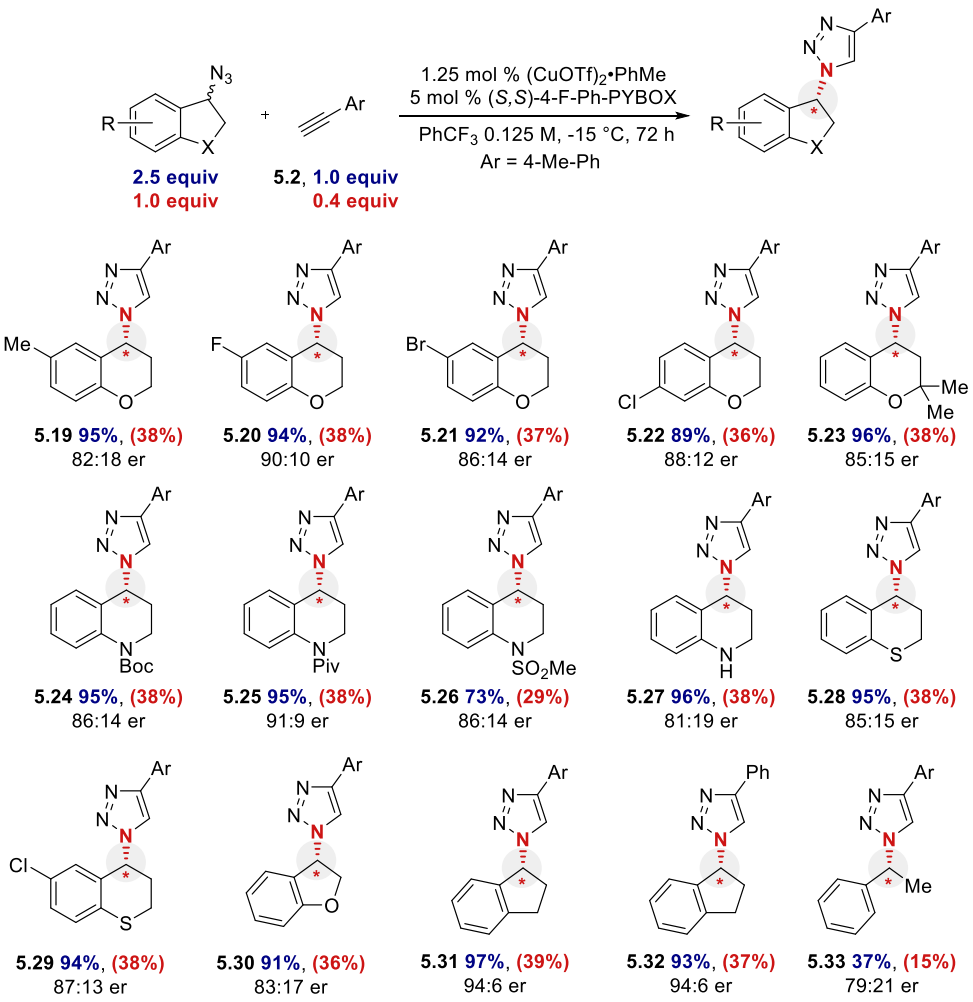

Isolated yields are reported. The yield is calculated based on either the **alkyne** (limiting reagent) or **azide** (kinetic resolution component, in parentheses). Enantiomeric ratio was determined by chiral HPLC. Yield and er values are the average of duplicate trials.

Chiral alkyne **5.34** was used to test for matched/mismatched behavior (Scheme 5.4). Treating azide *rac*-**5.1** with chiral alkyne **5.34** and either enantiomer of ligand **L4** resulted in moderate yield with opposite diastereoselectivity (14:1 and 1:13). This reversal of diastereoselectivity indicates this reaction is under catalyst control.

Scheme 5.4 Matched/Mismatched Experiment

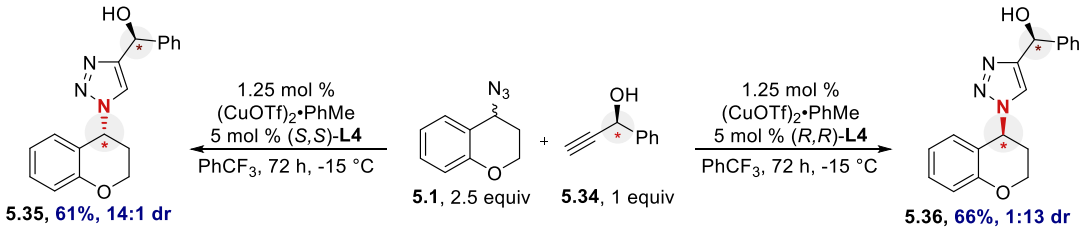

The kinetic resolution could be successfully scaled to provide more than one gram of triazole product (Scheme 5.5). The initial enantioselectivity was 89:11 er which corresponds to an s = 13.5. The enantiopurity could be enhanced upon recrystallization (99:1 er). The excess azide was recovered (76:24 er) and racemized upon exposure to catalytic $AgPF_6$.[28] The azide could then be recycled and used in a subsequent reaction. The ability to recycle the recovered azide improves the overall efficiency of the reaction. The (*R*)-**5.1** enantiomer preferentially reacted with the catalyst derived from ligand (*S,S*)-**L5**. This was determined by analyzing scalemic azide recovered from the reaction. The scalemic azide was compared to a sample of (*S*)-**5.1** which was accessed via diazo transfer from commercially available (*S*)-3,4-dihydro-2H-chromen-4-amine. The same analysis was conducted with azide recovered in the synthesis of triazoles **5.12** and **5.18**, which confirmed the absolute configuration of the product. The configuration of the other triazole products were assigned based on analogy.

Scheme 5.5 Gram Scale Reaction and Racemization of Recovered Azide

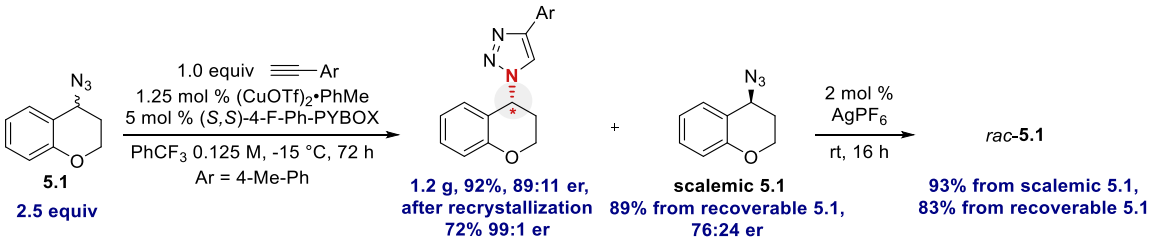

5.3 Conclusion

This report describes an expanded scope for both the azide and alkyne coupling partners in an E-CuAAC. The products of this kinetic resolution are α-*N*-chiral triazoles and can be obtained in up to 97% yield and up to 97:3 er. The reaction can be conducted to isolate more than one gram of product and the excess azide can be recovered, racemized and recycled. The er of the product triazoles can be readily improved to 99:1 with a single recrystallization.

5.4 References

(1) Tornøe, C. W.; Christensen, C.; Meldal, M. Peptidotriazoles on Solid Phase : [1,2,3]-Triazoles by Regiospecific Copper (I)-Catalyzed 1,3-Dipolar Cycloadditions of Terminal Alkynes to Azides. *J. Org. Chem.* **2002**, *67*, 3057–3064.

(2) Rostovtsev, V. V.; Green, L. G.; Fokin, V. V.; Sharpless, K. B. A Stepwise Huisgen Cycloaddition Process: Copper(I)-Catalyzed Regioselective "Ligation" of Azides and Terminal Alkynes. *Angew. Chem. Int. Ed.* **2002**, *41*, 2596–2599.

(3) Meldal, M.; Tornøe, C. W. Cu-Catalyzed Azide-Alkyne Cycloaddition. *Chem. Rev.* **2008**, *108*, 2952–3015.

(4) Pedersen, D. S.; Abell, A. 1,2,3-Triazoles in Peptidomimetic Chemistry. *Eur. J. Org. Chem.* **2011**, 2399–2411.

(5) Finn, M. G.; Fokin, V. V. Click Chemistry: Function Follows Form. *Chem. Soc. Rev.* **2010**, *39*, 1231–1232.

(6) Kolb, H. C.; Finn, M. G.; Sharpless, K. B. Click Chemistry: Diverse Chemical Function from a Few Good Reactions. *Angew. Chem. Int. Ed.* **2001**, *40*, 2004–2021.

(7) Ellman, J. A.; Jain, R. K.; Wood, W. J. L.; Tsuruoka, H.; Patterson, A. W. Substrate Activity Screening: A Fragment-Based Method for the Rapid Identification of Nonpeptidic Protease Inhibitors. *J. Am. Chem. Soc.* **2005**, *127*, 15521–15527.

(8) Lee, T.; Cho, M.; Ko, S.-Y.; Youn, H.-J.; Baek, D. J.; Cho, W.-J.; Kang, C.-Y.; Kim, S. Synthesis and Evaluation of 1,2,3-Triazole Containing Analogues of the Immunostimulane Alpha-GalCer. *J. Med. Chem.* **2007**, *50*, 585–589.

(9) Patterson, A. W.; Wood, W. J. L.; Hornsby, M.; Lesley, S.; Spraggon, G.; Ellman, J. A. Identification of Selective, Nonpeptidic Nitrile Inhibitors of Cathepsin S Using the Substrate Activity Screening Method. *J. Med. Chem.* **2006**, *49*, 6298–6307.

(10) Huber, K.; Hamad, B.; Kirkpatrick, P. Fresh from the Pipeline: Ticagrelor. *Nat. Rev. Drug Discov.* **2011**, *10*, 255–256.

(11) Deprez-Poulain, R.; Hennuyer, N.; Bosc, D.; Liang, W. G.; Marechal, X.; Charton, J.; Totobenazara, J.; Berte, G.; Jahklal, J.; Verdelet, T.; et al. Catalytic Site Inhibition of Insulin-Degrading Enzyme by a Small Molecule Induces Glucose Intolerance in Mice. *Nat. Commun.* **2015**, *6*, 1–13.

(12) Mocharla, V. P.; Walsh, J. C.; Padgett, H. C.; Su, H.; Fueger, B.; Weber, W. A.; Czernin, J.; Kolb, H. C. From In Situ to In Vivo : An In Situ Click-Chemistry-Derived Carbonic Anhydrase II Imaging Agent for Positron Emission Tomography. *ChemMedChem* **2013**, *8*, 43–48.

(13) Rodionov, V. O.; Fokin, V. V.; Finn, M. G. Mechanism of the Ligand-Free CuI-Catalyzed Azide-Alkyne Cycloaddition Reaction. *Angew. Chem. Int. Ed.* **2005**, *44*, 2210–2215.

(14) Meng, J. C.; Fokin, V. V.; Finn, M. G. Kinetic Resolution by Copper-Catalyzed Azide-Alkyne Cycloaddition. *Tetrahedron Lett.* **2005**, *46*, 4543–4546.

(15) Brittain, W. D. G.; Buckley, B. R.; Fossey, J. S. Kinetic Resolution of Alkyne-Substituted Quaternary Oxindoles via Copper Catalysed Azide-Alkyne

Cycloadditions. *Chem. Commun.* **2015**, *51*, 17217–17220.
(16) Brittain, W. D. G.; Chapin, B. M.; Zhai, W.; Lynch, V. M.; Buckley, B. R.; Anslyn, E. V.; Fossey, J. S. The Bull-James Assembly as a Chiral Auxiliary and Shift Reagent in Kinetic Resolution of Alkyne Amines by the CuAAC Reaction. *Org. Biomol. Chem.* **2016**, *14*, 10778–10782.
(17) Liu, E.-C.; Topczewski, J. J. Enantioselective Copper Catalyzed Alkyne-Azide Cycloaddition by Dynamic Kinetic Resolution. *J. Am. Chem. Soc.* **2019**, *141*, 5135–5138.
(18) Zhou, F.; Tan, C.; Tang, J.; Zhang, Y. Y.; Gao, W. M.; Wu, H. H.; Yu, Y. H.; Zhou, J. Asymmetric Copper(I)-Catalyzed Azide-Alkyne Cycloaddition to Quaternary Oxindoles. *J. Am. Chem. Soc.* **2013**, *135*, 10994–10997.
(19) Page, P.; Martin, J.; Stephenson, G.; Gaumont, A.-C.; Deschamps, D.; Buttress, J.; Lancelot, M.; Sheldon, A.; Alayrac, C. An Investigation of the Asymmetric Huisgen 'Click' Reaction. *Synlett* **2013**, *24*, 2723–2729.
(20) Zheng, Z.-J.; Song, T.; Xu, L.-W.; Deng, Y.; Xu, Z.; Zhou, W.; Li, L. Enantioselective Copper-Catalyzed Azide-Alkyne Click Cycloaddition to Desymmetrization of Maleimide-Based Bis(Alkynes). *Chem. - Eur. J.* **2014**, *21*, 554–558.
(21) Osako, T.; Uozumi, Y. Enantioposition-Selective Copper-Catalyzed Azide-Alkyne Cycloaddition for Construction of Chiral Biaryl Derivatives. *Org. Lett.* **2014**, *16*, 5866–5869.
(22) Brittain, W. D. G. G.; Buckley, B. R.; Fossey, J. S. Asymmetric Copper-Catalyzed Azide-Alkyne Cycloadditions. *ACS Catal.* **2016**, *6*, 3629–3636.
(23) Ott, A. A.; Goshey, C. S.; Topczewski, J. J. Dynamic Kinetic Resolution of Allylic Azides via Asymmetric Dihydroxylation. *J. Am. Chem. Soc.* **2017**, *139*, 7737–7740.
(24) Porter, M. R.; Shaker, R. M.; Calcanas, C.; Topczewski, J. J. Stereoselective Dynamic Cyclization of Allylic Azides : Synthesis of Tetralins, Chromanes, and Tetrahydroquinolines. *J. Am. Chem. Soc.* **2018**, *140*, 1211–1214.
(25) Ott, A. A.; Packard, M. H.; Ortuño, M. A.; Johnson, A.; Suding, V. P.; Cramer, C. J.; Topczewski, J. J. Evidence for a Sigmatropic and an Ionic Pathway in the Winstein Rearrangement. *J. Org. Chem.* **2018**, *83*, 8214–8224.
(26) Keith, J. M.; Larrow, J. F.; Jacobsen, E. N. Practical Considerations in Kinetic Resolution Reactions. *Adv. Synth. Catal.* **2001**, *343*, 5–26.
(27) Worrell, B. T.; Malik, J. A.; Fokin, V. V. Direct Evidence of a Dinuclear Copper Intermediate in Cu(I)-Catalyzed Azide-Alkyne Cycloadditions. *Science* **2013**, *340*, 457–461.
(28) Ott, A. A.; Topczewski, J. J. Catalytic Racemization of Activated Organic Azides. *Org. Lett.* **2018**, *20*, 7253–7256.

Chapter 6. Efforts Towards a DKR with Activated Azides

6.1 Introduction

Chiral amines are ubiquitous in bioactive molecules, natural products, and agrochemicals.[1] In particular, fully substituted chiral amines are challenging to access synthetically. The ability to synthesize these molecules using a DKR of activated azides would be a novel approach to chiral amine synthesis. Efforts in our group were initially focused on using allylic azides as substrates for these transformations to provide access to the desired chiral amine motif. Allylic azides might be suitable substrates because they often exist as mixtures of isomers due to their propensity to rearrange at ambient temperature via the Winstein rearrangement.[2] Using symmetric substrates, this rearrangement was utilized as the racemization pathway for a DKR.[3,4] However, non-symmetric allylic azides that do not have an achiral isomer do not racemize via the Winstein rearrangement because it is a concerted, stereospecific process. However, racemization of these allylic azides could be promoted using a Lewis acid catalyst.[5] Other activated (non-allylic) azides could be racemized under similar conditions. With a pathway for racemization identified, efforts to identify an appropriate reaction to complete the DKR were undertaken (Scheme 6.1).

Scheme 6.1 General DKR Strategy with Activated Azides

6.2 E-CuAAC Reaction via DKR of Azides

Due to our lab's experience with asymmetric click reactions,[4,6] the possibility of coupling the enantioselective copper(I) catalyzed azide-alkyne cycloaddition (E-CuAAC) reaction to the previously identified catalytic racemization was explored. If successful, this would generate α-chiral triazoles, which have applications across a range of fields.[7–10] Our previous work identified benzylic azides as suitable substrates for kinetic resolution by the E-CuAAC reaction.[6] Slightly modified conditions provided triazole **6.3** in good yield with 85:15 er (Scheme 6.2a). This result provided a starting point for translating the kinetic resolution to a dynamic kinetic resolution.

Scheme 6.2 a) Kinetic Resolution of Azide **6.1**. b) Attempted DKR with Azide **6.1**.

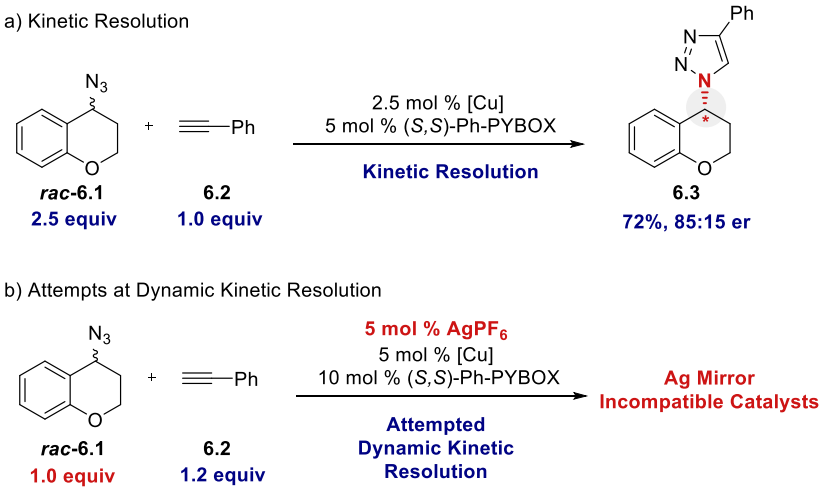

An initial experiment using azide **6.1** and alkyne **6.2** under E-CuAAC conditions with added $AgPF_6$ resulted in no product formation (Scheme 6.2b). Addition of the racemization catalyst to the reaction mixture led to immediate color change and formation of silver mirror. The Cu(I) salt and the Ag(I) salt undergo a facile redox reaction to form

Cu(II) and Ag(0).[11] This outcome highlights the complications involved in developing a DKR from a kinetic resolution. Individually, each catalyst can perform the desired reaction. However, when these catalysts are combined in the same reaction vessel, the potential for catalyst-catalyst interactions cannot be overlooked. For a successful reaction, it is necessary for one catalyst to promote the racemization and a second catalyst to perform the desired E-CuAAC reaction (Scheme 6.3a). Unfortunately, Ag(I) salts were incompatible with the CuAAC reaction; however, it was unclear if other racemization catalysts could be used in its place.

Scheme 6.3 a) General Approach for DKR of Activated Azides using an E-CuAAC Reaction. b) Flow Chart of Requirements for Successful E-CuAAC Reaction

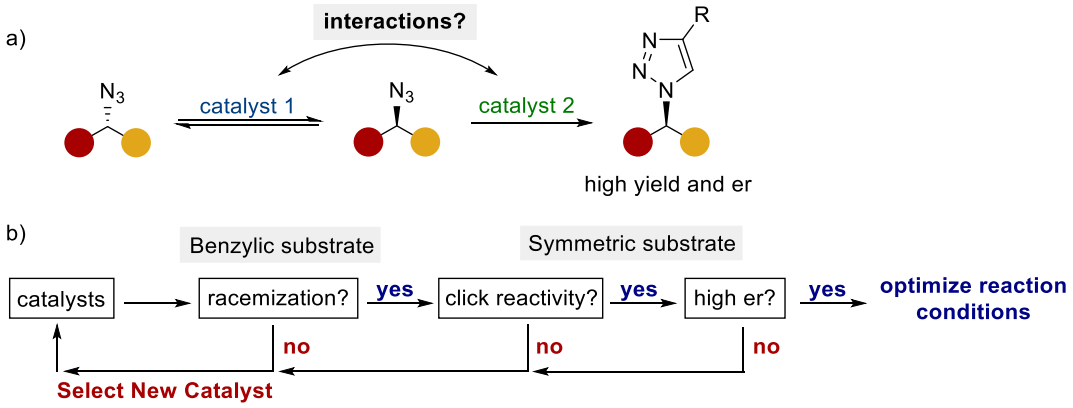

It was important to develop an assay to quickly identify whether conditions would i) promote racemization, ii) promote click reactivity and iii) be enantioselective (Scheme 6.3b). Using an enantioenriched azide, it was straightforward to determine whether certain conditions resulted in racemization. To probe the reactivity and enantioselectivity of the desired transformation, the reaction was conducted using a symmetric allylic azide

substrate. Liu had reported using symmetric allylic azide substrates for an E-CuAAC reaction.[4] With symmetric azide **6.4** and Liu's unoptimized reaction conditions, the desired triazole was synthesized (Table 6.1 entry 1, 86:14 er). This reaction provided a benchmark for comparison when adding a racemization catalyst.

Table 6.1 Effect of Racemization Catalyst on er of Triazole **6.5**[a]

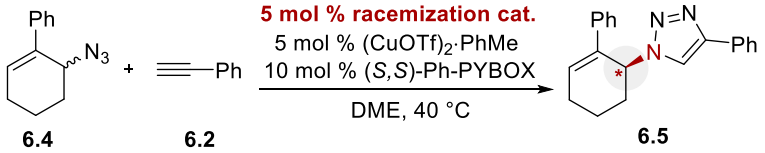

6.4 **6.2** **6.5**

entry	racemization cat.	er[a]	entry	racemization cat.	er[b]
1	none	86:14	8	$B(C_6F_5)_3$	--
2	JohnPhosAuSbF$_6$	67:33	9	BF_3•OEt_2	--
3	$Zn(OTf)_2$	53:47	10	$Ti(O^iPr)_4$	78:22
4	$Cu(OTf)_2$	51:49	11	$Y(OTf)_3$	57:43
5	$Al(O^iPr)_3$	80:20	12	$Dy(OTf)_3$	63:37
6	$Al(O^tBu)_3$	80:20	13	$Er(OTf)_3$	59:41
7	BPh_3	86:14	14	$Pr(OTf)_3$	63:37

[a]Reaction conducted with azide **6.4** (0.05 mmol), alkyne **6.2** (0.06 mmol), [Cu] catalyst (1.25 μmol) ligand (5 μmol), and racemization catalyst (1.25 μmol) in DME (0.17 M) at 40 °C for 24 h. [b]er measured by chiral HPLC analysis.

A variety of racemization catalysts were screened in this manner (Table 6.1). Other catalysts previously shown to promote racemization, JohnPhosAuSbF$_6$ and $Zn(OTf)_2$,[5] resulted in reduced enantioselectivity (entries 2 and 3). Use of $Cu(OTf)_2$ led to near racemic formation of the desired triazole (entry 4). A moderate reduction in enantioselectivity was observed with aluminum Lewis acids (entries 5 and 6). To our delight, BPh_3 provided no loss of enantioselectivity (entry 7). Other boron Lewis acids inhibited triazole formation

(entries 8 and 9). Lanthanide triflates and $Y(OTf)_3$ provided lower enantioselectivities compared to the benchmark reaction (entries 11-14).

Some Lewis acid catalysts provided only a slight decrease in enantioselectivity of the desired triazole **6.5**, however, it was uncertain whether they would promote racemization of the desired benzylic azide starting material (**6.1**). Both aluminum- and boron-based Lewis acids were investigated for their ability to racemize enantioenriched azide **6.1** (Table 6.2).

Table 6.2 Catalytic Racemization of Azide **6.1**[a]

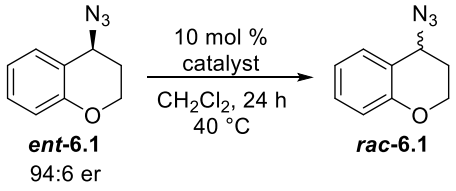

***ent*-6.1**
94:6 er

***rac*-6.1**

entry	catalyst	er[b]
1	$Al(O^iPr)_3$	94:6
2	$Al(O^tBu)_3$	94:6
3	BPh_3	94:6
4	$B(C_6F_5)_3$	50:50

[a]Reaction conducted with azide **6.1** (5.7 μM) and catalyst (0.57 μM) in CH_2Cl_2 (0.05 M) at 40 °C. [b]er measured by chiral HPLC analysis.

Unfortunately, no racemization was observed using $Al(O^iPr)_3$, $Al(O^tBu)_3$, or BPh_3 (entries 1-3). The stronger Lewis acid, $B(C_6F_5)_3$, did result in racemization (entry 4), however, it shuts down the E-CuAAC reaction (see Table 6.1, entry 8). While not effective for the E-CuAAC reaction, racemization using $B(C_6F_5)_3$ was further studied (see section 6.6 Experimental). Of the catalysts investigated, none met the three required criteria listed in

the flow chart (Scheme 6.2b). Weaker Lewis acids generally did not inhibit the reactivity of the reaction but were either not able to promote racemization or resulted in diminished enantioselectivity. Stronger Lewis acids greatly diminished the conversion, often resulting in only trace amounts of product. Other racemization conditions besides addition of Lewis acid catalysis were also investigated. A combination of Dowex 50Wx4 in HFIP was found to racemize azide **6.1** (for more details see 6.6 Experimental). Unfortunately, both the acidic resin and HFIP inhibited the E-CuAAC reaction.

The observed catalyst compatibility issues likely arise between the Lewis basic PYBOX ligand and the Lewis acidic racemization catalyst. The Cu(I) salt and the chiral ligand are stirred to generate the chiral Cu(I) complex which results in an orange solution. However, upon addition of several of the racemization catalysts, the orange color rapidly dissipated and the solution became colorless. Presumably the PYBOX ligand is binding to the racemization catalyst rather than the Cu center, thereby mitigating the enantioselectivity and diminishing the enhanced reactivity via ligand accelerated catalysis.[12] Currently, there are no ongoing investigations into alternate catalysts to promote this transformation. Rather, the insights gained from this project were used to investigate other reactions that may be more amenable to the racemization conditions.

6.3 Azide Reduction using Chiral Catalysts

The direct reduction of racemic tertiary azides via DKR was investigated. This reduction would directly afford α,α-disubstituted amines. Azide **6.9** was identified as a suitable substrate to explore this transformation. The synthesis of azide **6.9** began with ketone **6.6**. A simple methyl addition (MeMgBr or MeLi) proved to be insufficient to

access tertiary alcohol **6.7** in a reasonable yield. However, utilizing $CeCl_3$ in combination with MeLi provided clean conversion to alcohol **6.7** (Scheme 6.4). Treatment of alcohol **6.7** with $Zn(OTf)_2$ and TMS-N_3 resulted in formation of azide **6.8**. Reduction with $LiAlH_4$ provided racemic amine **6.9**.

Scheme 6.4 Synthesis of Azide **6.8** and Amine **6.9**

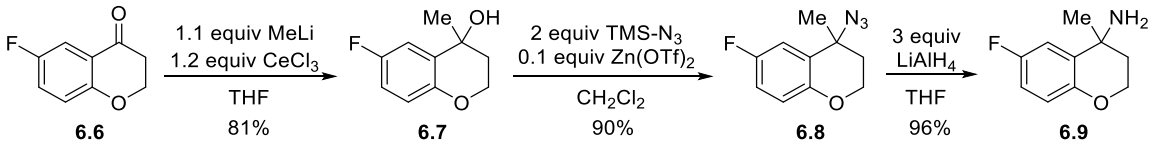

With azide **6.8** in hand, attention was turned to investigating various reduction conditions to generate amine **6.9**. As amines tend to be good ligands for metals, it was unclear whether there would be significant product inhibition under catalytic conditions. Therefore, initial efforts focused on conversion. Using 5:2 HCO_2H /TEA as the hydrogen source with various ruthenium catalysts in either MeCN or MeOH provided good conversion (Table 6.3, entries 1-6).

Table 6.3 Reduction of Azide **6.8** Using Ruthenium Catalysts[a]

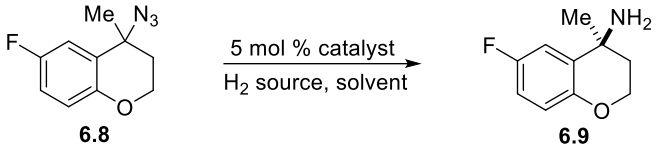

6.8 **6.9**

entry	catalyst	H_2 source	solvent	temp	conv (%)[b]	er[c]
1	RuCl[(*R,R*)-FsDPEN](*p*-cymene)	HCO_2H/TEA	MeCN	60 °C	>95	nd
2	RuCl[(*S,S*)-Teth-TsDPEN]	HCO_2H/TEA	MeCN	60 °C	>95	nd
3	RuCl[(S,S)-Ts-DPEN](*p*-cymene)	HCO_2H/TEA	MeCN	60 °C	61	nd
4	RuCl[(*R,R*)-FsDPEN](*p*-cymene)	HCO_2H/TEA	MeOH	60 °C	79	nd
5	RuCl[(*S,S*)-Teth-TsDPEN]	HCO_2H/TEA	MeOH	60 °C	>95	nd
6	RuCl[(S,S)-Ts-DPEN](*p*-cymene)	HCO_2H/TEA	MeOH	60 °C	70	nd
7[d]	RuCl[(*R,R*)-FsDPEN](*p*-cymene)	HCO_2Na	H_2O/DMF	60 °C	>95	nd
8[d]	RuCl[(*S,S*)-Teth-TsDPEN]	HCO_2Na	H_2O/DMF	60 °C	>95	nd
9[d]	RuCl[(S,S)-Ts-DPEN](*p*-cymene)	HCO_2Na	H_2O/DMF	60 °C	>95	nd
10[d]	RuCl[(*S,S*)-Teth-TsDPEN]	HCO_2Na	H_2O/DMF	rt	92	nd
11[d]	RuCl[(*S,S*)-Teth-TsDPEN]	HCO_2H/TEA	MeOH	rt	<10	nd
12[e]	RuCl[(*S,S*)-Teth-TsDPEN]	HCO_2H/TEA	MeOH	60 °C	29	51:49
13[e]	RuCl[(*S,S*)-Teth-TsDPEN]	HCO_2Na	H_2O/DMF	rt	52	50:50

[a]Reaction conducted with azide **6.8** (0.05 mmol), catalyst (2.5 μM), sodium HCO_2Na (0.25 mmol) or 5:2 HCO_2H/TEA (0.5 mL/mmol) in solvent (0.25 M). [b]Conversion was determined by GC-FID analysis using 4-F-biphenyl as a standard. [c]er determined by chiral HPLC analysis. [d]Conversion determined by ^{1}H NMR using 4-F-biphenyl as a standard. [e]2.5 mol% catalyst loading. nd = not determined, rt = room temperature.

Alternatively, sodium formate in a mixture of H_2O/DMF at 60 °C resulted in full conversion of the starting material (entries 7-9). Only a slight decrease in conversion was observed when the reaction was conducted at room temperature (entry 10). No enantioselectivity was observed when the reaction was stopped before completion (kinetic resolution conditions) using RuCl[(*S,S*)-Teth-TsDPEN] as the catalyst under either the HCO_2H/TEA conditions or the sodium formate conditions (entries 12-13).

Efforts shifted to other classes of ruthenium catalysts that are known for promoting enantioselective hydrogenations (Table 6.4).[13,14] In IPA under an atmosphere of H_2, near full conversion was observed with several catalysts (entries 1, 3-4).

Table 6.4 Reduction of Azide **6.8** using H_2 with Ruthenium Catalysts[a]

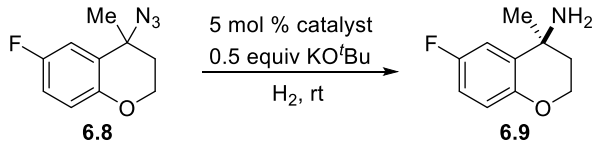

6.8 **6.9**

entry	catalyst	solvent	conv (%)[b]	er[c]
1	$RuCl_2$[(*R*)-DM-BINAP]-[(*R*)-DAIPEN]	IPA	>95	nd
2	$RuCl_2$[(*R*)-(DM-SEGPHOS)]-[(*R*)-DAIPEN]	IPA	10	nd
3	$RuCl_2$[(*R*)-DM-BINAP]-[(*R,R*)-DPEN]	IPA	>95	nd
4	$RuCl_2$[(*R*)-(DM-SEGPHOS)]-[(*R,R*)-DPEN]	IPA	>95	nd
5	$RuCl_2$[(*R*)-(DM-SEGPHOS)]-[(*R,R*)-DPEN]	THF	>95	nd
6	$RuCl_2$[(*R*)-(DM-SEGPHOS)]-[(*R,R*)-DPEN]	PhMe	>95	nd
7	$RuCl_2$[(*R*)-DM-BINAP]-[(*R*)-DAIPEN]	IPA	26	53:47
8	$RuCl_2$[(*R*)-DM-BINAP]-[(*R,R*)-DPEN]	IPA	19	53:47

[a]Reaction conducted with azide **6.8** (0.05 mmol), catalyst (2.5 μM), KO^{t}Bu (0.025 mmol) in solvent (0.1 M). [b]Conversion was determined by GC-FID analysis using 4-F-biphenyl used as standard. [c]er determined by chiral HPLC analysis. nd = not determined

Switching solvents from IPA to THF or PhMe had a minimal impact on the conversion (entries 5-6). Neither $RuCl_2$[(*R*)-DM-BINAP]-[(*R*)-DAIPEN] nor $RuCl_2$[(*R*)-DM-BINAP]-[(*R,R*)-DPEN] resulted in enantioselective formation of the amine under kinetic resolution conditions (53:47, entries 7 and 8).

With the vast array of available chiral phosphine ligands, the enantioselective hydrogenation using $Pd_2(dba)_3$ was explored under an atmosphere of hydrogen. Unfortunately, none of the chiral phosphines investigated provided any appreciable enantioselectivity (Table 6.5).

Table 6.5 Reduction of azide **6.8** using $Pd_2(dba)_3$ and H_2[a]

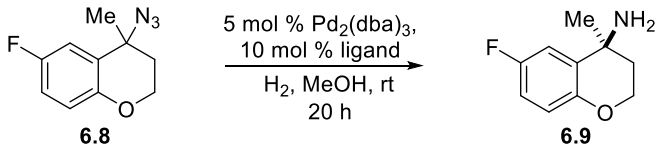

6.8 **6.9**

entry	ligand	conv (%)[b]	er[c]	entry	ligand	conv (%)[b]	er[c]
1	(*R*)-BINAP	45	51:49	9	(*S,S*)-BDPP	11	50:50
2	(*R,R*)-NorPhos	22	51:49	10	(*S,S*)-DIOP	58	51:49
3	(*R*)-SynPhos	42	50:50	11[d]	(*S*)-Tol-BINAP	28	52:48
4	(*R,R*)-Me-DuPhos	55	50:50	12[d]	(*R*)-MeO-BIPHEP	28	50:50
5	(*R*)-QuinoxP	25	51:49	13[d]	(*R*)-DTBM-SEGPHOS	33	50:50
6	(*S,S*)-ChiraPhos	12	50:50	14	(*R*)-L1	43	48:52
7	(*R*)-PhanePhos	36	51:49	15[e]	(*R,R*)-L2	36	50:50
8	(*R,R*)-DIPAMP	49	52:48	16	(*S,S*)-L3	45	51:49

[a]Reaction conducted with azide **6.8** (0.05 mmol), in MeOH (0.5 mL), with $Pd_2(dba)_3$ (2.5 μmol) and ligand (5.0 μmol) under an atmopshere of H_2. [b]Conversion was determined by GC-FID analysis using 4-F-biphenyl as a standard. [c]Chiral HPLC was used to determine er. [d]Reaction used 2.5 mol % $Pd_2(dba)_3$, 5 mol % ligand and was stopped after 4 h. [e]Reaction stopped after 2 h.

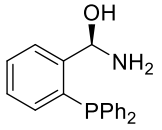

(*R*)-L1

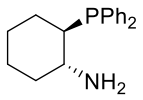

(*R,R*)-L2

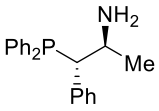

(*S,S*)-L3

Due to the lack of enantioselectivity observed upon reduction of azide **6.8**, other substrates, such as azide **6.12**, were considered. In azide **6.12**, the heteroatom could potentially bind to the catalyst and help bias the reduction of one enantiomer. This substrate was prepared in three steps form ketone **6.6** (Scheme 6.5). Treatment of ketone **6.6** with chloroiodomethane and ^{n}BuLi afforded chlorohydrin **6.10**. An *in situ* Finkelstein reaction followed by nucleophilic displacement by methoxide generated alcohol **6.11**. Azide **6.12** was formed via a Lewis acid catalyzed substitution reaction. Reduction using $LiAlH_4$ afforded amine **6.13**.

Scheme 6.5 Synthesis of Azide **6.12** and Amine **6.13**

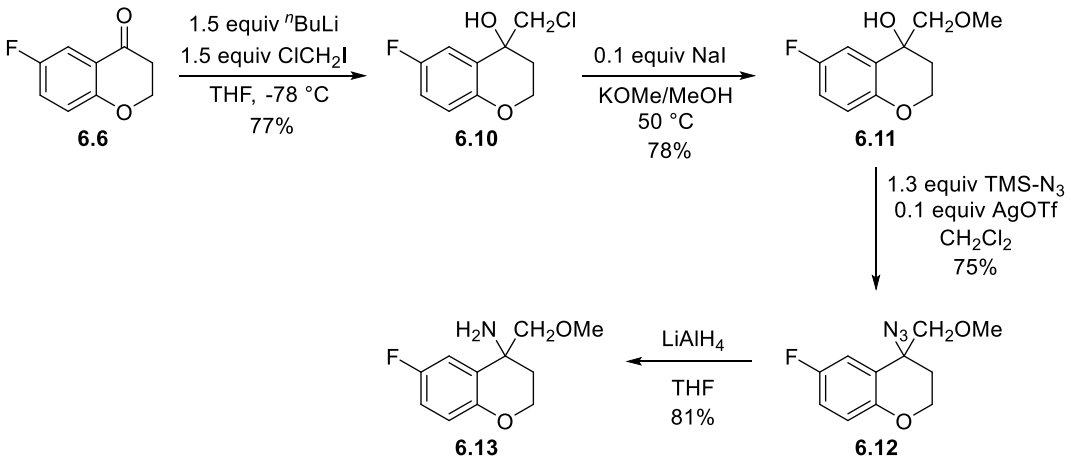

Either low conversion (Table 6.6, entry 1) or lack of enantioselectivity (entries 2-3) was observed using ruthenium catalysts in MeOH with HCO_2H/TEA. Attempts to reduce azide **6.12** using (diamine)$RuCl_2$(bisphosphine) catalysts resulted in poor enantioselectivity (entries 4-5). Other ruthenium catalysts bearing different chiral ligands could be investigated for this transformation.

Table 6.6 Reduction of Azide **6.12** Using Ruthenium Catalysts[a]

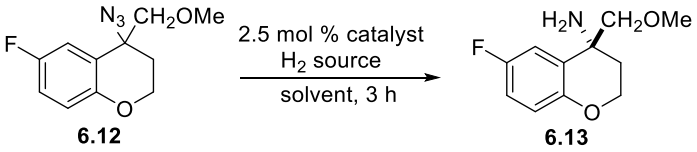

entry	catalyst	H_2 source	solvent	temp	conv (%)[a]	er[b]
1	RuCl[(*S,S*)-Teth-TsDPEN]	HCO_2H/TEA	MeOH	60 °C	<10	nd
2	RuCl[(*R,R*)-FsDPEN](*p*-cymene)	HCO_2H/TEA	MeOH	60 °C	22	50:50
3	RuCl[(S,S)-Ts-DPEN](*p*-cymene)	HCO_2H/TEA	MeOH	60 °C	30	50:50
4[c]	$RuCl_2$[(*R*)-DM-BINAP]-[(*R*)-DAIPEN]	H_2	IPA	rt	64	52:48
5[c]	$RuCl_2$[(*R*)-(DM-SEGPHOS)]-[(*R*)-DAIPEN]	H_2	IPA	rt	21	53:47

[a]Reaction conducted with azide **6.12** (34 μmol) and catalyst (1.7 μmol) in solvent (0.1 M). [b]Conversion was determined by GC-FID analysis using 4-F-biphenyl as a standard. [b]er determined by chiral HPLC analysis. [c]Reaction conducted with 0.5 equiv KO^{t}Bu and was stopped after 5 h. nd = not determined, rt = room temperature.

Chiral iridium catalysts with H_2 have been used for the enantioselective hydrogenation of imines.[15,16] The enantioselectivity can vary depending on the presence or absence of additives, such as iodine.[17–19] Using $[Ir(COD)Cl]_2$ with phosphoramidite ligand **L4** under an atmosphere of H_2 resulted in low conversion (Table 6.7, entry 1). Using the same conditions with KI as an additive did not improve the conversion (entry 2). The addition of I_2, led to moderate conversion, albeit no product formation (entry 3). Switching from a monodentate phosphine ligand to bidentate phosphine ligands resulted in decreased conversion and no product formation (entries 4-5).

Table 6.7 Reduction of Azide **6.12** using H_2 with Iridium or Rhodium Catalysts[a]

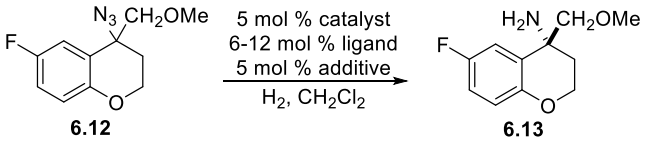

6.12 **6.13**

entry	catalyst	ligand	additive	conv (%)[b]
1[c]	$[Ir(COD)Cl]_2$	(*S,S,S*)-L4	none	15
2[c]	$[Ir(COD)Cl]_2$	(*S,S,S*)-L4	I_2	60
3[c]	$[Ir(COD)Cl]_2$	(*S,S,S*)-L4	KI	<10
4[d]	$[Ir(COD)Cl]_2$	(*S,S*)-ChiraPhos	I_2	25
5[d]	$[Ir(COD)Cl]_2$	(*R*)-BINAP	I_2	28
6	$Rh(COD)_2BF_4$	(*S,S,S*)-L4	none	<10
7	$Rh(COD)_2BF_4$	(*S,S*)-ChiraPhos	none	14
8	$Rh(COD)_2BF_4$	(*R*)-MonoPhos	none	15
9	$Rh(COD)_2BF_4$	(*R,R*)-Me-DuPhos	none	17
10	$Rh(COD)_2BF_4$	(*R*)-QuinoxP	none	<10

[a]Reaction conducted with azide **6.12** (0.05 mmol), catalyst (2.5 μM), ligand (3 or 6 μM). [b]Conversion was determined by GC-FID analysis using biphenyl as a standard. [c]2 mol % catalyst loading, 4.4 mol % ligand. [d]3 mol % catalyst, 6.6 mol % ligand

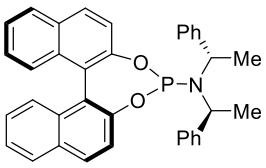

(*S,S,S*)-L4

Cationic rhodium complexes have been shown to promote asymmetric hydrogenation of various types of alkenes.[20] Attempting a reduction using $Rh(COD)BF_4$ with phosphoramidite ligand **L4** (Table 6.7, entry 6) and several bidentate phosphine ligands resulted in low conversion and no product formation (entries 7-10). At this point, it was clear that this was a complex project as there are several catalysts (Ru, Ir, Rh), solvents (e.g. MeOH, MeCN), possible additives (e.g. I_2), and H_2 sources (e.g H_2, HCO_2H/TEA) to consider. As well, we do not have access to a high-pressure reactor to conduct experiments at high pressures of H_2 which many hydrogenation reactions require. Therefore, at this time we have decided to explore other projects.

6.4 Azide Reduction using Chiral Rhodium Catalyst and Acceptor/Acceptor Diazo Compounds

During our lab's efforts to explore a cyclopropanation reaction on allylic azide **6.14**, the desired cyclopropane product **6.16** was not observed (Scheme 6.6a). Instead, diketone **6.19** was observed by both ^1H NMR and HRMS. This product could be observed if the metal carbene reacted with azide rather than the alkene, presumably forming imine **6.17**. Hydrolysis upon work up could result in diketone **6.19**. Li and coworkers reported of a few alkyl azides reacting in this manner.[21]

Scheme 6.6 a) Rhodium-Catalyzed Reaction of Allylic Azide **6.14** with Aryldiazoacetate **6.15** b) Rhodium-Catalyzed Reaction of Tertiary Azide **6.8**

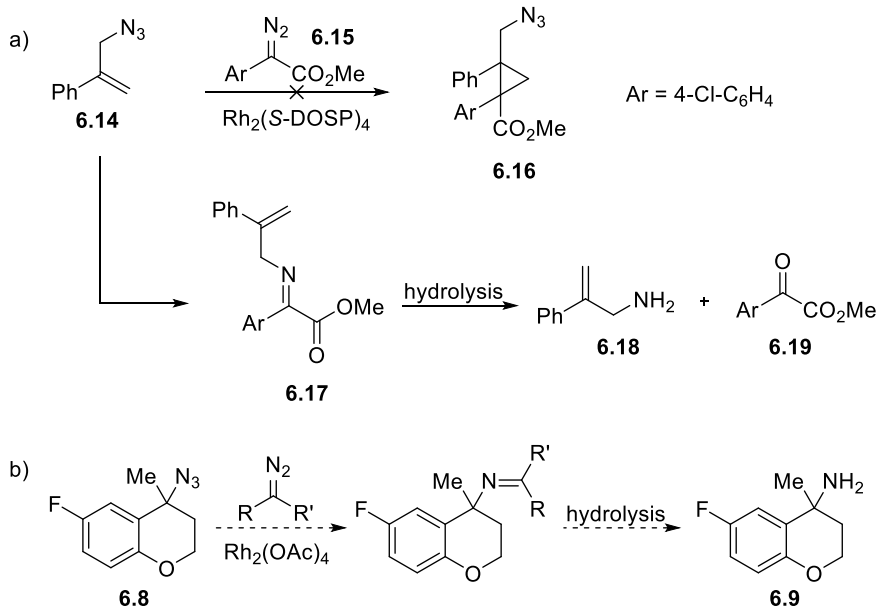

Based on this observation and the report from Li and coworkers,[21] attention was turned to investigate whether tertiary azides could react in same manner to afford chiral amines (Scheme 6.6b). Initial investigations began with tertiary azide **6.8**, $Rh_2(OAc)_4$ and donor/acceptor aryldiazoacetate **6.15**. Unfortunately, azide **6.8** was unreactive under the reaction conditions. While the nucleophilicity of the primary azide was matched with the electrophilicity of the metal carbene generated from aryldiazoacetate **6.15**, the lower nucleophilicity of the tertiary azide resulted in no reactivity under the same conditions. We sought to identify a suitably electrophilic diazo coupling partner.

There are three different classes of diazo compounds: Acceptor/acceptor, donor/acceptor, and donor/donor. These are defined by the electronics on either side of the diazo group (Figure 6.1). Aryldiazoacetate **6.15** is a donor/acceptor derivative, which has intermediary reactivity to form a metal carbene. Potentially, using aryldiazoacetate **6.15**

the metal carbene formed rapidly and dimerized before the carbene could be intercepted by the azide. Moving to a donor/donor diazo compound would likely exacerbate this issue because they more readily form metal carbenes. Therefore, efforts focused on exploring acceptor/acceptor diazo compounds which more slowly generate the metal carbene. Within the class of acceptor/acceptor diazo compounds there are various types depending on the substituents (Figure 6.1, Y and Z) which tunes the nature of the diazo species.

Figure 6.1 Classes of Diazo Compounds

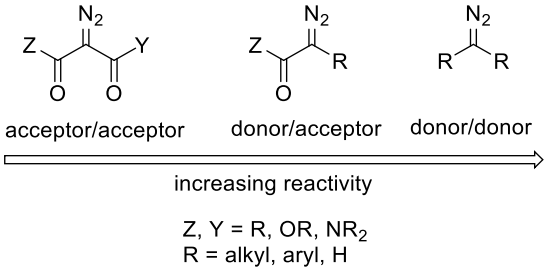

A few different types of acceptor/acceptor diazo compounds were synthesized and their reactivity with tertiary azides was explored (Scheme 6.7). Details regarding the synthesis of the diazo compounds can be found in section 6.6 Experimental. Azide **6.8** was consumed using $Rh_2(OAc)_4$ with diazo ester **6.20**. Low conversion was observed with diazo compounds **6.21**-**6.23**.

Scheme 6.7 Reactivity Screen of Diazo Compounds with Azide **6.8**[a]

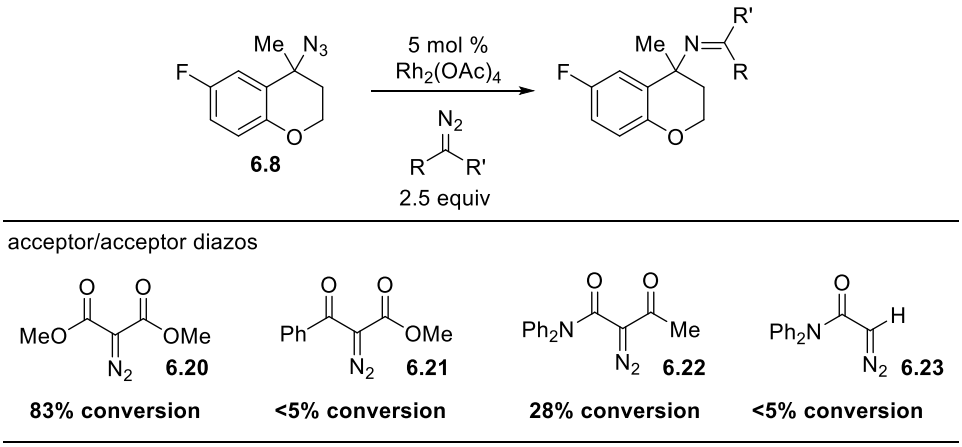

[a]Reaction conducted with azide **6.8** (0.05 mmol), diazo compound (0.125 mmol) and catalyst (2.5 μmol) in CH_2Cl_2 (0.1 M) at 40 °C under argon. Conversion of azide **6.8** was determined by calibrated GC-FID analysis using biphenyl as a standard.

Using diazo ester **6.20,** imine **6.24** was identified and characterized. With a suitable match in reactivity between azide **6.8** and diazo ester **6.20**, further optimizations were conducted (Table 6.8). Using two equivalents of diazo ester **6.20** and 5 mol % $Rh_2(OAc)_4$ formed imine **6.25** in 67% yield (entry 1). Conducting the reaction with $Cu(MeCN)_4PF_6$ or Ag(I) salts in place of $Rh_2(OAc)_4$ was ineffective (entries 2-4). Increasing the equivalents of diazo ester **6.20** improved the yield, however, resulted in formation of dimer **6.25** which is difficult to separate from imine **6.24 (**entries 5-6). Decreasing the catalyst loading resulted in a significant drop in yield (entry 7), while increasing the catalyst loading provided good yield of imine **6.24** (entry 8).

Table 6.8 Reaction Optimization[a]

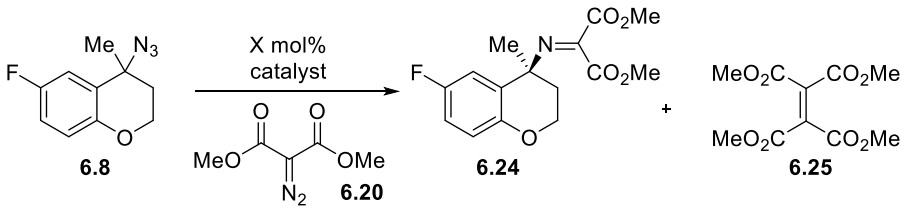

entry	catalyst	X	diazo equiv	yield (%)[b]
1	$Rh_2(OAc)_4$	5	2.0	67
2[c]	$Cu(MeCN)PF_6$	10	2.5	16
3[c]	$AgSbF_6$	10	2.0	--
4[c]	$AgPF_6$	10	2.0	--
5	$Rh_2(OAc)_4$	5	3.0	74
6	$Rh_2(OAc)_4$	5	5.0	83
7	$Rh_2(OAc)_4$	1	2.0	10
8	$Rh_2(OAc)_4$	10	2.0	86

[a]Reaction conducted with azide **6.8** (0.05 mmol), diazo ester **6.20** (0.1 - 0.25 mmol) and catalyst (0.5 - 50 μmol) in CH_2Cl_2 (0.2 M) at room temperature under argon. [b]Yield was determined by calibrated GC-FID analysis using biphenyl as a standard.[c]Reaction conducted at 40 °C.

Next, the effect of Ag(I) salts on the reaction was investigated (Table 6.9). Ag(I) salts had previously been identified as suitable catalysts to promote racemization for a series of azide substrates.[5] Adding $AgSbF_6$ or $AgPF_6$ to the reaction with $Rh_2(OAc)_4$ had minimal effect on the consumption of azide **6.8** (entries 2-3). This was encouraging because often, catalyst/catalyst interactions can be detrimental to product formation (*vide supra* attempts at DKR E-CuAAC reaction). Before attempting a DKR, a reasonable er from a kinetic resolution is necessary. A kinetic resolution was attempted using commercially available chiral rhodium catalysts. Unfortunately, none of the catalysts investigated provided reasonable enantioselectivity (entries 4-6).

Table 6.9 Effect of Ag(I) Salt and Chiral Catalysts[a]

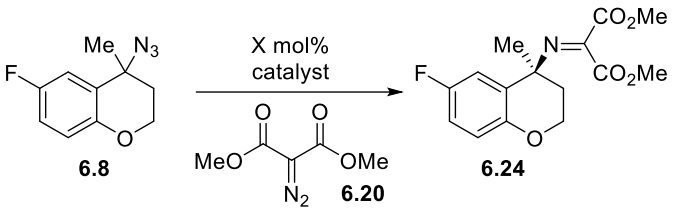

6.8 **6.20** **6.24**

entry	X	catalyst	additive[b]	conv. (%)[c]	er[d]
1	10	$Rh_2(OAc)_4$	--	75	--
2	10	$Rh_2(OAc)_4$	$AgSbF_6$	69	--
3	10	$Rh_2(OAc)_4$	$AgPF_6$	74	--
4[e]	1	Rh_2(*S*-DOSP)$_4$	--	41	48:52
5[e]	2.5	Rh_2(*R*-BTPCP)$_4$	--	<5	--
6[e]	2.5	Rh_2(*S*-PTAD)$_4$	--	8	55:45

[a]Reaction conducted with azide **6.8** (0.05 mmol), diazo ester **6.20** (0.1 mmol) and catalyst (5 μmol) in CH_2Cl_2 (0.1 M) at room temperature under argon for 15 h. [b]2:1 ratio between catalyst and additive. [c]Conversion was determined by calibrated GC-FID analysis using biphenyl as a standard. [d]Chiral HPLC used to determine er. [e]Reaction conducted with 1.2 equiv diazo ester **6.20**.

The rhodium catalyzed reaction of azide **6.12** with diazo ester **6.20** was investigated (Table 6.10). Azide **6.12** was consumed using $Rh_2(OAc)_4$ as a catalyst (entry 1). Chiral rhodium catalysts, Rh_2(*S*-DOSP)$_4$ and Rh_2(*R*-BTPCP)$_4$, resulted in near racemic formation of imine **6.26** (entries 2-3). A measurable er (55:45) was observed with Rh_2(*S*-PTAD)$_4$ (entry 4). Further optimization could be conducted to identify conditions that provide higher enantiomeric ratios. For example, alternate diazo esters generated from other symmetric esters, such as the trichloroethyl or trifluoroethyl ester could be explored.

Table 6.10 Chiral Rhodium Catalysts with Azide **6.12**[a]

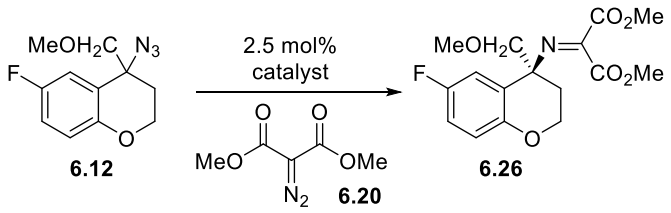

entry	catalyst	conv. (%)[b]	er[c]	entry	catalyst	conv. (%)[b]	er[c]
1[d]	$Rh_2(OAc)_4$	81	--	3	Rh_2(*R*-BTPCP)$_4$	67	52:48
2	Rh_2(*S*-DOSP)$_4$	56	51:49	4	Rh_2(*S*-PTAD)$_4$	65	55:45

[a]Reaction conducted with azide **6.12** (0.05 mmol), diazo **6.20** (0.06 mmol) and catalyst (2.5 μmol) in CH_2Cl_2 (0.2 M) at room temperature under argon for 6 h. [b]Conversion was determined by GC-FID analysis using biphenyl as a standard. [c]Chiral HPLC used to determine er. [d]Reaction conducted with 5 mol % catalyst.

6.5 Conclusions

The summation of this research provides proof-of-concept that allylic azides can be used for a DKR. Several catalysts promote racemization for non-symmetric systems, including other activated substrates (i.e. benzylic). The racemization has been used in combination with a kinetic resolution to access chiral triazoles and recycle the excess scalemic azide. Initial investigations into utilizing the racemization for a DKR E-CuAAC reaction or reduction have been unfruitful up to this point. A key challenge is the compatibility of the desired reaction conditions and the racemization catalyst. The formal reduction using chiral rhodium catalysts was tolerant of the racemization catalyst, albeit only low enantiomeric ratios have been observed up to this point. Future efforts should be focused on reactions that are tolerant of Lewis acids or Au/Ag(I) salts.

6.6 Experimental

Azide Safety. Azides are known to be high energy materials and explosions have been reported when working with azides.[22] In the course of this work, no issues were encountered. All of the azides synthesized in this report have C/N ratios equal to or above the recommended guideline of 3. Precautionary safety shields were used for all reactions using or producing more than 1 mmol of azide. Safety shields were used both in the fume hood and during rotary evaporation. All waste and aqueous solution which could be contaminated with azide were kept in individually labeled containers and were kept STRICTLY free of acid to avoid the accidental production on HN_3 – DO NOT use aqueous HCl during work up of any of the reactions reported herein. Further reading on azide safety is available.[23,24]

General Methods. All reactions conducted at elevated temperature used aluminum heating blocks with magnetic stirrings (500 rpm). Reported temperatures were based on an external thermal couple. All commercially available chemicals were used without further purification. Dry tetrahydrofuran, toluene, dimethoxyethane, *N*,*N*-dimethylforamide and methylene chloride were obtained from a commercial solvent system utilizing activated alumina columns under a positive pressure of argon. Thin-layer chromatography (TLC) was used for monitoring reaction progress. Visualization was conducted by using UV light, $KMnO_4$, or PMA stains. Organic solutions were concentrated using a rotary evaporator under reduced pressure at or below 40 ˚C. Flash chromatography was performed on a Teledyne Isco CombiFlash Rf system utilizing normal phase pre-column load cartridges and gold high performance columns. All proton (^1H) nuclear magnetic resonance spectra were recorded at 400 MHz or 500 MHz. All carbon (^{13}C) nuclear magnetic resonance

spectra were recorded at 100 MHz or 125 MHz. The fluorine (^{19}F) nuclear magnetic resonance spectra was recorded at 376 MHz or 471 MHz with proton decoupling. Chemical shifts are expressed in parts per million and are referenced to residual solvent ($CDCl_3$: 7.27 ppm, CD_3CN: 1.94 ppm), to the central carbon in the NMR solvent ($CDCl_3$: 77.2 ppm, CD_3CN 118.3). Data is presented as follows: chemical shift, multiplicity (s = singlet, d = doublet, ad = apparent doublet – para disubstituted pattern, t = triplet, q = quartet and m = multiplet), integration, and coupling constant in Hertz (Hz). Infrared (IR) spectra were taken in a Nicolet Nexus 670 FT-IR with salt plates. IR spectra were reported in cm^{-1}. Enantiomeric excesses were determined using a Shimadzu HPLC with a PDA detector.

Screening procedure for E-CuAAC reaction:

In a glove box, a vial was charged with $(CuOTf)_2$ PhMe (6.5 mg, 13 µmol) and Ph-PYBOX (18.8 mg, 50.9 µmol), and sealed with a septum screw cap. The vial was removed from the glovebox and connected to an argon filled Schlenk line via needle. Solvent (DME, 1.0 mL) was added by syringe to make a copper(I) catalyst stock solution. The resulting solution was stirred at ambient temperature for 10 min. Under air, a separate vial was charged with azide **6.4** (107 mg, 0.534 mmol), phenylacetylene (66 µL, 0.60 mmol), and DME (1.1 mL), making a substrate stock solution. A new vial was charged with $Zn(OTf)_2$ (0.9 mg, 3 µmol) and a stir bar. To this vial was added the substrate stock solution (0.1 mL, 0.05 mmol azide and 0.06 mmol alkyne, respectively), an aliquot of copper(I) catalyst solution (0.1 mL, 1.3 µmol [Cu], 5.0 µmol ligand, respectively) and additional DME (0.1 mL). (Note: For Lewis acids that are liquids, a solution was prepared such that 0.1 mL of the Lewis acid solution was added. In this case no additional DME was used). The vial was

sealed with a Teflon-lined cap under air. After 24 h at room temperature, the reaction was quenched by the addition of silver nitrate (50 μL, 0.1 M in 10% water in DME). The mixture was passed through a plug of silica, rinsed (70% EtOAc in hexanes), and concentrated under reduced pressure. The crude sample was reconstituted in IPA/hexanes and analyzed by chiral HPLC to determine er.

Screening procedure for reduction using [Pd]:

In a glove box, a vial was charged with $Pd_2(dba)_3$ (2.1 mg, 2.3 μmol) and (*S,S*)-DIOP (2.3 mg, 4.6 μmol), sealed with a septum screw cap and removed from the glove box. Under air, a separate vial was charged with azide **6.8** (90 mg, 0.44 mmol), 4-F-biphenyl (25 mg, 0.14 mmol), and MeOH (4.5 mL), making a substrate stock solution. The substrate stock solution (0.5 mL) was added to the vial containing the catalyst. After stirring for 30 min, the reaction mixture was purged with a continuous flow of hydrogen gas. After 5 min, the flow of hydrogen was ceased, and the vessel was sealed under a positive pressure of hydrogen gas (balloon). After 20 h, an aliquot of the reaction mixture was filtered through silica, rinsing with EtOAc, into a vial for analysis by GC-FID to determine conversion. The remaining sample was concentrated under reduced pressure, reconstituted in CH_2Cl_2 and filtered through silica. First the silica was rinsed with 30% EtOAc/hexanes (~5 mL) to remove excess starting material. Then, into a separate vial, the silica was rinsed with EtOAc (~5 mL) and the sample was concentrated under reduced pressure. The crude material was reconstituted in IPA/hexanes for analysis by HPLC.

Screening procedure 1 for reduction using [Ru]:

In a glove box, a vial was charged with RuCl[(*S*,*S*)-Teth-TsDPEN] (1.0 mg, 2.6 μmol), sealed with a septum screw cap and removed from the glove box. A separate vial was charged with azide **6.12** (30 mg, 0.13 mmol), 4-F-biphenyl (5.7 mg, 0.033 mmol), and MeOH (0.5 mL), making a substrate stock solution. The substrate stock solution (0.15 mL) was added to the vial containing the catalyst followed by a solution of 5:2 TEA/HCO_2H (17 μL) in MeOH (0.15 mL). After 3 h, an aliquot of the reaction mixture was filtered through silica, rinsing with EtOAc, into a vial for analysis by GC-FID to determine conversion. The remaining sample was concentrated under reduced pressure, reconstituted in CH_2Cl_2 and filtered through silica. First the silica was rinsed with 30% EtOAc/hexanes (~5 mL) to remove excess starting material. Then, into a separate vial, the silica was rinsed with EtOAc (~5 mL) and the sample was concentrated under reduced pressure. The crude material was reconstituted in IPA/hexanes for analysis by HPLC.

Screening procedure 2 for reduction using [Ru]:

In a glove box, a vial was charged with $RuCl_2$[(*R*)-BINAP]-[(*R*)-DAIPEN] (1.4 mg, 1.1 μmol), KO*t*Bu (2.2 mg, 20 μmol), sealed with a septum screw cap and removed from the glove box. A separate vial was charged with azide **6.12** (30 mg, 0.13 mmol), biphenyl (12 mg, 0.076 mmol), and IPA (1.25 mL), making a substrate stock solution. The substrate stock solution (0.5 mL) was added to the vial containing the catalyst. The reaction mixture was purged with a continuous flow of hydrogen gas. After 5 min, the flow of hydrogen was ceased, and the vessel was sealed under a positive pressure of hydrogen gas (balloon). After 5 h, an aliquot of the reaction mixture was filtered through silica, rinsing with EtOAc, into a vial for analysis by GC-FID to determine conversion. The remaining sample was

concentrated under reduced pressure, reconstituted in CH_2Cl_2 and filtered through silica. First the silica was rinsed with 30% EtOAc/hexanes (~5 mL) to remove excess starting material. Then, into a separate vial, the silica was rinsed with EtOAc (~5 mL) and the sample was concentrated under reduced pressure. The crude material was reconstituted in IPA/hexanes for analysis by HPLC.

Screening procedure for reduction using [Ir]:

In a glove box, a vial was charged with $[Ir(COD)Cl]_2$ (1.3 mg, 1.9 μmol) and (*S,S*)-ChiraPhos (1.6 mg, 3.8 μmol), sealed with a septum screw cap and removed from the glove box. Under air, a separate vial was charged with azide **6.12** (74 mg, 0.31 mmol), biphenyl (16 mg, 0.10 mmol), and CH_2Cl_2 (0.65 mL), making a substrate stock solution. The substrate stock solution (0.1 mL) was added to the vial containing the catalyst followed by a solution of I_2 in CH_2Cl_2 (0.1 mL, 25 μM). After stirring for 10 min, the reaction mixture was purged with a continuous flow of hydrogen gas. After 5 min, the flow of hydrogen was ceased, and the vessel was sealed under a positive pressure of hydrogen gas (balloon). After 20 h, an aliquot of the reaction mixture was filtered through silica, rinsing with EtOAc, into a vial for analysis by GC-FID to determine conversion. The remaining sample was filtered through silica, first rinsing with 30% EtOAc/hexanes (~5 mL) to remove excess starting material. Then, into a separate vial, the silica was rinsed with EtOAc (~5 mL) and the sample was concentrated under reduced pressure. The crude material was reconstituted in IPA/hexanes for analysis by HPLC.

Screening procedure for reduction using [Rh]:

In a glove box, a vial was charged with $Rh(COD)_2BF_4$ (1.2 mg, 2.9 μmol) and (*R*,*R*)-Me-DuPhos (1.3 mg, 4.2 μmol), sealed with a septum screw cap and removed from the glove box. Under air, a separate vial was charged with azide **6.12** (78 mg, 0.33 mmol), biphenyl (48 mg, 0.31 mmol), and MeOH (3.25 mL), making a substrate stock solution. The substrate stock solution (0.5 mL) was added to the vial containing the catalyst. After stirring for 10 min, the reaction mixture was purged with a continuous flow of hydrogen gas. After 5 min, the flow of hydrogen was ceased, and the vessel was sealed under a positive pressure of hydrogen gas (balloon). After 20 h, an aliquot of the reaction mixture was filtered through silica, rinsing with EtOAc, into a vial for analysis by GC-FID to determine conversion. The remaining sample was concentrated under reduced pressure, reconstituted in CH_2Cl_2 and filtered through silica. First the silica was rinsed with 30% EtOAc/hexanes (~5 mL) to remove excess starting material. Then, into a separate vial, the silica was rinsed with EtOAc (~5 mL) and the sample was concentrated under reduced pressure. The crude material was reconstituted in IPA/hexanes for analysis by HPLC.

Screening procedure for formal reduction using $Rh_2(OAc)_4$:

A vial was charged with $Rh_2(OAc)_4$ (1.3 mg, 2.9 μmol), sealed with a septum screw cap and purged with argon for 5 min. A separate vial was charged with azide **6.8** (85 mg, 0.41 mmol), biphenyl (17 mg, 0.11 mmol), and CH_2Cl_2 (1.7 mL), making a substrate stock solution. The substrate stock solution (0.2 mL) was added to the vial containing the catalyst followed by a solution of diazo ester **6.20** (20 mg, 0.13 mmol) in CH_2Cl_2 (0.3 mL) and was

heated to 40 °C. After 15 h, an aliquot of the reaction mixture was filtered through silica, rinsing with EtOAc, into a vial for analysis by GC-FID to determine conversion.

Racemization of azide 6.1

A solution of *rac*-azide **6.1** (11.7 mg, 66.8 μmol) was prepared in CH_2Cl_2 (2.3 mL). This solution was dispensed via syringe in 0.2 mL aliquots into 4 mL vials. The CH_2Cl_2 was allowed to evaporate at room temperature. A solution of triphenylborane (1.2 mg, 5.0 μmol) in CH_2Cl_2 (1.4 mL) was prepared. An aliquot of this solution (0.2 mL) was added to each vial containing neat azide 6.1 and heated to 40 °C. After 24 h, the reaction mixture was filtered through silica gel, rinsed with excess CH_2Cl_2, and concentrated under reduced pressure. The sample was reconstituted in hexanes (~1 mL) and filtered into an HPLC vial for analysis.

Table 6.11 Racemization of Azide **6.1** with $B(C_6F_5)_3$[a]

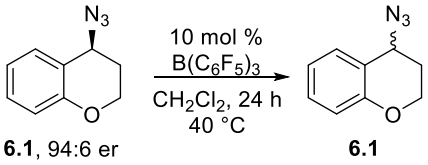

6.1, 94:6 er **6.1**

entry	T (°C)	time	er[b]	% azide remaining[c]
1	50	10 min	52:48	90
2	50	30 min	53:47	97
3	50	1 h	50:50	86
4	50	1.5 h	50:50	70
5	50	24 h	51:49	50
6	rt	0.5 h	70:30	88
7	rt	1 h	58:42	82
8	rt	6 h	52:48	81

[a]Reaction conducted with azide 6.1 (6 μmol) and $B(C_6F_5)_3$ (0.6 μmol) in CH_2Cl_2 (0.03 M). [b]er determined by chiral HPLC analysis. [c]Determined by calibratied HPLC analysis using 4,4'-di-*tert*-butylbiphenyl as a standard.

Table 6.12 Racemization of Azide **6.27**[a]

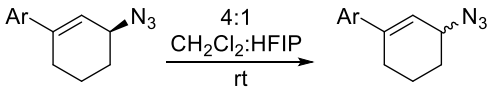

***ent*-6.27** **rac-6.27**

Ar = 4-Me-C_6H_5

entry	time	er[b]
1	1.5 h	71:30
2	2.5 h	63:37
3	24 h	50:50

[a]Reaction conducted with azide **6.27** (2.3 μmol) in solvent (4.6 mM). [b]er determined by chiral HPLC analysis.

Table 6.13 Racemization of Azide **6.1** with Dowex 50Wx4[a]

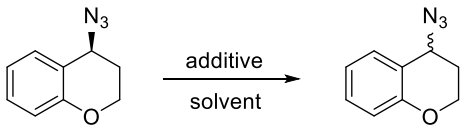

***ent*-6.1** ***rac*-6.1**

entry	solvent	additive	temp	time	er[b]
1	HFIP	--	rt	24 h	99:1
2	HFIP	--	50 °C	24 h	93:7
3	HFIP	Dowex 50Wx4	rt	1 h	50:50
4	CH_2Cl_2	Dowex 50Wx4	rt	1 h	>99:1 er
5	CH_2Cl_2	Dowex 50Wx4	rt	5 h	>99:1 er
6[c]	CH_2Cl_2/HFIP	Dowex 50Wx4	rt	5 h	>99:1 er

[a]Reactions conducted with azide **6.1** (2.9 μmol) and Dowex 50Wx4 (10 mg/0.1 mL) in solvent (10 mM). [b]er determined by chiral HPLC analysis. [c]2:1 CH_2Cl_2:HFIP

Azide **6.1** and azide **6.4** were synthesized following reported procedures.[4,5]

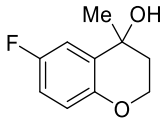

Alcohol **6.7**. In a nitrogen-filled glove box, a flask was charged with anhydrous $CeCl_3$ (1.6 g, 6.6 mmol). Outside of the glove box, the flask was connected to a Schlenk line before adding THF (20 mL). After stirring for 2 h the resulting suspension was cooled to in a dry ice/acetone bath, and MeLi (3.7 mL, 1.6 M in Et_2O, 5.9 mmol) was added dropwise via syringe. After 0.5 h, 6-fluoro-chromanone (831 mg, 5.00 mmol) in THF (3 mL) was added dropwise via syringe. After 4 h, the reaction mixture was poured onto water. The resulting mixture was extracted with EtOAc (3 × 25 mL). The combined organic phases were washed with brine, dried ($MgSO_4$), filtered, and concentrated under reduced pressure to yield alcohol **6.7** as a white solid (0.75 g, 4.0 mmol, 81%). This material was used without further purification.

^{1}H NMR (400 MHz, CD_3CN) δ 7.23 (dd, *J* = 9.8, 3.1 Hz, 1H), 6.95 – 6.87 (m, 1H), 6.77 (dd, *J* = 9.0, 4.9 Hz, 1H), 4.28 – 4.14 (m, 2H), 3.36 (s, 1H), 2.03-2.00 (m, 2H), 1.55 (s, 3H) **^{13}C NMR (100 MHz, CD_3CN)** δ 157.7 (d, J_{C-F} = 235.5 Hz), 151.0 (d, J_{C-F} = 1.9 Hz), 131.7 (d, J_{C-F} = 6.4 Hz), 118.7 (d, J_{C-F} = 8.0 Hz), 116.2 (d, J_{C-F} = 23.5 Hz), 113.6 (d, J_{C-F} = 23.3 Hz), 66.6, 64.4, 38.3, 30.1. **^{19}F NMR (376 MHz, CD_3CN)** δ -125.3. **IR (NaCl, thin film, cm^{-1})** 3338, 2989, 2916, 1485, 1424, 1199, 819, 746. **HRMS (EI):** *m/z* calcd for $C_{10}H_{11}FO_2^+$ $[M]^+$ 182.0738, observed 182.0736.

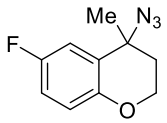

Azide **6.8.** To a solution of alcohol **6.7** (413 mg, 2.27 mmol) in CH_2Cl_2 (4.5 mL) cooled in an ice bath was added $TMSN_3$ (0.60 mL, 5.2 mmol) and $Zn(OTf)_2$ (83 mg, 0.23 mmol).

The vessel was sealed. After 20 min, the solution was quenched with triethylamine (0.5 mL) and MeOH (0.5 mL). The reaction mixture was filtered through basic alumina and washed with excess CH_2Cl_2. The resulting solution was concentrated under reduced pressure. Purification by column chromatography (gradient elution 0-20% EtOAc in hexanes) afforded azide **6.8** as a yellow oil (371 mg, 2.04 mmol, 90%).

^{1}H NMR (500 MHz, CD_3CN) δ 7.22 (dd, *J* = 9.6, 3.1 Hz, 1H), 7.07 – 6.99 (m, 1H), 6.87 (dd, *J* = 9.0, 4.9 Hz, 1H), 4.29 – 4.17 (m, 2H), 2.12 – 2.03 (m, 2H), 1.67 (s, 3H).**^{13}C NMR (125 MHz, CD_3CN)** δ 157.5 (d, $J_{C\text{-}F}$ = 236.7 Hz), 151.3, 125.9 (d, $J_{C\text{-}F}$ = 6.6 Hz), 119.6 (d, $J_{C\text{-}F}$ = 7.5 Hz), 117.6 (d, $J_{C\text{-}F}$ = 23.4 Hz), 113.8 (d, $J_{C\text{-}F}$ = 23.9 Hz), 59.5, 63.8, 35.8, 26.6. **^{19}F NMR (471 MHz, CD_3CN)** δ -124.5. **IR (NaCl, thin film, cm^{-1})** 2977, 2887, 2102, 1493. **HRMS (EI):** *m/z* calcd for $C_{10}H_{10}FO^+$ $[M - N_3]^+$ 165.0710, observed 165.0705.

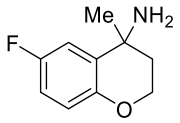

Amine **6.9**. To a solution of azide **6.8** (107 mg, 0.516 mmol) in THF (5.1 mL) cooled in an ice bath was added $LiAlH_4$ (61 mg, 1.6 mmol). After 24 h, the reaction was poured onto a saturated aqueous solution of Rochelle's salt. The resulting mixture was extracted with EtOAc (3 × 15 mL). The combined organic phases were washed with brine, dried ($MgSO_4$), filtered, and concentrated under reduced pressure to yield amine **6.9** as a yellow solid (90 mg, 0.49 mmol, 96%). This material was used without further purification.

^{1}H NMR (400 MHz, $CDCl_3$) δ 7.14 (dd, *J* = 9.6, 3.0 Hz, 1H), 6.83 (ddd, *J* = 8.9, 7.8, 3.0 Hz, 1H), 6.75 (dd, *J* = 9.0, 4.9 Hz, 1H), 4.29 – 4.15 (m, 2H), 2.05 – 1.92 (m, 2H), 1.65 (s, 2H), 1.50 (s, 3H).**^{13}C NMR (100 MHz, $CDCl_3$)** δ 157.2 (d, $J_{C\text{-}F}$ = 237.9 Hz), 149.6 (d, $J_{C\text{-}F}$ = 2.0 Hz), 132.2 (d, $J_{C\text{-}F}$ = 6.0) 118.1 (d, $J_{C\text{-}F}$ = 7.7 Hz), 115.1 ($J_{C\text{-}F}$, *J* = 23.3 Hz), 112.5

(d, $J_{C\text{-}F}$ = 23.1 Hz), 63.6, 47.8, 39.2, 31.4. **^{19}F NMR (376 MHz, $CDCl_3$)** δ -123.2. **IR (NaCl, thin film, cm^{-1})** 3355, 2968, 1594, 1493, 1421, 1258, 1062, 744. **HRMS (EI):** *m/z* calcd for $C_{10}H_{12}FNO^+$ $[M]^+$ 181.0897, observed 181.0891. **HPLC:** Reflect-C 3μ column, 0.1% TEA in hexanes/IPA = 75:25 at 1.0 mL/min, λ = 286 nm: t_r = 5.4 min. and t_r = 5.9 min.

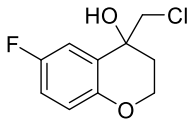

Chlorohydrin **6.10**. Adapting a known procedure,[25] a solution of ketone **6.6** (0.83 g, 5.0 mmol) in THF (10 mL) was cooled in a dry ice/acetone bath and $ClCH_2I$ (0.55 mL, 7.5 mmol) was added via syringe. Over the course of three hours, ^{n}BuLi (3.0 mL, 2.5 M in hexanes) was added dropwise via syringe, maintaining the temperature. After complete addition, the reaction was allowed to stir for 1 h in the dry ice/acetone bath. The reaction mixture was quenched cold using with an aqueous saturated NH_4Cl solution and allowed to warm to room temperature. The reaction mixture was extracted with EtOAc (3 ×20 mL) The combined organic layers were washed with brine, dried (Na_2SO_4), filtered, and concentrated under reduced pressure. Purification by flash chromatography (gradient elution 20 – 50% EtOAc in hexanes) afforded the product **6.10** (0.83 g, 77%) as a yellow oil.

^{1}H NMR (500 MHz, $CDCl_3$) δ 7.16 (dd, *J* = 9.1, 3.1 Hz, 1H), 6.95 (ddd, *J* = 9.0, 7.8, 3.1 Hz, 1H), 6.82 (dd, *J* = 9.0, 4.8 Hz, 1H), 4.28 (ddd, *J* = 11.7, 7.2, 3.6 Hz, 1H), 4.20 (ddd, *J* = 11.6, 8.5, 3.2 Hz, 1H), 3.92 (d, *J* = 11.6 Hz, 1H), 3.80 (d, *J* = 11.6 Hz, 1H), 2.64 (s, 1H), 2.39 (ddd, *J* = 14.2, 7.2, 3.2 Hz, 1H), 2.13 (ddd, *J* = 14.2, 8.6, 3.6 Hz, 1H). **^{13}C NMR (125 MHz, $CDCl_3$)** δ 157.0 (d, $J_{C\text{-}F}$ = 239.3 Hz), 150.8, 124.9 (d, $J_{C\text{-}F}$ = 6.6 Hz), 118.5 (d, $J_{C\text{-}F}$

= 7.8 Hz), 117.2 (d, $J_{C\text{-}F}$ = 23.3 Hz), 112.7 (d, $J_{C\text{-}F}$ = 23.6 Hz), 68.4, 63.3, 52.5, 33.0. **^{19}F NMR (471 MHz, $CDCl_3$)** δ -122.3. **IR (NaCl, thin film, cm^{-1})** 3441. 2965, 2889, 1494, 1427, 1261, 1200. **HRMS (EI):** *m/z* calcd for $C_{10}H_{10}ClFO_2^+$ $[M]^+$ 216.0348, observed 216.0343.

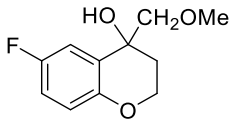

Alcohol **6.11**. A solution of KOMe in MeOH (10 mL, 25 wt % in MeOH) was added to chlorohydrin **6.10** (0.54 g, 2.5 mmol) and NaI (70 mg, 0.46 mmol) and heated to 50 °C. After 2 h, the solution was quenched with aqueous saturated NH_4Cl and extracted with EtOAc (3 × 15 mL) The combined organic layers were washed with brine, dried (Na_2SO_4), filtered, and concentrated under reduced pressure. Purification by flash chromatography (gradient elution 20 – 50% EtOAc in hexanes) afforded the product **6.11** (0.53 g, 78%) as a yellow oil.

^{1}H NMR (400 MHz, $CDCl_3$) δ 7.21 (dd, *J* = 9.4, 3.1 Hz, 1H), 6.90 (ddd, *J* = 9.0, 7.8, 3.1 Hz, 1H), 6.78 (dd, *J* = 9.0, 4.8 Hz, 1H), 4.29 – 4.14 (m, 2H), 3.58 (d, *J* = 9.5 Hz, 1H), 3.53 (d, *J* = 9.5 Hz, 1H), 3.46 (s, 3H), 3.04 (s, 1H), 2.19 (ddd, *J* = 14.0, 7.4, 3.7 Hz, 1H), 2.04 (ddd, *J* = 14.0, 7.6, 3.8 Hz, 1H). **^{13}C NMR (100 MHz, $CDCl_3$)** δ 157.0 (d, $J_{C\text{-}F}$ = 238.1 Hz), 150.9, 125.8 (d, $J_{C\text{-}F}$ = 6.6 Hz), 118.1 (d, $J_{C\text{-}F}$ = 7.8 Hz), 116.5 (d, $J_{C\text{-}F}$ = 23.4 Hz), 113.3 (d, $J_{C\text{-}F}$ = 23.5 Hz), 78.8, 68.2, 63.5, 59.5, 33.1. **^{19}F NMR (376 MHz, $CDCl_3$)** δ -123.1. **IR (NaCl, thin film, cm^{-1})** 3448, 2931, 2890, 1494, 1429, 1261, 1199, 1105. **HRMS (EI):** *m/z* calcd for $C_{11}H_{13}FO_3^+$ $[M]^+$ 212.0843, observed 212.0839.

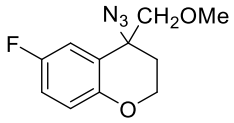

Azide **6.12**. To a solution of alcohol **6.11** (0.33 g, 1.6 mmol) in CH_2Cl_2 (3.2 mL) cooled in an ice bath was added $TMSN_3$ (0.27 mL, 2.1 mmol) and AgOTf (42 mg, 0.16 mmol). The vessel was sealed. After 24 h, the reaction mixture was quenched with triethylamine (0.3 mL) and MeOH (0.3 mL), filtered through basic alumina and washed with excess CH_2Cl_2. The resulting solution was concentrated under reduced pressure. Purification by column chromatography (gradient elution 15% EtOAc in hexanes) afforded azide **6.12** (0.28 g, 1.2 mmol, 75%) as a colorless oil.

^{1}H NMR (400 MHz, $CDCl_3$) δ 7.15 (dd, *J* = 9.3, 3.1 Hz, 1H), 6.96 (ddd, *J* = 9.1, 7.7, 3.1 Hz, 1H), 6.84 (dd, *J* = 9.0, 4.9 Hz, 1H), 4.32 – 4.19 (m, 2H), 3.69 (d, *J* = 9.9 Hz, 1H), 3.65 (d, *J* = 10.0 Hz, 1H), 3.04 (s, 3H), 2.31 (ddd, *J* = 14.1, 7.7, 4.6 Hz, 1H), 2.10 (ddd, *J* = 14.2, 5.9, 3.8 Hz, 1H). **^{13}C NMR (100 MHz, $CDCl_3$)** δ 156.8 (d, $J_{C\text{-}F}$ = 239.0 Hz), 150.9, 121.8 (d, $J_{C\text{-}F}$ = 6.8 Hz), 118.7 (d, $J_{C\text{-}F}$ = 7.8 Hz), 117.2 (d, $J_{C\text{-}F}$ = 23.2 Hz), 113.4 (d, $J_{C\text{-}F}$ = 23.9 Hz), 78.0, 62.9, 60.5, 59.6, 30.1. **^{19}F NMR (376 MHz, $CDCl_3$)** δ -122.5. **IR (NaCl, thin film, cm^{-1})** 2891, 2106, 1493, 1426, 1262, 1201. **HRMS (EI):** *m/z* calcd for $C_{11}H_{12}FN_3O_2^+$ $[M]^+$ 237.0908, observed 237.0900.

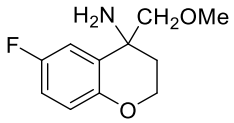

Amine **6.13**. To a solution of azide **6.12** (0.10 g, 0.42 mmol) in THF (2.0 mL) cooled in an ice bath was added $LiAlH_4$ (45 mg, 1.2 mmol). After 24 h, the reaction was poured onto a saturated aqueous solution of Rochelle's salt. The resulting mixture was extracted with EtOAc (3 × 10 mL). The combined organic phases were washed with brine, dried ($MgSO_4$), filtered, and concentrated under reduced pressure. Purification by column chromatography

(gradient elution 5 - 20% MeOH in CH_2Cl_2) afforded azide **6.13** (73 mg, 0.34 mmol, 81%) as a colorless oil.

^{1}H NMR (400 MHz, $CDCl_3$) δ 7.21 (dd, *J* = 9.7, 3.1 Hz, 1H), 6.84 (ddd, *J* = 8.9, 7.7, 3.1 Hz, 1H), 6.74 (dd, *J* = 9.0, 4.9 Hz, 1H), 4.20 – 4.18 (m, 2H), 3.48 (d, *J* = 9.1 Hz, 1H), 3.43 (d, *J* = 9.2 Hz, 1H), 3.39 (s, 3H), 2.22 – 2.16 (m, 1H), 1.93 – 1.78 (m, 1H), 1.74 (s, 2H). **^{13}C NMR (100 MHz, $CDCl_3$)** δ 157.0 (d, J_{C-F} = 237.7 Hz), 150.6 (d, J_{C-F} = 2.1 Hz), 128.2 (d, J_{C-F} = 6.4 Hz), 118.0 (d, J_{C-F} = 7.9 Hz), 115.5 (d, J_{C-F} = 23.4 Hz), 113.4 (d, J_{C-F} = 23.4 Hz), 80.2, 63.4, 59.4, 50.7, 34.5. **^{19}F NMR (376 MHz, $CDCl_3$)** δ -123.3. **IR (NaCl, thin film, cm^{-1})** 3372, 3308, 2927, 2890, 1492, 1424, 1259, 1197, 1107. **HRMS (ESI):** *m/z* calcd for $C_{11}H_{15}FNO_2^+$ $[M + H]^+$ 212.1081, observed 212.1081. **HPLC:** Reflect-C 3μ column, 0.1% TEA in hexanes/IPA = 98:2 at 0.75 mL/min, λ = 300 nm: t_r = 15.3 min. and t_r = 16.1 min.

p-ABSA (3.1 g, 13 mmol, 66%) was prepared using a reported procedure.[26]

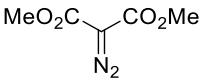

Dizao ester **6.20**. To a solution of dimethylmalonate (0.92 g, 7.0 mmol) and TEA (1.1 mL, 7.7 mmol) in acetonitrile (10 mL) cooled in an ice bath was added *p*-ABSA (1.7 g, 8.1 mmol). After 24 h, the reaction mixture was concentrated under reduced pressure then triturated was ether/petroleum ether (1:1). After filtration and concentration under reduced pressure, purification by flash column chromatography yielded diazo ester **6.20** (0.97 g, 5.8 mmol, 83%) as a yellow oil.

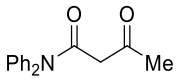

Amide **6.28**. Following a reported procedure, amide **6.28** (1.2 g, 4.7 mmol, 94%) was isolated as a red solid.[27]

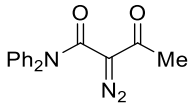

Diazo amide **6.22**. Following a reported procedure, diazo amide **6.22** (0.36 g, 1.3 mmol, 85%) was isolated.[27]

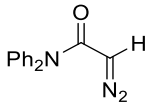

Diazo amide **6.23**. Following a reported procedure, diazo compound **6.23** (0.15 g, 0.62 mmol, 58%) was isolated.[27]

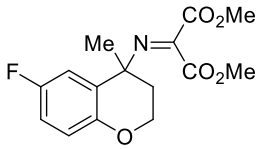

Imine **6.24**. A vial was charged with $Rh_2(OAc)_4$ (4.0 mg, 9.0 μmol) and purged with argon. A solution of azide **6.8** (75 mg, 0.36 mmol) in CH_2Cl_2 (0.2 mL) and a solution of diazo **6.20** (77 mg, 0.49 mmol) in CH_2Cl_2 (0.3 mL) were added subsequently. After 24 h, the reaction mixture was concentrated under reduced pressure and purified by flash chromatography (gradient elution 0 – 50% EtOAc in hexanes) to afford the product **6.24** (46 mg, 41%) as a white solid.

^{1}H NMR (400 MHz, $CDCl_3$) δ 6.92-6.86 (m, 2H), 6.77 (dd, *J* = 8.8, 4.9 Hz, 1H), 4.25 – 4.10 (m, 2H), 3.89 (s, 3H), 3.38 (s, 3H), 2.35 (ddd, *J* = 13.9, 5.6, 3.3 Hz, 1H), 2.10 (ddd, *J*

= 13.6, 8.8, 4.2 Hz, 1H), 1.79 (s, 3H). **^{13}C NMR (125 MHz, $CDCl_3$)** δ 162.8 (d, $J_{C\text{-}F}$ = 144.1 Hz), 157.4, 155.5, 151.2, 150.7, 124.6 (d, $J_{C\text{-}F}$ = 6.3 Hz), 118.0 (d, $J_{C\text{-}F}$ = 7.7 Hz), 116.7 (d, $J_{C\text{-}F}$ = 23.2 Hz), 115.2 (d, $J_{C\text{-}F}$ = 23.3 Hz), 62.9, 59.8, 53.7, 52.3, 36.3, 30.1. **^{19}F NMR (471 MHz, $CDCl_3$)** δ -123.8. **IR (NaCl, thin film, cm^{-1})** 2955, 1745, 1725, 1492, 1429, 1261, 1069. **HRMS (ESI):** *m/z* calcd for $C_{15}H_{16}FNO_5Na^+$ $[M + Na]^+$ 332.0905, observed 332.0917. **HPLC:** Reflect-C 3μ column, hexanes/IPA = 97:3 at 1.0 mL/min, λ = 210 nm: t_r = 8.6 min and t_r = 9.1 min.

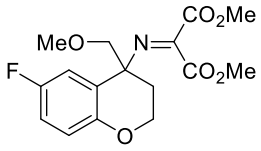

Imine **6.26**. A vial was charged with $Rh_2(OAc)_4$ (2.9 mg, 6.4 μmol) and purged with argon. A solution of azide **6.12** (52 mg, 0.22 mmol) in CH_2Cl_2 (0.4 mL) and a solution of diazo **6.20** (72 mg, 0.45 mmol) in CH_2Cl_2 (0.6 mL) were added subsequently. After 24 h, the reaction mixture was concentrated under reduced pressure and purified by flash chromatography (gradient elution 20 – 50% EtOAc in hexanes) to afford the product **6.26** (23 mg, 32%) as a yellow oil.

^{1}H NMR (400 MHz, $CDCl_3$) δ 6.96 – 6.86 (m, 2H), 6.79 (dd, *J* = 9.8, 4.8 Hz, 1H), 4.26-4.16 (m, 2H), 3.88 (s, 3H), 3.85 (d, *J* = 9.7 Hz, 1H), 3.82 (d, *J* = 9.7 Hz, 1H), 3.42 (s, 3H), 3.33 (s, 3H), 2.40 (ddd, *J* = 14.0, 6.8, 4.4 Hz, 1H), 2.25 (ddd, *J* = 14.0, 6.6, 4.4 Hz, 1H) **^{13}C NMR (100 MHz, $CDCl_3$)** δ 163.0, 162.2, 156.5 (d, $J_{C\text{-}F}$ = 238.5 Hz), 152.2, 152.0, 122.0, 118.0 (d, $J_{C\text{-}F}$ = 7.8 Hz), 116.9 (d, $J_{C\text{-}F}$ = 23.2 Hz), 115.4 (d, $J_{C\text{-}F}$ = 23.7 Hz), 79.6, 63.0, 62.9, 59.8, 53.6, 52.2, 31.6. **^{19}F NMR (376 MHz, $CDCl_3$)** δ -123.4. **IR (NaCl, thin film, cm^{-1})** 2955, 1746, 1719, 1493, 1260, 1070. **HRMS (ESI):** *m/z* calcd for $C_{16}H_{18}FNO_6Na^+$

$[M + Na]^+$ 362.1010, observed 362.1017. **HPLC:** Reflect-C 3μ column, hexanes/IPA = 97:3 at 1.0 mL/min, $\lambda = 285$ nm: $t_r = 9.7$ min and $t_r = 10.3$ min.

6.7 References

(1) Nugent, T. C. *Chiral Amine Synthesis: Methods, Developments and Applications*; Wiley, 2010.

(2) Gagneux, A.; Winstein, S.; Young, W. G. Rearrangement of Allyl Azides. *J. Am. Chem. Soc.* **1960**, *82*, 5956–5957.

(3) Ott, A. A.; Goshey, C. S.; Topczewski, J. J. Dynamic Kinetic Resolution of Allylic Azides via Asymmetric Dihydroxylation. *J. Am. Chem. Soc.* **2017**, *139*, 7737–7740.

(4) Liu, E.-C.; Topczewski, J. J. Enantioselective Copper Catalyzed Alkyne–Azide Cycloaddition by Dynamic Kinetic Resolution. *J. Am. Chem. Soc.* **2019**, *141*, 5135–5138.

(5) Ott, A. A.; Topczewski, J. J. Catalytic Racemization of Activated Organic Azides. *Org. Lett.* **2018**, *20*, 7253–7256.

(6) Alexander, J. R.; Ott, A. A.; Liu, E.-C.; Topczewski, J. J. Kinetic Resolution of Cyclic Secondary Azides, Using an Enantioselective Copper-Catalyzed Azide-Alkyne Cycloaddition. *Org. Lett.* **2019**, *21*, 4355–4358.

(7) Finn, M. G.; Fokin, V. V. Click Chemistry: Function Follows Form. *Chem. Soc. Rev.* **2010**, *39*, 1231–1232.

(8) Pedersen, D. S.; Abell, A. 1,2,3-Triazoles in Peptidomimetic Chemistry. *Eur. J. Org. Chem.* **2011**, 2399–2411.

(9) Ellman, J. A.; Jain, R. K.; Wood, W. J. L.; Tsuruoka, H.; Patterson, A. W. Substrate Activity Screening: A Fragment-Based Method for the Rapid Identification of Nonpeptidic Protease Inhibitors. *J. Am. Chem. Soc.* **2005**, *127*, 15521–15527.

(10) Lee, T.; Cho, M.; Ko, S.-Y.; Youn, H.-J.; Baek, D. J.; Cho, W.-J.; Kang, C.-Y.; Kim, S. Synthesis and Evaluation of 1,2,3-Triazole Containing Analogues of the Immunostimulane Alpha-GalCer. *J. Med. Chem.* **2007**, *50*, 585–589.

(11) Vanysek, P. Electrochemical Series. In *CRC Handbook of Chemistry and Physics*; Haynes, W. H., Lide, D. R., Bruno, T. J., Eds.; CRC Press, 2012.

(12) Rodionov, V. O.; Presolski, S. I.; Díaz, D. D.; Fokin, V. V.; Finn, M. G. Ligand-Accelerated Cu-Catalyzed Azide-Alkyne Cycloaddition: A Mechanistic Report. *J. Am. Chem. Soc.* **2007**, *129*, 12705–12712.

(13) Ohkuma, T.; Koizumi, M.; Doucet, H.; Pham, T.; Kozawa, M.; Murata, K.; Katayama, E.; Yokozawa, T.; Ikariya, T.; Noyori, R. Asymmetric Hydrogenation of Alkenyl, Cyclopropyl, and Aryl Ketones. $RuCl_2$(Xylbinap)(1,2-Diamine) as a Precatalyst Exhibiting a Wide Scope. *J. Am. Chem. Soc.* **1998**, *120*, 13529–13530.

(14) Hems, W. P.; Groarke, M.; Zanotti-Gerosa, A.; Grasa, G. A. [(Bisphosphine) Ru(II) Diamine] Complexes in Asymmetric Hydrogenation: Expanding the Scope of the Diamine Ligand. *Acc. Chem. Res.* **2007**, *40*, 1340–1347.

(15) Spindler, F.; Blaser, H. U. Enantioselective Hydrogenation of C=N Functions and Enamines. In *The Handbook of Homogeneous Hydrogenation*; Wiley-VCH Verlag GmbH & Co., 2007; pp 1193–1214.

(16) Baeza, A.; Pfaltz, A. Iridium-Catalyzed Asymmetric Hydrogenation of Imines. *Chem. - Eur. J.* **2010**, *16*, 4003–4009.

(17) Verzijl, G. K. M.; Schuster, C.; Dax, T.; De Vries, A. H. M.; Lefort, L. Asymmetric Synthesis of a Key Intermediate for Tofacitinib via a Dynamic Kinetic Resolution-Reductive Amination Protocol. *Org. Process Res. Dev.* **2018**, *22*, 1817–1822.
(18) Verzijl, G. K. M.; Hassfeld, J.; De Vries, A. H. M.; Lefort, L. Enantioselective Synthesis of a 2,3-Benzodiazepine Intermediate of BET Inhibitor BAY 1238097 via Catalytic Asymmetric Hydrogenation. *Org. Process Res. Dev.* **2020**, *24*, 255–260.
(19) Hou, C. J.; Wang, Y. H.; Zheng, Z.; Xu, J.; Hu, X. P. Chiral Phosphine-Phosphoramidite Ligands for Highly Efficient Ir-Catalyzed Asymmetric Hydrogenation of Sterically Hindered N-Arylimines. *Org. Lett.* **2012**, *14*, 3554–3557.
(20) Etayo, P.; Vidal-Ferran, A. Rhodium-Catalysed Asymmetric Hydrogenation as a Valuable Synthetic Tool for the Preparation of Chiral Drugs. *Chem. Soc. Rev.* **2013**, *42*, 728–754.
(21) Gu, P.; Wu, X.; Su, Y.; Li, X.-Q.; Xue, P.; Li, R. Rhodium-Catalyzed Intermolecular Reaction of Alkyl Azides with Diazo-(Aryl)Acetates. *Synlett* **2014**, *25*, 535–538.
(22) Kolb, H. C.; Finn, M. G.; Sharpless, K. B. Click Chemistry: Diverse Chemical Function from a Few Good Reactions. *Angew. Chem. Int. Ed.* **2001**, *40*, 2004–2021.
(23) Bräse, S.; Gil, C.; Knepper, K.; Zimmermann, V. Organic Azides: An Exploding Diversity of a Unique Class of Compounds. *Angew. Chem. Int. Ed.* **2005**, *44*, 5188–5240.
(24) Brase, S.; Banert, K. *Organic Azides: Synthesis and Applications*; John Wiley and Sons: Chichester, 2010.
(25) Lautens, M.; Maddess, M. L.; Sauer, E. L. O.; Ouellet, S. G. Enantioselective Allylation of β,γ-Unsaturated Aldehydes Generated via Lewis Acid Induced Rearrangement of 2-Vinyloxiranes. *Org. Lett.* **2002**, *4*, 83–86.
(26) Davies, H. M. L.; Cantrell, C. J. R.; Romines, K. R.; Baum, J. S. Synthesis of Furans via Rhodium(II) Acetate-Catalyzed Reaction of Acetylenes with α-Diazocarbonyls: Ethyl 2-Methyl-5-Phenyl-3-Furancarboxylate. *Org. Synth.* **1998**, *70*, 93–97.
(27) Doben, N.; Yan, H.; Kischkewitz, M.; Mao, J.; Studer, A. Intermolecular Acetoxyaminoalkylation of A-Diazo Amides with (Diacetoxyiodo)Benzene and Amines. *Org. Lett.* **2018**, *20*, 7933–7936.

Bibliography

Chapter 1.

(1) Lovering, F.; Bikker, J.; Humblet, C. Escape from Flatland: Increasing Saturation as an Approach to Improving Clinical Success. *J. Med. Chem.* **2009**, *52*, 6752–6756.

(2) Lovering, F. Escape Form Flatland 2: Complexity and Promiscuity. *Medchemcomm* **2013**, *4*, 515–519.

(3) Brill, Z. G.; Condakes, M. L.; Ting, C. P.; Maimone, T. J. Navigating the Chiral Pool in the Total Synthesis of Complex Terpene Natural Products. *Chem. Rev.* **2017**, *117*, 11753–11795.

(4) Crosby, J. Synthesis of Optically Active Compounds: A Large Scale Perspective. *Tetrahedron* **1991**, *47*, 4789–4846.

(5) Paek, S. M.; Jeong, M.; Jo, J.; Heo, Y. M.; Han, Y. T.; Yun, H. Recent Advances in Substrate-Controlled Asymmetric Induction Derived from Chiral Pool α-Amino Acids for Natural Product Synthesis. *Molecules* **2016**, *21*, 951–963.

(6) Nugent, W. A.; RajanBabu, T. V.; Burk, M. J. Beyond Nature's Chiral Pool: Enantioselective Catalysis in Industry. *Science* **1993**, *259*, 479–483.

(7) Noyori, R. *Asymmetric Catalysis in Organic Synthesis*; John Wiley & Sons, Ltd: New York, 1994.

(8) Noyori, R. Asymmetric Catalysis: Science and Opportunities. *Adv. Synth. Catal.* **2003**, *345*, 15–30.

(9) Ault, A. The Nobel Prize in Chemistry for 2001. *J. Chem. Educ.* **2002**, *79*, 572–577.

(10) Jacques, J.; Collet, A.; Willen, S. H. *Enantiomers, Racemates, and Resolutions*; John Wiley & Sons, Ltd, 1981.

(11) Pellissier, H. H. Recent Developments in Dynamic Kinetic Resolution. *Tetrahedron* **2011**, *67*, 3769–3802.

(12) Keith, J. M.; Larrow, J. F.; Jacobsen, E. N. Practical Considerations in Kinetic Resolution Reactions. *Adv. Synth. Catal.* **2001**, *343*, 5–26.

(13) Porter, W. H. Resolution of Chiral Drugs. *Pure Appl. Chem.* **1991**, *63*, 1119–1122.

(14) Carey, J. S.; Laffan, D.; Thomson, C.; Williams, M. T. Analysis of the Reactions Used for the Preparation of Drug Candidate Molecules. *Org. Biomol. Chem.* **2006**, *4*, 2337–2347.

(15) Larrow, J. F.; Jacobsen, E. N. (R,R)-*N*,*N*'-Bis(3,5-Di-*Tert*-Butylsalicylidene)-1,2-Cyclohexanediamino Manganese(III) Chloride, A Highly Enantioselective Epoxidation Catalyst. *Org. Synth.* **1998**, *75*, 1–6.

(16) Reider, P. J. Advances in AIDS Chemotherapy: The Asymmetric Synthesis of Crixivan®. *Chimia* **1997**, *51*, 306–308.

(17) Ahuja, S. *Chiral Separations by Chromatography*; Oxford University Press: New York, 2000.

(18) Ahuja, S.; Zeid, R. L.; Amoss, C. A.; Maier, N. M.; Ning, J. G.; Ye, Y. K.; Webster, G. K.; DePianta, R.; Douville, K.; Nickerson, B.; et al. *Chiral Separation Methods for Pharmaceutical and Biotechnological Products*; John Wiley & Sons, Ltd: Hoboken, 2011.

(19) Zhang, Y.; Wu, D.-R.; Wang-Iverson, D. B.; Tymiak, A. A. Enantioselective Chromatography in Drug Discovery. *Drug Discov. Today* **2005**, *10*, 571–577.
(20) Rossi, D.; Marra, A.; Rui, M.; Brambilla, S.; Juza, M.; Collina, S. "Fit-for-Purpose" Development of Analytical and (Semi)Preparative Enantioselective High Performance Liquid and Supercritical Fluid Chromatography for the Access to a Novel Sigma-1 Recepotr Agonist. *J. Pharm. Biomed. Anal.* **2016**, *118*, 363–369.
(21) Nelson, T. D.; Welch, C. J.; Rosen, J. D.; Smitrovich, J. H.; Huffman, M. A.; Namara, J. M. M. C.; Mathre, D. J. Effective Use of Preparative Chiral HPLC in a Preclinical Drug Synthesis. *Chirality* **2004**, *16*, 609–613.
(22) Leek, H.; Andersson, S. Preparative Scale Resolution of Enantiomers Enables. *Molecules* **2017**, *22*, 158–166.
(23) Martin, V. S.; Woodard, S. S.; Katsuki, T.; Yamada, Y.; Ikeda, M. M.; Sharpless, K. B. Kinetic Resolution of Racemic Allylic Alcohols by Enantioselective Epoxidation. A Route to Substances of Absolute Enantiomeric Purity? *J. Am. Chem. Soc.* **1981**, *103*, 6237–6240.
(24) Adam, W.; Lazarus, M.; Boss, B.; Saha-mo, C. R. Enzymatic Resolution of Chiral 2-Hydroxy Carboxylic Acids by Enantioselective Oxidation with Molecular Oxygen Catalyzed by the Glycolate Oxidase from Spinach (Spinacia Oleracea). *J. Org. Chem.* **1997**, *3263*, 7841–7843.
(25) Dieth, S.; Tritsch, D.; Biellman, J.-F. Resolution of Allylic Alcohols by Cholesterol Oxidase Iosolated from Rhodococcus Erythropolis. *Tetrahedron Lett.* **1995**, *36*, 2243–2246.
(26) Patel, R. N.; Banerjee, A.; Nanduri, V.; Goswami, A.; Comezoglu, F. T. Enzymatic Resolution of Racemic Secondary Alcohols by Lipase B from *Candida Antarctica*. *J. Am. Oil Chem. Soc.* **2000**, *77*, 1015–1019.
(27) Sonnet, P. E.; Baillargeon, M. W. Kinetic Resolution of Secondary Alcohols with Commerical Lipases: Application to Rootworm Sex Pheromone Synthesis. *J. Chemcial Ecol.* **1987**, *13*, 1279–1292.
(28) Ruble, J. C.; Latham, H. A.; Fu, G. C. Effective Kinetic Resolution of Secondary Alcohols with a Planar-Chiral Analogue of 4-(Dimethylamino) Pyridine. Use of the Fe(C_5Ph_5) Group in Asymmetric Catalysis. *J. Am. Chem. Soc.* **1997**, *119*, 1492–1493.
(29) Spivey, A. C.; Fekner, T.; Spey, S. E. Axially Chiral Analogues of 4-(Dimethylamino) Pyridine: Novel Catalysts for Nonenzymatic Enantioselective Acylations. *J. Org. Chem.* **2000**, *65*, 3154–3159.
(30) Kawabata, T.; Nagato, M.; Takasu, K.; Fuji, K. Nonenzymatic Kinetic Resolution of Racemic Alcohols through an "Induced Fit" Process. *J. Am. Chem. Soc.* **1997**, *119*, 3169–3170.
(31) Vedejs, E.; Daugulis, O. 2-Aryl-4,4,8-Trimethyl-2-Phophabicyclo[3.3.0]Octanes:Reactive Chiral Phosphine Catalysts for Enantioselective Acylation. *J. Am. Chem. Soc.* **1999**, *121*, 5813–5814.
(32) Tokunaga, M.; Larrow, J. F.; Kakiuchi, F.; Jacobsen, E. N. Asymmetric Catalysis with Water: Efficient Kinetic Resolution of Terminal Epoxides by Means of Catalytic Hydrolysis. *Science* **1997**, *277*, 936–938.
(33) Jacobsen, E. N. Asymmetric Catalysis of Epoxide Ring-Opening Reactions. *Acc. Chem. Res.* **2000**, *33*, 421–431.

(34) Kim, G.-J.; Lee, H.; Kim, S.-J. Catalytic Activity and Recyclability of New Enantioselective Chiral Co-Salen Complexes in the Hydrolytic Kinetic Resolution of Epichlorohydrine. *Tetrahdron Lett.* **2003**, *44*, 5005–5008.
(35) Dorling, E. K.; Elisabeth, Ö.; Mantoulidis, A.; Mulzer, J. Concise Synthesis of the C3-C14-Fragment of the Antitumor Agent Laulimalide. Application of Jacobsen's HKR Reaction. *Synlett* **2001**, 1105–1108.
(36) Chavez, D. E.; Jacobsen, E. N. Total Synthesis of Fostriecin (CI-920). *Angew. Chem. Int. Ed.* **2001**, *40*, 3667–3670.
(37) Jiang, S.; Liu, Z.; Sheng, G.; Zeng, B.; Cheng, X.; Wu, Y.-L.; Yao, Z.-J. Mimicry of Annonaceous Acetogenins: Enantioselective Synthesis of a (4R)-Hydroxy Analogue Having Potent Antitumor Activity. *J. Org. Chem.* **2002**, *67*, 3404–3408.
(38) HKR Epoxides. *Aldrich ChemFiles* **2005**, *5.4*, 17.
(39) Seeman, J. I.; Farone, W. A. Analytical Solution to the Curtin-Hammett/Winstein-Holness Kinetic System. *J. Org. Chem.* **1978**, *43*, 1854–1864.
(40) Jurkauskas, V.; Buchwald, S. L. Dynamic Kinetic Resolution via Asymmetric Conjugate Reduction: Enantio- and Diastereoselective Synthesis of 2,4-Dialkyl Cyclopentanones. *J. Am. Chem. Soc.* **2002**, *124*, 2892–2893.
(41) Wang, G.-Z.; Backvall, J.-E. Ruthenium-Catalysed Oxidation of Alcohols by Acetone. *J. Chem. Soc. Chem. Commun.* **1992**, 337–339.
(42) Almeida, M. L. S.; Beller, M.; Wang, G.; Backvall, J. Ruthenium(II)-Catalyszed Oppenauer-Type Oxidation of Secondary Alcohols. *Chem. Eur. J.* **1996**, *2*, 1533–1536.
(43) Larsson, A. L. E.; Persson, B. A.; Backvall, J.-E. Enzymatic Resolution of Alcohols Coupled with Ruthenium-Catalyzed Racemization of the Substrate Alcohol. *Angew. Chem. Int. Ed.* **1997**, *36*, 1211–1212.
(44) Leijondahl, K.; Borén, L.; Braun, R.; Bäckvall, J. E. Enzyme- and Ruthenium-Catalyzed Dynamic Kinetic Asymmetric Transformation of 1,5-Diols. Application to the Synthesis of (+)-Solenopsin A. *J. Org. Chem.* **2009**, *74*, 1988–1993.
(45) Steinreiber, J.; Griengl, H. De-Racemization of Enantiomers versus De-Epimerization of Diastereomers — Classification of Dynamic Kinetic Asymmetric. *Chem. - Eur. J.* **2008**, *14*, 8060–8072.
(46) Dornan, P. K.; Kou, K. G. M.; Houk, K. N.; Dong, V. M. Dynamic Kinetic Resolution of Allylic Sulfoxides by Rh-Catalyzed Hydrogenation: A Combined Theoretical and Experimental Mechanistic Study. *J. Am. Chem. Soc.* **2014**, *136*, 291–298.
(47) Arnold, S.; Nguyen, H. M. Rhodium-Catalyzed Dynamic Kinetic Asymmetric Transformations of Racemic Tertiary Allylic Trichloroacetimidates with Anilines. *J. Am. Chem. Soc.* **2012**, *134*, 8380–8383.
(48) Yang, Y.; Shi, S.-L.; Niu, D.; Liu, P.; Buchwald, S. L. Catalytic Asymmetric Hydroamination of Unactivated Internal Olefins to Aliphatic Amines. *Science* **2015**, *349*, 62–66.
(49) Nugent, T. C. *Chiral Amine Synthesis: Methods, Developments and Applications*; Wiley, 2010.
(50) Fleury-Brégeot, N.; de la Fuente, V.; Castillón, S.; Claver, C. Highlights of Transition Metal-Catalyzed Asymmetric Hydrogenation of Imines. *ChemCatChem* **2010**, *2*, 1346–1371.

(51) Hannedouche, J.; Schulz, E. Asymmetric Hydroamination: A Survey of the Most Recent Developments. *Chem. - Eur. J.* **2013**, *19*, 4972–4985.
(52) Trowbridge, A.; Walton, S. M.; Gaunt, M. J. New Strategies for the Transition-Metal Catalyzed Synthesis of Aliphatic Amines. *Chem. Rev* **2020**, *120*, 2613–2692.
(53) Kobayashi, S.; Ishitani, H. Catalytic Enantioselective Addition to Imines. *Chem. Rev.* **1999**, *99*, 1069–1094.
(54) Ukaji, Y.; Watai, T.; Sumi, T.; Fujisawa, T. Reversal of Diastereofacial Selectivity in the Addition Reaction of Organometallics to Chiral Imines. *Chem. Lett.* **1991**, 1555–1558.
(55) Fujihara, H.; Nagai, K.; Tomioka, K. Copper - Amidophosphine Catalyst in Asymmetric Addition of Organozinc to Imines. *J. Am. Chem. Soc.* **2000**, *122*, 12055–12056.
(56) Nishimura, T.; Yasuhara, Y.; Hayashi, T. Asymmetric Addition of Dimethylzinc to N-Tosylarylimines Catalyzed by a Rhodium− Diene Complex toward the Synthesis of Chiral 1-Arylethylamines. *Org. Lett.* **2006**, *8*, 979–981.
(57) Shintani, R.; Takeda, M.; Tsuji, T.; Hayashi, T. Rhodium-Catalyzed Asymmetric Arylation of N -Tosyl Ketimines Ketimines Provides Straightforward Access to Enantioenriched Chiral. **2010**, 13168–13169.
(58) Weix, D. J.; Shi, Y.; Ellman, J. A. Diastereoselective and Enantioselective Rh (I)-Catalyzed Additions of Arylboronic Acids to *N*-*Tert*-Butanesulfinyl and *N*-Diphenylphosphinoyl Aldimines. *J. Am.* **2005**, *127*, 1092–1093.
(59) Kuduk, S. D.; DiPardo, R. M.; Chang, R. K.; Ng, C.; Bock, M. G. Reversal of Diastereoselection in the Addition of Grignard Reagents to Chiral 2-Pyridyl *Tert*-Butyl (Ellman) Sulfinimines. *Tetrahedron Lett.* **2004**, *45*, 6641–6643.
(60) Han, Z.; Krishnamurthy, D.; Pflum, D.; Grover, P.; Wald, S. A.; Senanayake, C. H. First Application of Tunable Alkyl or Aryl Sulfinamides to the Stereoselective Synthesis of a Chiral Amine: Asymmetric Synthesis of (*R*)-Didesmethylsibutramine ((*R*)-DDMS) Using (*R*)-Triethylmethylsulfinamide ((*R*)-TESA). *Org. Lett.* **2002**, 4025–4028.
(61) Brinner, K. M.; Ellman, J. A. A Rapid and General Method for the Asymmetric Synthesis of 2-Substituted Pyrrolidines Using *Tert*-Butanesulfinamide. *Org. Biomol. Chem.* **2005**, *3*, 2109–2113.
(62) Robak, M. T.; Herbage, M. A.; Ellman, J. A. Synthesis and Applications of Tert-Butanesulfinamide. *Chem. Rev.* **2010**, *110*, 3600–3740.
(63) Wu, Y.; Guernon, J.; Shi, J.; Marcin, L.; Higgins, M.; Rajamani, R.; Muckelbauer, J.; Lewis, H.; Chang, C.; Camac, D.; et al. Discovery of S3-Truncated, C-6 Heteroaryl Substituted Aminothiazine B-Site APP Cleaving Enzyme-1 (BACE1) Inhibitors. *J. Med. Chem.* **2016**, *59*, 8593–8600.
(64) Shibasaki, M.; Kanai, M. Asymmetric Synthesis of Tertiary Alcohols and α-Tertiary Amines via Cu-Catalyzed C-C Bond Formation to Ketones and Ketimines. *Chem. Rev.* **2008**, *108*, 2853–2873.
(65) Jiang, C.; Lu, Y.; Hayashi, T. High Performance of a Palladium Phosphinooxazoline Catalyst in the Asymmetric Arylation of Cyclic N-Sulfonyl Ketimines. *Angew. Chem. Int. Ed.* **2014**, *53*, 9936–9939.
(66) Jiang, T.; Wang, Z.; Xu, M. H. Rhodium-Catalyzed Asymmetric Arylation of

Cyclic N-Sulfonyl Aryl Alkyl Ketimines: Efficient Access to Highly Enantioenriched α-Tertiary Amines. *Org. Lett.* **2015**, *17*, 528–531.
(67) Wieland, L. C.; Vieira, E. M.; Snapper, M. L.; Hoveyda, A. H.; Hill, C. Mannich Reactions of Alpha-Ketoimine Esters . Development of a Method and Investigation of Its Mechanism. *J. Am. Chem. Soc.* **2009**, *131*, 570–576.
(68) Kalek, M.; Fu, G. C. Phosphine-Catalyzed Doubly Stereoconvergent Γ-Additions of Racemic Heterocycles to Racemic Allenoates: The Catalytic Enantioselective Synthesis of Protected α,α-Disubstituted A-Amino Acid Derivatives. *J. Am. Chem. Soc.* **2015**, *137*, 9438–9442.
(69) Mandal, M.; Wu, Y.; Misiaszek, J.; Li, G.; Buevich, A.; Caldwell, J. P.; Liu, X.; Mazzola, R. D.; Orth, P.; Strickland, C.; et al. Structure-Based Design of an Iminoheterocyclic β-Site Amyloid Precursor Protein Cleaving Enzyme (BACE) Inhibitor That Lowers Central Aβ in Nonhuman Primates. *J. Med. Chem.* **2016**, *59*, 3231–3248.
(70) Yan, T. Q.; Orihuela, C.; Swanson, D. The Application of Preparative Batch HPLC, Supercritical Fluid Chromatography, Steady-State Recycling, and Simulated Moving Bed for the Resolution of a Racemic Pharmaceutical Intermediate. *Chirality* **2008**, *20*, 139–146.
(71) Jr, W. R. L.; Henderson, D. W.; Miller, R. A.; Spencer, G. A.; Sudah, O. S.; Biba, M.; Welch, C. J. Strategic Use of Preparative Chiral Chromatography for the Synthesis of a Preclinical Pharmaceutical Candidate. *Chirality* **2007**, *19*, 693–700.
(72) Overman, L. E. Molecular Rearrangements in the Construction of Complex Molecules. *Tetrahedron*. 2009, 6432–6446.
(73) Clayden, J.; Donnard, M.; Lefranc, J.; Tetlow, D. J. Quaternary Centres Bearing Nitrogen (Alpha-Tertiary Amines) as Products of Molecular Rearrangements. *Chem. Commun.* **2011**, *47*, 4624–4639.
(74) Nocquet, P. A.; Henrion, S.; Macé, A.; Carboni, B.; Villalgordo, J. M.; Carreaux, F. The Allyl Cyanate/Isocyanate Rearrangement: An Efficient Tool for the Stereocontrolled Formation of Allylic C–N Bonds. *Eur. J. Org. Chem.* **2017**, 1295–1307.
(75) Billeter, O. Ueber Organische Sulfocyanverbindungen. *Ber. Dtsch. Chem. Ges* **1875**, *8*, 462–466.
(76) Gerlich, G. Ueber Psendoyropyl- Und Allylrhodaniir. *Justus Liebigs Ann. Chem* **1875**, *198*, 80–91.
(77) Billeter, O. Notice Sur La Transposisition Des Thiocyanates En Senevols. *Helv. Chim. Acta* **1925**, *11*, 337–338.
(78) Mumm, O.; Richter, H. Versuche Zur Theorie Der Allyl-Umlagerung. *Berichte der Dtsch. Chem. Gesellschaft* **1940**, *73*, 843–860.
(79) Smith, A. S.; Emerson, D. W. The Isomerization of Alkyl Thiocyanates to Isothiocyanates. *J. Am. Chem. Soc.* **1992**, *82*, 3076–3082.
(80) Gonda, J.; Martinkova, M.; Raschmanova, J.; Balentova, E. Creation of Quarternary Stereocentres via [3,3]- Sigmatropic Rearrangement of Allylic Thiocyanates. A Synthetic Appraoch to (+)-Myriocin. *Tetrahedron Asymmetry* **2006**, *17*, 1875–1882.
(81) Christophersen, C.; Holm, A. Formation of 1-Methylallyl and 2-Butenyl Isocyanate from Crotyl Bromide and Silver Cyanate. *Acta Chem. Scand.* **1970**, *24*,

1852–1854.
(82) Christophersen, C.; Holm, A. Alkyl Cyanates. XIV. Isomerization of Allylic Cyanates and Allylic Thionoderivatives. *Acta Chemica Scandinavica*. 1970, pp 1512–1526.
(83) Ichikawa, Y. New Synthetic Method for Allylic Isocyanates Through [3,3] Sigmatropic Rearrangement of Allylic Cyanates. *Synlett* **1991**, 238–240.
(84) Ichikawa, Y. Evolution, Development and Personal Experience in Studies of the Allyl Cyanate-to-Isocyanate Rearrangement. *Synlett* **2007**, 2927–2936.
(85) Ichikawa, Y.; Okumura, K.; Matsuda, Y.; Hasegawa, T.; Nakamura, M.; Fujimoto, A.; Masuda, T.; Nakano, K.; Kotsuki, H. Synthesis of Manzacidin A and C: Efficient Construction of Quaternary Carbon Stereocenters Bearing Nitrogen Substituents. *Org. Biomol. Chem.* **2012**, *10*, 614–622.
(86) Yokoyama, R.; Matsumoto, S.; Nomura, S.; Higaki, T.; Yokoyama, T.; Kiyooka, S. Enantioselective Construction of Nitrogen-Substituted Quaternary Carbon Centers Adjacent to the Carbonyl Group in the Cyclohexane Ring: First Asymmetric Synthesis of Anesthetic (*S*) -Ketamine with High Selectivity. *Tetrahedron* **2009**, *65*, 5181–5191.
(87) Noyori, R.; Ohkuma, T. Asymmetric Catalysis by Architectural and Functional Molecular Engineering: Practical Chemo- and Stereoselective Hydrogenation of Ketones. *Angew. Chem. Int. Ed.* **2001**, *40*, 40–73.
(88) Yoshimura, M.; Tanaka, S.; Kitamura, M. Recent Topics in Catalytic Asymmetric Hydrogenation of Ketones. *Tetrahedron Lett.* **2014**, *55*, 3635–3640.
(89) Echeverria, P. G.; Ayad, T.; Phansavath, P.; Ratovelomanana-Vidal, V. Recent Developments in Asymmetric Hydrogenation and Transfer Hydrogenation of Ketones and Imines through Dynamic Kinetic Resolution. *Synth.* **2016**, *48*, 2523–2539.
(90) Shende, V. S.; Singh, P.; Bhanage, B. M. Recent Trends in Organocatalyzed Asymmetric Reduction of Prochiral Ketones. *Catal. Sci. Technol.* **2018**, *8*, 955–969.
(91) Noyori, R.; Tomino, I.; Yamada, M.; Nishizawa, M. Synthetic Applications of the Enantioselective Reduction by Binaphthol-Modified Lithium Aluminum Hydride Reagents. *J. Am. Chem. Soc.* **1984**, *106*, 6717–6725.
(92) Noyori, R.; Tomino, I.; Tanimoto, Y.; Nishizawa, M. Rational Designing of Efficient Chiral Reducing Agents. Highly Enantioselective Reduction of Aromatic Ketones by Binaphthol-Modified Lithium Aluminum Hydride Reagents. *J. Am. Chem. Soc.* **1984**, *106*, 6709–6716.
(93) Arbour, M.; Roy, S.; Godbout, C.; Spino, C. Stereoselective Synthesis of (+)-Euphococcinine and (-)-Adaline. *J. Org. Chem.* **2009**, *74*, 3806–3814.
(94) Roulland, E.; Monneret, C.; Florent, J.; Bennejean, C.; Renard, P. Enantioselective Synthesis of 12-Amino Alkylidenecyclopentenone Prostaglandins Biological Activities of Cyclopentenone Prostaglandins. *J. Org. Chem.* **2002**, No. 67, 4399–4406.
(95) Overman, L. E. Thermal and Mercuric Ion Catalyzed [3,3]-Sigmatropic Rearrangement of Allylic Trichloroacetimidates. The 1,3 Transposition of Alcohol and Amine Functions. *J. Am. Chem. Soc.* **1974**, *96*, 597–599.
(96) Overman, L. E. A General Method for the Synthesis of Amines by the

Rearrangement of Allylic Trichloroacetimidates. 1,3 Transposition of Alcohol and Amine Functions. *J. Am. Chem. Soc.* **1976**, *1*, 2901–2910.
(97) Chida, N.; Takeoka, J.; Tsutsumi, N.; Ogawa, S. Total Syntheis of (+)-Lactacystin from D-Glucose. *J. Chem. Soc. Chem. Commun.* **1995**, *20*, 793–794.
(98) Kang, S. H.; Kang, S. Y.; Lee, H. S.; Buglass, A. J. Total Synthesis of Natural Tert-Alkylamino Hydroxy Carboxylic Acids. *Chem. Rev.* **2005**, *105*, 4537–4558.
(99) Nishikawa, T.; Asai, M.; Ohyabu, N.; Yamamoto, N.; Fukuda, Y.; Isobe, M. Synthesis of a Common Key Intermediate for (-)-Tetrodotoxin and Its Analogs. *Tetrahedron* **2001**, *57*, 3875–3883.
(100) Nishikawa, T.; Urabe, D.; Isobe, M. An Efficient Total Synthesis of Optically Active Tetrodotoxin. *Angew. Chem. Int. Ed.* **2004**, *43*, 4782–4785.
(101) Overman, L. E.; Owen, C. E.; Pavan, M. M.; Richards, C. J. Catalytic Asymmetric Rearrangement of Allylic N-Aryl Trifluoroacetimidates. A Useful Method for Transforming Prochiral Allylic Alcohols to Chiral Allylic Amines. *Org. Lett.* **2003**, *5*, 1809–1812.
(102) Xin, Z. Q.; Fischer, D. F.; Peters, R. Catalytic Asymmetric Formation of Secondary Allylic Amines by Aza-Claisen Rearrangement of Trifluoroacetimidates. *Synlett* **2008**, 1495–1499.
(103) Fischer, D. F.; Barakat, A.; Xin, Z. Q.; Weiss, M. E.; Peters, R. The Asymmetric Aza-Claisen Rearrangement: Development of Widely Applicable Pentaphenylferrocenyl Palladacycle Catalysts. *Chem. - Eur. J.* **2009**, *15*, 8722–8741.
(104) Fischer, D. F.; Xin, Z.; Peters, R. Asymmetric Formation of Allylic Amines with N-Substituted Quaternary Stereocenters by PdII-Catalyzed Aza-Claisen Rearrangements. *Angew. Chem. Int. Ed.* **2007**, *46*, 7704–7707.
(105) *Molecular Rearrangements in Organic Synthesis*; Rojas, C. M., Ed.; John Wiley and Sons, 2015.
(106) Gagneux, A.; Winstein, S.; Young, W. G. Rearrangement of Allyl Azides. *J. Am. Chem. Soc.* **1960**, *82*, 5956–5957.
(107) Askin, D.; Angst, C.; Danishefsky, S. A Total Syntheis of *N*-Acetylactinobolamine. *J. Org. Chem.* **1985**, *50*, 5005–5007.

Chapter 2.

(1) Gagneux, A.; Winstein, S.; Young, W. G. Rearrangement of Allyl Azides. *J. Am. Chem. Soc.* **1960**, *82*, 5956–5957.
(2) Vekariya, R. H.; Liu, R.; Aubé, J. A Concomitant Allylic Azide Rearrangement/Intramolecular Azide-Alkyne Cycloaddition Sequence. *Org. Lett.* **2014**, *16*, 1844–1847.
(3) Craig, D.; Harvey, J. W.; O'Brien, A. G.; White, A. J. P. Claisen Rearrangements of Equilibrating Allylic Azides. *Org. Biomol. Chem.* **2011**, *9*, 7057–7061.
(4) Lauzon, S.; Tremblay, F.; Gagnon, D.; Godbout, C.; Chabot, C.; Mercier-Shanks, C.; Perreault, S.; DeSeve, H.; Spino, C. Sterically Biased 3,3-Sigmatropic Rearrangement of Chiral Allylic Azides: Application to the Total Syntheses of Alkaloids. *J. Org. Chem.* **2008**, *73*, 6239–6250.
(5) Cardillo, G.; Fabbroni, S.; Gentilucci, L.; Perciaccante, R.; Piccinelli, F.;

Tolomelli, A. Highly Diastereoselective Allylic Azide Formation and Isomerization . Synthesis of 3(2′-Amino)-β-Lactams. *Org. Lett.* **2005**, *3*, 5087–5090.
(6) Padwa, A.; Sa, M. M. Intramolecular O-H Insertion Reaction of Azido Substituted Diazoesters and Its Relevance to the Mechanism of the Allylic Azide Rearrangement. *Tetrahedron Lett.* **1997**, *38*, 5087–5090.
(7) Panek, J.; Yang, M.; Muler, I. Sequential Diastereoselective Addition and Allylic Azide Isomerization of Syn- and Anti-α-Azido-β-(Dimethylphenylsilyl)-(*E*)-Hex-4-Enoates with Acetals: Asymmetric Synthesis of γ- Hydroxy-α-Amino Acid Synthons. *J. Org. Chem.* **1992**, *54*, 4063–4064.
(8) VanderWerf, C. A.; Heasley, L. Studies on the Preparation and Rearrangements of Allylic Azides. *J. Org. Chem.* **1966**, *31*, 3534–3537.
(9) Feldman, A. K.; Colasson, B.; Sharpless, K. B.; Fokin, V. V. The Allylic Azide Rearrangement: Achieving Selectivity. *J. Am. Chem. Soc.* **2005**, *127*, 13444–13445.
(10) Liu, R.; Gutierrez, O.; Tantillo, D. J.; Aubé, J. Stereocontrol in a Combined Allylic Azide Rearrangement and Intramolecular Schmidt Reaction. *J. Am. Chem. Soc.* **2012**, *134*, 6528–6531.
(11) Pellissier, H. H. Recent Developments in Dynamic Kinetic Resolution. *Tetrahedron* **2011**, *67*, 3769–3802.
(12) Steinreiber, J.; Griengl, H. De-Racemization of Enantiomers versus De-Epimerization of Diastereomers — Classification of Dynamic Kinetic Asymmetric. *Chem. - Eur. J.* **2008**, *14*, 8060–8072.
(13) Pellissier, H. Recent Developments in Dynamic Kinetic Resolution. *Tetrahedron* **2008**, *64*, 1563–1601.
(14) Pellissier, H. H. Dynamic Kinetic Resolution. *Tetrahedron* **2003**, *59*, 8291–8327.
(15) Faber, K. Non-Sequential Processes for the Transformation of a Racemate into a Single Stereoisomeric Product : Proposal for Stereochemical Classification. *Chem. - Eur. J.* **2001**, *7*, 5004–5010.
(16) Pamies, O.; Backvall, J.-E. Combination of Enzymes and Metal Catalysts. A Powerful Approach In. *Chem. Rev.* **2003**, *103*, 3247–3261.
(17) Bhat, V.; Welin, E. R.; Guo, X.; Stoltz, B. M. Advances in Stereoconvergent Catalysis from 2005 to 2015: Transition-Metal-Mediated Stereoablative Reactions, Dynamic Kinetic Resolutions, and Dynamic Kinetic Asymmetric Transformations. *Chem. Rev.* **2017**, *117*, 4528–4561.
(18) Chen, X.; Fong, J. Z. M.; Xu, J.; Mou, C.; Lu, Y.; Yang, S.; Song, B. A.; Chi, Y. R. Carbene-Catalyzed Dynamic Kinetic Resolution of Carboxylic Esters. *J. Am. Chem. Soc.* **2016**, *138*, 7212–7215.
(19) Koszelewski, D.; Brodzka, A.; Żądło, A.; Paprocki, D.; Trzepizur, D.; Zysk, M.; Ostaszewski, R. Dynamic Kinetic Resolution of 3-Aryl-4-Pentenoic Acids. *ACS Catal.* **2016**, 3287–3292.
(20) Piotrowski, D. W.; Kamlet, A. S.; Dechert-Schmitt, A. M. R.; Yan, J.; Brandt, T. A.; Xiao, J.; Wei, L.; Barrila, M. T. Regio- and Enantioselective Synthesis of Azole Hemiaminal Esters by Lewis Base Catalyzed Dynamic Kinetic Resolution. *J. Am. Chem. Soc.* **2016**, *138*, 4818–4823.
(21) Zhang, G.; Yang, S.; Zhang, X.; Lin, Q.; Das, D. K.; Liu, J.; Fang, X. Dynamic

Kinetic Resolution Enabled by Intramolecular Benzoin Reaction: Synthetic Applications and Mechanistic Insights. *J. Am. Chem. Soc.* **2016**, *138*, 7932–7938.
(22) Zhang, Q.; Stockdale, D. P.; Mixdorf, J. C.; Topczewski, J. J.; Nguyen, H. M. Iridium-Catalyzed Enantioselective Fluorination of Racemic, Secondary Allylic Trichloroacetimidates. *J. Am. Chem. Soc.* **2015**, *137*, 11912–11915.
(23) Bhadra, S.; Yamamoto, H. Catalytic Asymmetric Synthesis of *N*-Chiral Amine Oxides. *Angew. Chem. Int. Ed.* **2016**, *55*, 13043–13046.
(24) Woods, B. P.; Orlandi, M.; Huang, C. Y.; Sigman, M. S.; Doyle, A. G. Nickel-Catalyzed Enantioselective Reductive Cross-Coupling of Styrenyl Aziridines. *J. Am. Chem. Soc.* **2017**, *139*, 5688–5691.
(25) Bartlett, S. L.; Keiter, K. M.; Johnson, J. S. Synthesis of Complex Tertiary Glycolates by Enantioconvergent Arylation of Stereochemically Labile α-Keto Esters. *J. Am. Chem. Soc.* **2017**, *139*, 3911–3916.
(26) Rasu, L.; John, J. M.; Stephenson, E.; Endean, R.; Kalapugama, S.; Clément, R.; Bergens, S. H. Highly Enantioselective Hydrogenation of Amides via Dynamic Kinetic Resolution Under Low Pressure and Room Temperature. *J. Am. Chem. Soc.* **2017**, *139*, 3065–3071.
(27) Applegate, G. A.; Berkowitz, D. B. Exploiting Enzymatic Dynamic Reductive Kinetic Resolution (DYRKR) in Stereocontrolled Synthesis. *Adv. Synth. Catal.* **2015**, *357*, 1619–1632.
(28) Noyori, R.; Ikeda, T.; Ohkuma, T.; Widhalm, M.; Kitamura, M.; Takaya, H.; Akutagawa, S.; Sayo, N.; Saito, T.; Taketomi, T.; et al. Stereoselective Hydrogenation via Dynamic Kinetic Resolution. *J. Am. Chem. Soc.* **1999**, *111*, 9134–9135.
(29) Trost, B. M.; Toste, F. D. Palladium-Catalyzed Kinetic and Dynamic Kinetic Asymmetric Transformation of Synthesis of (-) -Aflatoxin B Lactone. *J. Am. Chem. Soc.* **1999**, *121*, 3543–3544.
(30) Rainka, M. P.; Milne, J. E.; Buchwald, S. L. Dynamic Kinetic Resolution of α,β -Unsaturated Lactones through Asymmetric Copper-Catalyzed Conjugate Reduction: Application to the Total Synthesis of Eupomatilone-3. *Angew. Chem. Int. Ed.* **2005**, *44*, 6177–6180.
(31) Jurkauskas, V.; Buchwald, S. L. Dynamic Kinetic Resolution via Asymmetric Conjugate Reduction: Enantio- and Diastereoselective Synthesis of 2,4-Dialkyl Cyclopentanones. *J. Am. Chem. Soc.* **2002**, *124*, 2892–2893.
(32) Petersen, K. S. Chiral Brønsted Acid Catalyzed Kinetic Resolutions. *Asian J. Org. Chem* **2016**, *5*, 308–320.
(33) Lu, G.; Birman, V. B. Dynamic Kinetic Resolution of Azlactones Catalyzed by Chiral Brønsted Acids. *Org. Lett.* **2011**, *13*, 356–358.
(34) Weisenburger, G. A.; Faibish, N. C.; Pippel, D. J.; Beak, P. Temperature- and Electrophile-Dependent Stereocontrol: A Structural and Mechanistic Investigation of (-)-Sparteine-Mediated Asymmetric Lithiation-Substitution Sequences of *N*-Boc-*N*-*p*-Methoxyphenyl) Cinnamylamine. *J. Am. Chem. Soc.* **1999**, *121*, 9522–9530.
(35) Pellissier, H. Organocatalyzed Dynamic Kinetic Resolution. *Adv. Synth. Catal.* **2011**, *353*, 659–676.
(36) Berkessel, A.; Cleemann, F.; Mukherjee, S.; Müller, T. N.; Lex, J. Highly Efficient

Dynamic Kinetic Resolution of Azlactones by Urea-Based Bifunctional Organocatalysts. *Angew. Chem. Int. Ed.* **2005**, *44*, 807–811.
(37) Tang, L.; Deng, L. Dynamic Kinetic Resolution via Dual-Function Catalysis of Modified Cinchona Alkaloids : Asymmetric Synthesis of α-Hydroxy Carboxylic Acids. *J. Am. Chem. Soc.* **2002**, *124*, 2870–2871.
(38) Dornan, P. K.; Kou, K. G. M.; Houk, K. N.; Dong, V. M. Dynamic Kinetic Resolution of Allylic Sulfoxides by Rh-Catalyzed Hydrogenation: A Combined Theoretical and Experimental Mechanistic Study. *J. Am. Chem. Soc.* **2014**, *136*, 291–298.
(39) Wu, Y.; Guernon, J.; Shi, J.; Marcin, L.; Higgins, M.; Rajamani, R.; Muckelbauer, J.; Lewis, H.; Chang, C.; Camac, D.; et al. Discovery of S3-Truncated, C-6 Heteroaryl Substituted Aminothiazine B-Site APP Cleaving Enzyme-1 (BACE1) Inhibitors. *J. Med. Chem.* **2016**, *59*, 8593–8600.
(40) Ghosh, A. K.; Osswald, H. L. BACE1 (β-Secretase) Inhibitors for the Treatment of Alzheimer's Disease. *Chem. Soc. Rev.* **2014**, *43*, 6765–6813.
(41) Kolb, H. C.; VanNieuwenhze, M. S.; Sharpless, K. B. Catalytic Asymmetric Dihydroxylation. *Chem. Rev.* **1994**, *94*, 2483–2547.
(42) Hu, Z.; Liu, J.; Li, G.; Dong, Z.; Li, W. Synthesis of Asymmetric Triarylbenzenes by Using $SOCl_2$ -C_2H_5OH Reagent. *J. Chinese Chem. Soc.* **2004**, *51*, 581–583.
(43) Hoffmann, R.; Radom, L.; Pople, J. A.; Schleyer, P. von R.; Hehre, W. J.; Salem, L. Strong Conformational Consequences of Hyperconjugation. *J. Am. Chem. Soc.* **1972**, *94*, 6221–6223.
(44) Radom, L.; Hehre, W. J.; Pople, J. A. Molecular Orbital Theory of the Electronic Structure of Organic Compounds XIII. Fourier Component Analysis of Internal Rotation Potential Functions in Saturated Molecules. *J. Am. Chem. Soc.* **1972**, *94*, 2371–2381.
(45) Patonay, T.; Kónya, K.; Juhász-Tóth, É. Syntheses and Transformations of α-Azido Ketones and Related Derivatives. *Chem. Soc. Rev.* **2011**, *40*, 2797–2847.
(46) Robak, M. T.; Herbage, M. A.; Ellman, J. A. Synthesis and Applications of *Tert*-Butanesulfinamide. *Chem. Rev.* **2010**, *110*, 3600–3740.

Chapter 3.

(1) Lutz, R. P. Catalysis of the Cope and Claisen Rearrangements. *Chem. Rev.* **1984**, *84*, 206–243.
(2) Nakai, T.; Mikami, K. [2,3]-Wittig Sigmatropic Rearrangements in Organic Synthesis. *Chem. Rev.* **1986**, *86*, 885–902.
(3) Wilson, S. R.; Price, M. F. The Ester Enolate Carroll Rearrangment. *J. Org. Chem.* **1984**, *49*, 722–725.
(4) Kantor, S. W.; Hauser, C. R. Rearrangements of Benzyltrimethylammonium Ion and Related Quaternary Ammonium Ions by Sodium Amide Involving Migration into the Ring. *J. Am. Chem. Soc.* **1951**, *73*, 4122–4131.
(5) Evans, D. A.; Andrews, G. C. Allylic Sulfoxides: Useful Intermediates in Organic Synthesis. *Acc. Chem. Res.* **1974**, *7*, 147–155.
(6) Albini, A. Synthetic Utility of Amine *N*-Oxides. *Synthesis* **1992**, 263–277.
(7) Overman, L. E. Allylic and Propargylic Imidic Esters in Organic Synthesis. *Acc.*

Chem. Res. **1980**, *13*, 218–224.
(8) Nubbemeyer, U. Recent Advances in Asymmetric [3 ,3]-Sigmatropic Rearrangements. *Synthesis* **2003**, *7*, 961–1008.
(9) Jones, A. C.; May, J. A.; Sarpong, R.; Stoltz, B. M. Toward a Symphony of Reactivity : Cascades Involving Catalysis and Sigmatropic Rearrangements. *Angew. Chem. Int. Ed.* **2014**, *53*, 2556–2591.
(10) Ilardi, E. A.; Stivala, C. E.; Zakarian, A. [3,3]-Sigmatropic Rearrangements: Recent Applications in the Total Synthesis of Natural Products. *Chem. Soc. Rev.* **2009**, *38*, 3133–3148.
(11) Gagneux, A.; Winstein, S.; Young, W. G. Rearrangement of Allyl Azides. *J. Am. Chem. Soc.* **1960**, *82*, 5956–5957.
(12) Doering, W. V. E.; Roth, W. R. Thermal Rearrangements. *Angew. Chem. Int. Ed.* **1963**, *2*, 115–122.
(13) Overman, L. E.; Fredrick, K. M. Palladium (II)-Catalyzed Rearrangement of Allylic Acetates. *Tetrahedron Lett.* **1979**, *20*, 321–234.
(14) Marion, N.; Gealageas, R.; Nolan, S. P. [(NHC)Au(I)]-Catalyzed Rearrangement of Allyic Acetates. *Org. Lett.* **2007**, *9*, 2653–2656.
(15) Kreiman, H. W.; Batali, M. E.; Jamieson, C. S.; Lyon, M. A.; Duncan, J. A. CASSCF Calculations Reveal Competitive Chair (Pericyclic) and Boat (Pseudopericyclic) Transition States for the [3,3] Sigmatropic Rearrangement of Allyl Esters. *J. Org. Chem.* **2018**, *83*, 1717–1726.
(16) VanderWerf, C. A.; Heisler, R. V; McEwen, W. E. The Reaction of Sodium Azide with Some Representative Epoxides. *J. Am. Chem. Soc.* **1954**, *76*, 1231–1235.
(17) VanderWerf, C. A.; Heasley, L. Studies on the Preparation and Rearrangements of Allylic Azides. *J. Org. Chem.* **1966**, *31*, 3534–3537.
(18) Le Noble, W. J. The Effect of Pressure on the Equilibration of α- and γ-Methylallyl Azide. *J. Phys. Chem.* **1963**, *67*, 2451–2453.
(19) Padwa, A.; Sa, M. M. Intramolecular O-H Insertion Reaction of Azido Substituted Diazoesters and Its Relevance to the Mechanism of the Allylic Azide Rearrangement. *Tetrahedron Lett.* **1997**, *38*, 5087–5090.
(20) Gagnon, D.; Lauzon, S.; Godbout, C.; Spino, C. Sterically Biased 3,3-Sigmatropic Rearrangement of Azides: Efficient Preparation of Nonracemic α-Amino Acids and Heterocycles. *Org. Lett.* **2005**, *7*, 4769–4771.
(21) Jabbari, A. Transition States and Activation Barriers for [3,3]-Sigmatropic Shift of Allyl Azides. *Org. Chem. J.* **2010**, *1*, 6–14.
(22) Kang, H.; Kang, Y. K. Allylic Azide Rearrangements Investigated by Density Functional Theory Calculations. *Bull. Korean Chem. Soc.* **2017**, *38*, 1419–1426.
(23) Porta, E. O. J.; Vallejos, M. M.; Bracca, A. B. J.; Labadie, G. R. Experimental and Theoretical Studies of the [3,3]- Sigmatropic Rearrangement of Prenyl Azides. *RSC Adv.* **2017**, *7*, 47527–47538.
(24) Askin, D.; Angst, C.; Danishefsky, S. A Total Syntheis of *N*-Acetylactinobolamine. *J. Org. Chem.* **1985**, *50*, 5005–5007.
(25) Liu, R.; Gutierrez, O.; Tantillo, D. J.; Aubé, J. Stereocontrol in a Combined Allylic Azide Rearrangement and Intramolecular Schmidt Reaction. *J. Am. Chem. Soc.* **2012**, *134*, 6528–6531.
(26) Vekariya, R. H.; Liu, R.; Aubé, J. A Concomitant Allylic Azide

Rearrangement/Intramolecular Azide-Alkyne Cycloaddition Sequence. *Org. Lett.* **2014**, *16*, 1844–1847.
(27) Feldman, A. K.; Colasson, B.; Sharpless, K. B.; Fokin, V. V. The Allylic Azide Rearrangement: Achieving Selectivity. *J. Am. Chem. Soc.* **2005**, *127*, 13444–13445.
(28) Craig, D.; Harvey, J. W.; O'Brien, A. G.; White, A. J. P. Claisen Rearrangements of Equilibrating Allylic Azides. *Org. Biomol. Chem.* **2011**, *9*, 7057–7061.
(29) Moynihan, L.; Chadda, R.; Mcardle, P.; Murphy, P. V. Allylic Azide Rearrangement in Tandem with Huisgen Cycloaddition for Stereoselective Annulation: Synthesis of *C*-Glycosyl Iminosugars. *Org. Lett.* **2015**, *17*, 6226–6229.
(30) Chadda, R.; Mcardle, P.; Murphy, P. V. Allylic Azide Rearrangement in Tandem with Intramolecular Huisgen Cycloaddition for Iminosugar and Glycomimetic Synthesis: Functionalized Piperidine, Pyrrolidine, and Pyrrolotriazoles from D-Mannose. *Synthesis* **2017**, *49*, 2138–2152.
(31) Packard, M. H.; Cox, J. H.; Suding, V. P.; Topczewski, J. J. The Effect of Proximal Functionality on the Allylic Azide Equilibrium. *Eur. J. Org. Chem.* **2017**, 6365–6368.
(32) Ott, A. A.; Goshey, C. S.; Topczewski, J. J. Dynamic Kinetic Resolution of Allylic Azides via Asymmetric Dihydroxylation. *J. Am. Chem. Soc.* **2017**, *139*, 7737–7740.
(33) Porter, M. R.; Shaker, R. M.; Calcanas, C.; Topczewski, J. J. Stereoselective Dynamic Cyclization of Allylic Azides : Synthesis of Tetralins, Chromanes, and Tetrahydroquinolines. *J. Am. Chem. Soc.* **2018**, *140*, 1211–1214.
(34) Hassner, A.; Fibiger, R.; Andisik, D. Lewis Acid Catalyzed Conversion of Alkenes and Alcohols to Azides. *J. Org. Chem.* **1984**, *49*, 4237–4244.
(35) Carlson, A. S.; Calcanas, C.; Brunner, R. M.; Topczewski, J. J. Regiocontrolled Wacker Oxidation of Cinnamyl Azides. *Org. Lett.* **2018**, *20*, 1604–1607.
(36) Panek, J.; Yang, M.; Muler, I. Sequential Diastereoselective Addition and Allylic Azide Isomerization of Syn- and Anti-α-Azido-β-(Dimethylphenylsilyl)-(*E*)-Hex-4-Enoates with Acetals: Asymmetric Synthesis of γ- Hydroxy-α-Amino Acid Synthons. *J. Org. Chem.* **1992**, *54*, 4063–4064.
(37) Doherty, W.; Evans, P. Aminooxylation Horner-Wadsworth-Emmons Sequence for the Synthesis of Enantioenriched γ-Functionalized Vinyl Sulfones. *J. Org. Chem.* **2016**, *81*, 1416–1424.
(38) Cope, A. C.; Hardy, E. M. The Introduction of Substituted Vinyl Groups. V. A Rearrangement Involving the Migration of an Allyl Group in a Three-Carbon System. *J. Am. Chem. Soc.* **1940**, *62*, 441–444.
(39) Safi, M.; Fahrang, R.; Sinou, D. Palladium(0)-Catalyzed Azidation of Allyl Esters with Trimethylsilyl Azide. *Tetrahedron Lett.* **1990**, *31*, 527–530.
(40) Maag, H.; J, R. M. R. An Allylic Azide Route to 4'-Azido Carbocyclic Nucleosides. Synthesis of (±)-(1'α,2'α,3'β)- and (±)-(1'α,2'β,3'β)-1-[1-Azido-2-Hydroxy-1-(Hydroxymethyl)-3-Cyclopentyl]Thymine. *J. Org. Chem.* **1992**, *57*, 5823–5831.
(41) Banert, K.; Hagedorn, M.; Liedtke, C.; Melzer, A.; Schöffler, C. Reactions of Unsaturated Azides, 12 Azido-1,2,3-Triphenylpropenes of Varying Stabilities: A

Corrigendum of Structure Assignment. *Eur. J. Org. Chem.* **2000**, 257–267.
(42) Goswami, P. P.; Suding, V. P.; Carlson, A. S.; Topczewski, J. J. Direct Conversion of Aldehydes and Ketones into Azides by Sequential Nucleophilic Addition and Substitution. *Eur. J. Org. Chem.* **2016**, 4805–4809.
(43) Marenich, A. V; Cramer, C. J.; Truhlar, D. G. Universal Solvation Model Based on Solute Electron Density and on a Continuum Model of the Solvent Defined by the Bulk Dielectric Constant and Atomic Surface Tensions. *J. Phys. Chem. B.* **2009**, *113*, 6378–6396.
(44) Zhao, Y.; Truhlar, D. G. The M06 Suite of Density Functionals for Main Group Thermochemistry, Thermochemical Kinetics, Noncovalent Interactions, Excited States, and Transition Elements: Two New Functionals and Systematic Testing of Four M06-Class Functionals and 12 Other Function. *Theor. Chem. Acc.* **2008**, *120*, 215–241.
(45) Sharma, S.; Rajale, T.; Unruh, D. K.; Birney, D. M. Competitive Pseudopericyclic [3,3]- and [3,5]-Sigmatropic Rearrangements of Trichloroacetimidates. *J. Org. Chem.* **2015**, *80*, 11734–11743.
(46) Sharma, S.; Rajale, T.; Cordes, D. B.; Hung-Low, F.; Birney, D. M. Experimental and Computational Studies on the [3,3]- and [3,5]- Sigmatropic Rearrangements of Acetoxycyclohexadienones: A Non- Ionic Mechanism for Acyl Migration. *J. Am. Chem. Soc.* **2013**, *135*, 14438.
(47) Klepper, F.; Jahn, E. M.; Hickmann, V.; Carell, T. Synthesis of the Transfer-RNA Nucleoside Queuosine by Using a Chiral Allyl Azide Intermediate. *Angew. Chem. Int. Ed.* **2007**, *46*, 2325–2327.
(48) Espenson, J. H. *Chemical Kinetics and Reaction Mechanisms*; McGraw-Hill, Inc: New York, 1995.

Chapter 4.

(1) Pellissier, H. H. Recent Developments in Dynamic Kinetic Resolution. *Tetrahedron* **2011**, *67*, 3769–3802.
(2) Pellissier, H. H. Dynamic Kinetic Resolution. *Tetrahedron* **2003**, *59*, 8291–8327.
(3) Verho, O.; Bäckvall, J. E. Chemoenzymatic Dynamic Kinetic Resolution: A Powerful Tool for the Preparation of Enantiomerically Pure Alcohols and Amines. *J. Am. Chem. Soc.* **2015**, *137*, 3996–4009.
(4) Bhat, V.; Welin, E. R.; Guo, X.; Stoltz, B. M. Advances in Stereoconvergent Catalysis from 2005 to 2015: Transition-Metal-Mediated Stereoablative Reactions, Dynamic Kinetic Resolutions, and Dynamic Kinetic Asymmetric Transformations. *Chem. Rev.* **2017**, *117*, 4528–4561.
(5) El Gihani, M. T.; Williams, J. M. J. Dynamic Kinetic Resolution. *Curr. Opin. Chem. Biol.* **1999**, *3*, 11–15.
(6) Huerta, F.; Minidis, A. Racemisation in Asymmetric Synthesis. Dynamic Kinetic Resolution and Related Processes in Enzyme and Metal Catalysis. *Chem. Soc. Rev.* **2001**, *30*, 321–331.
(7) Keith, J. M.; Larrow, J. F.; Jacobsen, E. N. Practical Considerations in Kinetic Resolution Reactions. *Adv. Synth. Catal.* **2001**, *343*, 5–26.
(8) Tai, A.; Wantanabe, H.; Harada, T. Stereochemical Studies of the Hydrogenation

with Asymmetrically Modified Nickel Catalysts; The Hydrogenation of Methyl 2-Alkyl-3-Oxobutyrate. *Bull. Chem. Soc. Jpn.* **1979**, *52*, 1468–1472.
(9) Noyori, R.; Ikeda, T.; Ohkuma, T.; Widhalm, M.; Kitamura, M.; Takaya, H.; Akutagawa, S.; Sayo, N.; Saito, T.; Taketomi, T.; et al. Stereoselective Hydrogenation via Dynamic Kinetic Resolution. *J. Am. Chem. Soc.* **1999**, *111*, 9134–9135.
(10) Jurkauskas, V.; Buchwald, S. L. Dynamic Kinetic Resolution via Asymmetric Conjugate Reduction: Enantio- and Diastereoselective Synthesis of 2,4-Dialkyl Cyclopentanones. *J. Am. Chem. Soc.* **2002**, *124*, 2892–2893.
(11) Carmona, J. A.; Hornillos, V.; Ramírez-López, P.; Ros, A.; Iglesias-Sigüenza, J.; Gómez-Bengoa, E.; Fernández, R.; Lassaletta, J. M. Dynamic Kinetic Asymmetric Heck Reaction for the Simultaneous Generation of Central and Axial Chirality. *J. Am. Chem. Soc.* **2018**, *140*, 11067–11075.
(12) Ott, A. A.; Goshey, C. S.; Topczewski, J. J. Dynamic Kinetic Resolution of Allylic Azides via Asymmetric Dihydroxylation. *J. Am. Chem. Soc.* **2017**, *139*, 7737–7740.
(13) Porter, M. R.; Shaker, R. M.; Calcanas, C.; Topczewski, J. J. Stereoselective Dynamic Cyclization of Allylic Azides : Synthesis of Tetralins, Chromanes, and Tetrahydroquinolines. *J. Am. Chem. Soc.* **2018**, *140*, 1211–1214.
(14) Ding, P. G.; Hu, X. S.; Zhou, F.; Zhou, J. Catalytic Enantioselective Synthesis of α-Chiral Azides. *Org. Chem. Front.* **2018**, *5*, 1542–1559.
(15) Gagneux, A.; Winstein, S.; Young, W. G. Rearrangement of Allyl Azides. *J. Am. Chem. Soc.* **1960**, *82*, 5956–5957.
(16) Feldman, A. K.; Colasson, B.; Sharpless, K. B.; Fokin, V. V. The Allylic Azide Rearrangement: Achieving Selectivity. *J. Am. Chem. Soc.* **2005**, *127*, 13444–13445.
(17) Liu, R.; Gutierrez, O.; Tantillo, D. J.; Aubé, J. Stereocontrol in a Combined Allylic Azide Rearrangement and Intramolecular Schmidt Reaction. *J. Am. Chem. Soc.* **2012**, *134*, 6528–6531.
(18) Ott, A. A.; Packard, M. H.; Ortuño, M. A.; Johnson, A.; Suding, V. P.; Cramer, C. J.; Topczewski, J. J. Evidence for a Sigmatropic and an Ionic Pathway in the Winstein Rearrangement. *J. Org. Chem.* **2018**, *83*, 8214–8224.
(19) Trost, B. M.; Pulley, S. R. On the Flexibility of Allylic Azides as Synthetic Intermediates. *Tetrahedron Lett.* **1995**, *36*, 8737–8740.
(20) Liu, R. A Combined Allylic Azide Rearrangement and Intramolecular Schmidt Reaction - Discovery, Development, And Application. *Ph.D Diss. Univ. Kansas* **2003**.
(21) Lalonde, R. L.; Sherry, B. D.; Kang, E. J.; Toste, F. D. Gold (I)-Catalyzed Enantioselective Intramolecular Hydroamination of Allenes. *J. Am. Chem. Soc.* **2007**, *129*, 2452–2453.
(22) Espenson, J. H. *Chemical Kinetics and Reaction Mechanisms*; McGraw-Hill, Inc: New York, 1995.
(23) Jaffe, H. H. A Reexamination of the Hammett Equation. *Chem. Rev.* **1973**, *53*, 191–261.
(24) Dash, C.; Yousufuddin, M.; Cundari, T. R.; Dias, H. V. R. Gold-Mediated Expulsion of Dinitrogen from Organic Azides. *J. Am. Chem. Soc.* **2013**, *135*,

15479–15488.

Chapter 5.

(1) Tornøe, C. W.; Christensen, C.; Meldal, M. Peptidotriazoles on Solid Phase : [1,2,3]-Triazoles by Regiospecific Copper (I)-Catalyzed 1,3-Dipolar Cycloadditions of Terminal Alkynes to Azides. *J. Org. Chem.* **2002**, *67*, 3057–3064.

(2) Rostovtsev, V. V.; Green, L. G.; Fokin, V. V.; Sharpless, K. B. A Stepwise Huisgen Cycloaddition Process: Copper(I)-Catalyzed Regioselective "Ligation" of Azides and Terminal Alkynes. *Angew. Chem. Int. Ed.* **2002**, *41*, 2596–2599.

(3) Meldal, M.; Tornøe, C. W. Cu-Catalyzed Azide-Alkyne Cycloaddition. *Chem. Rev.* **2008**, *108*, 2952–3015.

(4) Pedersen, D. S.; Abell, A. 1,2,3-Triazoles in Peptidomimetic Chemistry. *Eur. J. Org. Chem.* **2011**, 2399–2411.

(5) Finn, M. G.; Fokin, V. V. Click Chemistry: Function Follows Form. *Chem. Soc. Rev.* **2010**, *39*, 1231–1232.

(6) Kolb, H. C.; Finn, M. G.; Sharpless, K. B. Click Chemistry: Diverse Chemical Function from a Few Good Reactions. *Angew. Chem. Int. Ed.* **2001**, *40*, 2004–2021.

(7) Ellman, J. A.; Jain, R. K.; Wood, W. J. L.; Tsuruoka, H.; Patterson, A. W. Substrate Activity Screening: A Fragment-Based Method for the Rapid Identification of Nonpeptidic Protease Inhibitors. *J. Am. Chem. Soc.* **2005**, *127*, 15521–15527.

(8) Lee, T.; Cho, M.; Ko, S.-Y.; Youn, H.-J.; Baek, D. J.; Cho, W.-J.; Kang, C.-Y.; Kim, S. Synthesis and Evaluation of 1,2,3-Triazole Containing Analogues of the Immunostimulane Alpha-GalCer. *J. Med. Chem.* **2007**, *50*, 585–589.

(9) Patterson, A. W.; Wood, W. J. L.; Hornsby, M.; Lesley, S.; Spraggon, G.; Ellman, J. A. Identification of Selective, Nonpeptidic Nitrile Inhibitors of Cathepsin S Using the Substrate Activity Screening Method. *J. Med. Chem.* **2006**, *49*, 6298–6307.

(10) Huber, K.; Hamad, B.; Kirkpatrick, P. Fresh from the Pipeline: Ticagrelor. *Nat. Rev. Drug Discov.* **2011**, *10*, 255–256.

(11) Deprez-Poulain, R.; Hennuyer, N.; Bosc, D.; Liang, W. G.; Marechal, X.; Charton, J.; Totobenazara, J.; Berte, G.; Jahklal, J.; Verdelet, T.; et al. Catalytic Site Inhibition of Insulin-Degrading Enzyme by a Small Molecule Induces Glucose Intolerance in Mice. *Nat. Commun.* **2015**, *6*, 1–13.

(12) Mocharla, V. P.; Walsh, J. C.; Padgett, H. C.; Su, H.; Fueger, B.; Weber, W. A.; Czernin, J.; Kolb, H. C. From In Situ to In Vivo : An In Situ Click-Chemistry-Derived Carbonic Anhydrase II Imaging Agent for Positron Emission Tomography. *ChemMedChem* **2013**, *8*, 43–48.

(13) Rodionov, V. O.; Fokin, V. V.; Finn, M. G. Mechanism of the Ligand-Free CuI-Catalyzed Azide-Alkyne Cycloaddition Reaction. *Angew. Chem. Int. Ed.* **2005**, *44*, 2210–2215.

(14) Meng, J. C.; Fokin, V. V.; Finn, M. G. Kinetic Resolution by Copper-Catalyzed Azide-Alkyne Cycloaddition. *Tetrahedron Lett.* **2005**, *46*, 4543–4546.

(15) Brittain, W. D. G.; Buckley, B. R.; Fossey, J. S. Kinetic Resolution of Alkyne-Substituted Quaternary Oxindoles via Copper Catalysed Azide-Alkyne Cycloadditions. *Chem. Commun.* **2015**, *51*, 17217–17220.
(16) Brittain, W. D. G.; Chapin, B. M.; Zhai, W.; Lynch, V. M.; Buckley, B. R.; Anslyn, E. V.; Fossey, J. S. The Bull-James Assembly as a Chiral Auxiliary and Shift Reagent in Kinetic Resolution of Alkyne Amines by the CuAAC Reaction. *Org. Biomol. Chem.* **2016**, *14*, 10778–10782.
(17) Liu, E.-C.; Topczewski, J. J. Enantioselective Copper Catalyzed Alkyne-Azide Cycloaddition by Dynamic Kinetic Resolution. *J. Am. Chem. Soc.* **2019**, *141*, 5135–5138.
(18) Zhou, F.; Tan, C.; Tang, J.; Zhang, Y. Y.; Gao, W. M.; Wu, H. H.; Yu, Y. H.; Zhou, J. Asymmetric Copper(I)-Catalyzed Azide-Alkyne Cycloaddition to Quaternary Oxindoles. *J. Am. Chem. Soc.* **2013**, *135*, 10994–10997.
(19) Page, P.; Martin, J.; Stephenson, G.; Gaumont, A.-C.; Deschamps, D.; Buttress, J.; Lancelot, M.; Sheldon, A.; Alayrac, C. An Investigation of the Asymmetric Huisgen 'Click' Reaction. *Synlett* **2013**, *24*, 2723–2729.
(20) Zheng, Z.-J.; Song, T.; Xu, L.-W.; Deng, Y.; Xu, Z.; Zhou, W.; Li, L. Enantioselective Copper-Catalyzed Azide-Alkyne Click Cycloaddition to Desymmetrization of Maleimide-Based Bis(Alkynes). *Chem. - Eur. J.* **2014**, *21*, 554–558.
(21) Osako, T.; Uozumi, Y. Enantioposition-Selective Copper-Catalyzed Azide-Alkyne Cycloaddition for Construction of Chiral Biaryl Derivatives. *Org. Lett.* **2014**, *16*, 5866–5869.
(22) Brittain, W. D. G. G.; Buckley, B. R.; Fossey, J. S. Asymmetric Copper-Catalyzed Azide-Alkyne Cycloadditions. *ACS Catal.* **2016**, *6*, 3629–3636.
(23) Ott, A. A.; Goshey, C. S.; Topczewski, J. J. Dynamic Kinetic Resolution of Allylic Azides via Asymmetric Dihydroxylation. *J. Am. Chem. Soc.* **2017**, *139*, 7737–7740.
(24) Porter, M. R.; Shaker, R. M.; Calcanas, C.; Topczewski, J. J. Stereoselective Dynamic Cyclization of Allylic Azides : Synthesis of Tetralins, Chromanes, and Tetrahydroquinolines. *J. Am. Chem. Soc.* **2018**, *140*, 1211–1214.
(25) Ott, A. A.; Packard, M. H.; Ortuño, M. A.; Johnson, A.; Suding, V. P.; Cramer, C. J.; Topczewski, J. J. Evidence for a Sigmatropic and an Ionic Pathway in the Winstein Rearrangement. *J. Org. Chem.* **2018**, *83*, 8214–8224.
(26) Keith, J. M.; Larrow, J. F.; Jacobsen, E. N. Practical Considerations in Kinetic Resolution Reactions. *Adv. Synth. Catal.* **2001**, *343*, 5–26.
(27) Worrell, B. T.; Malik, J. A.; Fokin, V. V. Direct Evidence of a Dinuclear Copper Intermediate in Cu(I)-Catalyzed Azide-Alkyne Cycloadditions. *Science* **2013**, *340*, 457–461.
(28) Ott, A. A.; Topczewski, J. J. Catalytic Racemization of Activated Organic Azides. *Org. Lett.* **2018**, *20*, 7253–7256.

Chapter 6.

(1) Nugent, T. C. *Chiral Amine Synthesis: Methods, Developments and Applications*; Wiley, 2010.

(2) Gagneux, A.; Winstein, S.; Young, W. G. Rearrangement of Allyl Azides. *J. Am. Chem. Soc.* **1960**, *82*, 5956–5957.
(3) Ott, A. A.; Goshey, C. S.; Topczewski, J. J. Dynamic Kinetic Resolution of Allylic Azides via Asymmetric Dihydroxylation. *J. Am. Chem. Soc.* **2017**, *139*, 7737–7740.
(4) Liu, E.-C.; Topczewski, J. J. Enantioselective Copper Catalyzed Alkyne–Azide Cycloaddition by Dynamic Kinetic Resolution. *J. Am. Chem. Soc.* **2019**, *141*, 5135–5138.
(5) Ott, A. A.; Topczewski, J. J. Catalytic Racemization of Activated Organic Azides. *Org. Lett.* **2018**, *20*, 7253–7256.
(6) Alexander, J. R.; Ott, A. A.; Liu, E.-C.; Topczewski, J. J. Kinetic Resolution of Cyclic Secondary Azides, Using an Enantioselective Copper-Catalyzed Azide-Alkyne Cycloaddition. *Org. Lett.* **2019**, *21*, 4355–4358.
(7) Finn, M. G.; Fokin, V. V. Click Chemistry: Function Follows Form. *Chem. Soc. Rev.* **2010**, *39*, 1231–1232.
(8) Pedersen, D. S.; Abell, A. 1,2,3-Triazoles in Peptidomimetic Chemistry. *Eur. J. Org. Chem.* **2011**, 2399–2411.
(9) Ellman, J. A.; Jain, R. K.; Wood, W. J. L.; Tsuruoka, H.; Patterson, A. W. Substrate Activity Screening: A Fragment-Based Method for the Rapid Identification of Nonpeptidic Protease Inhibitors. *J. Am. Chem. Soc.* **2005**, *127*, 15521–15527.
(10) Lee, T.; Cho, M.; Ko, S.-Y.; Youn, H.-J.; Baek, D. J.; Cho, W.-J.; Kang, C.-Y.; Kim, S. Synthesis and Evaluation of 1,2,3-Triazole Containing Analogues of the Immunostimulane Alpha-GalCer. *J. Med. Chem.* **2007**, *50*, 585–589.
(11) Vanysek, P. Electrochemical Series. In *CRC Handbook of Chemistry and Physics*; Haynes, W. H., Lide, D. R., Bruno, T. J., Eds.; CRC Press, 2012.
(12) Rodionov, V. O.; Presolski, S. I.; Díaz, D. D.; Fokin, V. V.; Finn, M. G. Ligand-Accelerated Cu-Catalyzed Azide-Alkyne Cycloaddition: A Mechanistic Report. *J. Am. Chem. Soc.* **2007**, *129*, 12705–12712.
(13) Ohkuma, T.; Koizumi, M.; Doucet, H.; Pham, T.; Kozawa, M.; Murata, K.; Katayama, E.; Yokozawa, T.; Ikariya, T.; Noyori, R. Asymmetric Hydrogenation of Alkenyl, Cyclopropyl, and Aryl Ketones. $RuCl_2$(Xylbinap)(1,2-Diamine) as a Precatalyst Exhibiting a Wide Scope. *J. Am. Chem. Soc.* **1998**, *120*, 13529–13530.
(14) Hems, W. P.; Groarke, M.; Zanotti-Gerosa, A.; Grasa, G. A. [(Bisphosphine) Ru(II) Diamine] Complexes in Asymmetric Hydrogenation: Expanding the Scope of the Diamine Ligand. *Acc. Chem. Res.* **2007**, *40*, 1340–1347.
(15) Spindler, F.; Blaser, H. U. Enantioselective Hydrogenation of C=N Functions and Enamines. In *The Handbook of Homogeneous Hydrogenation*; Wiley-VCH Verlag GmbH & Co., 2007; pp 1193–1214.
(16) Baeza, A.; Pfaltz, A. Iridium-Catalyzed Asymmetric Hydrogenation of Imines. *Chem. - Eur. J.* **2010**, *16*, 4003–4009.
(17) Verzijl, G. K. M.; Schuster, C.; Dax, T.; De Vries, A. H. M.; Lefort, L. Asymmetric Synthesis of a Key Intermediate for Tofacitinib via a Dynamic Kinetic Resolution-Reductive Amination Protocol. *Org. Process Res. Dev.* **2018**, *22*, 1817–1822.
(18) Verzijl, G. K. M.; Hassfeld, J.; De Vries, A. H. M.; Lefort, L. Enantioselective

Synthesis of a 2,3-Benzodiazepine Intermediate of BET Inhibitor BAY 1238097 via Catalytic Asymmetric Hydrogenation. *Org. Process Res. Dev.* **2020**, *24*, 255–260.

(19) Hou, C. J.; Wang, Y. H.; Zheng, Z.; Xu, J.; Hu, X. P. Chiral Phosphine-Phosphoramidite Ligands for Highly Efficient Ir-Catalyzed Asymmetric Hydrogenation of Sterically Hindered N-Arylimines. *Org. Lett.* **2012**, *14*, 3554–3557.

(20) Etayo, P.; Vidal-Ferran, A. Rhodium-Catalysed Asymmetric Hydrogenation as a Valuable Synthetic Tool for the Preparation of Chiral Drugs. *Chem. Soc. Rev.* **2013**, *42*, 728–754.

(21) Gu, P.; Wu, X.; Su, Y.; Li, X.-Q.; Xue, P.; Li, R. Rhodium-Catalyzed Intermolecular Reaction of Alkyl Azides with Diazo-(Aryl)Acetates. *Synlett* **2014**, *25*, 535–538.

(22) Kolb, H. C.; Finn, M. G.; Sharpless, K. B. Click Chemistry: Diverse Chemical Function from a Few Good Reactions. *Angew. Chem. Int. Ed.* **2001**, *40*, 2004–2021.

(23) Bräse, S.; Gil, C.; Knepper, K.; Zimmermann, V. Organic Azides: An Exploding Diversity of a Unique Class of Compounds. *Angew. Chem. Int. Ed.* **2005**, *44*, 5188–5240.

(24) Brase, S.; Banert, K. *Organic Azides: Synthesis and Applications*; John Wiley and Sons: Chichester, 2010.

(25) Lautens, M.; Maddess, M. L.; Sauer, E. L. O.; Ouellet, S. G. Enantioselective Allylation of β,γ-Unsaturated Aldehydes Generated via Lewis Acid Induced Rearrangement of 2-Vinyloxiranes. *Org. Lett.* **2002**, *4*, 83–86.

(26) Davies, H. M. L.; Cantrell, C. J. R.; Romines, K. R.; Baum, J. S. Synthesis of Furans via Rhodium(II) Acetate-Catalyzed Reaction of Acetylenes with α-Diazocarbonyls: Ethyl 2-Methyl-5-Phenyl-3-Furancarboxylate. *Org. Synth.* **1998**, *70*, 93–97.

(27) Doben, N.; Yan, H.; Kischkewitz, M.; Mao, J.; Studer, A. Intermolecular Acetoxyaminoalkylation of A-Diazo Amides with (Diacetoxyiodo)Benzene and Amines. *Org. Lett.* **2018**, *20*, 7933–7936.

Appendix. HPLC and NMR Images

Table 6.1 entry 1. Phenomenex Lux® 3µm Cellulose-1, hexane/IPA= 85:15 at 1.0 mL/min, λ = 210 nm: t_r = 9.5 min, t_r = 10.6 min

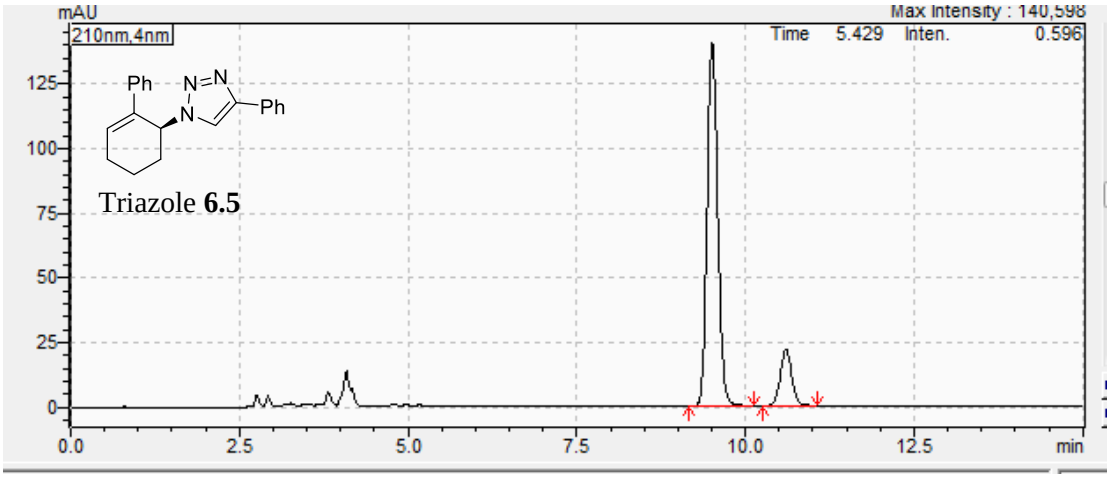

Peak#	Ret. Time	Area	Area%
1	9.509	1525966	85.673
2	10.603	255181	14.327
Total		1781147	100.000

Table 6.1 entry 2

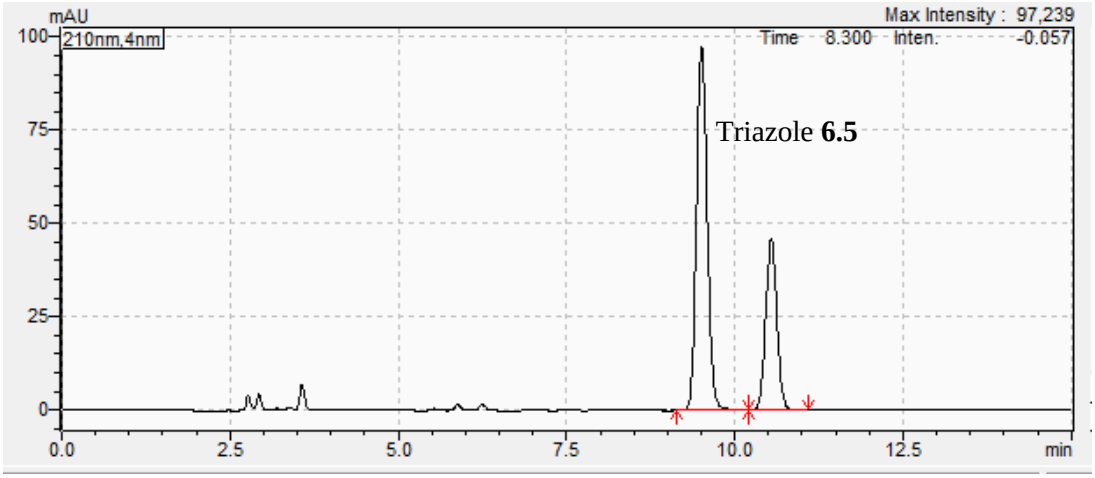

Peak#	Ret. Time	Area	Area%
1	9.509	1078330	66.905
2	10.544	533398	33.095
Total		1611728	100.000

Table 6.1 entry 3

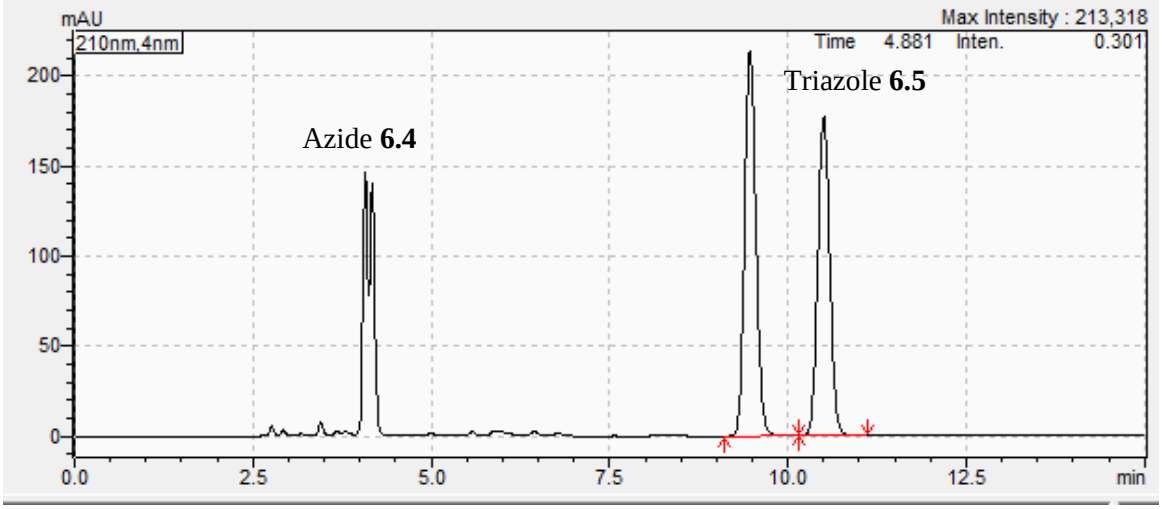

Peak#	Ret. Time	Area	Area%
1	9.469	2351286	53.290
2	10.504	2060945	46.710
Total		4412231	100.000

Table 6.1 entry 5

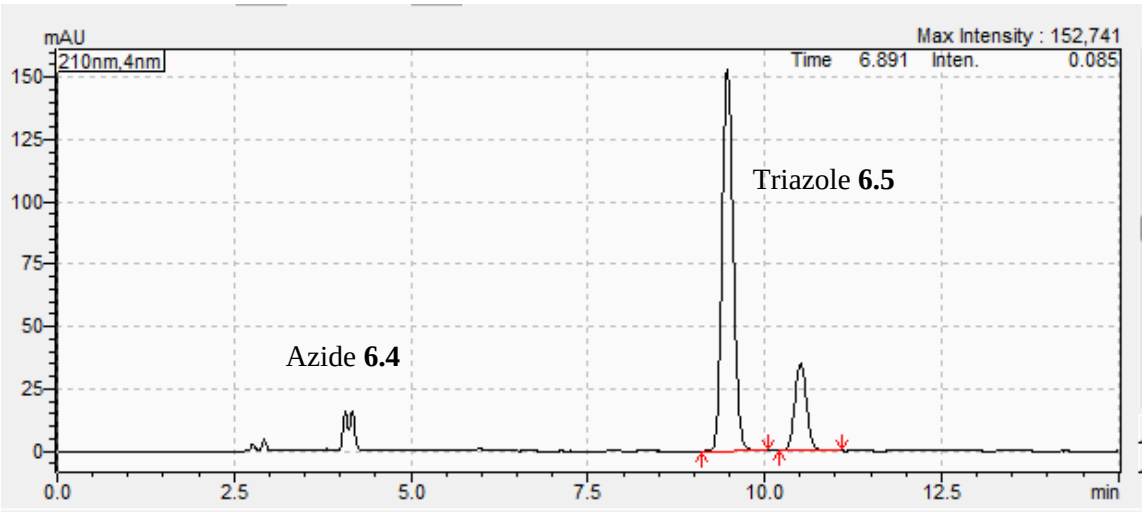

Peak#	Ret. Time	Area	Area%
1	9.474	1665208	80.395
2	10.511	406084	19.605
Total		2071293	100.000

Table 6.1 entry 7

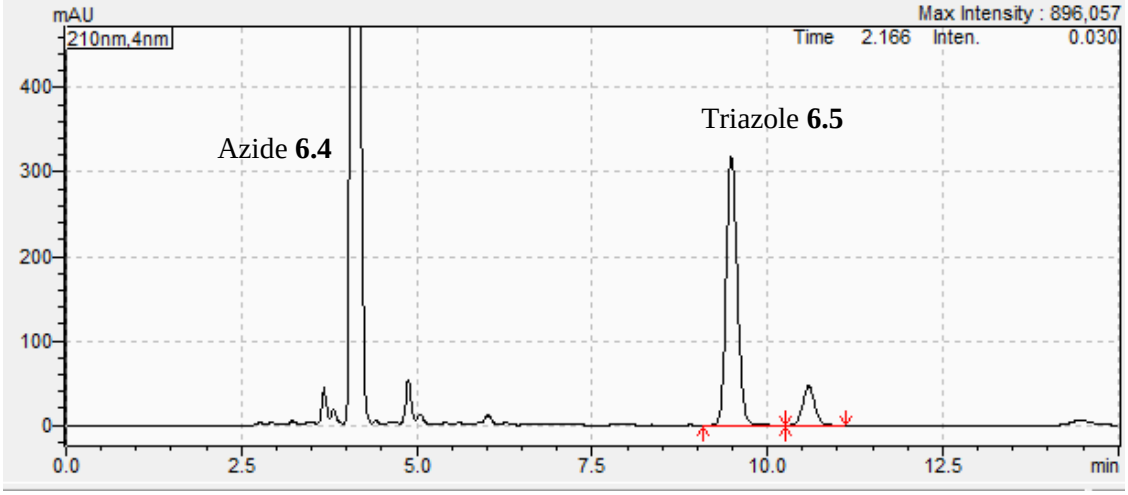

Peak#	Ret. Time	Area	Area%
1	9.487	3469267	86.377
2	10.590	547142	13.623
Total		4016409	100.000

Table 6.1 entry 13

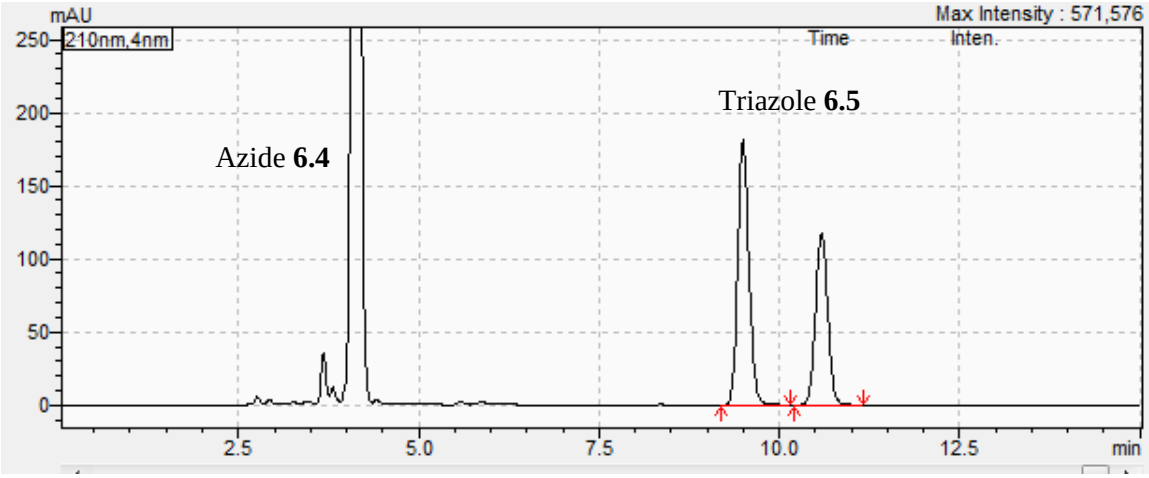

Peak#	Ret. Time	Area	Area%
1	9.496	1973155	58.710
2	10.587	1387697	41.290
Total		3360852	100.000

Amine 6.9. Reflect-C 3µ column, 0.1% TEA in hexanes/IPA = 75:25 at 1.0 mL/min, λ = 286 nm: t_r = 5.4 min. and t_r = 5.9 min.

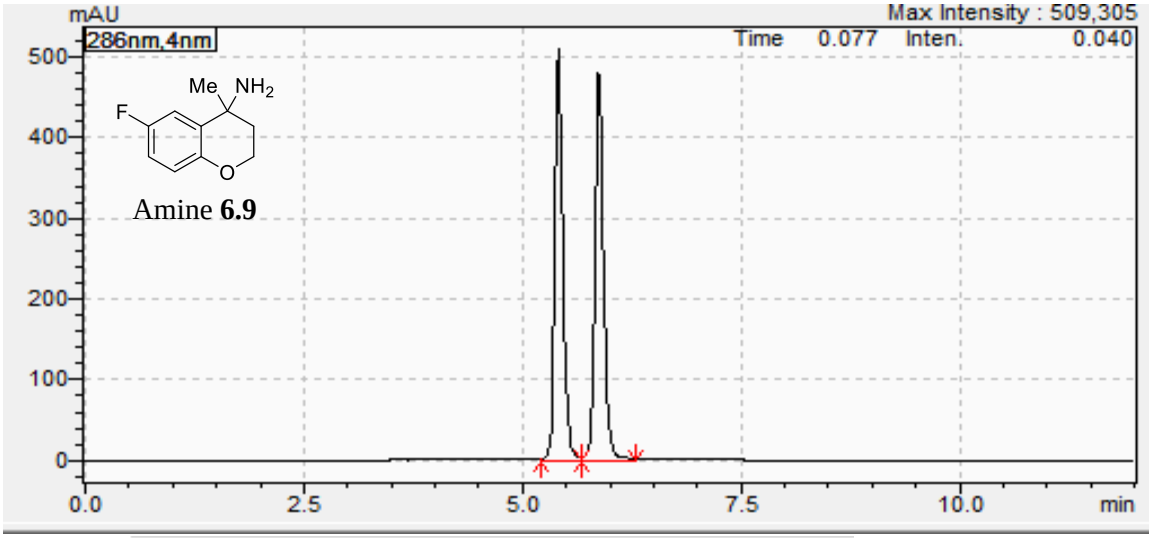

Peak#	Ret. Time	Height	Area	Area%
1	5.410	509134	3257340	49.568
2	5.871	480425	3314173	50.432
Total		989559	6571512	100.000

Table 6.5 entry 5

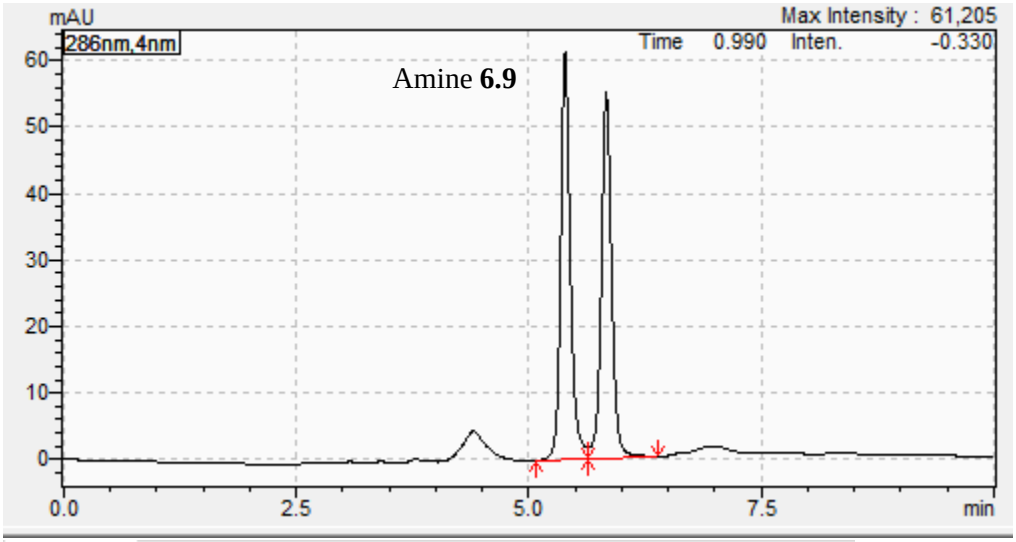

Peak#	Ret. Time	Height	Area	Area%
1	5.392	61224	442083	51.187
2	5.833	55173	421586	48.813
Total		116397	863668	100.000

Table 6.5 entry 6.

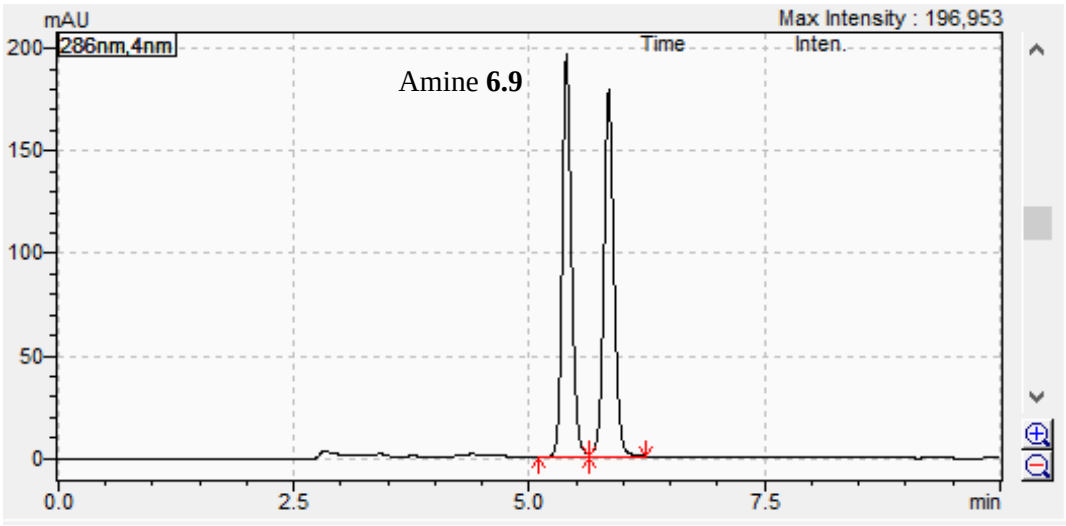

Peak#	Ret. Time	Height	Area	Area%
1	5.398	196612	1335423	49.779
2	5.842	179165	1347277	50.221
Total		375777	2682700	100.000

Amine 6.13. Reflect-C 3µ column, 0.1% TEA in hexanes/IPA = 98:2 at 0.75 mL/min, λ = 300 nm: t_r = 15.3 min. and t_r = 16.1 min.

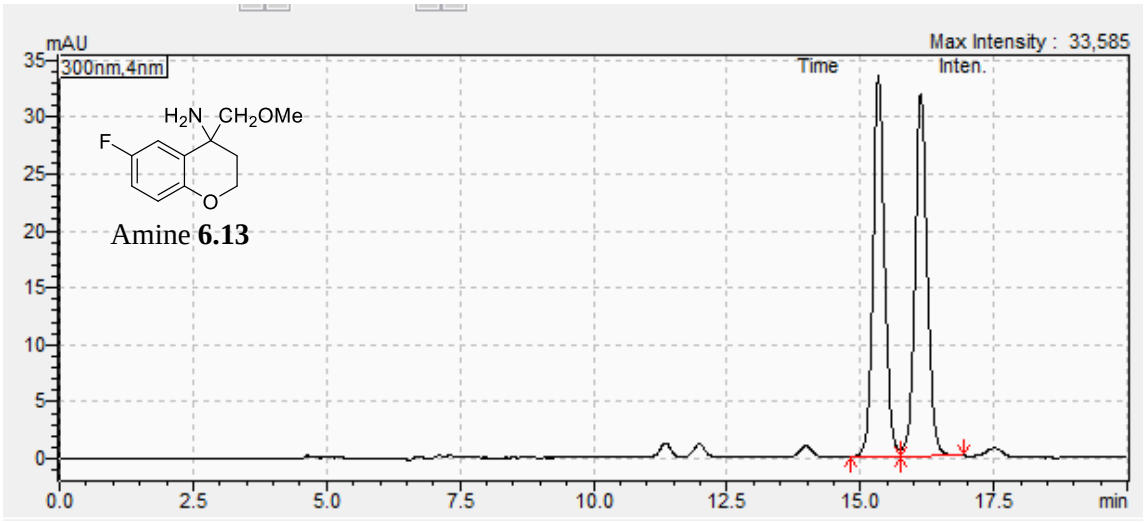

Peak#	Ret. Time	Area	Area%
1	15.339	504046	49.771
2	16.132	508675	50.229
Total		1012720	100.000

Table 6.6 entry 3

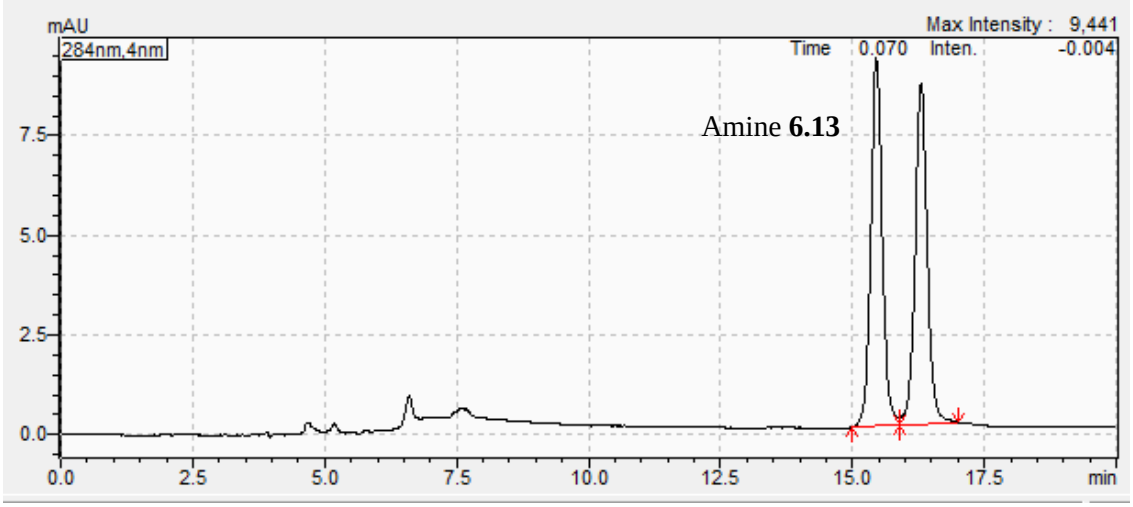

Peak#	Ret. Time	Area	Area%
1	15.455	139713	50.346
2	16.302	137790	49.654
Total		277503	100.000

Table 6.6 entry 4

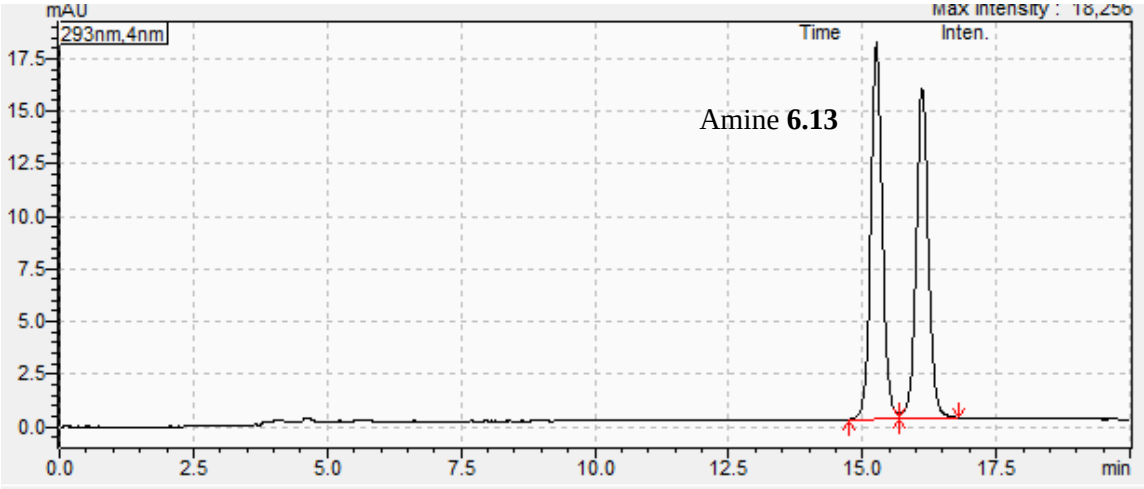

Peak#	Ret. Time	Area	Area%
1	15.261	268104	51.855
2	16.116	248918	48.145
Total		517022	100.000

Imine 6.24. Reflect-C 3µ column, hexanes/IPA = 97:3 at 1.0 mL/min, λ = 210 nm: t_r = 8.6 min and t_r = 9.1 min.

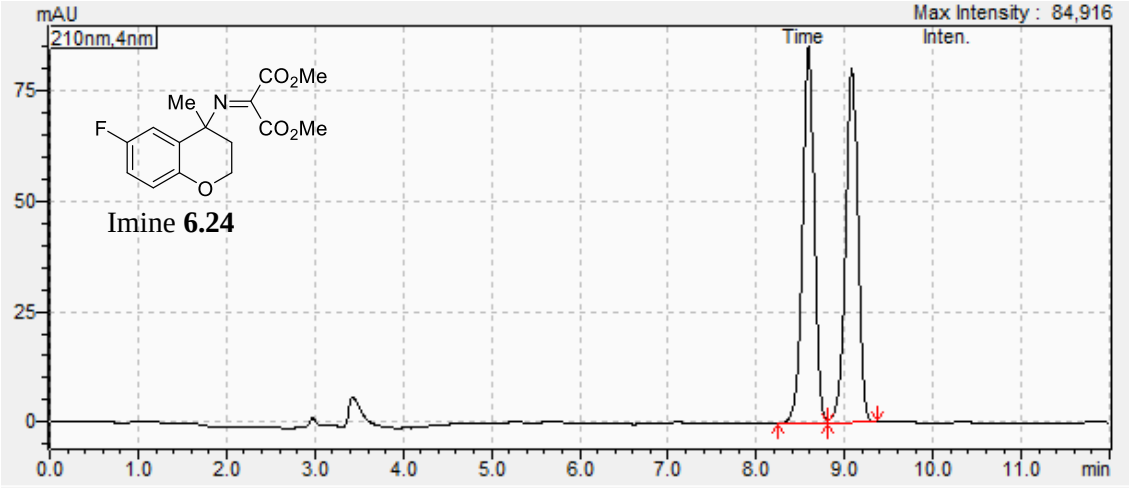

Peak#	Ret. Time	Area	Area%
1	8.595	768610	50.293
2	9.085	759640	49.707
Total		1528249	100.000

Table 6.9 entry 4

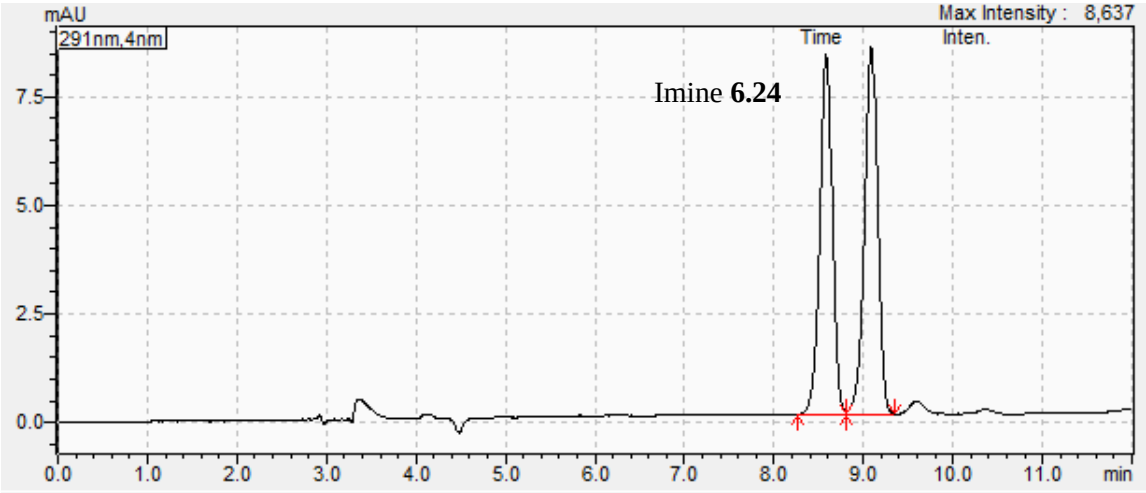

Peak#	Ret. Time	Area	Area%
1	8.588	79539	48.300
2	9.091	85137	51.700
Total		164676	100.000

Imine 6.26. Reflect-C 3µ column, hexanes/IPA = 97:3 at 1.0 mL/min, λ = 285 nm: t_r = 9.7 min and t_r = 10.3 min.

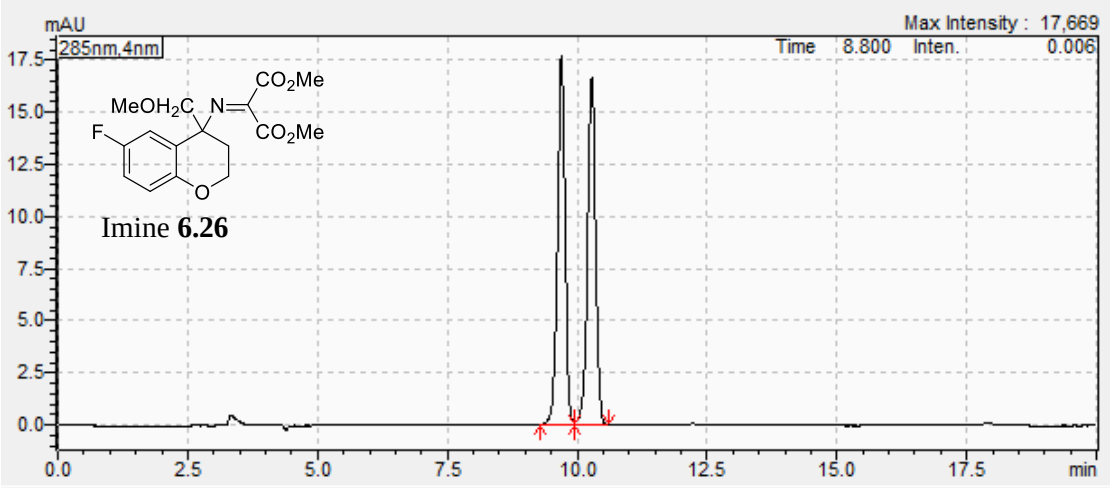

Peak#	Ret. Time	Area	Area%
1	9.698	179818	49.966
2	10.281	180066	50.034
Total		359884	100.000

Table 6.10 entry 3

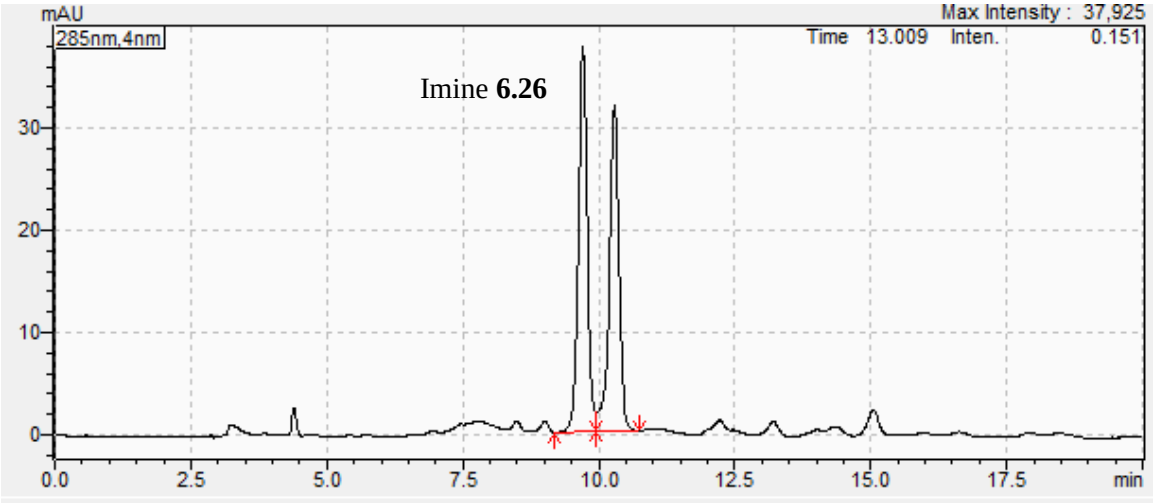

Peak#	Ret. Time	Area	Area%
1	9.709	430250	52.076
2	10.290	395944	47.924
Total		826193	100.000

Table 6.10 entry 4

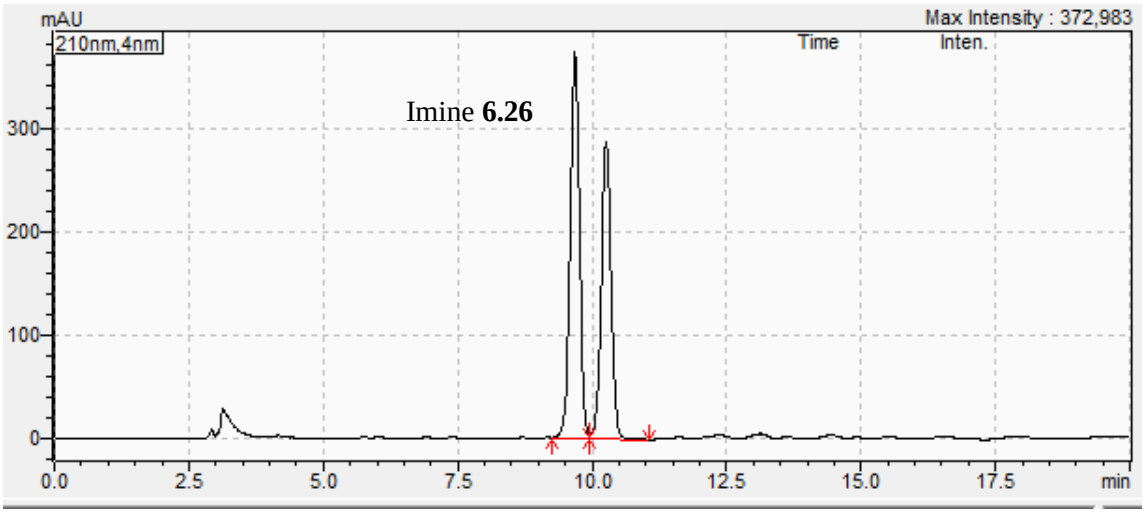

Peak#	Ret. Time	Area	Area%
1	9.682	4491621	55.225
2	10.262	3641624	44.775
Total		8133245	100.000

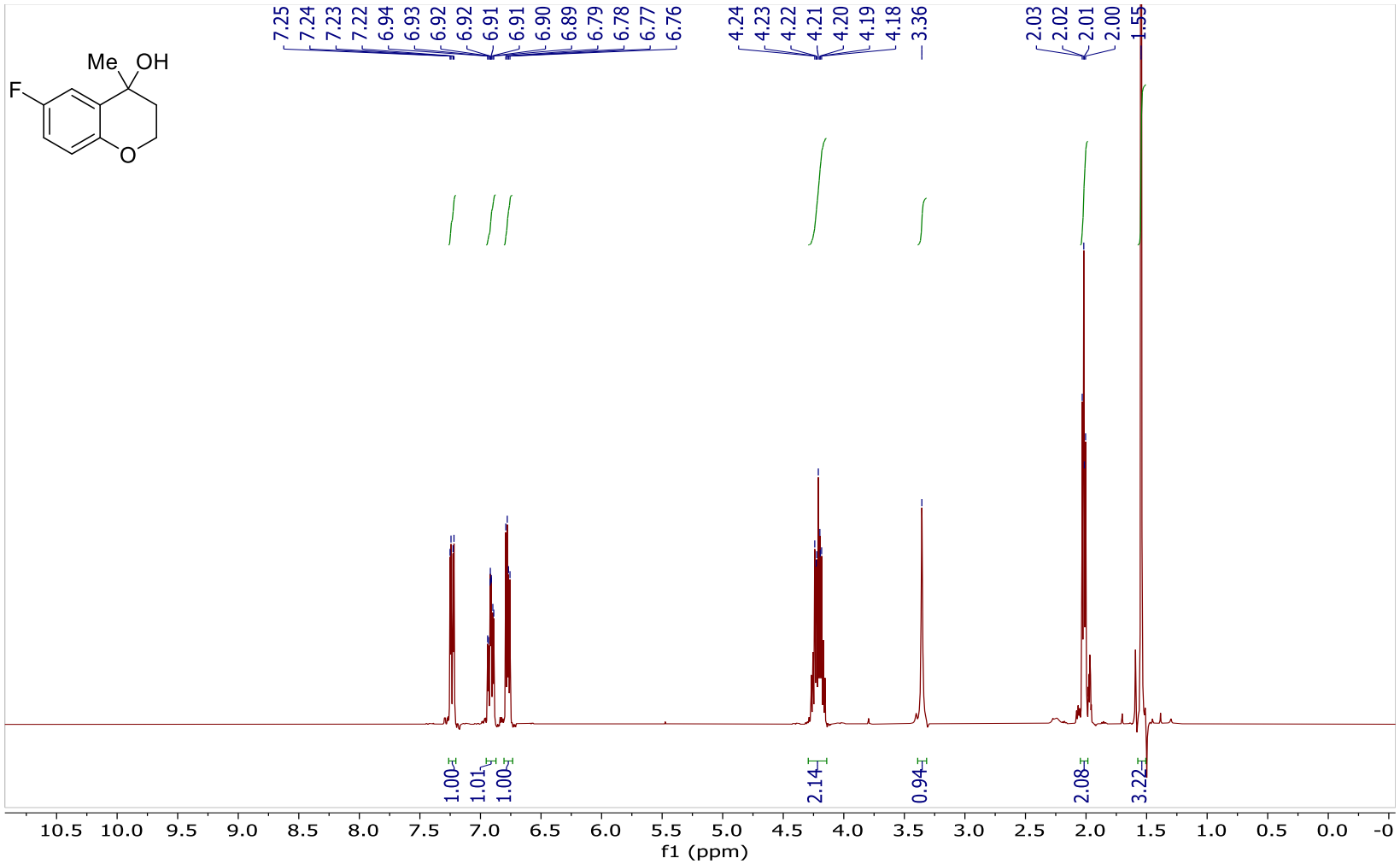

Compound **6.7**. 400 MHz ^{1}H NMR spectrum in CD_3CN

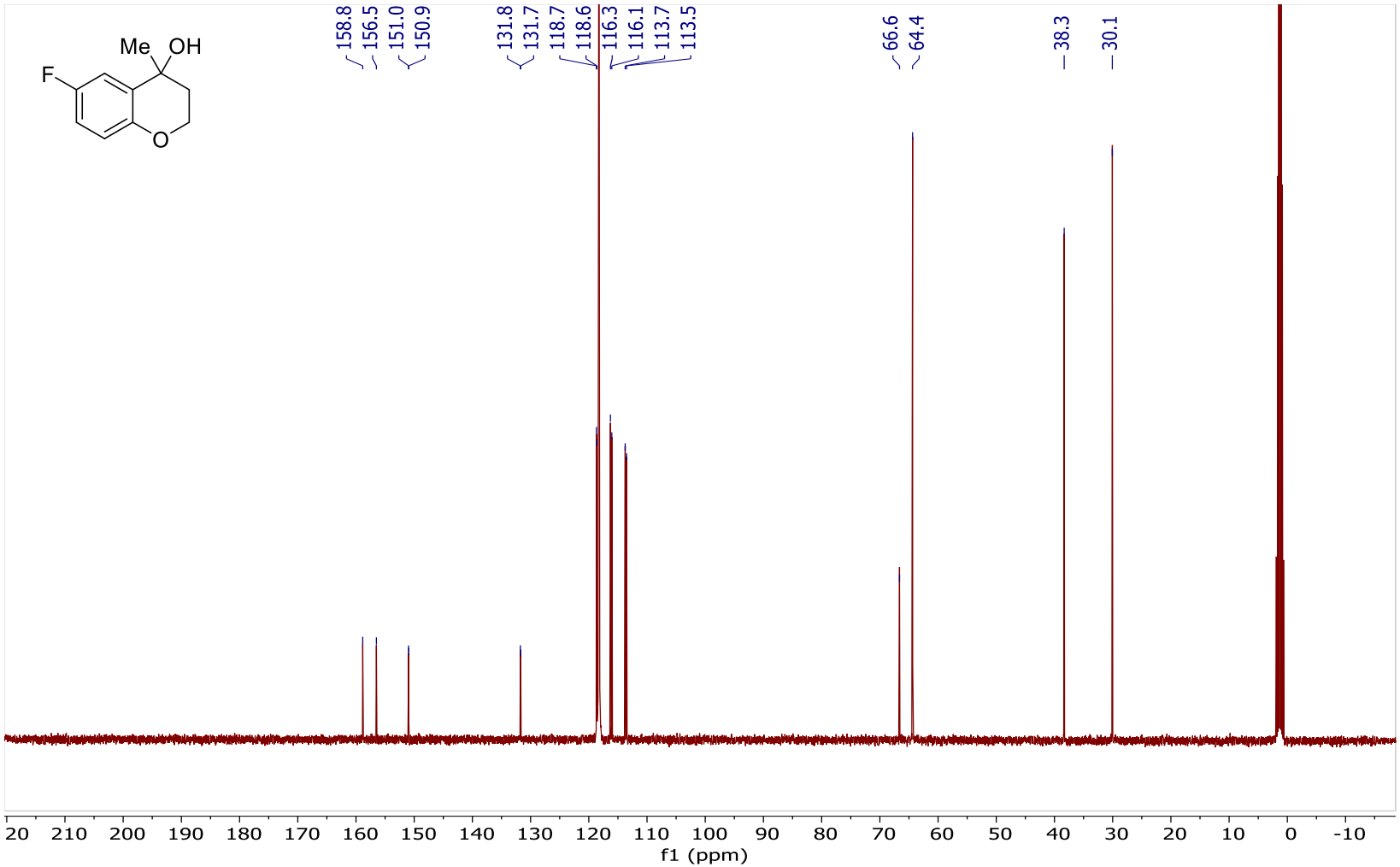

Compound **6.7**. 100 MHz $^{13}C\{^{1}H\}$ NMR spectrum in CD_3CN

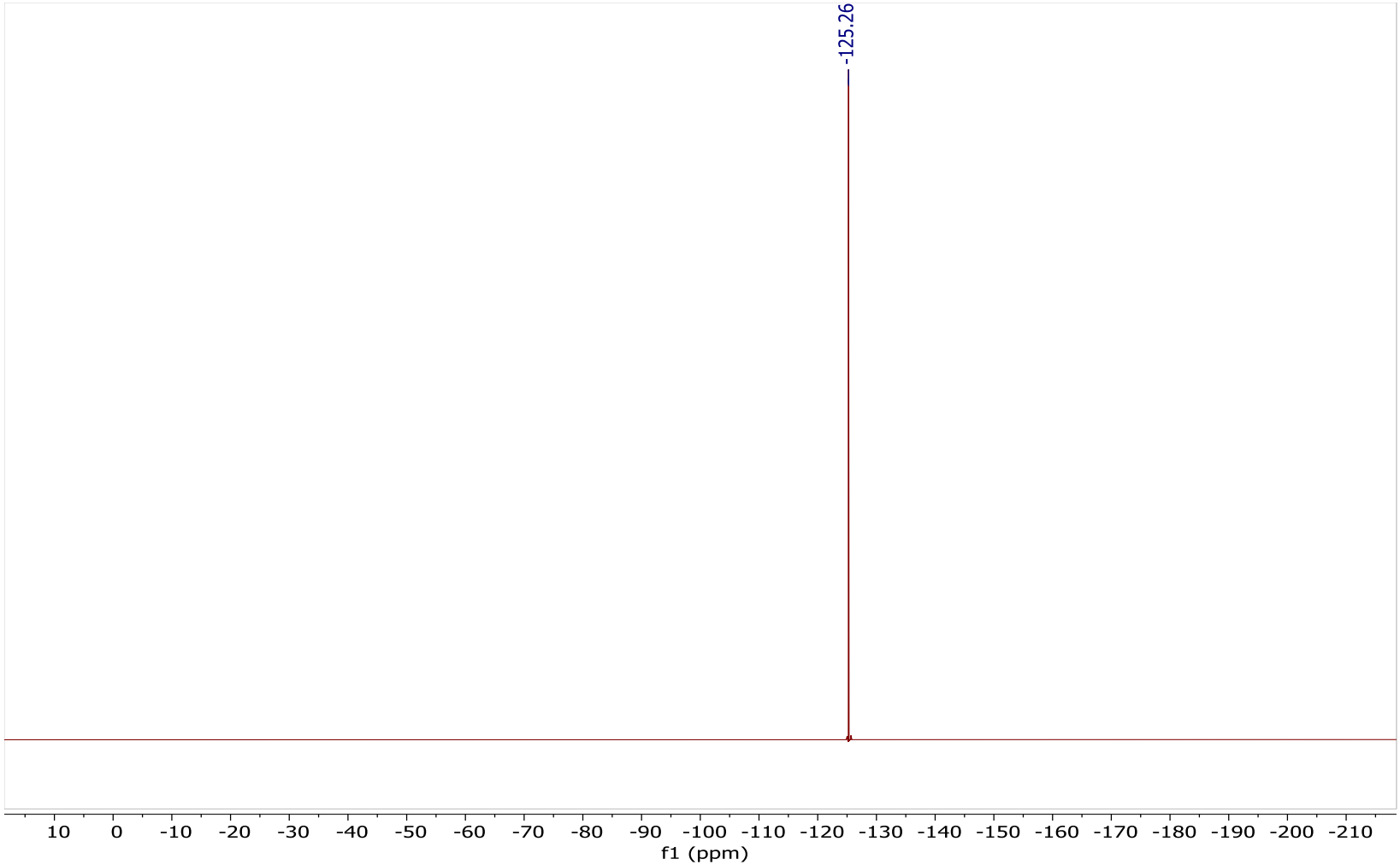

Compound **6.7**. 376 MHz $^{19}F\{^{1}H\}$ NMR spectrum in CD_3CN

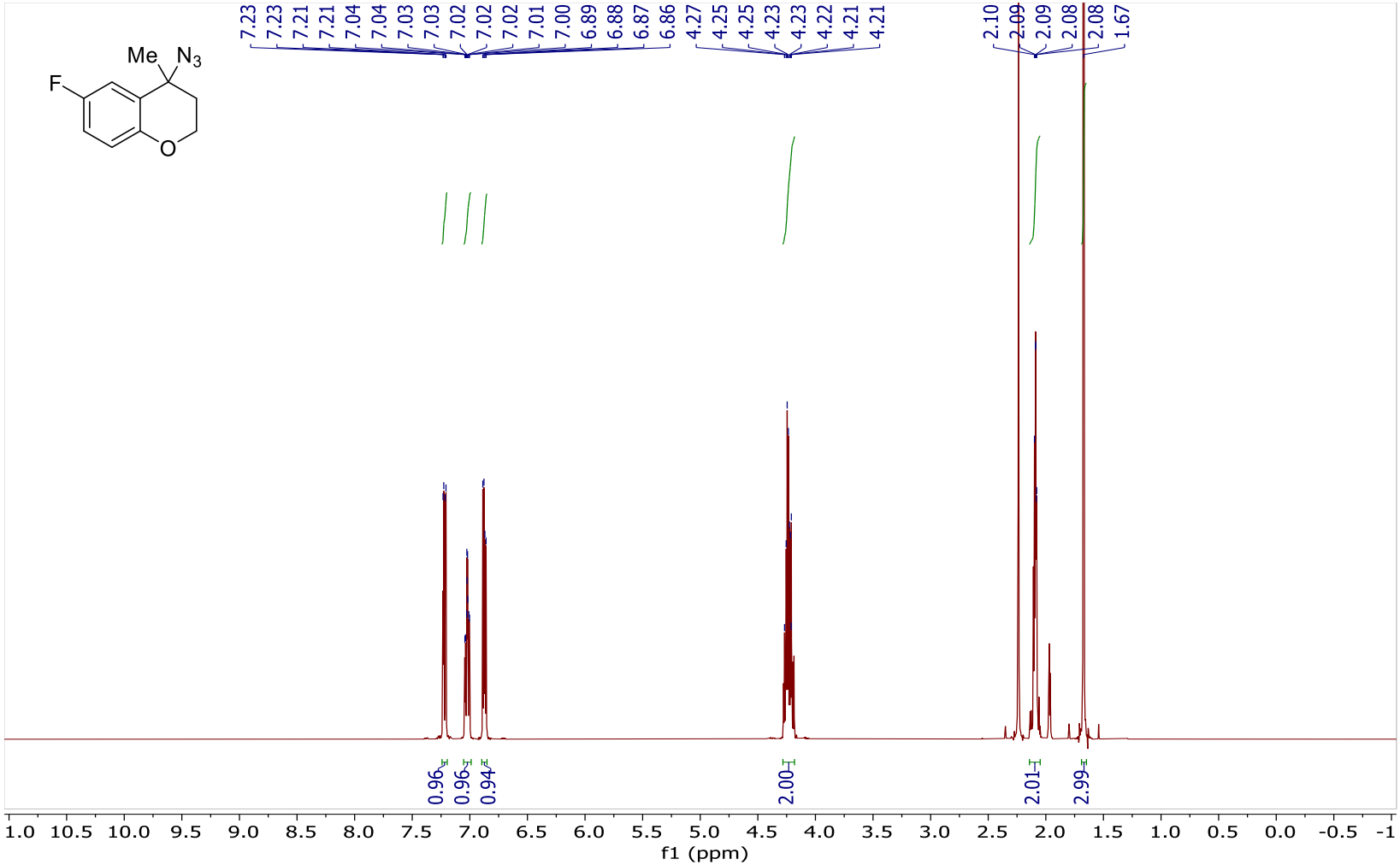

Compound **6.8**. 500 MHz ^{1}H NMR spectrum in $CDCl_3$

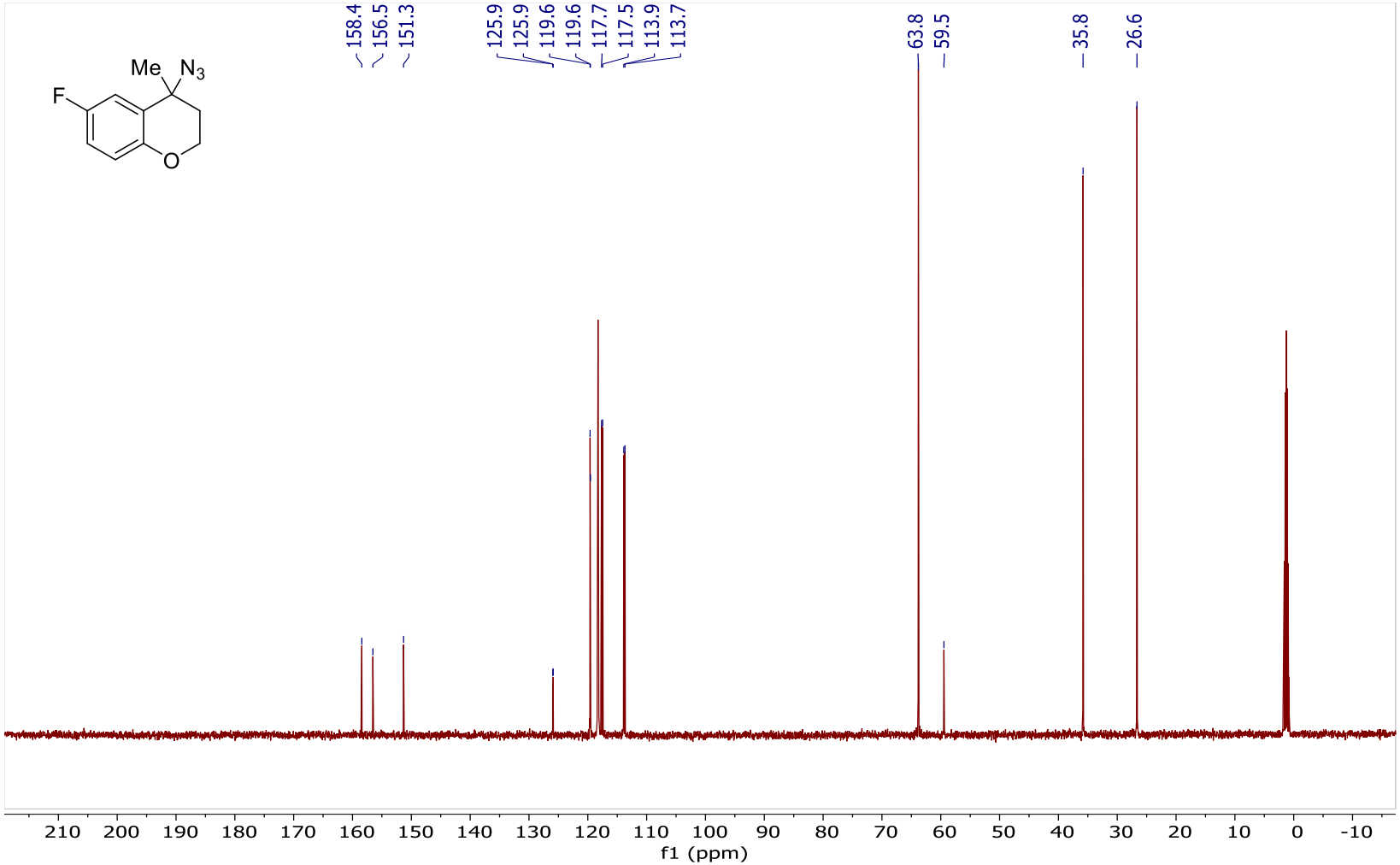

Compound **6.8**. 125 MHz $^{13}C\{^{1}H\}$ NMR spectrum in $CDCl_3$

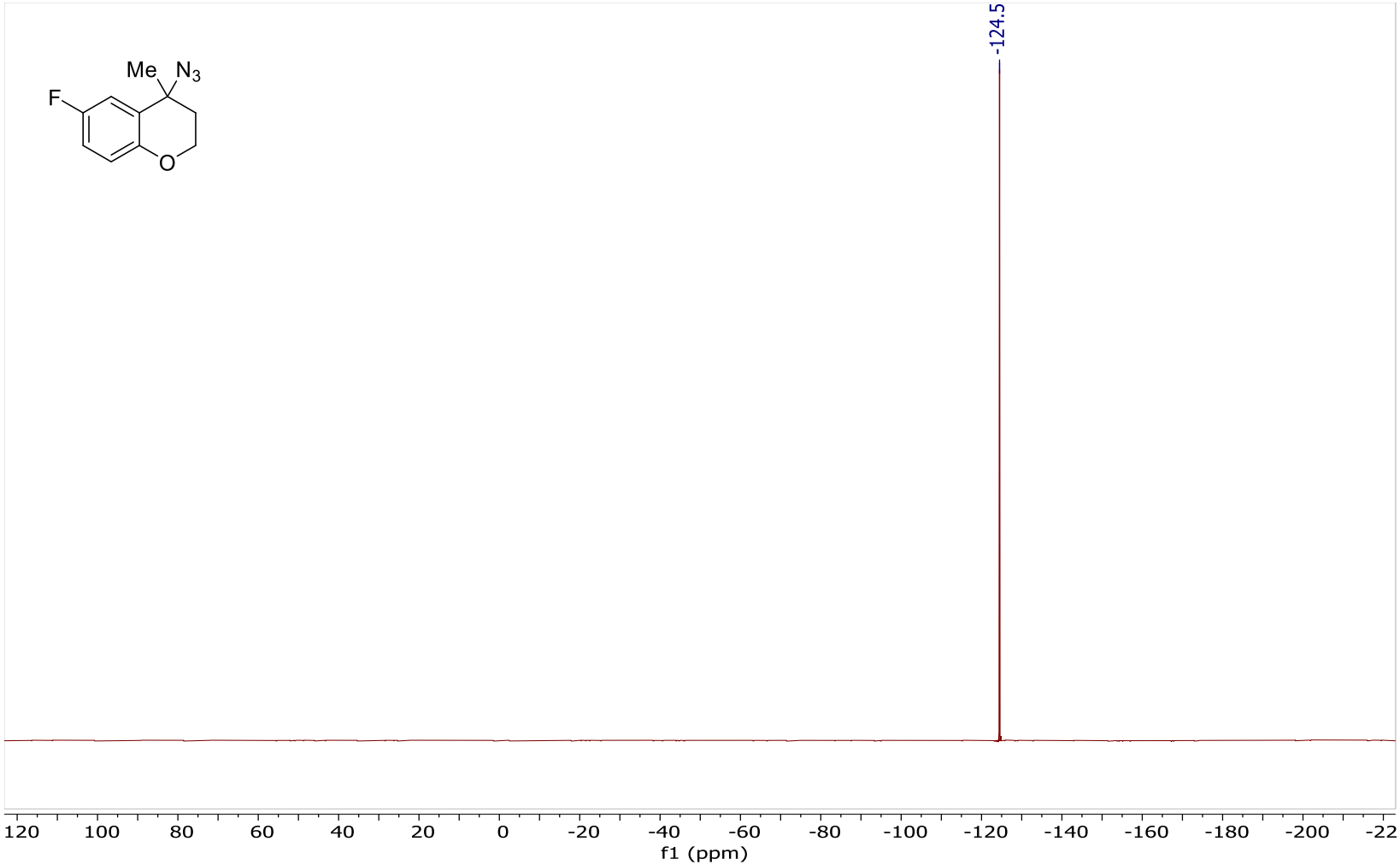

Compound **6.8**. 471 MHz $^{19}F\{^{1}H\}$ NMR spectrum in $CDCl_3$

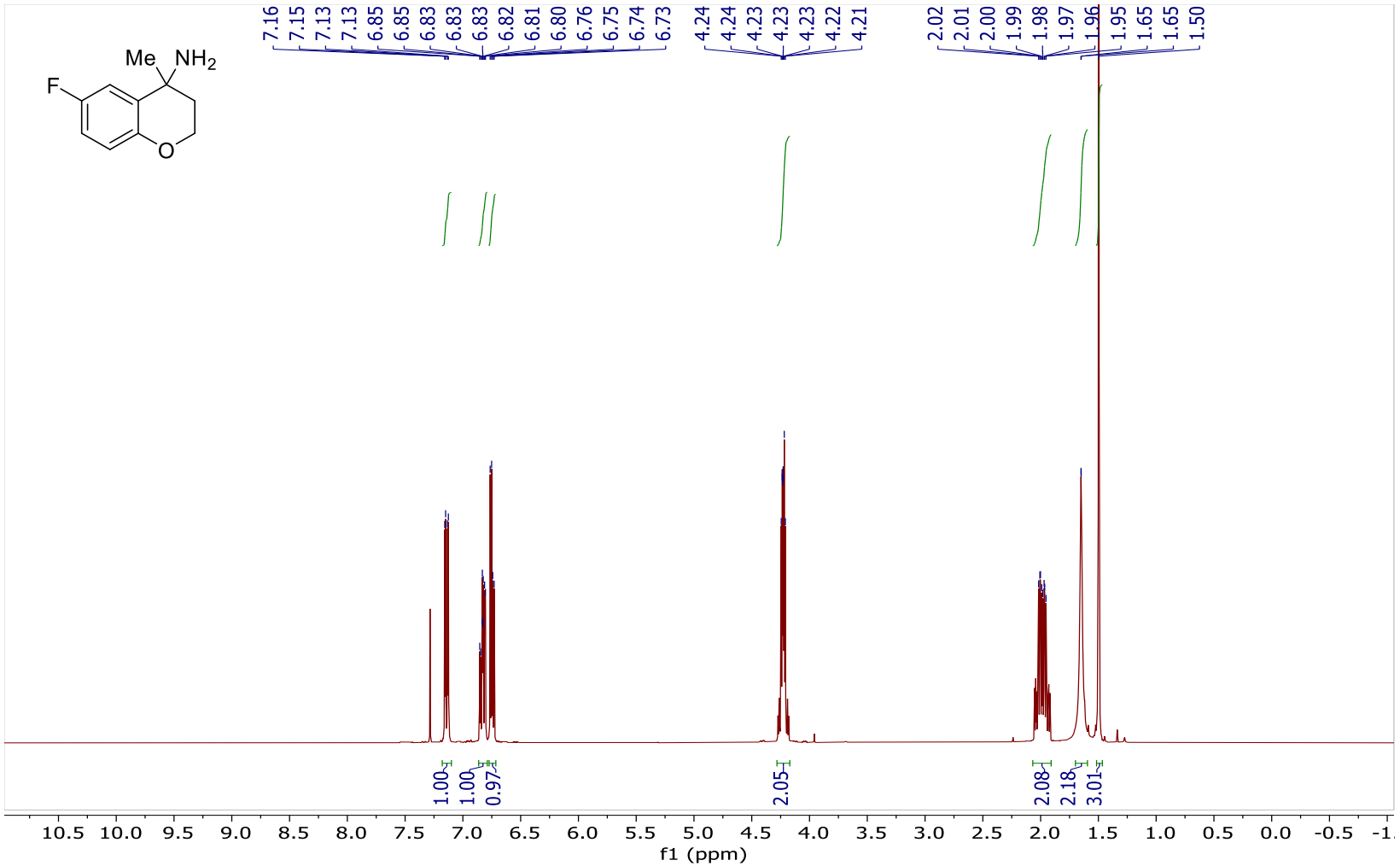

Compound **6.9**. 400 MHz ^{1}H NMR spectrum in $CDCl_3$

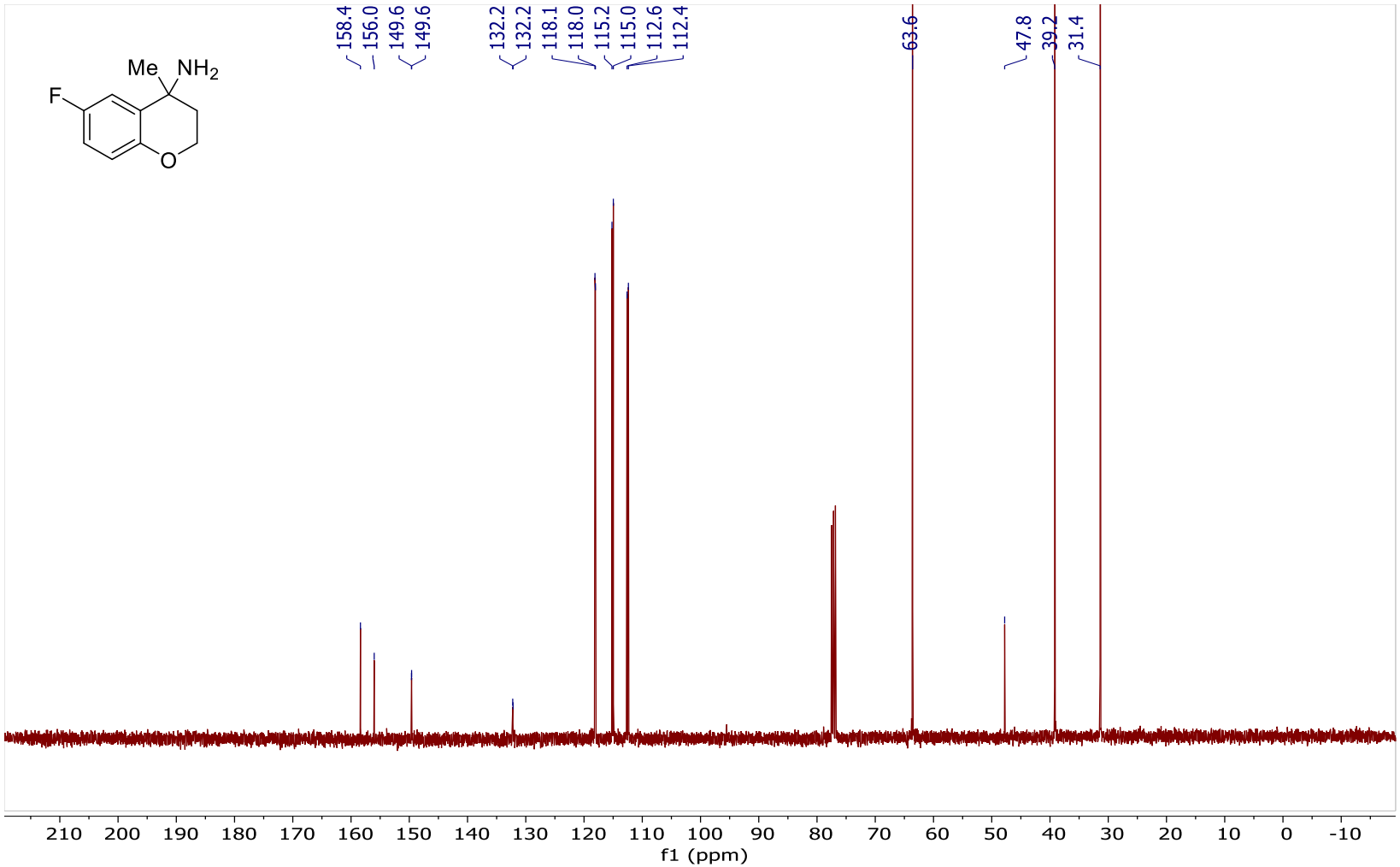

Compound **6.9**. 100 MHz $^{13}C\{^{1}H\}$ NMR spectrum in $CDCl_3$

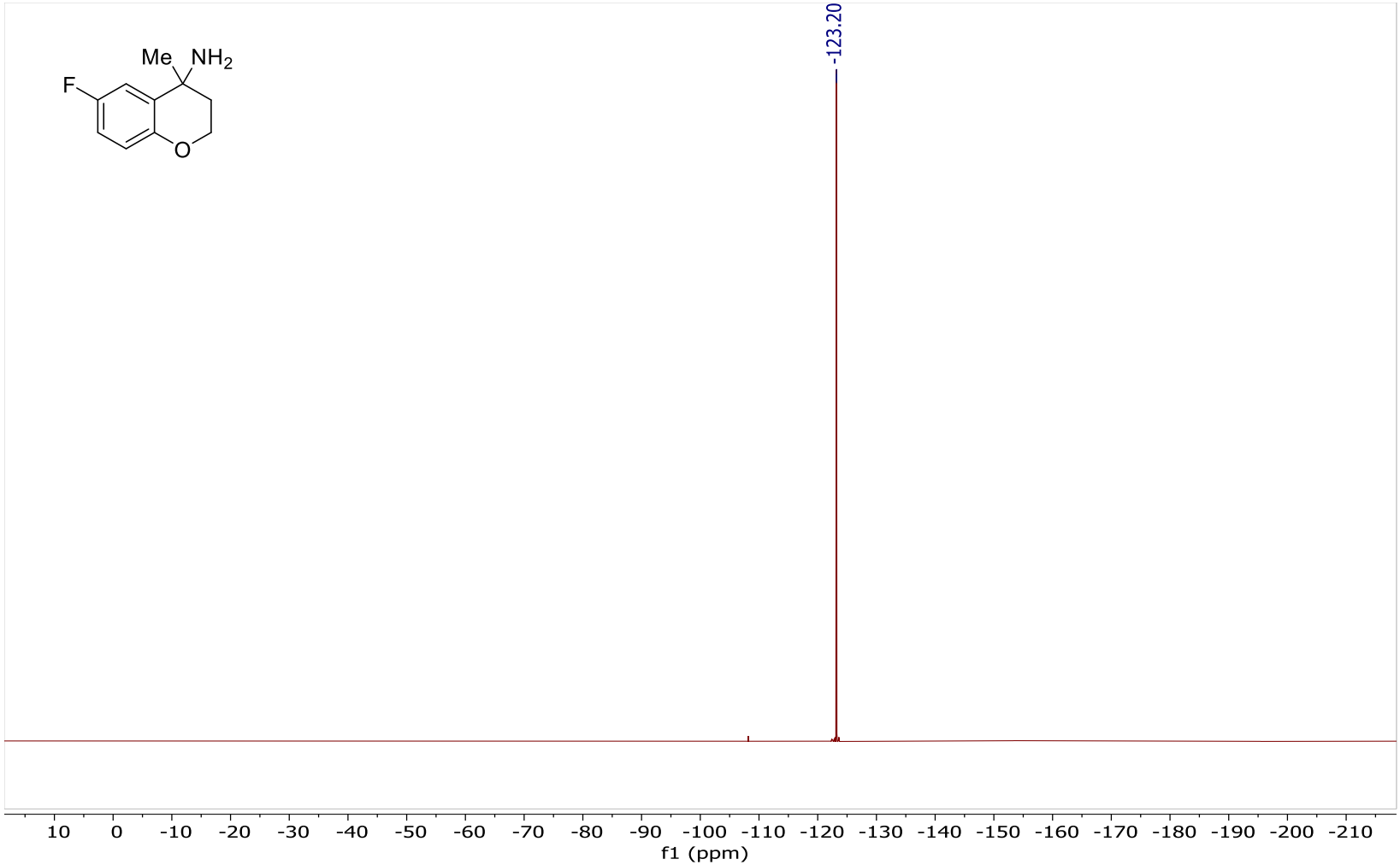

Compound **6.9**. 376 MHz $^{19}F\{^{1}H\}$ NMR spectrum in $CDCl_3$

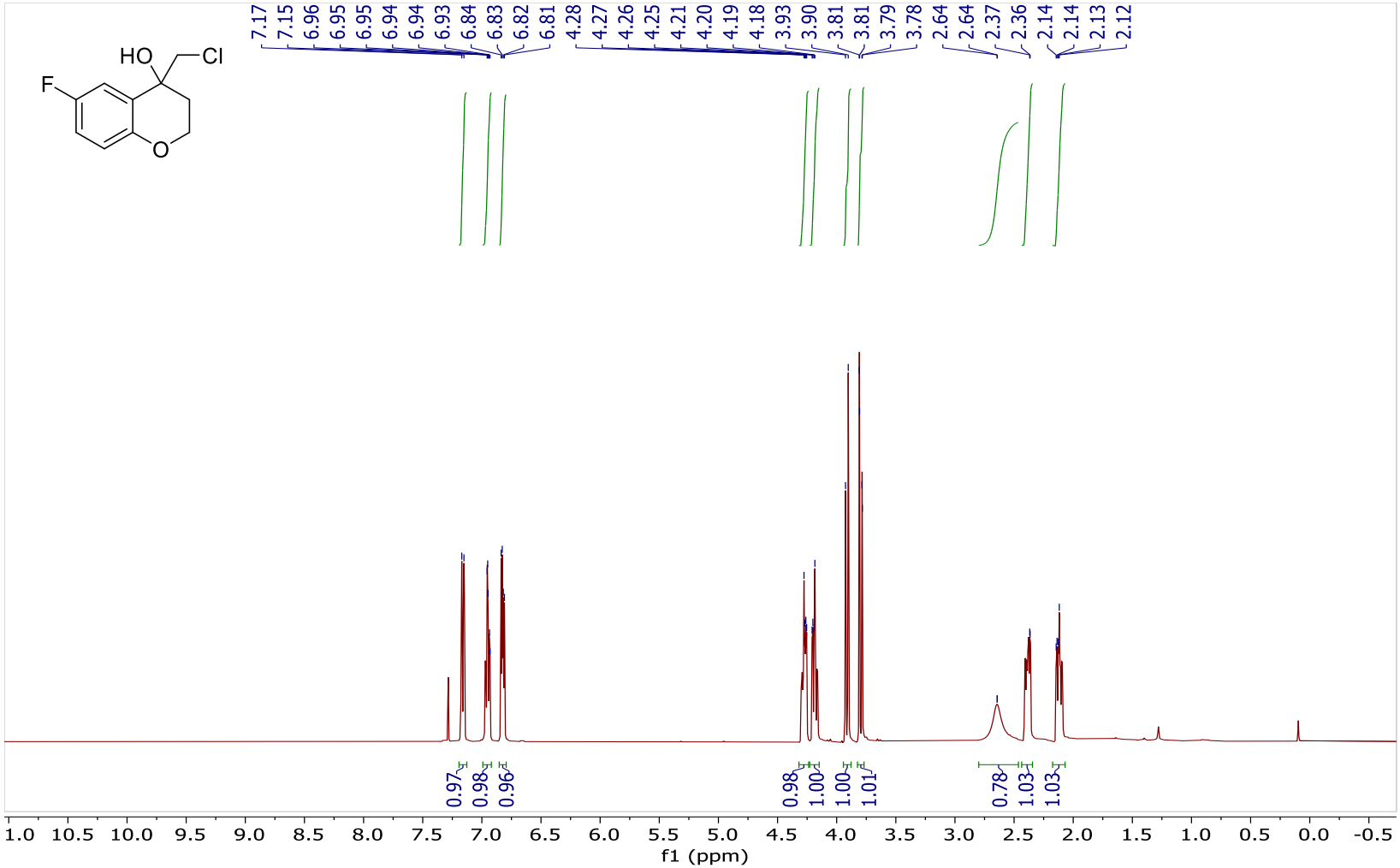

Compound **6.10**. 500 MHz ^{1}H NMR spectrum in $CDCl_3$

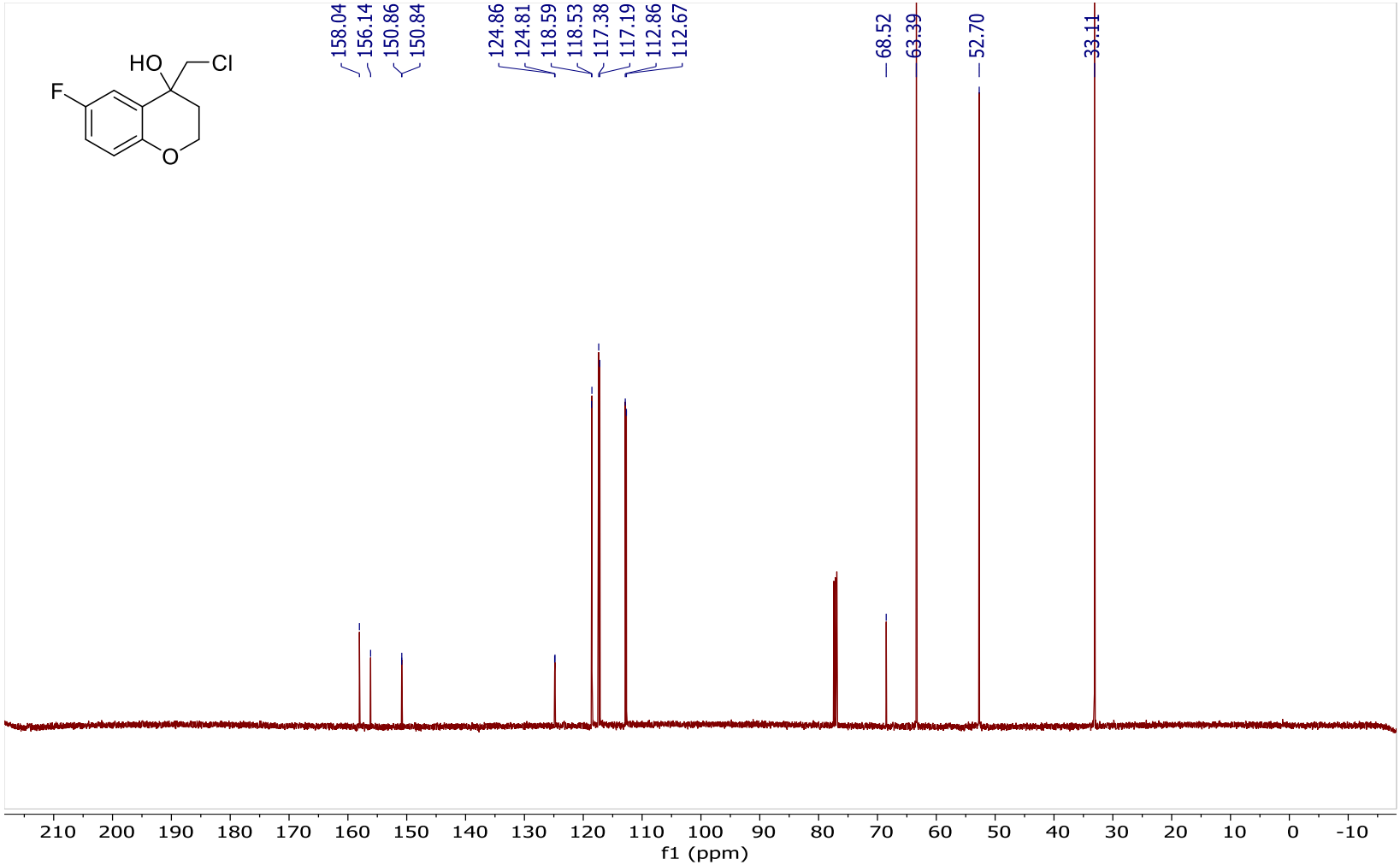

Compound **6.10**. 125 MHz $^{13}C\{^{1}H\}$ NMR spectrum in $CDCl_3$

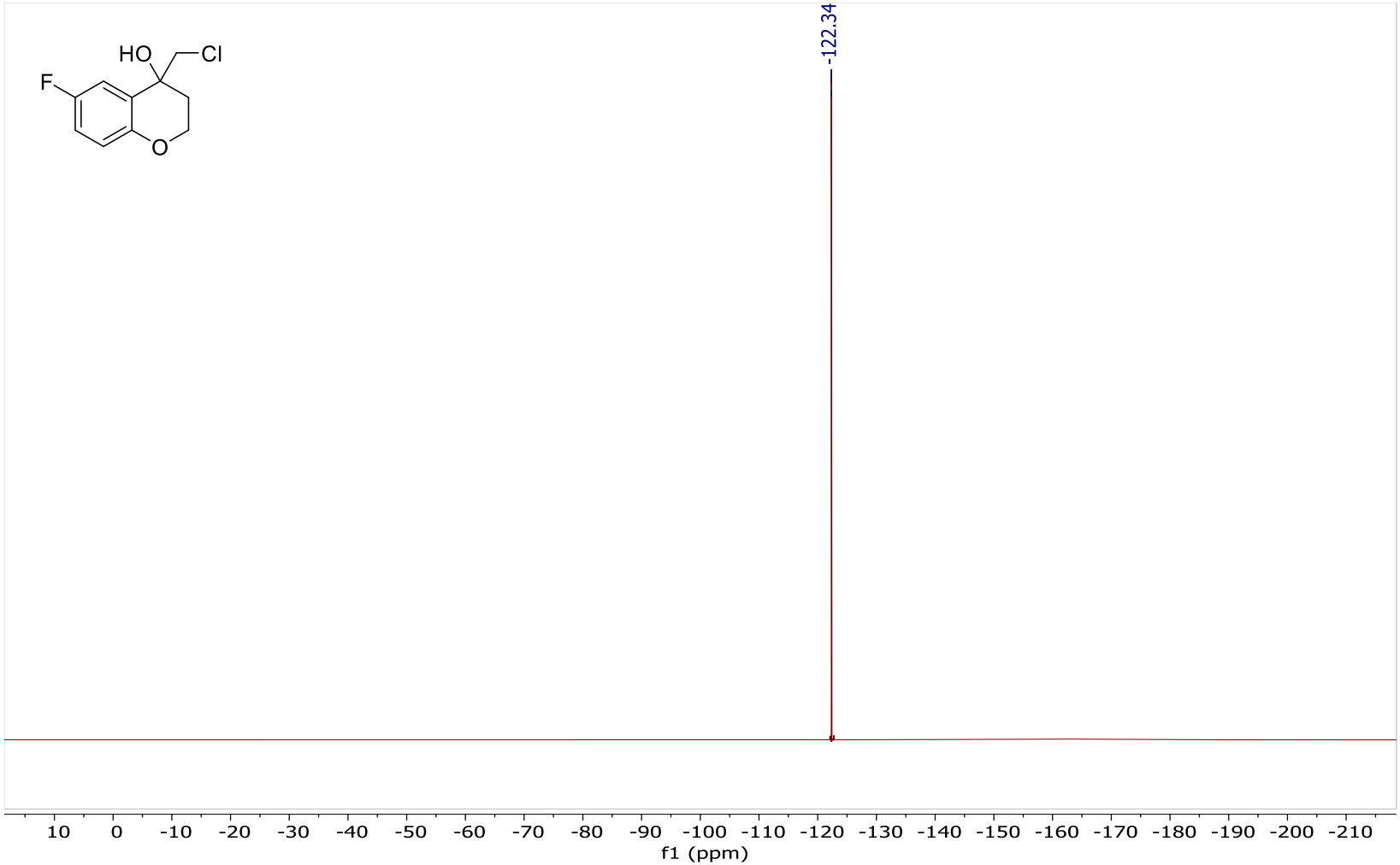

Compound **6.10**. 471 MHz $^{19}F\{^{1}H\}$ NMR spectrum in $CDCl_3$

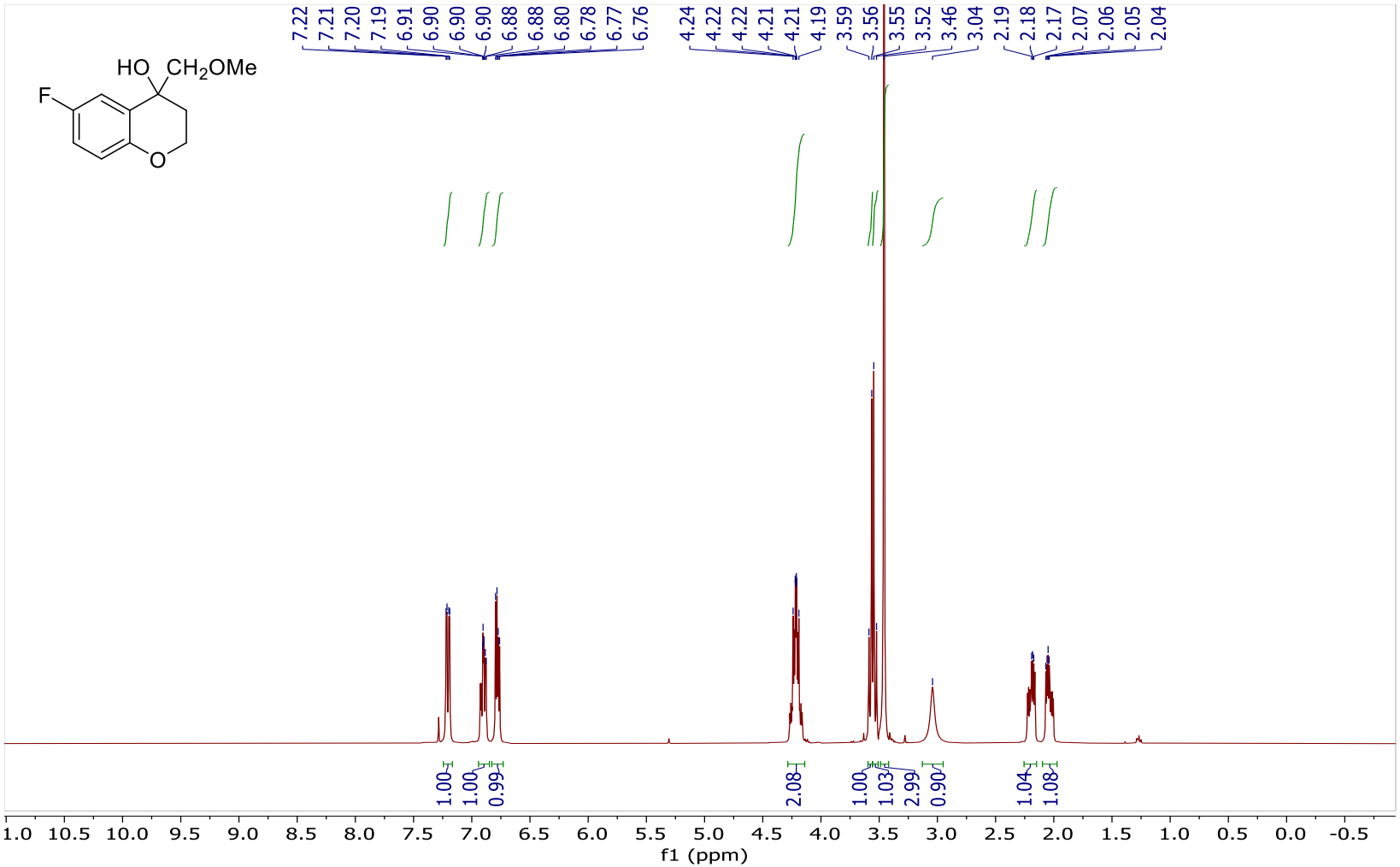

Compound **6.11**. 400 MHz ^{1}H NMR spectrum in $CDCl_3$

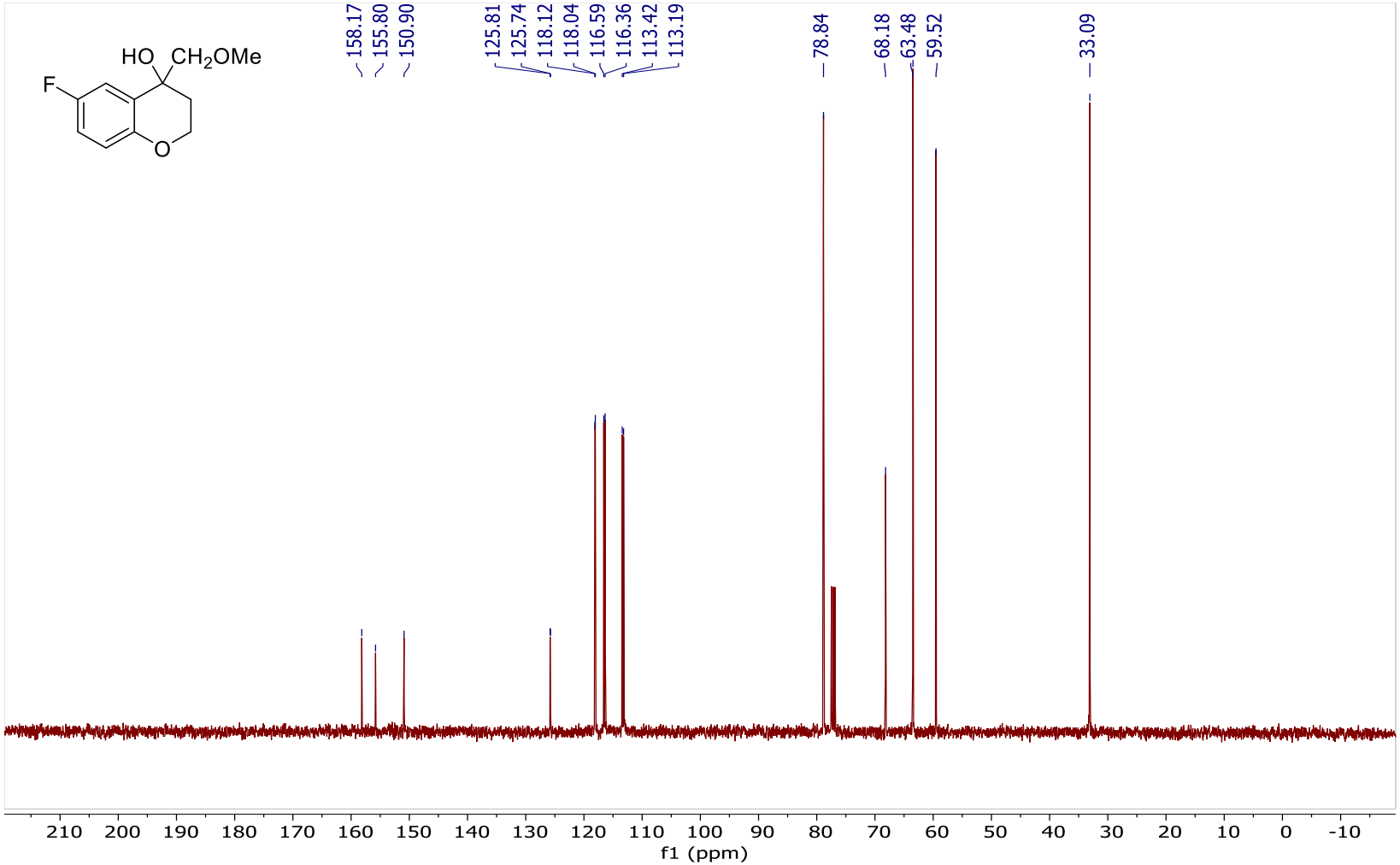

Compound **6.11**. 100 MHz $^{13}C\{^{1}H\}$ NMR spectrum in $CDCl_3$

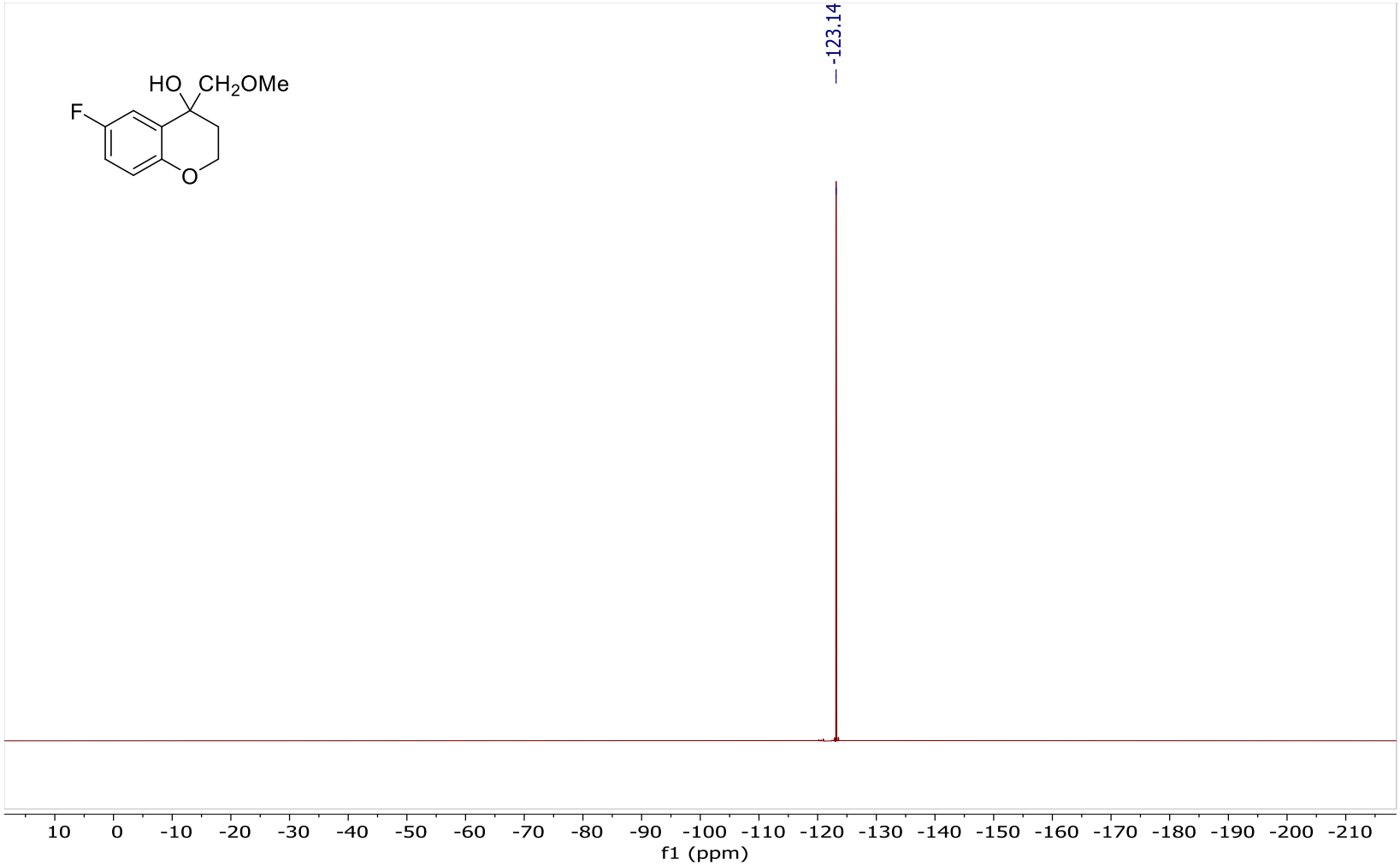

Compound **6.11**. 376 MHz $^{19}F\{^{1}H\}$ NMR spectrum in $CDCl_3$

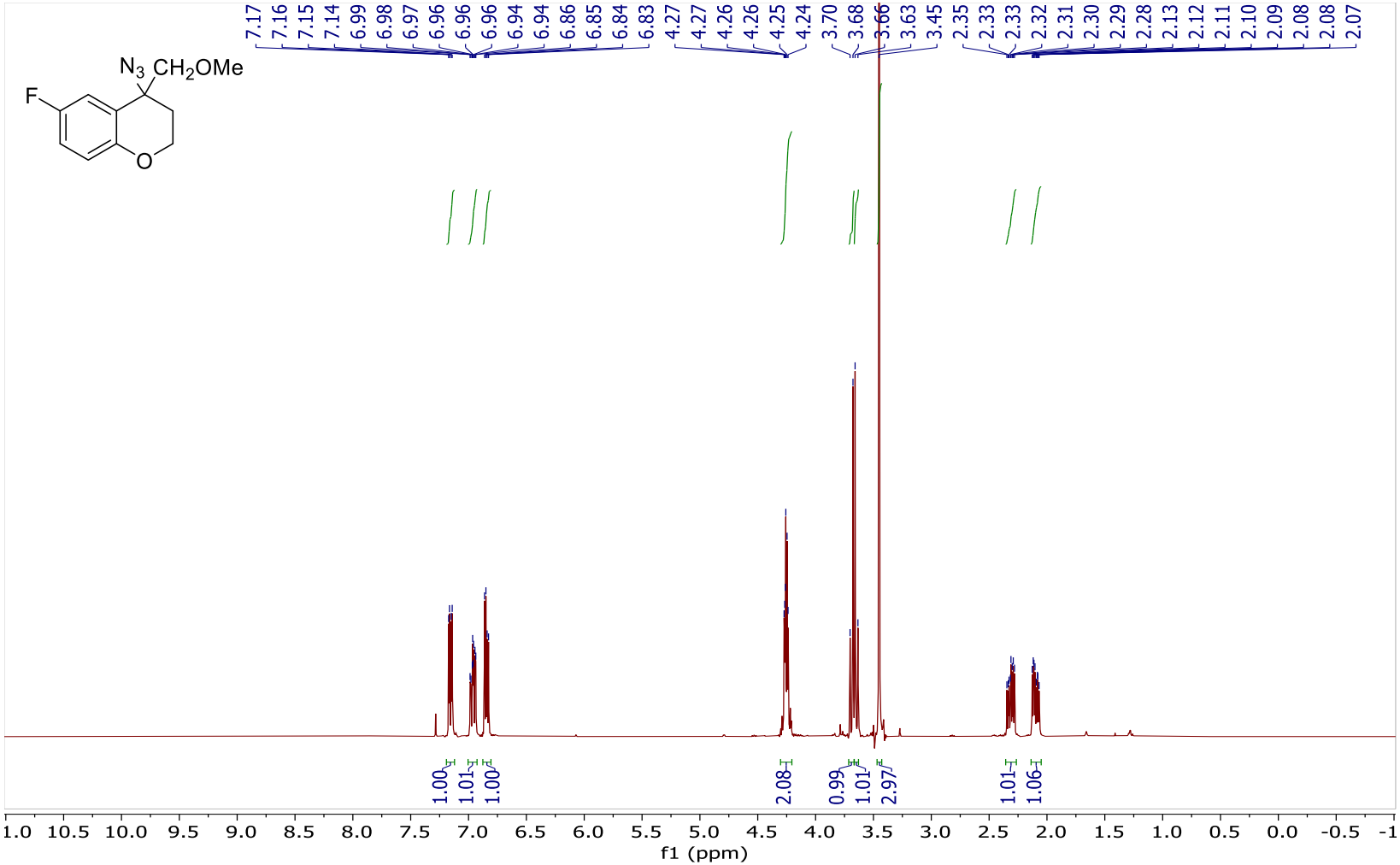

Compound **6.12**. 400 MHz ^{1}H NMR spectrum in $CDCl_3$

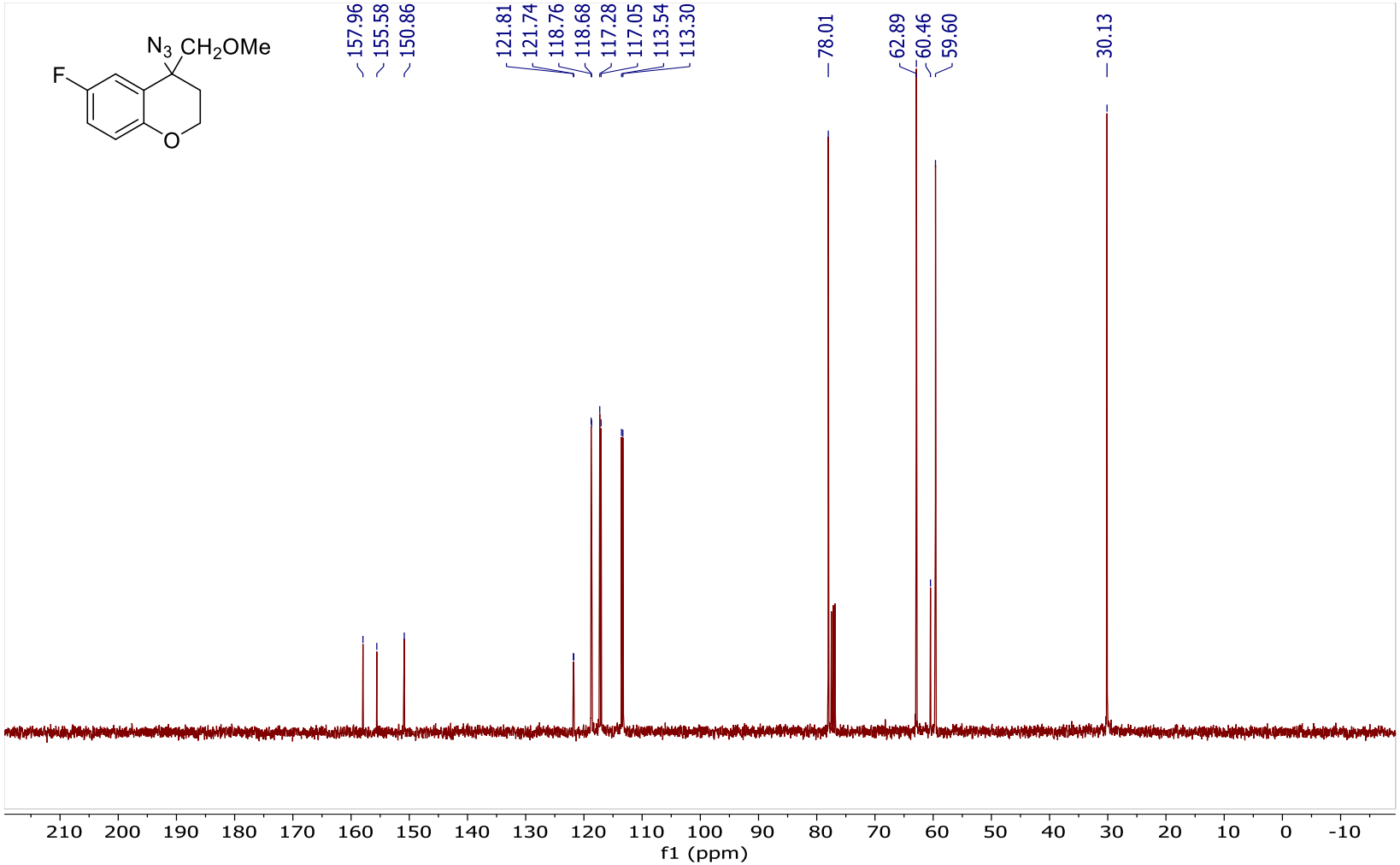

Compound **6.12**. 100 MHz $^{13}C\{^{1}H\}$ NMR spectrum in $CDCl_3$

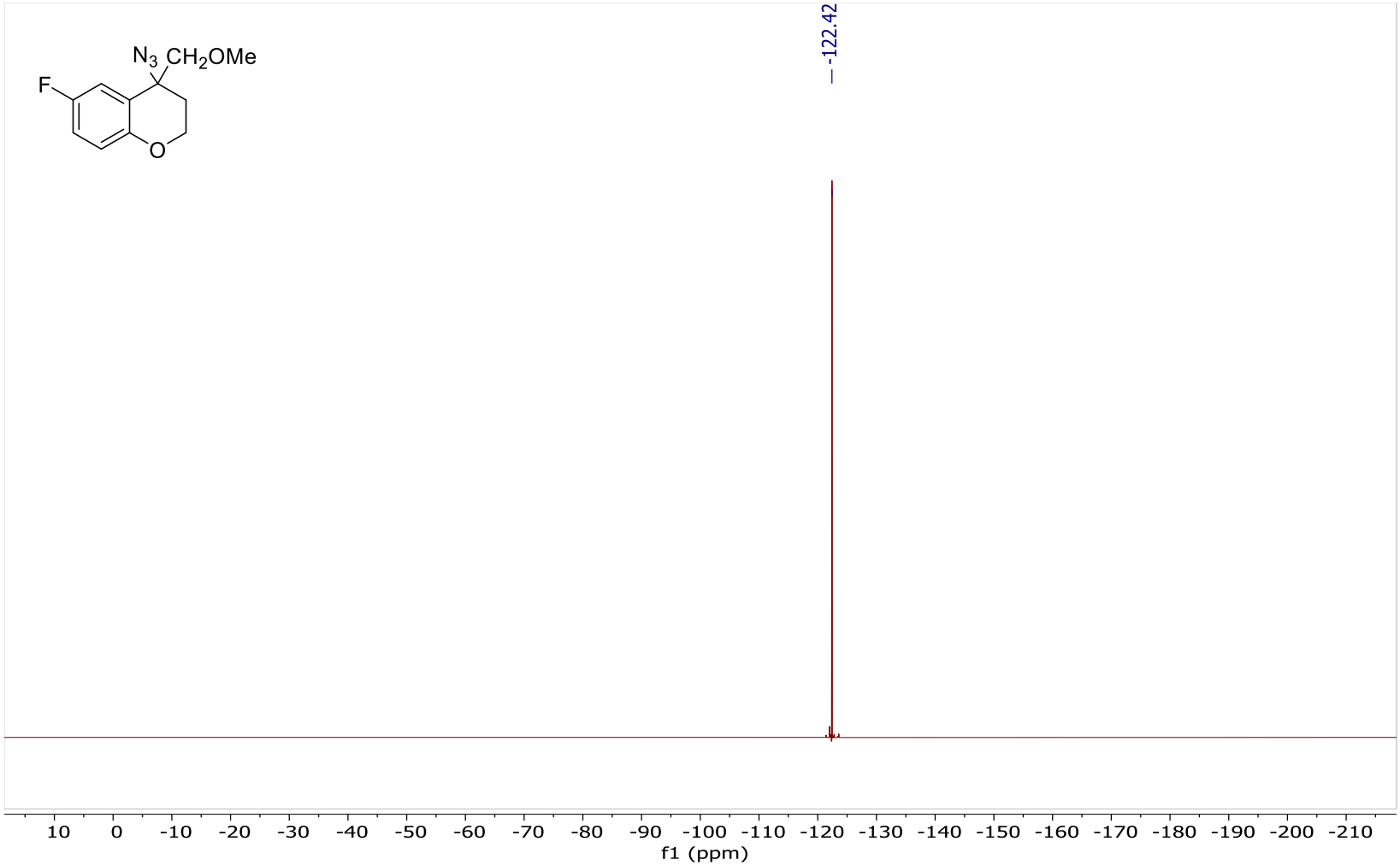

Compound **6.12**. 376 MHz $^{19}F\{^{1}H\}$ NMR spectrum in $CDCl_3$

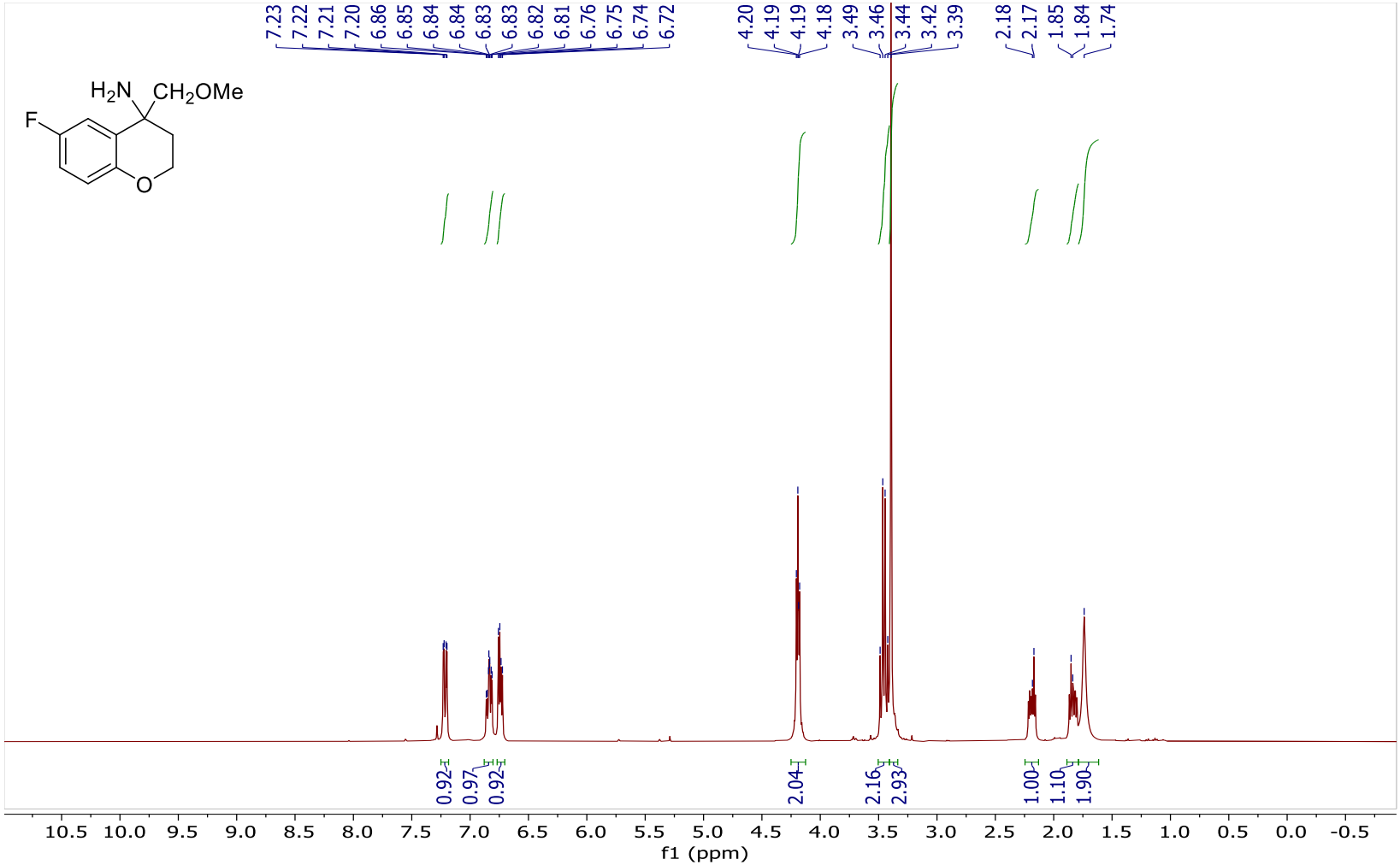

Compound **6.13**. 400 MHz ^{1}H NMR spectrum in $CDCl_3$

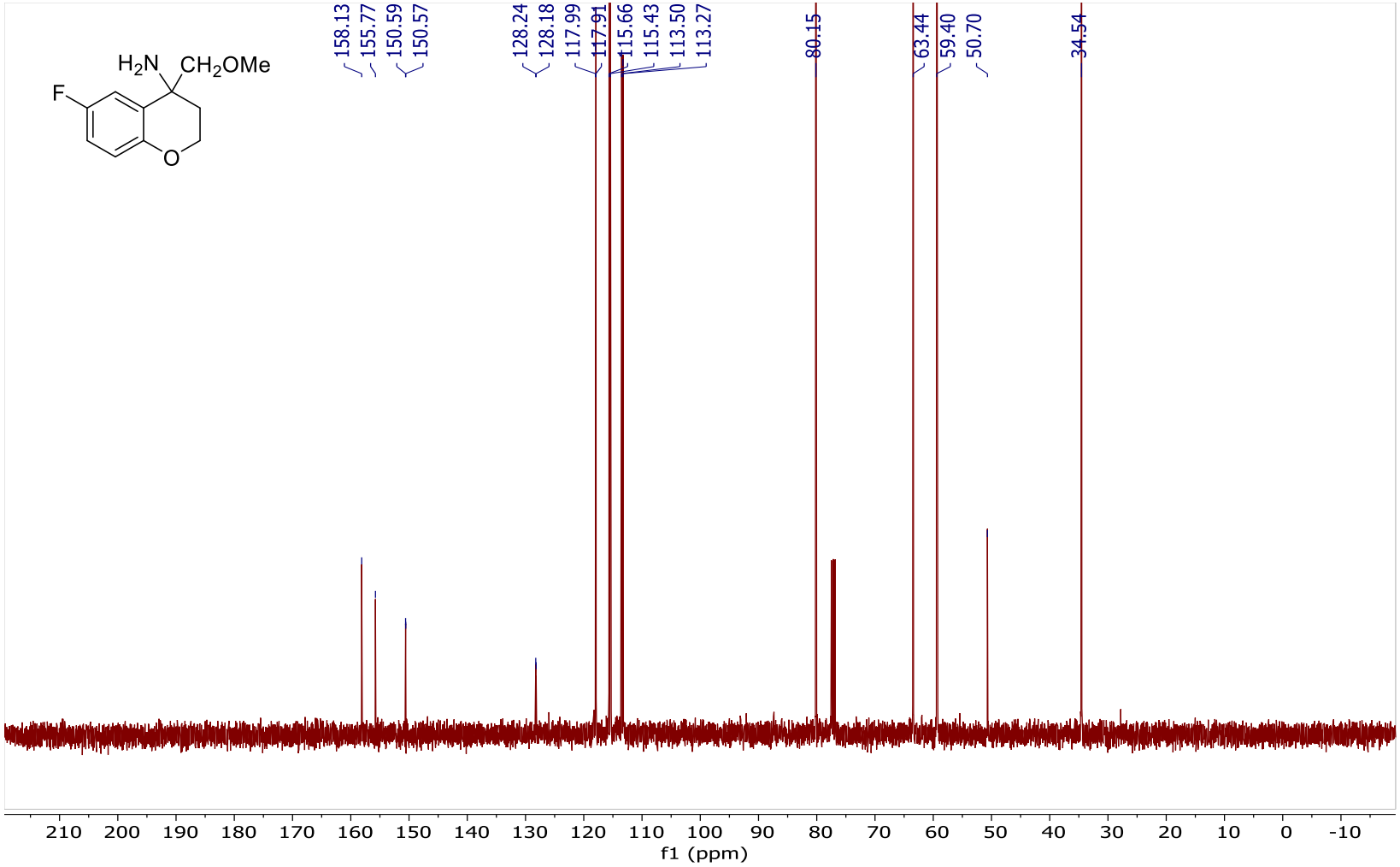

Compound **6.13**. 100 MHz $^{13}C\{^{1}H\}$ NMR spectrum in $CDCl_3$

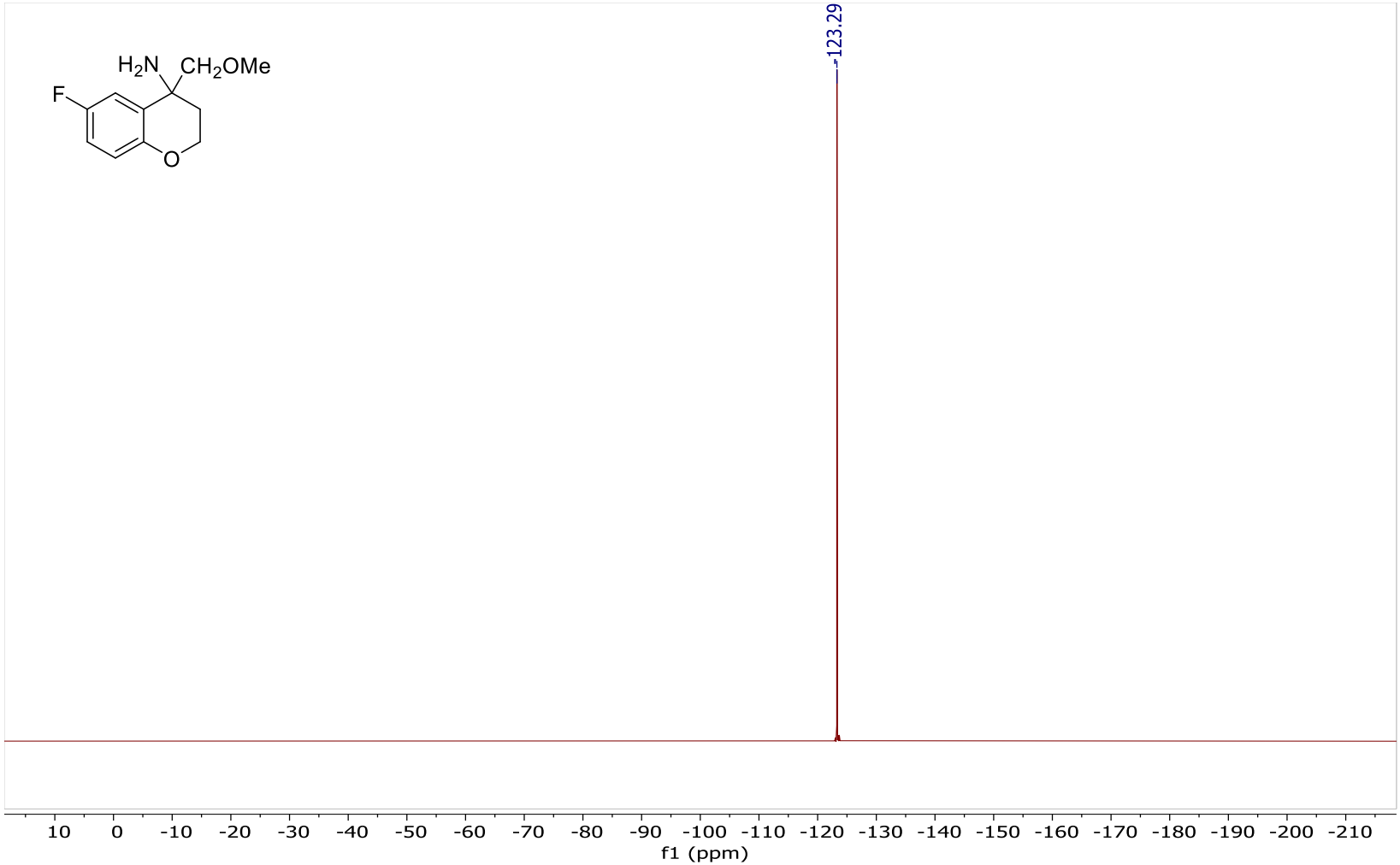

Compound **6.13**. 376 MHz $^{19}F\{^{1}H\}$ NMR spectrum in $CDCl_3$

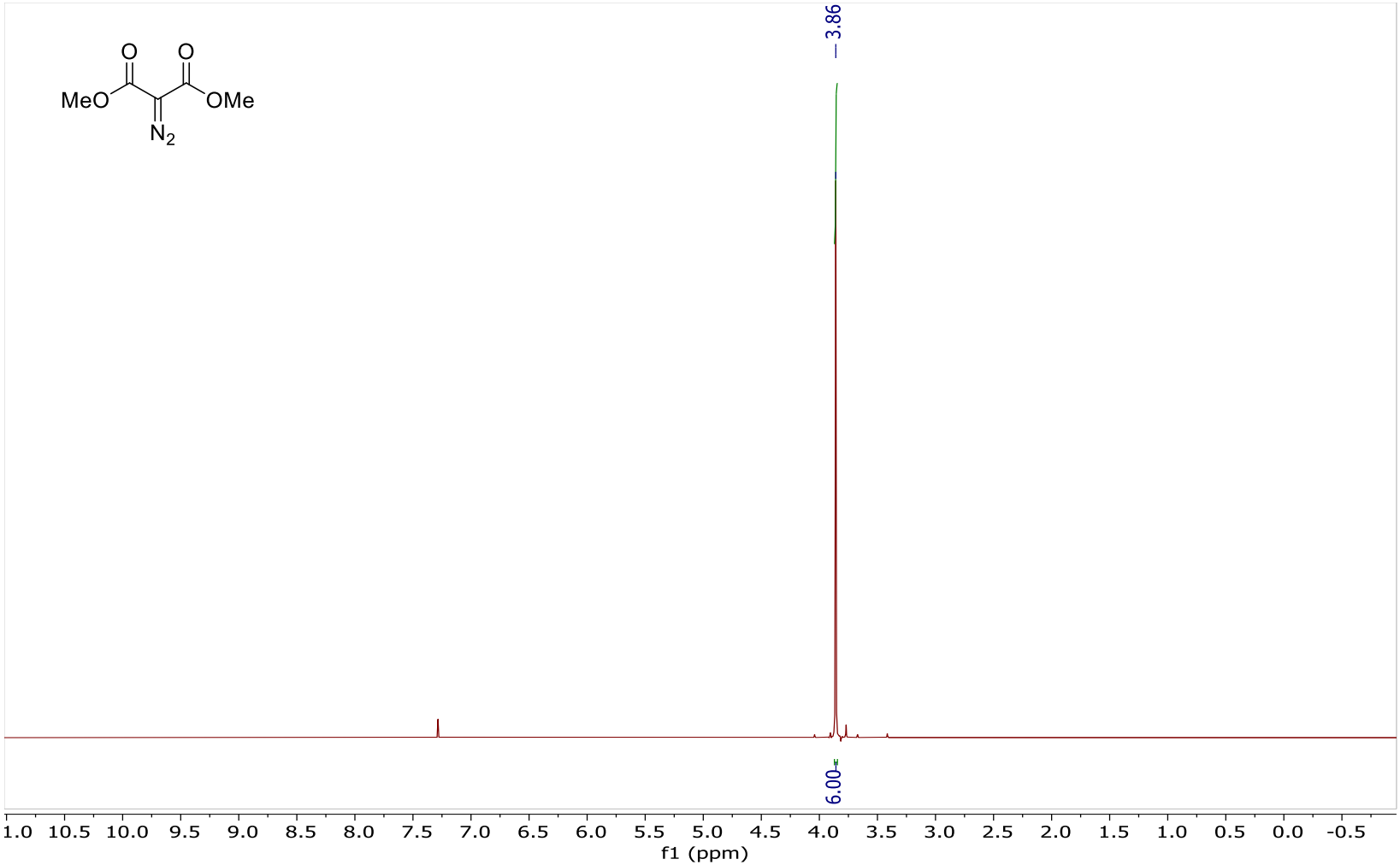

Compound **6.20**. 400 MHz ^{1}H NMR spectrum in $CDCl_3$

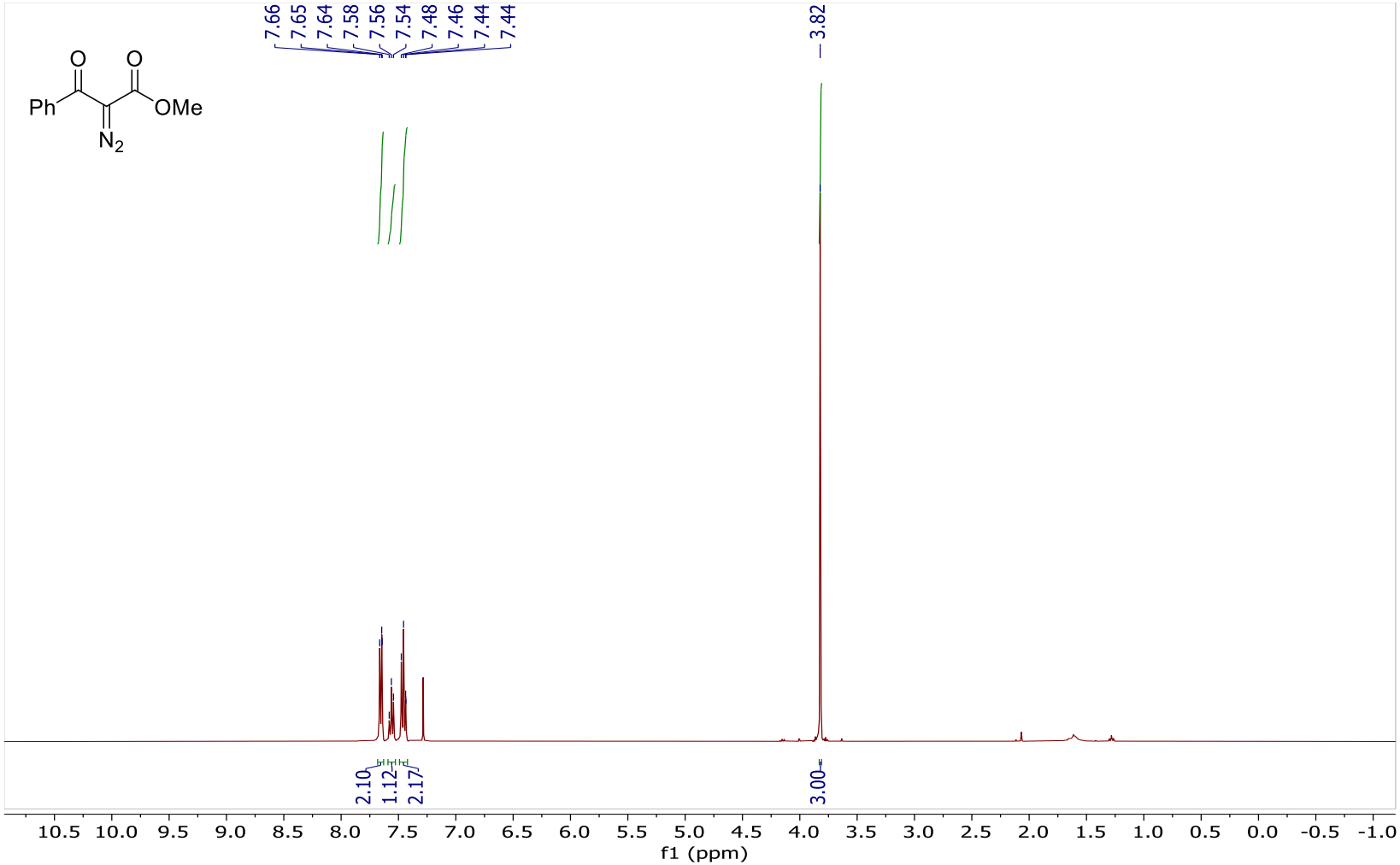

Compound **6.21**. 400 MHz ^{1}H NMR spectrum in $CDCl_3$

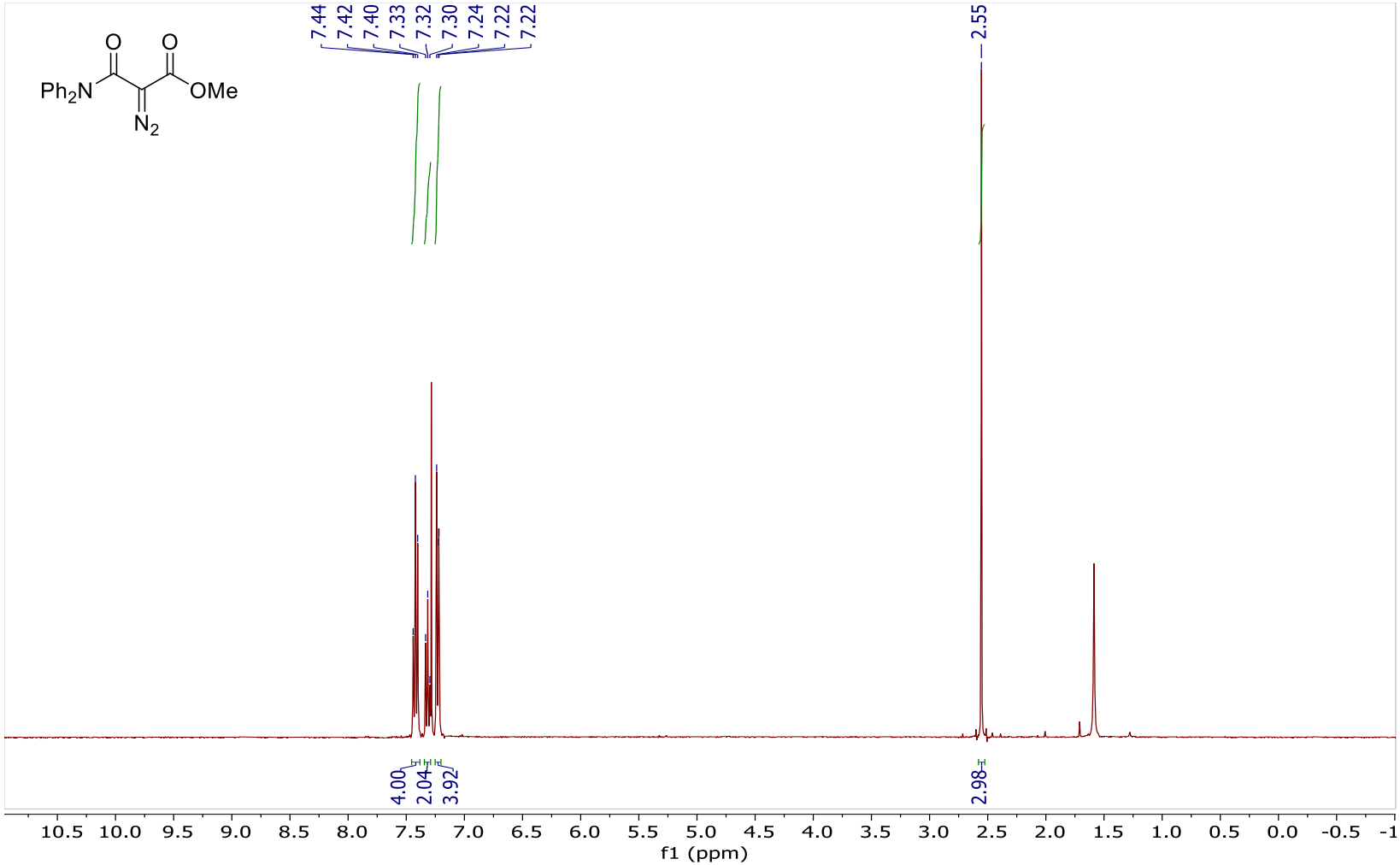

Compound **6.22**. 400 MHz ^{1}H NMR spectrum in $CDCl_3$

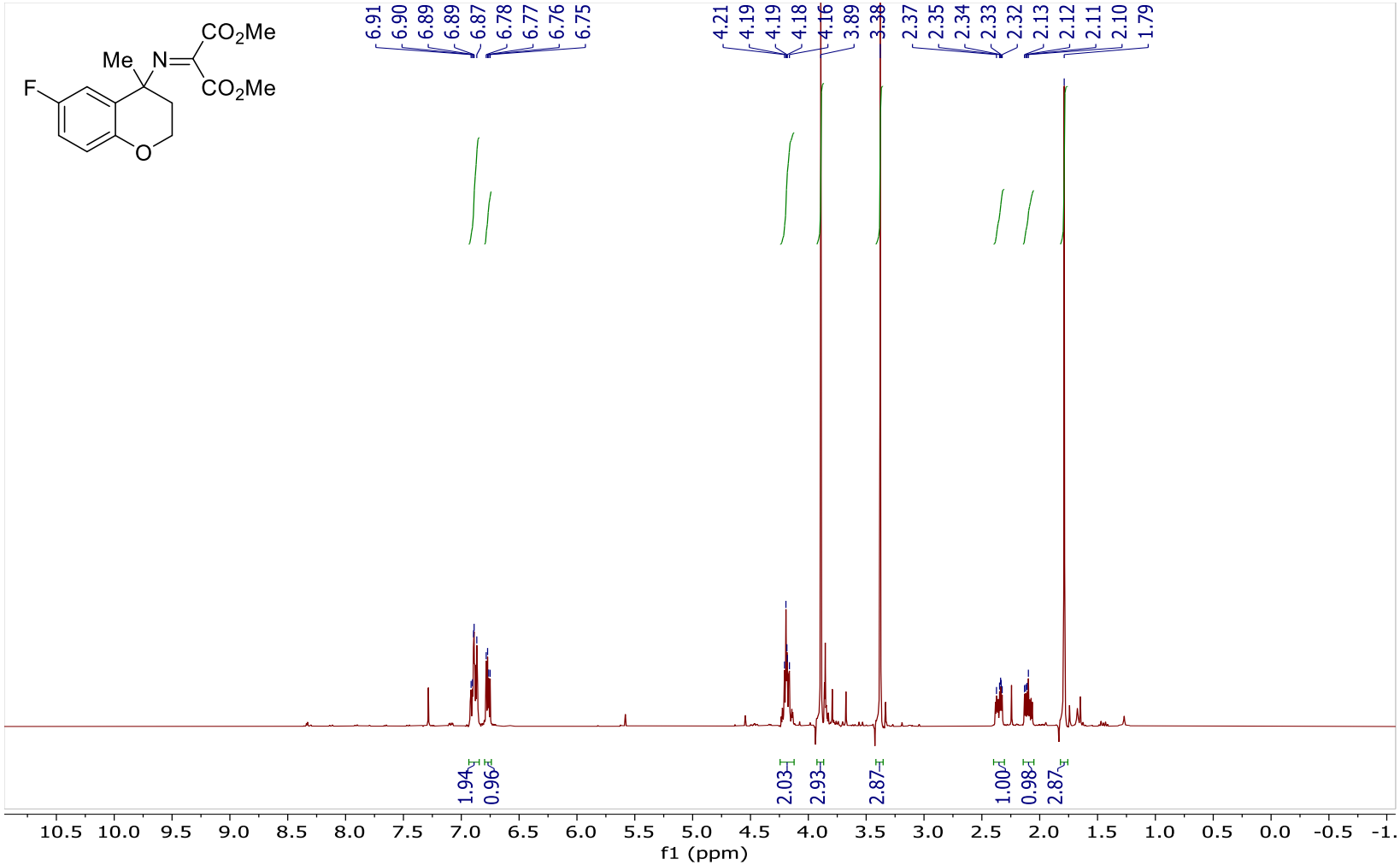

Compound **6.24**. 400 MHz ^{1}H NMR spectrum in $CDCl_3$

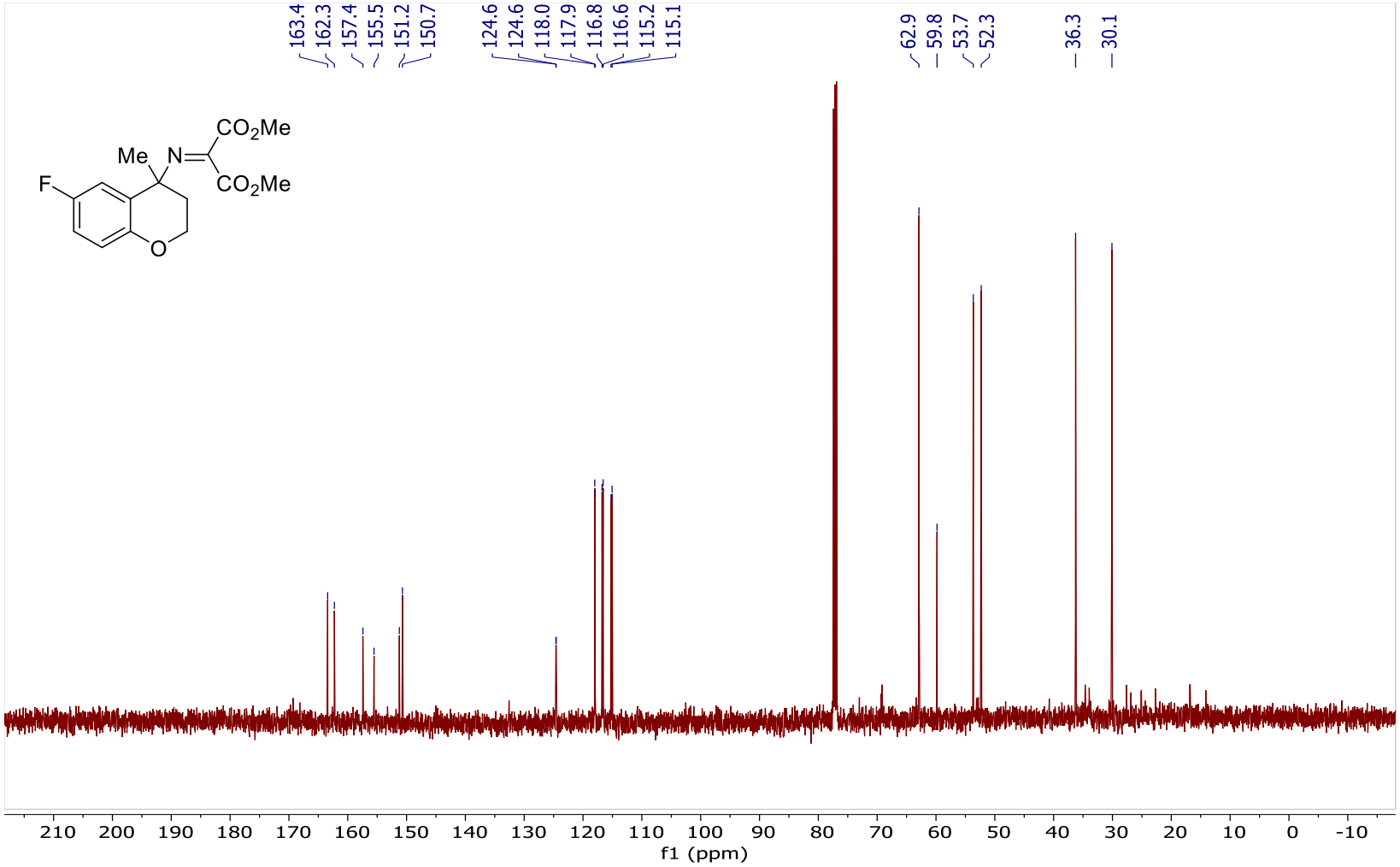

Compound **6.24** 125 MHz $^{13}C\{^{1}H\}$ NMR spectrum in $CDCl_3$

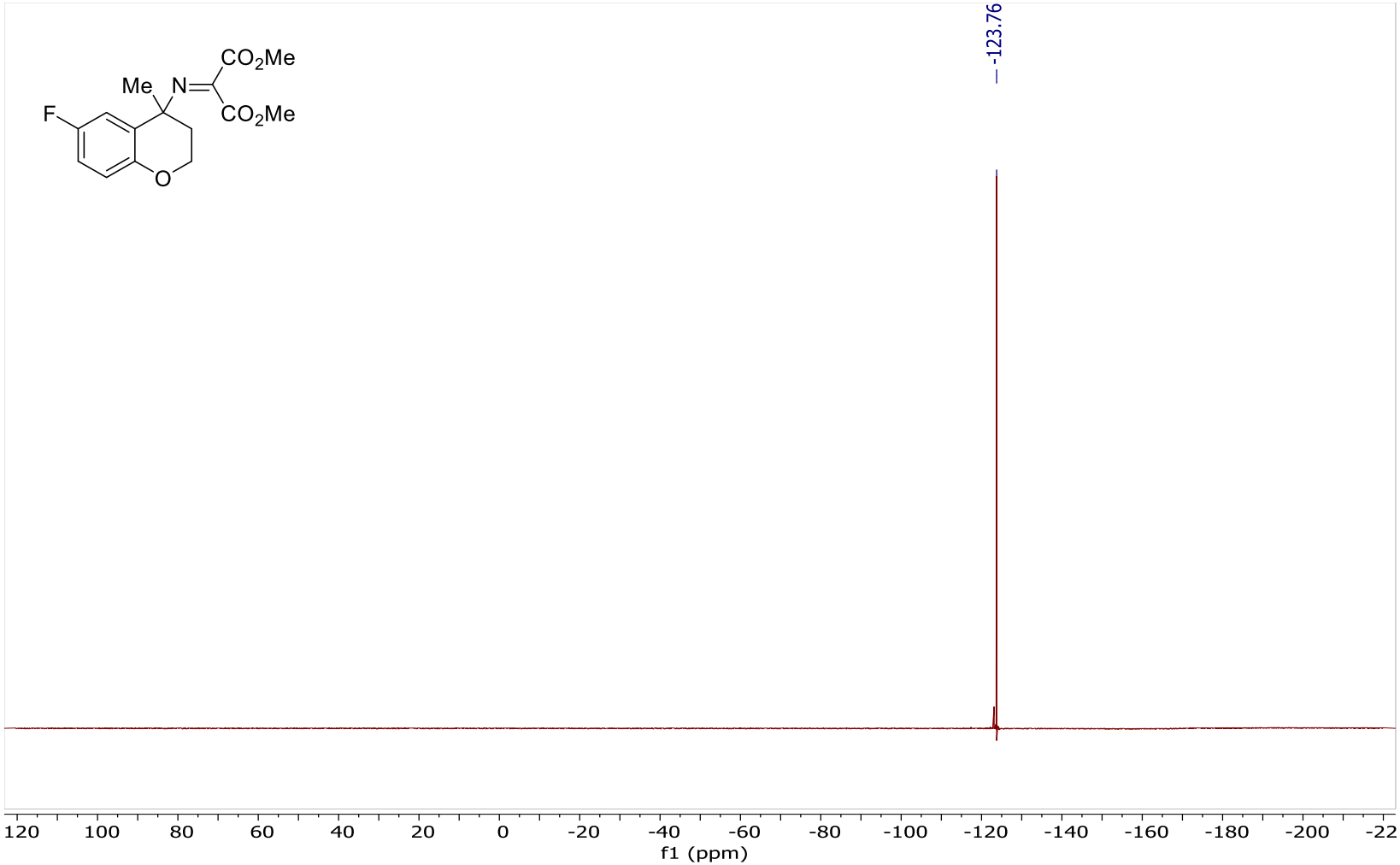

Compound **6.24** 471 MHz $^{19}F\{^{1}H\}$ NMR spectrum in $CDCl_3$

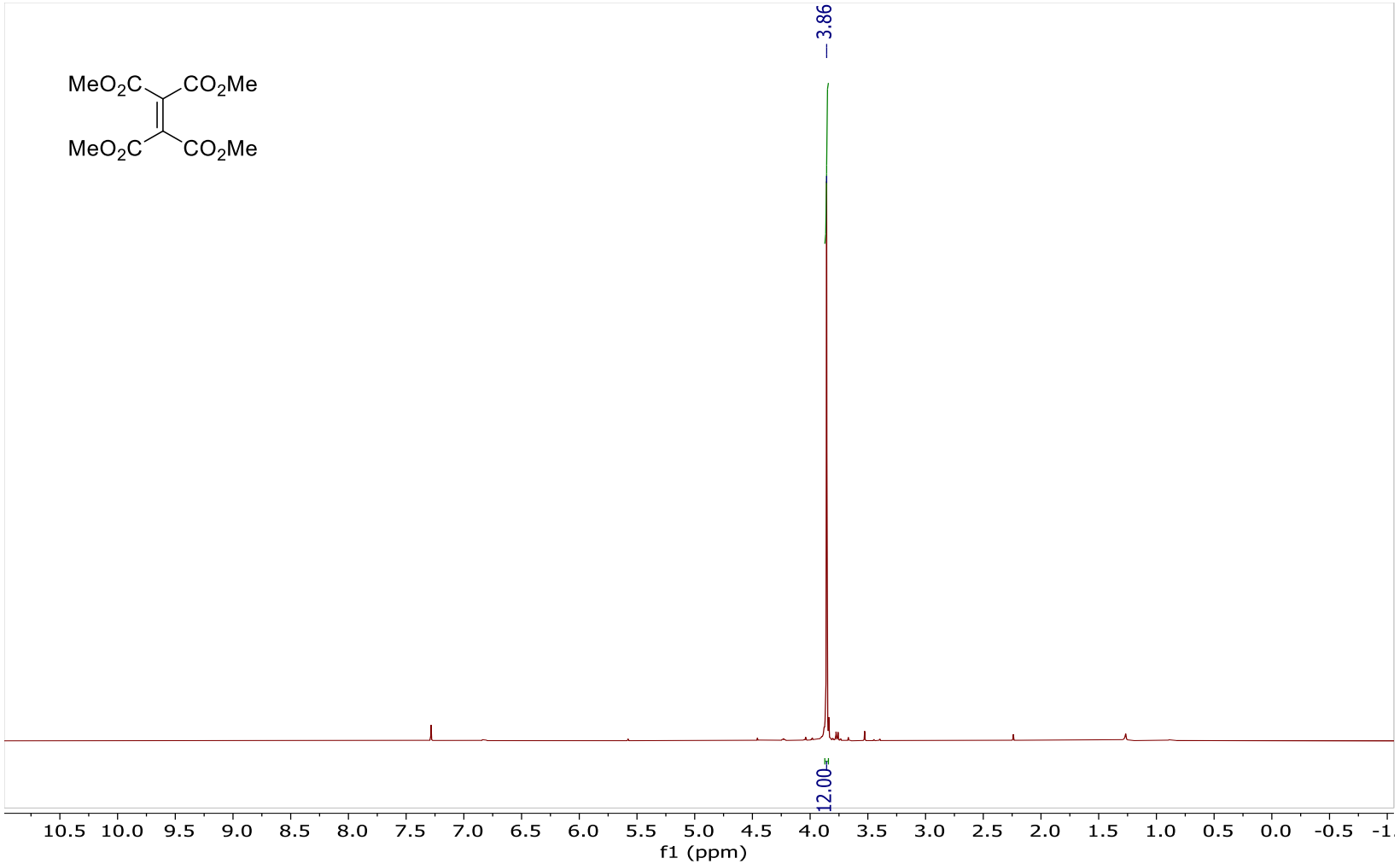

Compound **6.25**. 400 MHz ^{1}H NMR spectrum in $CDCl_3$

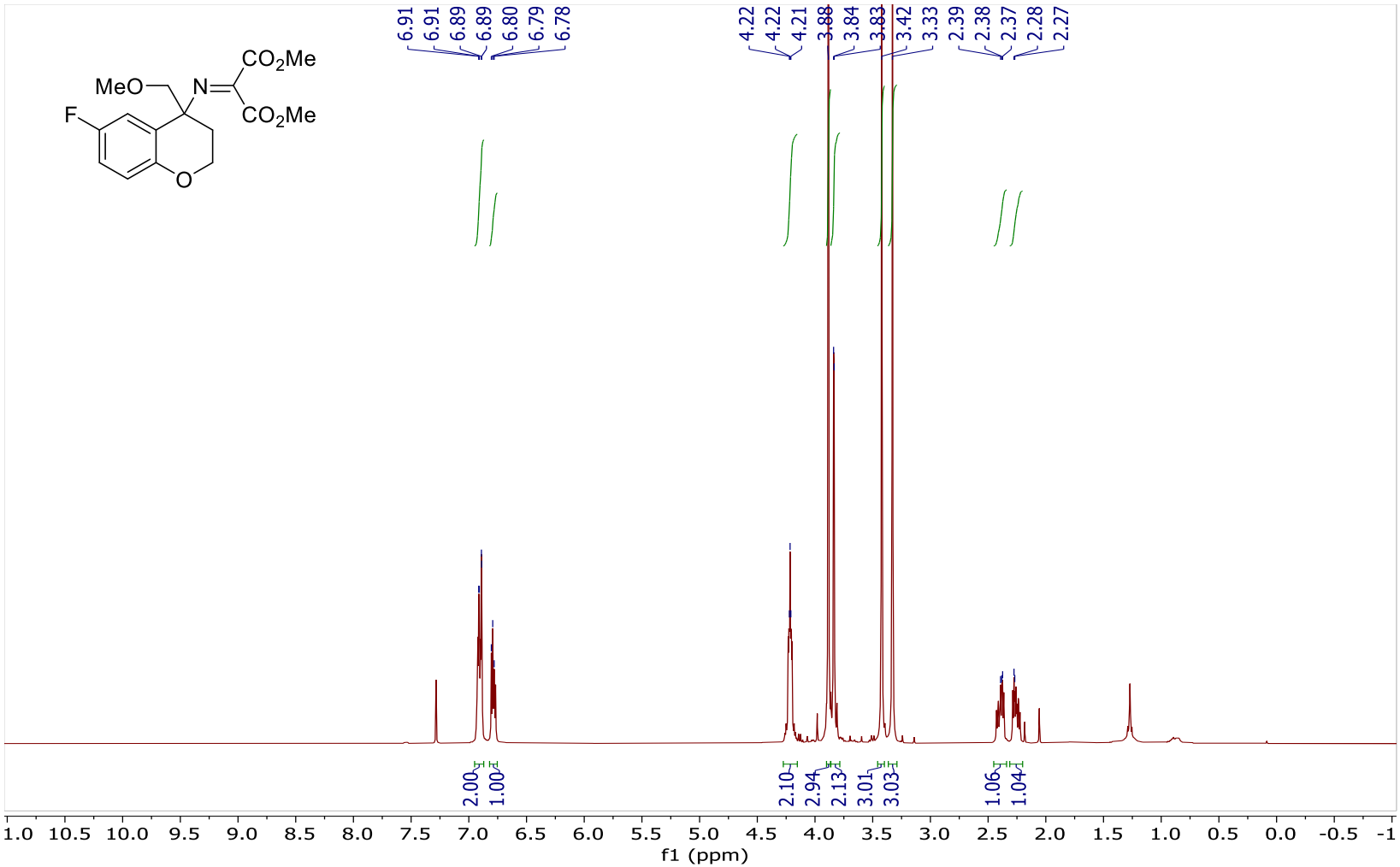

Compound **6.26**. 400 MHz ^{1}H NMR spectrum in $CDCl_3$

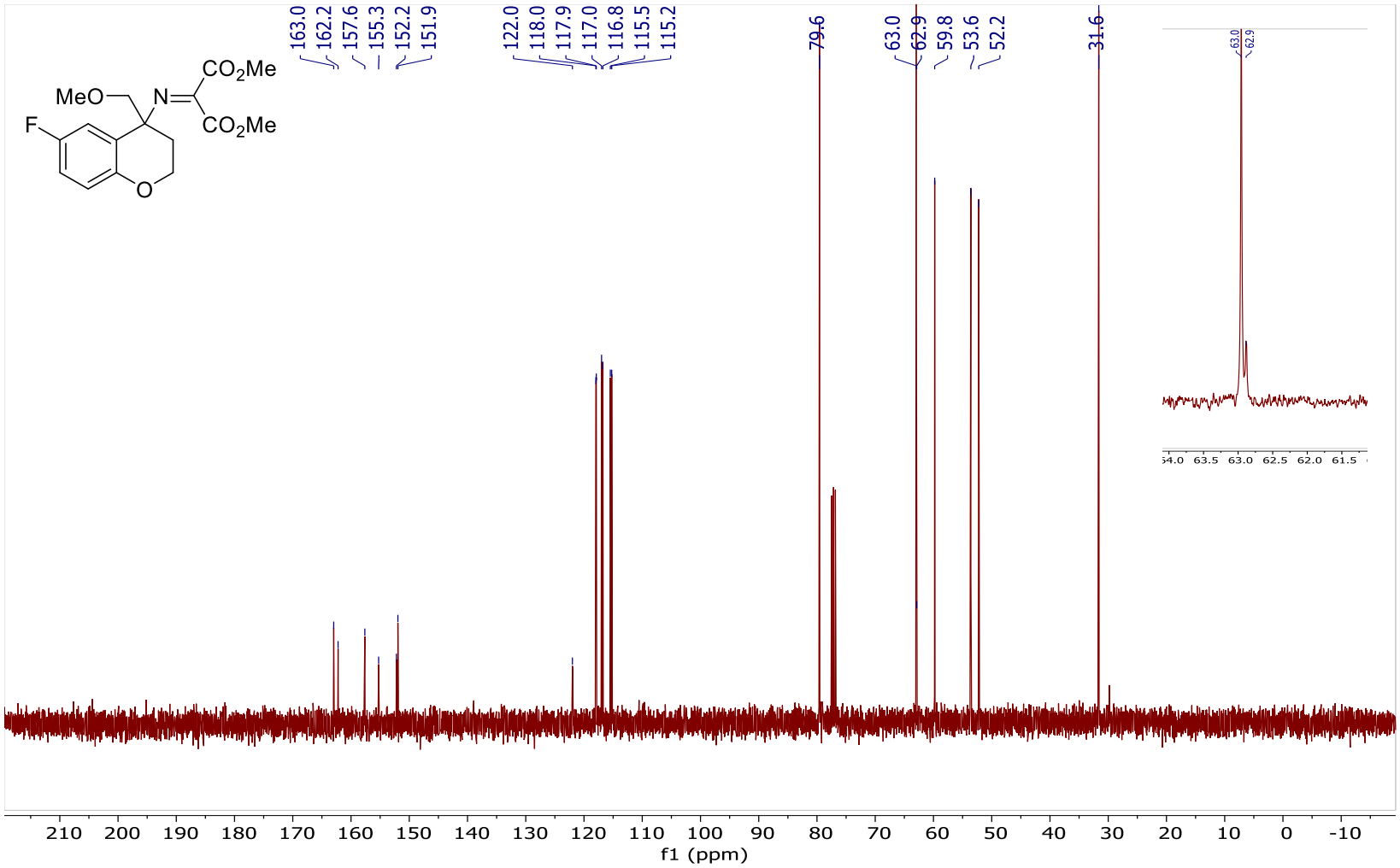

Compound **6.26** 100 MHz $^{13}C\{^{1}H\}$ NMR spectrum in $CDCl_3$

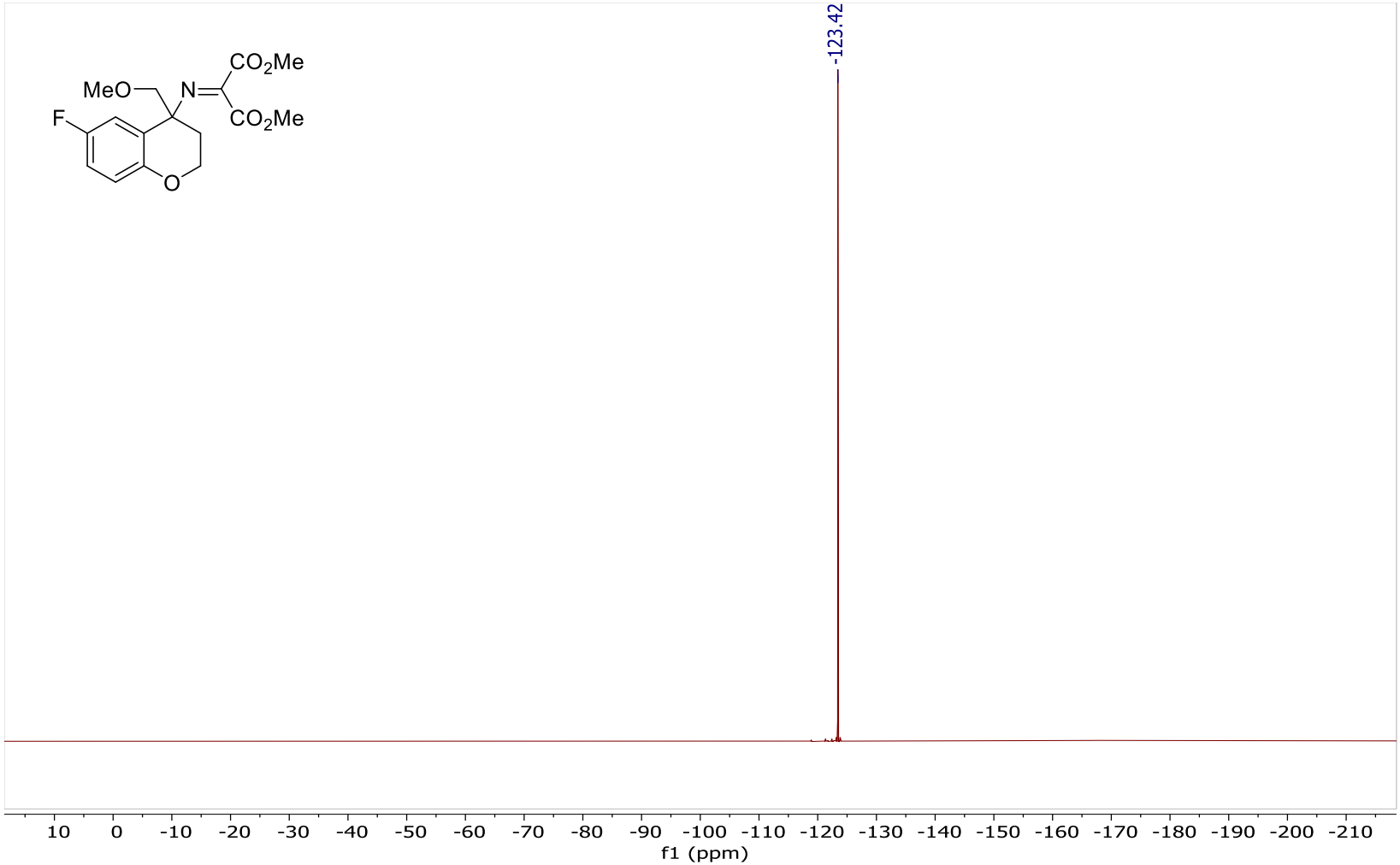

Compound **6.26** 376 MHz $^{19}F\{^{1}H\}$ NMR spectrum in $CDCl_3$